

Public-data File 88-42

APATITE FISSION-TRACK STUDY OF THE THERMAL HISTORY OF
PERMIAN TO TERTIARY SEDIMENTARY ROCKS IN THE
ARCTIC NATIONAL WILDLIFE REFUGE, NORTHEASTERN ALASKA

By

Paul O'Sullivan

Alaska Division of
Geological and Geophysical Surveys

December 1988

THIS REPORT HAS NOT BEEN REVIEWED FOR
TECHNICAL CONTENT (EXCEPT AS NOTED IN
TEXT) OR FOR CONFORMITY TO THE
EDITORIAL STANDARDS OF DGGS.

794 University Avenue, Suite 200
Fairbanks, Alaska 99709-3645

ABSTRACT

Apatite fission track analyses (AFTA) of four sedimentary rock outcrop areas in the Arctic National Wildlife Refuge (ANWR) of Alaska indicate that uplift events responsible for the formation of the Northeastern Brooks Range decrease in age to the north. AFTA data from a Permian to Albian section at Bathub Ridge indicate the section was uplifted > 2 km and eroded, cooling rapidly through ~125°-60°C at ~62 Ma. AFTA data from the Albian Arctic Creek exposures indicate that the section was uplifted, eroded, and rapidly cooled at ~37 Ma. Analyses of Lower Cretaceous to Paleocene rocks from the banks of the Canning River record two uplift-and-erosion events at ~45 Ma and ≤ 32 Ma. AFTA data from Upper Cretaceous to Eocene sedimentary rocks from the ANWR coastal plain indicate that these rocks have not been subjected to temperatures greater than 60°C since their deposition.

TABLE OF CONTENTS

ABSTRACT.....	3
TABLE OF CONTENTS.....	4
LIST OF FIGURES.....	8
ABBREVIATIONS USED IN THIS THESIS.....	10
LIST OF TABLES.....	11
ACKNOWLEDGEMENTS.....	12
INTRODUCTION.....	14
PURPOSE AND SCOPE.....	16
REGIONAL GEOLOGY.....	18
NORTH SLOPE OF ALASKA: STRATIGRAPHY.....	18
NORTH SLOPE OF ALASKA: STRUCTURAL HISTORY.....	18
STRUCTURE OF THE NORTHEASTERN BROOKS RANGE.....	20
STUDY LOCATIONS.....	21
Bathtub Ridge.....	21
Arctic Creek Region.....	23
Canning River Region.....	24
ANWR Coastal Plain.....	25
APATITE FISSION TRACK ANALYSIS: BACKGROUND, PROCEDURES, AND METHODOLOGY.....	26
FISSION TRACKS AND FISSION TRACK TECHNIQUES.....	26
FISSION TRACK LENGTHS.....	27
THERMAL HISTORIES FROM APATITE FISSION TRACK ANALYSIS.....	29
TECTONIC STUDIES.....	31
APATITE FISSION TRACK METHODS.....	34
Sample Descriptions and Sampling Details.....	34
Sample Preparation and Processing.....	35
Fission Track Age Calculations.....	36
Track Length Measurements.....	36
FISSION TRACK RESULTS AND INTERPRETATIONS.....	38
RESULTS.....	38
Bathtub Ridge.....	38
Arctic Creek Region.....	45

Canning River Region.....	46
ANWR Coastal Plain.....	48
Compositional Variation In Apatites.....	49
INTERPRETATIONS.....	50
Interpretation of Bathtub Ridge Results.....	51
Interpretation of Arctic Creek Results.....	55
Interpretation of Canning River Results.....	57
Interpretation of ANWR Coastal Plain Results.....	59
GEOLOGIC INTERPRETATION OF FISSION TRACK DATA.....	64
OVERVIEW.....	64
HEAT FLOW CONSTRAINTS.....	64
ALTERNATIVE MECHANISMS FOR RAPID COOLING.....	66
Rapid Decrease in Geothermal Gradient.....	66
Emplacement of Magma and Subsequent Cooling.....	67
Rapid Uplift and Denudation.....	68
SUMMARY AND CONCLUSIONS.....	74
Bathtub Ridge.....	74
Arctic Creek Region.....	74
Canning River Region.....	74
ANWR Coastal Plain.....	75
Overview of Proposed Uplift/Denudation History.....	75
APPENDIX A - FISSION TRACK ANALYSIS: SUMMARY OF	
THE TECHNIQUE AND INTERPRETATION OF RESULTS.....	79
INTRODUCTION.....	79
FISSION TRACKS AND FISSION TRACK TECHNIQUES.....	79
The Formation of a Fission Track.....	79
Track Etching.....	81
Etching Conditions.....	82
Fission Track Dating Methods.....	83
The External Detector Method.....	83
THE FISSION TRACK EQUATION, ZETA CALIBRATION,	
AND ERROR ANALYSIS.....	84
The Fission Track Equation.....	84
Zeta Calibration.....	86

Personal Zeta Calibration.....	87
Determination of Error.....	87
APATITE FISSION TRACK LENGTHS.....	92
Fission Track Annealing.....	92
The Effect of Composition on Apatite Annealing.....	96
Fission Track Length Annealing Studies.....	99
Measuring Fission Track Lengths.....	99
APATITE FISSION TRACK THERMAL HISTORIES.....	100
Track Length Distributions.....	101
Thermal Modeling.....	105
Applications.....	110
APPENDIX B - APATITE FISSION TRACK ANALYSIS	
SAMPLE PREPARATION.....	111
INTRODUCTION.....	111
SAMPLE TREATMENT.....	111
ROCK CRUSHING AND MINERAL SEPARATION.....	111
MINERAL MOUNTING, GRINDING, POLISHING, AND	
ETCHING TECHNIQUES.....	113
Summary of Materials and Methods.....	113
Mounting.....	113
Grinding and Polishing.....	114
Etching.....	114
PRE-IRRADIATION SAMPLE HANDLING FOR THE EXTERNAL	
DETECTOR METHOD.....	114
Mount-Mica Pairs and Wrapping.....	114
The Irradiation Package.....	115
Neutron Irradiation and Fluence Monitoring.....	115
POST-IRRADIATION SAMPLE HANDLING.....	115
MICROSCOPE EQUIPMENT AND COUNTING PROCEDURES.....	116
Fission Track Ages.....	116
Confined Fission Track-Lengths.....	118
APPENDIX C - INDIVIDUAL SAMPLE DATA.....	119
SAMPLE LOCATIONS.....	119
TRACK LENGTH DATA.....	121

Bathtub Ridge.....	121
Arctic Creek Region.....	123
Canning River Region.....	124
ANWR Coastal Plain.....	125
AGE DATA.....	128
Bathtub Ridge.....	129
Single-Grain Age Distributions: Bathtub Ridge.....	147
Arctic Creek Region.....	150
Single-Grain Age Distributions: Arctic Creek Region.....	157
Canning River Region.....	158
Single-Grain Age Distributions: Canning River Region.....	167
ANWR Coastal Plain.....	168
Single-Grain Age Distributions: ANWR Coastal Plain.....	175
REFERENCES CITED.....	176

LIST OF FIGURES

Figure 1.	Regional map showing the four areas sampled.....	17
Figure 2.	Generalized Ellesmerian and Brookian stratigraphy for northeastern Alaska.....	19
Figure 3.	Regional schematic cross sections.....	22
Figure 4.	Stratigraphic section of the Bathtub Ridge area.....	23
Figure 5.	Composite stratigraphic section of the Arctic Creek area.....	24
Figure 6.	Stratigraphic section of the Arctic Coastal Plain and Ignek Valley.....	25
Figure 7.	Comparison of parallel and fanning models to predict apatite annealing.....	28
Figure 8.	Idealized time-temperature paths with resultant apatite track length distributions.....	30
Figure 9.	Typical length distributions of confined tracks in rapidly cooled volcanic and related apatites.....	32
Figure 10.	Apatite fission track ages plotted against sample elevation for different regions in the Alps.....	33
Figure 11.	Cooling history of a sample from the Quottoon pluton, British Columbia.....	34
Figure 12.	Plot of fission track age vs. elevation for samples collected from Bathtub Ridge.....	44
Figure 13.	Apatite fission track data from representative samples collected from Bathtub Ridge.....	44
Figure 14.	Plot of fission track age vs. elevation for samples collected from the Arctic Creek exposures.....	45
Figure 15.	Apatite fission track data from representative samples collected from the Arctic Creek exposures.....	46
Figure 16.	Apatite fission track data from representative samples collected from the Canning River section.....	47
Figure 17.	Plot of relative changes in ages and mean track lengths throughout the Canning River section.....	47
Figure 18.	Apatite fission track data from representative samples collected from the Arctic Coastal Plain.....	48

Figure 19. Proposed thermal history for the upper part of the Bathtub Ridge section.....	52
Figure 20. Proposed thermal history for the lower part of the Bathtub Ridge section.....	54
Figure 21. Proposed thermal history for the Albian turbidites of the Arctic Creek section.....	56
Figure 22. Fission track interpretation of the Canning River section.....	58
Figure 23. Proposed thermal history for the upper part of the Canning River section.....	60
Figure 24. Proposed thermal history for the lower part of the Canning River section.....	61
Figure 25. Proposed thermal history for the Hue Shale on the Arctic Coastal Plain.....	63
Figure 26. Tectonic Map of the NEBR.....	76
Figure 27. Preliminary cross-section across the NEBR.....	77
Figure A1. The ion explosion spike mechanism for track formation in a simple crystalline solid.....	80
Figure A2. Track geometry showing V_{Gt} (bulk surface etching with time) and V_{Tt} (track etching with time).....	81
Figure A3. Results of a laboratory study of fading of fission tracks in apatite and sphene.....	93
Figure A4. Variation in apparent apatite fission track age with down-hole temperature in wells of the Otway Basin, South Australia.....	94
Figure A5. Arrhenius plot for fission track fading in apatite.....	95
Figure A6. Variation of apatite single grain ages with composition.....	97
Figure A7. Confined apatite fission track lengths as etched through fractures or other tracks.....	99
Figure A8. Fission track length distributions observed in apatites from the Otway Basin, South Australia at various depths (temperatures) in three drill-holes.....	101
Figure A9. Idealized time-temperature paths with the resultant apatite track length distributions.....	102

Figure A10. Characteristic confined track length distributions for different thermal histories.....	104
Figure A11. Apatite track length distributions resulting from different simple thermal histories.....	107
Figure A12. Thermal modeling of different thermal histories prior to cooling.....	109
Figure B1. Mount / mica pair mounted on a glass slide ready for counting and measuring track lengths.....	116

ABBREVIATIONS USED IN THIS THESIS

ADGGS - Alaska Division of Geological and Geophysical Surveys	NBS - National Bureau of Standards
AFTA - apatite fission track analysis	NEBR - northeastern Brooks Range
ANWR - Arctic National Wildlife Refuge	ppb - parts per billion
b.y. - billion years	ppm - parts per million
°C - degrees Celcius	R ₀ - Vitrinite Reflectance value
cm - centimeters	rpm - revolutions per minute
EDM - external detector method	s.d. - standard deviation
km - kilometers	TAI - Thermal Alteration Index
m - meters	µm - micrometers
Ma - million years before present	yr - year
m.y. - million years	

LIST OF TABLES

Table 1.	Analytical Data For Fission Track Age Determinations.....	39
Table 2.	Fission Track Length Data.....	42
Table 3.	Chlorine and Fluorine Contents in Selected Apatite Grains.....	49
Table A1.	Fission Track Counting of Standards for Personal Zeta Determination.....	88
Table B1.	Rock Crushing and Mineral Separation Summary.....	112
Table C1.	Sample Locations.....	119
Table C2.	Individual Track Length Distributions.....	126

ACKNOWLEDGEMENTS

This work was funded by a grant to the Alaska Division of Geological and Geophysical Surveys (ADGGS) from the U.S. Department of the Interior Minerals Management Service, through their Continental Margins Project.

I am indebted to many people who have contributed to this project, in particular, Dr. John Decker who has been instrumental in many ways from the beginning. John first proposed the thesis idea to me, patiently guided me to pertinent outcrops in the field, took time to teach me the proper ways of collecting data, and helped initiate a cooperative arrangement with Melbourne University Fission Track Research Group. He also arranged my financial support and provided employment with the ADGGS. Without John's excellent advice and support I would have never been able to complete this project.

I wish to thank my graduate advisory committee for their contributions and understanding, in particular Dr. Donald Turner and Dr. Steven Bergman. Don has labored many hours editing drafts and has given me advice and guidance since he first introduced me to geochronology as an undergraduate. Steve has been very supportive since the beginning of this project, taking time to edit preliminary drafts, answer questions, and offer excellent advice.

I am in debt to Dr. Paul Green, Dr. Andrew Gleadow, and Dr. Ian Duddy of the Melbourne University Fission Track Research Group. They willingly gave me access to their laboratory facilities, took time to help me with each step of apatite fission track analysis, and offered advice concerning the final interpretations. I am particularly grateful for their offer to allow me to return to Australia to start a PhD project.

A special thanks goes to Dr. Wesley K. Wallace for his expert advice and assistance with organizing the geologic interpretations.

I would also like to thank all my friends and colleagues who have helped me through the good and bad times associated with writing a thesis. These include my fiancée Andrea Byrnes, who assisted me with the initial data gathering and with assembling the final manuscript, and the crew of the "night shift". Finally, I will forever be indebted to my parents for all their support financially and morally throughout my college career. Thanks!

INTRODUCTION

The coastal plain of the Arctic National Wildlife Refuge (ANWR) in the northeastern Brooks Range (NEBR), Alaska has received a great deal of attention from the earth science community. The deep sedimentary basin beneath the ANWR coastal plain is believed by many to contain major hydrocarbon accumulations (Mast *et al.*, 1980). Hydrocarbons have been found in most North Slope stratigraphic units (Bird, 1987; Bird and Molenaar, 1987; Sedivy *et al.*, 1987). Analysis of basin development from detailed studies of Prudhoe Bay wells suggests that most of these hydrocarbon accumulations formed between 40 and 100 Ma (Bird, 1987). However, the geological relationships are complicated by deformation caused by the Brooks Range fold and thrust belt which extends northward across the coastal plain of ANWR. Determining the timing of deformation events within the fold and thrust belt could constrain the timing of formation of possible hydrocarbon traps.

The opening of the Canadian Basin during the Late Jurassic resulted in the initiation of the Late Jurassic to Tertiary Brookian orogeny (Mull, 1982). The structure of the NEBR records this orogenic event and is dominated by a series of generally east-trending anticlinoria cored by pre-Mississippian rocks (Leiggi, 1987; Wallace and Hanks, 1988a,b, and in review). The geometries of the anticlinoria are controlled by a north-vergent duplex consisting of fault-bounded slivers, or "horses", bounded at the base by a floor thrust in the pre-Mississippian rocks. The NEBR differs from the remainder of the Brooks Range in that deformation in the NEBR extends farther north but involves less displacement and shortening (Wallace and Hanks, 1988b).

Sedimentary rocks exposed in the NEBR provide a record of the timing of structural events within ANWR as well as a means of deciphering the thermal history of the rocks since Late Jurassic to Tertiary orogenic events. During uplift, material was shed from the northward-verging deformed rocks of the Brooks Range to form Cretaceous and Tertiary

deposits in the Colville Trough (Mull, 1985). Many details of the thermal and burial history of the post Jurassic sedimentary basin are poorly understood and timing of post Cretaceous structural events are poorly constrained.

Detrital apatites in sandstones from the study area preserve a record of their host rocks' thermal history which fission track analysis can reveal. Fission tracks are produced by spontaneous fission of the ^{238}U nucleus and are used for radiometric dating. However, the special interest of fission track geochronometers is that they are highly sensitive to temperature (Fleischer *et al.*, 1975). Fission track ages can be considered as cooling ages with the temperature depending on the mineral studied (Fleischer *et al.*, 1975; Mailhe *et al.*, 1986). Two minerals, apatite and zircon, have been used extensively to delineate the thermal histories of rocks (Gleadow and Duddy, 1984; Miller and Lakatos, 1983; Naeser, 1979b). Using this approach, it is possible to detect and date large vertical movements and to constrain rates of cooling, uplift and erosion in orogenic areas.

This thesis presents the results of an apatite fission track analysis (AFTA) study of Permian through Tertiary sedimentary rocks from four areas in ANWR. In this study, I have attempted to determine the timing of uplift and erosion events along major detachment horizons in the NEBR as well as to determine the thermal histories of the sedimentary rocks presently exposed in the four study areas. These uplift and erosion events resulted in the development of the east-trending anticlinoria in the NEBR. AFTA data from 42 samples (primarily sandstones), indicate that the uplift and erosion events responsible for the formation of these major anticlinoria decrease in age to the north. Since the Albian, major uplift and denudation events from south to north occurred at ~62 Ma, ~45 Ma, ~37 Ma, and ≤ 32 Ma. Farther north, rocks studied on the ANWR coastal plain near the northern coast of Alaska are unannealed and do not show any effects of the advancing fold and thrust belt.

PURPOSE AND SCOPE

This thesis reports AFTA data derived from forty-two samples from four areas: Bathtub Ridge, Arctic Creek, the ANWR coastal plain (along Carter Creek, the Jago River, and the Niguanak River) (Fig. 1), and along the Canning River west of the Sadlerochit Mountains. The objective of this study is to determine the timing of uplift and erosion events along major detachment horizons in the NEBR as well as the thermal history of selected Permian through Eocene sedimentary rocks from ANWR using AFTA data. The study was conceived to answer the following questions concerning the thermal history of Permian through Tertiary rocks exposed in ANWR:

1. What are the time-temperature paths for representative rocks from each area studied?
2. What do these time-temperature paths tell us about the structural development of the NEBR?
 - A. How much uplift and erosion has taken place?
 - B. When did uplift and erosion occur?
 - C. What does the timing of uplift and erosion events tell us about the thrust imbrication history of the NEBR?

The AFTA method involves determination of an apparent fission track age and a distribution of track lengths (an indication of the sample's thermal history). A discussion of this method is given in the section titled "Apatite Fission Track Analysis: Background, Procedures, and Methodology." A more detailed treatment is given in Appendix A. Fission track analysis of apatites is particularly useful because partial annealing of fission tracks occurs over a temperature range (60°-125°C) which coincides with that of oil generation (Gleadow *et al.*, 1983). By measuring and comparing fission track ages and

lengths in detrital apatites from sedimentary rocks, it is possible to construct an implied thermal history for the samples.

Selection of the sample localities was based on several factors including available exposures and logistics. Continuous exposures of Cretaceous and Tertiary units are limited to a few areas such as Bathrub Ridge. Field work for this study was conducted from June to September, 1987 as part of a joint field program by the ADGGS and the University of Alaska Department of Geology and Geophysics. The purpose of this continuing interagency field program is to better understand the structure, stratigraphy, and thermal history of strata in the NEBR.

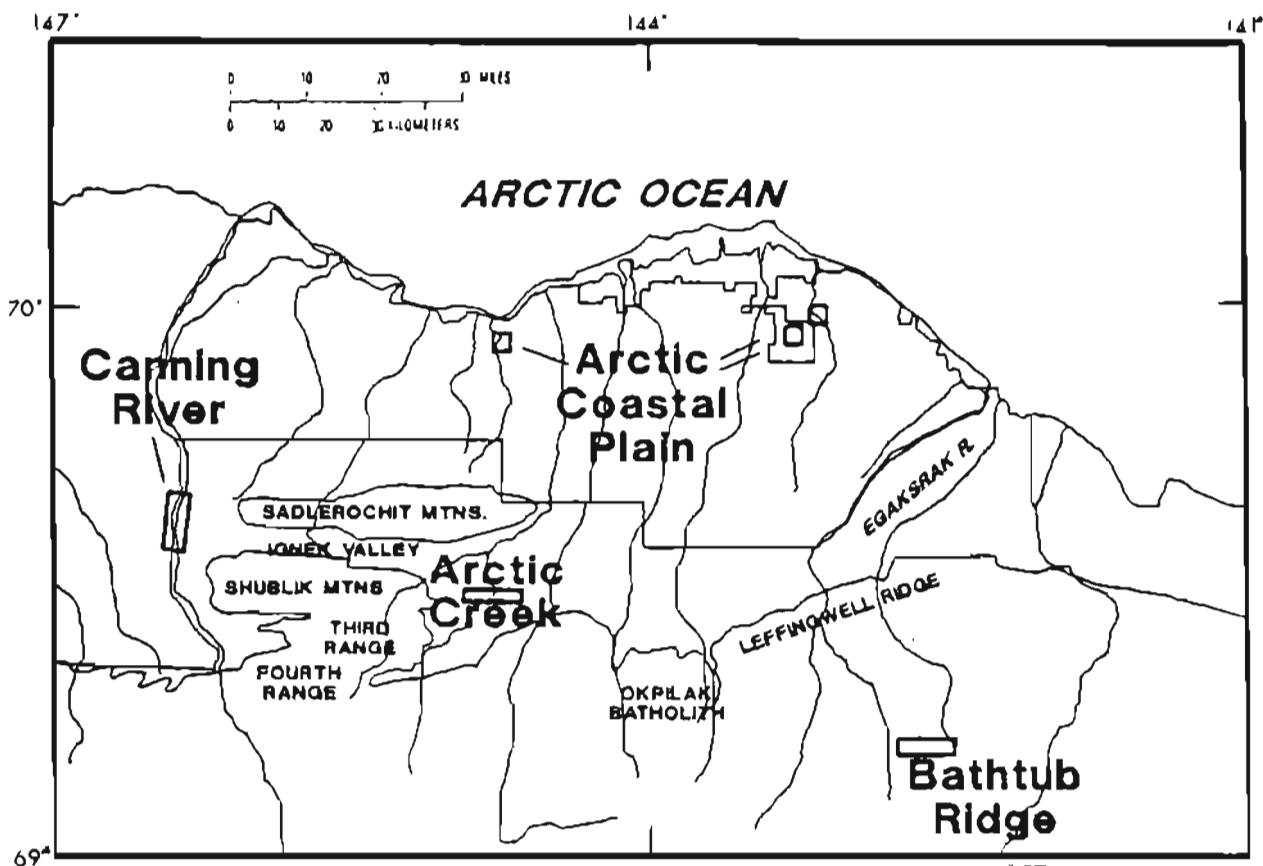


Figure 1. Regional map showing the four areas sampled. These include (1) Bathrub Ridge, (2) Arctic Creek area, (3) ANWR Coastal Plain, and (4) the Canning River area.

REGIONAL GEOLOGY

NORTH SLOPE OF ALASKA: STRATIGRAPHY

The ANWR coastal plain and North Slope of Alaska represent a combined passive continental margin and foreland basin bounded to the north by the Arctic Ocean and to the south by the Brooks Range, a Late Jurassic to Tertiary fold and thrust belt (Mull, 1982). The stratigraphy of the Brooks Range and the North Slope can be divided into three major unconformity-bounded stratigraphic sequences (Fig. 2) (Lerand, 1973; Mull, 1982; Bird and Molenaar, 1987). The Proterozoic to Middle Devonian **Franklinian** sequence, consisting of marine and nonmarine miogeoclinal and eugeoclinal sedimentary rocks (Grantz and May, 1983), documents a complex and poorly understood history culminating in a late Devonian orogenic event. The Mississippian to Lower Cretaceous **Ellesmerian** sequence was deposited on a south-facing (present coordinates) passive margin with both platformal and basinal stratigraphic components. The Lower Cretaceous and younger **Brookian** sequence consists of south-derived clastic deposits derived from erosion of the Brooks Range orogen. The stratigraphy of these sequences has been discussed in detail by many authors (e.g. Brosge and TAILLEUR, 1970; Detterman *et al.*, 1975; Palmer *et al.*, 1979; Grantz and May, 1983; Hubbard *et al.*, 1987).

NORTH SLOPE OF ALASKA: STRUCTURAL HISTORY

The North Slope has experienced a complicated structural history. Prior to the Late Devonian, the tectonic setting is highly speculative because of the fragmentary stratigraphic evidence (Bird, 1987; Hubbard *et al.*, 1987). During Late Devonian and Early Mississippian time, the Ellesmerian orogeny deformed the Franklinian rocks. Two belts of two-mica granitic intrusives, one along the core of the central Brooks Range and the other in the Romanzof Mountains, have Late Devonian (390-360 Ma) U-Pb zircon ages and are a result of this Devonian event (Sable, 1977; Dillon *et al.*, 1987). Subsequent erosion of

STRATIGRAPHIC COLUMN				
SEQUENCE	PERIOD	CENTRAL NORTH SLOPE	NORTHEASTERN BROOKS RANGE	
			SADLEROCHIT MTS	NORTHEASTERN ANWR
BROOKIAN	HOLOCENE	GUSIK FM & SURFICIAL DEPOSITS	GUSIK FM & SURFICIAL DEPOSITS	
	OLIGOCENE			
	MIOCENE			?
	PLIOCENE	SAGAANIRKTOK FM	SAGAANIRKTOK FM	
	EOCENE			
	PALEOCENE			?
				SABBATH CREEK UNIT
			CANNING FM	?
	LATE CRETACEOUS	COLVILLE GROUP		?
		NANUSHUK GP TOROK SHALE	HUE SHALE	
ELLESMERIAN	EARLY CRETACEOUS	KONGAKUT FM	PEBBLE SHALE UNIT KEMK SANDSTONE	SATYRUS GRAYWACKE & ARCTIC CREEK FACIES
				KONGAKUT FM
	JURASSIC	KINGAK SHALE	KINGAK SHALE	KINGAK SHALE
		SHUBLK FM	SHUBLK FM	SHUBLK FM
	TRIASSIC	SADLEROCHIT GROUP	SADLEROCHIT GROUP	SADLEROCHIT GROUP
	PERMIAN			
	PENNSYLVANIAN	LISBURNE GROUP	LISBURNE GROUP	LISBURNE GROUP
	MISSISSIPPIAN	ENDICOTT GROUP	ENDICOTT GROUP	ENDICOTT GROUP

Figure 2. Generalized Ellesmerian and Brookian stratigraphy for northeastern Alaska (from Vandergon, 1987).

the uplifted rocks created a major unconformity on which the Mississippian to Lower Cretaceous platform limestones and terrigenous clastic rocks of the Ellesmerian sequence were deposited. These deposits, derived from northern sources, record several transgressions and regressions in nonmarine and shallow marine environments along an east-west-trending shoreline (Hubbard *et al.*, 1987; Bird, 1987).

Rifting during the Jurassic and Early Cretaceous formed the proto-Canada Basin and caused renewed basement uplift along the east-west trending Barrow Arch (Hubbard *et al.*, 1987). The Barrow Arch is a long-lived buried basement high located approximately along the present northern shoreline of Alaska.

During Neocomian time, uplift of the rifted margin to the north resulted in a regional erosional unconformity. In the south, continental subduction and mountain building created the ancestral Brooks Range (Bird, 1987). The relationship between the rifting and the Brooks Range orogeny is unknown. This orogeny shifted the sediment source from north to south and later formed many of the structural features preserved in the area. The influx of synorogenic clastic sediment prograding northeastward into the Colville trough (the foredeep of the Brooks Range; Mull, 1985) is the first sedimentologic evidence of the Brooks Range orogen (Grantz and May, 1983).

STRUCTURE OF THE NORTHEASTERN BROOKS RANGE

Major tectonic elements of the NEBR are dominated by the Brooks Range fold-thrust belt which formed in the mid-to-Late Cretaceous (Leiggi, 1987). Rocks of the Brooks Range may be divided into several belts which trend sub-parallel to the strike of the range. The core of the range is characterized by highly deformed allochthonous rocks representing estimated crustal shortening of up to 400 km (Rattee, 1987). In comparison, parautochthonous rocks in the NEBR are relatively undeformed and represent significantly less shortening and displacement than in the core of the range (Mull, 1982; Oldow *et al.*,

1987). Most of the deformation in the core of the range ceased by earliest Tertiary time, but deformation continued episodically to the present time in the NEBR, resulting in northward progression of the deformation front and consequent uplift and exposure of the NEBR.

The mechanism for the development of the NEBR (Fig. 3), characterized by low-angle northward-directed thrust faulting (Bird, 1987) and crustal shortening, has been interpreted as a series of duplex structures (Leiggi, 1987). The key elements of a duplex system are a roof thrust, a basal detachment thrust, and a series of imbricate horses between these thrusts (e.g. Boyer and Elliot, 1982). Leiggi (1987) has described duplexing and the development of the Brooks Range in detail.

STUDY LOCATIONS

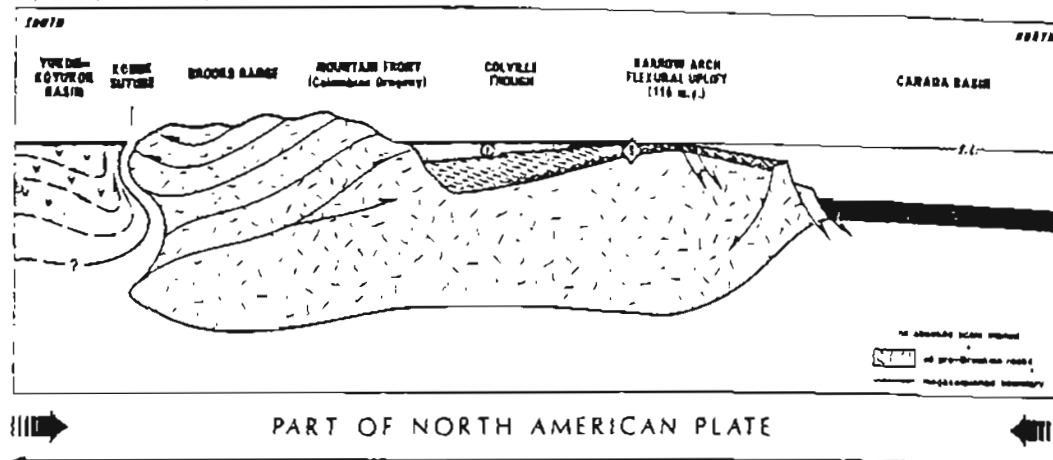
Four major areas within ANWR were selected for the purpose of separating out detrital apatites from sedimentary rocks from measured stratigraphic sections along Bathtub Ridge, Arctic Creek, and the Canning River (Fig. 1) for AFTA. Locations on Carter Creek, the Jago River, and the Niguanik River on the ANWR coastal plain were also selected for AFTA work..

Bathtub Ridge

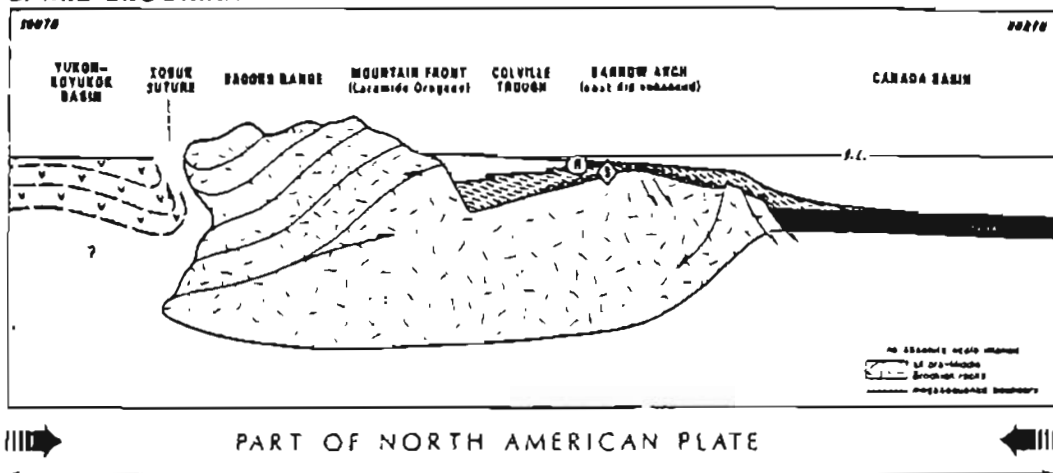
Bathtub Ridge, located near the center of the NEBR, consists of a 2600 meter section of Permian through Lower Cretaceous marine sedimentary rocks (Fig. 4). These consist of marine carbonates and sandstones (Permian to Triassic) in the lower half of the section. Black shale with local siltstone beds (Jurassic to Lower Cretaceous), manganiferous shale, interbedded shale and siltstone turbidites (Albian) and sandstone turbidites (Albian?) comprise the upper half of the section.

The Bathtub Ridge section is divided into two parts based on the relative amount of deformation in each part. The lower section is bounded at the top by the Triassic Ivishak

A) EARLY BROOKIAN



B) MID-BROOKIAN



C) LATE BROOKIAN

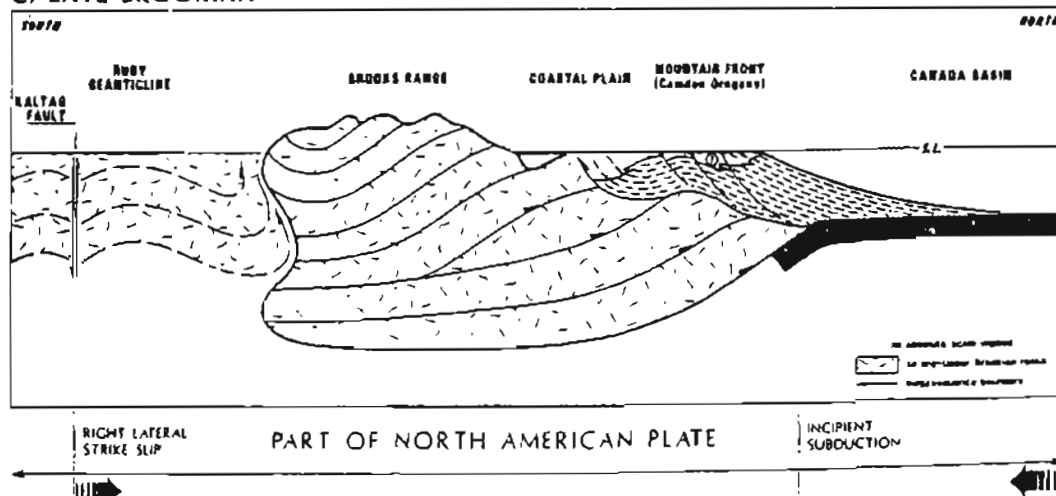


Figure 3. Regional schematic cross sections. Diagrammatic representation for the development of the Brooks Range and the Colville Trough during the Brookian orogeny. A, Early Brookian; B, Mid-Brookian; C, Late Brookian. Sediment thicknesses are diagrammatic. The 'S' symbol denotes a hydrocarbon source rock and the 'R' denotes a hydrocarbon reservoir rock (from Hubbard *et al.*, 1987).

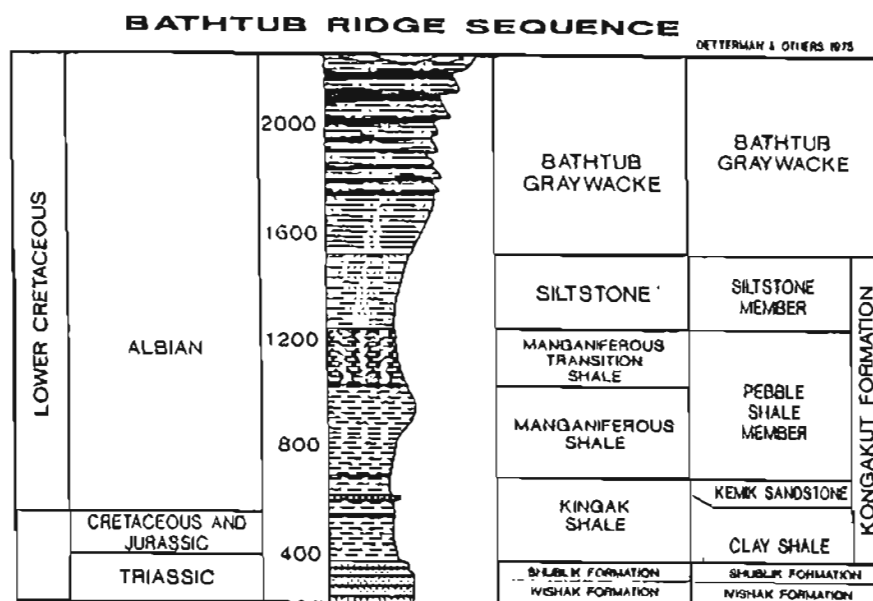


Figure 4. Stratigraphic section of the Bathtub Ridge area. Permian Echooka Formation not shown at base of Ivishak Formation (Detterman *et al.*, 1975).

Formation. The upper section comprises rocks of the Triassic Shublik Formation through the Albian Bathtub Graywacke. Rocks in the lower section are complexly folded and faulted due to compression along east-trending fold axes. Rocks in the upper section are folded into a broad open syncline. In post-Albian time the upper section was thrust over the lower section along a detachment surface at the base of the Shublik Formation. The upper section is relatively undeformed with some slight folding in the Shublik Formation whereas the lower section accommodated most of the shortening, producing tight isoclinal folds in the Ivishak Formation (Decker and O'Sullivan, unpublished data).

Arctic Creek Region

The Arctic Creek area, located approximately 85 km to the northwest of Bathtub Ridge, consists of deformed Albian turbidites and shales occurring in poorly exposed low-relief hills. The exposed sedimentary rocks (Fig. 5) include, in ascending order, Jurassic and

COMPOSITE STRATIGRAPHIC SECTION OF ARCTIC CREEK AREA


AGE	THICKNESS (m)		LITHOLOGY	BATHTUB UNITS
ALBIAN	1000m		MID-FAN FACIES TURBIDITES	BATHTUB GRAYWACKE
	1000m		OUTER FAN FACIES TURBIDITES	
	1000m		SILTSTONE TURBIDITES	SILTSTONE
LOWER CRETACEOUS			MANGANIFEROUS SHALE	MANGANIFEROUS TRANSITION AND MANGANIFEROUS SHALE
LOWER CRET. & JURASSIC			BLACK SHALE	KINGAK SHALE

Figure 5. Composite stratigraphic section of the Arctic Creek area (Decker *et al.*, 1987).

Lower Cretaceous black shale, Lower Cretaceous manganiferous shale, interbedded black shale and siltstone turbidites, and sandstone turbidites of Albian age (Decker *et al.*, 1988). These sedimentary rocks are thought to be distal equivalents of the upper half of the Bathtub Ridge section. Decker *et al.*, (1988) have proposed that the Arctic Creek and Bathtub Ridge sections were once part of a continuous depositional basin, with the Arctic Creek section having since been thrust northward into its present position.

Canning River Region

The Canning River section, located at the western end of Ignek Valley and the Sadlerochit Mountains, consists of poorly exposed, deformed Jurassic and Cretaceous marine deposits as well as Tertiary marine and non-marine deposits. The section includes the Kingak Shale (Jurassic to Neocomian), Kemik Sandstone (Hauterivian), Pebble Shale (Hauterivian-Barremian), Hue Shale (Aptian? to Santonian), turbidites of the Canning Formation (Campanian to Paleocene), and the Sagavanirktok Formation (Paleocene to Pliocene) (Fig. 6). Since the Paleocene (~50-65 Ma), the northward advancing fold and

IGNEK VALLEY SEQUENCE

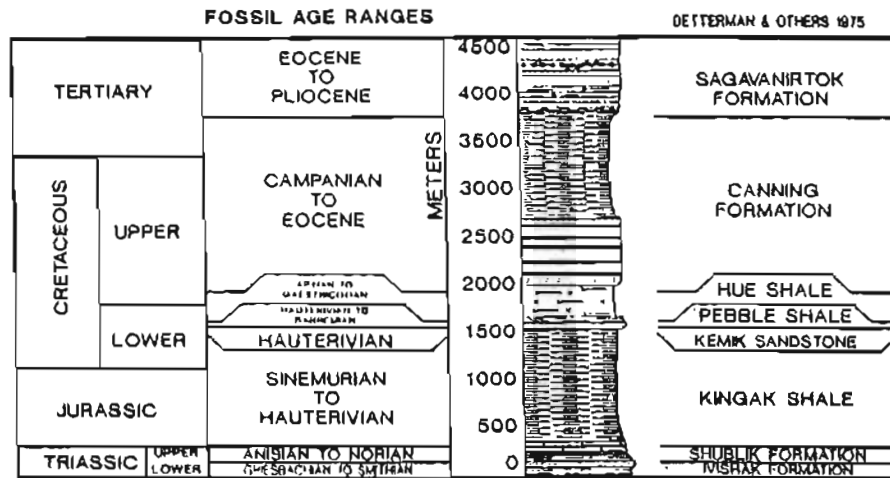


Figure 6. Stratigraphic section of the Arctic Coastal Plain and Ignek Valley (Detterman *et al.*, 1975).

thrust belt caused uplift of the Shublik and Sadlerochit Mountain ranges and deformation within the section.

ANWR Coastal Plain

Three ANWR coastal plain sections, located approximately 45 km to the north and 65 km to the northeast of Arctic Creek (Fig. 1), consist of the same sedimentary rocks and depositional environments exposed along the Canning River (Fig. 6). The stratigraphic sequence is complicated due to south-dipping imbricate faults (Bruns *et al.*, 1987). The timing of this deformation due to the northward advancement of the NEBR fold and thrust belt is post- Eocene (Bruns *et al.*, 1987).

APATITE FISSION TRACK ANALYSIS: BACKGROUND, PROCEDURES, AND METHODOLOGY

FISSION TRACKS AND FISSION TRACK TECHNIQUES

Apatite fission track analysis (AFTA) is a tool for thermal history studies and a relatively new application of fission track geochronology (Gleadow *et al.*, 1983). This section summarizes the AFTA technique and briefly reviews some applications of the technique. A more detailed presentation of the apatite fission track analysis technique is contained in Appendix A.

Fission track dating determines an *apparent* age using accumulated radiation damage caused by spontaneous nuclear fission of ^{238}U . During fission, two fast-moving, highly-charged fission fragments are shot through the crystal lattice producing regions (tracks 10-20 μm long) of crystal damage (Fleischer and Price, 1963; Fleischer *et al.*, 1975; Naeser, 1979a). These tracks are made visible by etching with a chemical solvent and can be observed with a conventional petrographic microscope.

The track density due to spontaneous fission of ^{238}U is determined by counting a statistically significant number of tracks in a given area. The observed track density is related to the length of time during which tracks have accumulated and to the ^{238}U concentration of the sample. By knowing the ^{238}U concentration of the mineral, the ^{238}U fission decay rate, and the number of fossil fission tracks which have accumulated, an age can be calculated.

The ^{238}U concentration is measured by counting fission tracks produced by induced fission of ^{235}U which takes place by bombarding the sample with thermal neutrons in a nuclear reactor. The ^{238}U concentration of the specimen is a function of the atomic ratio of $^{235}\text{U}/^{238}\text{U}$ in natural materials (7.252×10^{-3}), the observed density of induced fission tracks, the thermal neutron flux and the duration of the irradiation. The neutron flux is

determined using several flux monitors. By spacing these around samples being irradiated, the number of neutrons that pass through the samples can be determined.

Methods to measure the ^{235}U induced tracks are described by Hurford and Green (1982) and Gleadow (1981). The method used in this study registers the induced fission tracks in an external detector, such as a muscovite plate, held against the same surface in which the spontaneous tracks are counted. After neutron irradiation, the external detector is etched and the tracks caused by induced fission of ^{235}U in the specimen are counted.

FISSION TRACK LENGTHS

The stability of fission tracks is a function of temperature, time, and composition of the host phase (e.g. Naeser and Faul, 1969; Gleadow *et al.*, 1983; Green *et al.*, 1985a). Other factors such as pressure, shock, deformation, and presence of fluids have been shown to have very little to no effect compared with that of temperature (e.g. Naeser, 1979a; Gleadow *et al.*, 1983). In apatite, fission tracks that form with lengths of approximately 16 μm are stable for long periods of time at room temperature. The tracks shorten at elevated temperatures as the fission damage is repaired or *annealed*. This shortening acts to reduce or even reset the apparent age of a mineral. Shortening of tracks lengths is therefore very useful for thermal history studies, making certain minerals natural geochronothermometers.

Studies of apatite fission track annealing have shown that annealing takes place progressively over a range of temperatures (Green *et al.*, 1985a; Gleadow *et al.*, 1986a). This range is dependent on the apatite composition, in particular the Cl content. In apatite, the presence of chlorine has been shown to stabilize fission tracks to slightly higher temperatures (e.g. Green *et al.*, 1985a; Gleadow *et al.*, 1986a). Apatite grains which are most susceptible to annealing (F-rich) will give reduced ages (reflecting lower blocking temperatures) compared to grains which are more resistant to annealing (Cl-rich). The

effect of composition on apatite fission track annealing is treated in more detail in Appendix A.

The kinetics of fission track annealing in apatite have been extensively studied (Naeser and Faul, 1969; Green *et al.*, 1985a; Green *et al.*, 1986; Laslett *et al.*, 1987). Using results of Laslett *et al.*, (1987) (Fig. 7), one can predict the rate of track annealing in apatite as a function of temperature. For example at 100°C, it would take ~100 m.y. (fanning model) to 1 m.y. (parallel model) to decrease 16 μm tracks to 8 μm . In contrast at 50°C, respective times of 100 b.y. to 1 b.y. are required to achieve the same length reduction. With further work Laslett *et al.*, (1987) reported that a slightly fanning model gives the closest approximation to explain the kinetics of annealing.

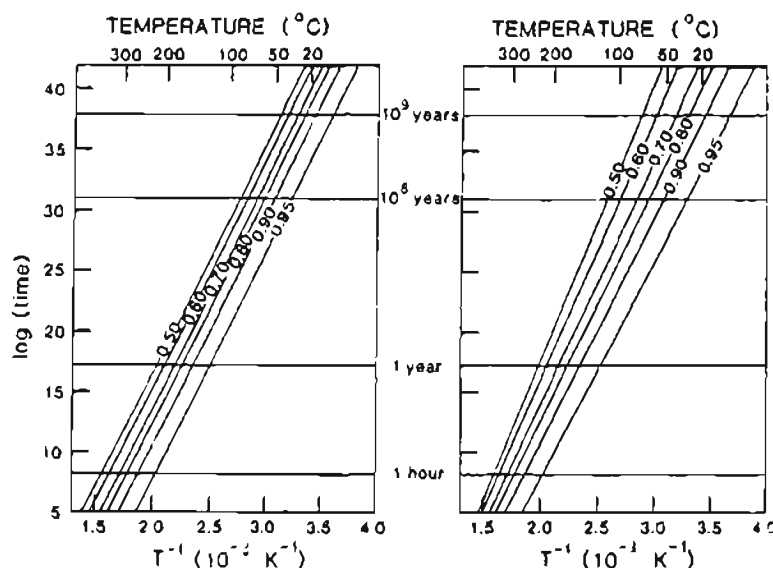


Figure 7. Comparison of parallel and fanning models to predict apatite annealing. On these Arrhenius plots, lines represent contours of predicted equal length reduction (l/l_0). In a parallel plot a single activation energy is represented throughout annealing. The fanning array has been interpreted in terms of activation energies increasing with degree of annealing. Differences between the two models are magnified by extrapolation. Plots are extrapolated from laboratory to geological time scales (from Laslett *et al.*, 1987).

The apatite fission track age is lowered during heating due to reduction of the proportion of etchable tracks by annealing. When they are formed, fission tracks in apatite

have a fairly constant mean length of about $16.3 \pm 0.9 \mu\text{m}$ (Gleadow *et al.*, 1983). Following their formation, fission tracks in apatite shorten progressively during thermal annealing. However, new tracks continuously form at approximately the initial length of $16.3 \pm 0.9 \mu\text{m}$. The distribution of track lengths in a crystal therefore reflects the integrated thermal record of its host rock. The shorter tracks have experienced higher temperatures ($>60^\circ\text{C}$ for millions of years) whereas long tracks ($13\text{-}16 \mu\text{m}$) have not experienced temperatures greater than $\sim 20\text{-}40^\circ\text{C}$ for significant lengths of time ($>1\text{-}5 \text{ m.y.}$) (Green, 1986).

THERMAL HISTORIES FROM APATITE FISSION TRACK ANALYSIS

The AFTA method was recently developed by researchers at the University of Melbourne (Gleadow and Duddy, 1981; Gleadow and Duddy, 1984; Gleadow *et al.*, 1983; Gleadow *et al.*, 1986b; and Green *et al.*, 1985b). This thermal history technique is based on the shortening of fission tracks as a function of temperature and time. Unlike other paleotemperature and maturation indicators (e.g. vitrinite reflectance and conodont alteration) which give only a single cumulative result to represent the entire thermal history, the fission track method can give information on paleotemperatures and their variation through time (Gleadow *et al.*, 1983).

With increasing temperature and time, fission tracks in apatite begin to anneal. Three temperature zones are distinguished for fission tracks in apatite (for times of the order of $1\text{-}10 \text{ m. y.}$): (a) the *annealing zone* ($>125^\circ\text{C}$) where fission tracks are totally annealed; (b) the *partial stability zone* ($60\text{-}125^\circ\text{C}$) where partial annealing occurs; and (c) the *zone of very slow annealing* ($<60^\circ\text{C}$) where very slight, slow annealing occurs. Several possible patterns of track lengths in apatites arising from distinct thermal histories are shown in Figure 8 (after Gleadow *et al.*, 1983). This figure shows a number of hypothetical temperature vs. time plots and the resulting track-length distributions. Examples A-C show

simple burial histories giving unimodal apatite length patterns with varying degrees of broadening due to varying periods of time with increasing temperatures in the partial stability zone. Examples D-F show the bimodal length distribution resulting from a past thermal event, the skewed distribution typical of slow cooling through the partial stability zone, and the entirely shortened unimodal distribution produced by a recent temperature increase.

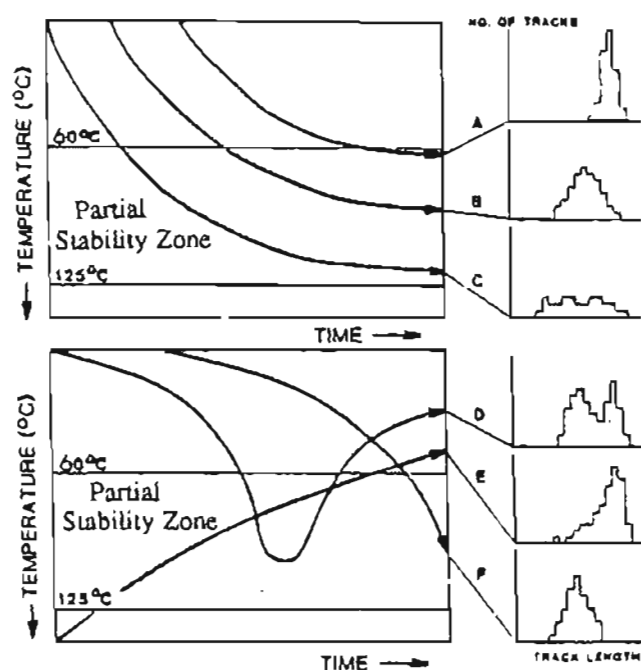


Figure 8. Idealized time-temperature paths with the resultant apatite track length distributions. See text for explanation (modified Gleadow *et al.*, 1983). The 60°C value for the upper boundary of the partial annealing zone is based on the work of Wagner *et al.*, 1977.

Bimodal distributions consist of two major length components: those that were annealed during a heating event and those that have formed since cooling to lower temperatures. By statistically separating the two components and estimating the contribution of the later group to the age of the mineral, the timing of the thermal event can be estimated. Skewed distributions are essentially the summation of the three length

distributions shown in the simple burial examples A-C. The shortened distribution resulting from a recent temperature increase is produced when all previously formed tracks are shortened together.

Green *et al.* (1985a, 1986) show that annealing occurs even at ambient surface temperatures and that as soon as a fission track is formed, it is in an "annealing environment." The annealing rate at different temperatures varies with time; at surface temperatures it is very slow and at temperatures above the zone of partial stability ($>125^{\circ}\text{C}$) it is essentially instantaneous. Therefore, the concept of a discrete apatite partial stability zone, although not strictly valid because of the linear Arrhenius relationship, is a useful concept and refers to a zone of "accelerated annealing" above the base of the partial stability zone (Green *et al.*, 1985a).

In rapidly cooled rocks (such as volcanics or those from rapidly uplifted terrains which have not been heated appreciably subsequent to their original cooling to $<20^{\circ}\text{C}$) the fission track length distributions are characteristically narrow (s.d. from 0.8 to 1.3 μm) with mean track lengths between ~ 14.0 and $15.7 \mu\text{m}$ (Fig. 9) (Gleadow *et al.*, 1986b). Therefore the majority of tracks in these samples have been subject only to low temperatures (less than $\sim 50^{\circ}\text{C}$) (Gleadow *et al.*, 1986b). Therefore one would expect apatites that experienced rapid cooling or uplift and erosion to low temperatures ($< 50^{\circ}\text{C}$) from high temperatures above the partial stability zone ($\geq 125^{\circ}\text{C}$) to have these *volcanic-type* length distributions (Gleadow *et al.*, 1986b). Slower rates of uplift and erosion would result in broadening of the length distributions and increasing the s.d. of the length histograms (see Appendix A).

TECTONIC STUDIES

Apatite fission track ages and track lengths can be used to study the thermal and uplift and erosion history of mountain ranges. For a simple cooling history, the fission track age represents the time that the sample cools below its effective closure temperature. In apatite

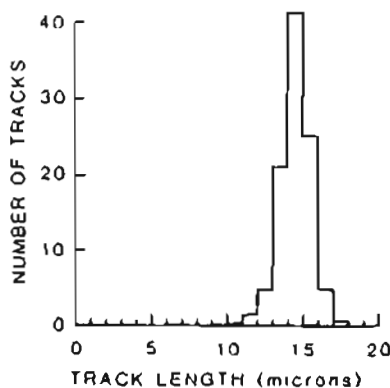


Figure 9. Typical length distribution of confined tracks in rapidly cooled samples (volcanics and related apatites). The distribution is characterized by mean track length values between ~ 14.1 and $15.7 \mu\text{m}$ and small standard deviations < 1.3 (from Gleadow *et al.*, 1986b).

this is equivalent to the time at which half the number of tracks become stable, and varies with the cooling rate (Wagner *et al.*, 1977). Therefore fission tracks in apatites from a thick sequence of rocks may record different times when parts of the sequence cooled through the effective apatite closure temperature. By estimating paleogeothermal gradient, the rate of uplift and denudation can be constrained for the sequence (e.g. Dodge and Naeser, 1968; Zeitler, 1985).

Fission track ages in apatite have been previously applied in many studies to constrain the cooling histories and uplift rates in the Himalayas (Zeitler *et al.*, 1982; Zeitler, 1985), the Alps (Wagner *et al.*, 1977), the western United States (Naeser, 1979b; Naeser *et al.*, 1983), the northern Appalachians (Miller and Lakatos, 1983), western British Columbia (Harrison *et al.*, 1979), and Antarctica (Gleadow and Fitzgerald, 1984; Gleadow and Fitzgerald, 1987). Three different approaches, all of which assume constant geothermal gradients with time have been utilized:

(1) The gradient of apatite fission track age plotted against sample elevation is taken to be the apparent *uplift rate* over the period given by the apatite ages (Fig. 10), (e.g. Wagner *et al.*, 1977; Gleadow and Fitzgerald, 1984).

(2) Extrapolation of an apatite fission track age from the sample elevation to its estimated depth of zero age gives an integrated uplift rate. This method requires assumed values for geothermal gradient and blocking temperature (e.g. Wagner *et al.*, 1977; Miller and Lakatos, 1983).

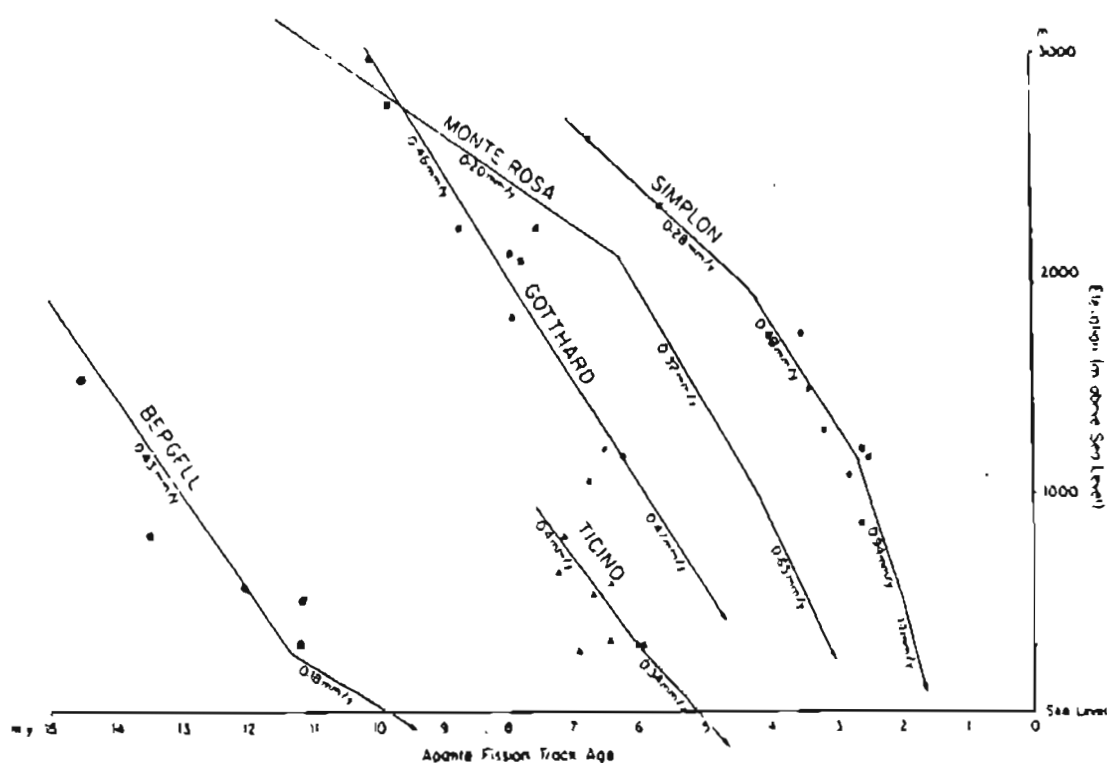


Figure 10. Apatite fission track ages plotted against sample elevation for different regions in the Alps. Paleo-uplift rates for the various regions were calculated from the slope of the various profiles. These profiles were all extrapolated to a zero age at depth calculated using an assumed geothermal gradient of $30^{\circ}\text{C}/\text{km}$ and a closure temperature of 120°C (from Wagner *et al.*, 1977).

(3) Dating different minerals with different blocking temperatures in different isotopic systems (e.g. Harrison *et al.*, 1979; Zeitler *et al.*, 1982) gives a cooling rate during the intervening temperature interval (Fig. 11). An uplift rate can be determined from this by

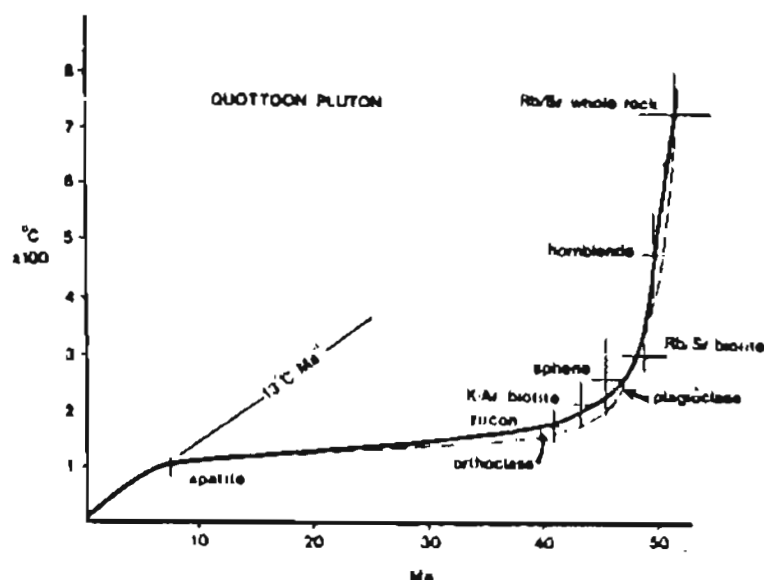


Figure 11. Cooling history of a sample from the Quotatoon pluton, British Columbia. Individual K-Ar, Rb-Sr, and fission track mineral dates are plotted against closure temperatures for each mineral and dating method used (from Harrison *et al.*, 1979).

dividing the cooling rate by the geothermal gradient. Alternatively, if ages of different minerals are available for different elevations in a given section, the uplift rate and the geothermal gradient can be estimated.

APATITE FISSION TRACK METHODS

This section briefly describes the 42 analyzed samples and summarizes the methods used to prepare these samples prior to counting and measuring fission track lengths. A more detailed discussion is contained in Appendix B.

Sample Descriptions and Sampling Details

The 42 analyzed samples are from clastic sedimentary rocks. The rocks, ranging in grain-size from siltstone to coarse-pebble conglomerate, are predominantly sandstones. These sandstones are lithic-rich with the majority of the framework grains being quartz and rock fragments. The lithics are predominantly sedimentary fragments and include chert, siltstone, mudstone, and shale. Metasedimentary and volcanic lithic fragments are present in some sandstones. The remaining components are feldspars, matrix, cements, and heavy

minerals. The predominant cement in most samples is calcite but some samples from Bathtub Ridge contain silica cement.

Eighteen siltstone to conglomerate samples are from Bathtub Ridge at the southern part of the NEBR. There 2600 m of Permian to Lower Cretaceous marine sedimentary rocks are exposed in a weakly deformed section. These samples are from various elevations (measured with an altimeter) along three main traverses designed to cover the largest possible vertical and stratigraphic intervals. Seven sandstone samples are from the Arctic Creek exposures located 85 km to the northwest. The Arctic Creek section consists of Upper Jurassic to Lower Cretaceous marine deposits. The seven samples were randomly collected from the Albian turbidites present at the top of the section due to poor outcrop control. Eight samples on the ANWR coastal plain are from Upper Cretaceous to Eocene sedimentary rocks. Very poor outcrop limited sampling to 5 locations with formations of different ages. Nine samples are from a continuous section of lower Cretaceous to Paleocene, marine to non-marine sedimentary rocks along the Canning River. Though the extent of the outcrop was relatively poor, all possible locations were sampled to cover the widest possible stratigraphic interval.

Sample Preparation and Processing

Apatites were separated from the outcrop samples by conventional heavy liquid and magnetic techniques. The mineral separates were mounted in epoxy resin on glass slides, ground and polished to expose internal surfaces of the grains, then etched to reveal the fossil tracks. Fission track ages were measured by the external detector method (EDM) described by Green (1986) using a special low-uranium muscovite (<5 ppb) to record induced tracks. The apatite mounts were etched in 5 mol HNO₃ for 20 seconds at 20°C to reveal the fossil tracks. The mica detectors were etched for 20 minutes in 40% HF at 20°C.

Neutron irradiations were carried out in a well thermalized flux in the Australian Atomic Energy Commission HIFAR reactor in Sydney. Thermal neutron fluences were monitored by counting tracks recorded in muscovite detectors attached to pieces of the NBS standard glass SRM612 (50 ppm U). Up to 15 grain/mica pairs were included in each irradiation cannister along with two glass/mica dosimeters, one at each end, to monitor any flux gradients present along the cannister. For a more detailed description of the sample preparation, see Appendix B.

Fission Track Age Calculations

Fission track densities were measured in the laboratories of the Department of Geology at Melbourne University, Melbourne, Australia. Ages were calculated using the standard fission track equation (Hurford and Green, 1982). Errors were calculated using the technique outlined by Green (1981). All errors are quoted as ± 2 sigma. A zeta calibration factor (Hurford and Green, 1982; Green, 1985) of 352.7 (see Table A1) was determined empirically by direct comparison with apatite age standards with independently known ages. The zeta calibration allows the reported fission track ages to be independent of uncertainties in the ^{238}U fission decay constant.

Fission tracks in each mount were counted in transmitted light using a dry 80x objective at a total magnification of 1250x. Approximately 20 grains were counted from each sample, depending on the number of suitable grains available, the available counting area per grain, and the spontaneous and induced track densities. The combined age for all grains counted was calculated for each sample from the pooled track counts.

Track Length Measurements

Only confined spontaneous track lengths were measured. Confined tracks are those that do not intersect the polished surface but have been etched due to contact with other tracks or fractures which intersect the exposed surface (see Fig. A7). Only fully etched and

horizontal confined tracks were measured in grains aligned parallel to the crystallographic c-axis. These give the closest representation of the true length distribution of confined tracks (Laslett *et al.*, 1984). A track is considered horizontal if it displays a uniform bright image under reflected light, or if it remains in sharp focus along its entire length when viewed with transmitted light. Such tracks were located by scanning systematically across the apatite mount using a 40x dry objective. Measurements were made with an 80x dry objective at a total magnification of 1250x. The lengths of suitable tracks were measured on a Hipad™ digitizing tablet calibrated using a stage micrometer. As many tracks as possible (up to 100) were measured from each sample. In most cases less than 100 tracks were recorded due to a scarcity of apatite grains, low U concentrations, and/or young ages for the samples.

FISSION TRACK RESULTS AND INTERPRETATIONS

RESULTS

Fission track age analytical results for 41 of the 42 samples are given in Table 1. One sample was undateable due to poor contact between the mica detector and the grain mount. The correlation coefficient for spontaneous and induced track pairs is included as a guide to the dispersion of single-grain ages, although its limitations for this purpose have been noted by Gleadow and Brooks (1979). Track length measurements were made on all 42 samples (Table 2). Sample locations, age data, and track length histograms are given in Appendix C. Fluorine and Chlorine contents of apatites from twelve samples from the four study areas are presented in Table 3.

Bathtub Ridge

The eighteen samples from Bathtub Ridge give apatite fission track ages which range from 49 ± 10 to 74 ± 15 Ma (2σ errors). The mean value for all 18 concordant ages is 61.8 Ma (Fig. 12). The samples collected along the stratigraphic section can be divided into two distinct groups based on measured track lengths: samples from the Permian to Upper Triassic section underlying the Shublik Formation (lower group), and those from the Upper Triassic to Albian section including and overlying the Shublik Formation (upper group) (Fig. 13). The twelve samples from the upper group possess mean track lengths ranging from 13.4 to 15.5 μm with s.d. between 0.6 and 2.6 μm (Table 2). Eleven of the twelve samples have mean lengths greater than 14 μm . The mean track length of these twelve samples is 14.7 μm with a s.d. of 1.3 μm . The typical shape of the track length distribution (see Appendix C for track length distributions) derived from these samples is an undisturbed volcanic-type distribution (defined by Gleadow *et al.*, 1986b) and discussed

Table 1 Analytical Data For Fission Track Age Determinations*

Sample number	Number of grains	Standard track density ($\times 10^6 \text{cm}^{-2}$)	Fossil track density ($\times 10^6 \text{cm}^{-2}$)	Induced track density ($\times 10^6 \text{cm}^{-2}$)	Correlation coefficient	Age (Ma \pm 2 σ)	Uranium content (ppm)
<i>Bathtub Ridge</i>							
POS106A	20	1.450 (5755)	0.464 (113)	1.843 (449)	0.961	64.0 \pm 13.6	17
POS104B	20	1.450 (5755)	0.265 (78)	1.059 (312)	0.928	63.6 \pm 16.2	10
POS103B	20	1.450 (5755)	0.402 (124)	1.381 (426)	0.935	74.0 \pm 15.2	13
POS102A	20	1.450 (5755)	0.424 (105)	1.691 (419)	0.955	63.8 \pm 14.0	15
POS97A	20	1.381 (5480)	0.338 (109)	1.182 (381)	0.948	69.3 \pm 15.2	11
POS86A	20	1.376 (5461)	0.420 (228)	1.815 (985)	0.954	55.9 \pm 8.4	17
JD78A	8	1.349 (5354)	0.436 (43)	1.774 (175)	0.966	58.2 \pm 19.8	17
POS96A	20	1.381 (5480)	0.250 (89)	0.940 (335)	0.929	64.4 \pm 15.4	9
POS90A	20	1.381 (5480)	0.440 (89)	1.710 (346)	0.859	62.3 \pm 15.0	16
POS88A	7	1.376 (5461)	0.659 (65)	2.970 (293)	0.999	53.6 \pm 14.8	29
POS111A	20	1.381 (5480)	0.446 (75)	1.796 (302)	0.729	60.2 \pm 15.6	17
POS76A	20	1.381 (5480)	0.587 (110)	2.900 (543)	0.917	49.1 \pm 10.4	28
POS117A	16	1.450 (5755)	0.375 (37)	1.318 (130)	0.742	72.4 \pm 27.0	12
JD87A	7	1.349 (5354)	0.144 (17)	0.560 (66)	0.746	81.0 \pm 33.2	6
POS115A	12	1.450 (5755)	0.299 (22)	1.238 (91)	0.919	61.5 \pm 29.2	11
POS99A	20	1.381 (5480)	0.265 (45)	1.058 (180)	0.693	60.6 \pm 20.2	10
POS98A	17	1.376 (5461)	0.120 (25)	0.481 (100)	0.713	60.4 \pm 27.0	5
POS113A	9	1.450 (5755)	0.432 (47)	1.876 (204)	0.865	58.6 \pm 19.0	17

Table 1 (continued). Analytical Data For Fission Track Age Determinations

Sample number	Number of grains	Standard track density ($\times 10^6 \text{cm}^{-2}$)	Fossil track density ($\times 10^6 \text{cm}^{-2}$)	Induced track density ($\times 10^6 \text{cm}^{-2}$)	Correlation coefficient	Age (Ma \pm 2 σ)	Uranium content (ppm)
<i>Arctic Creek</i>							
POS55A	20	1.450 (5755)	0.226 (35)	1.574 (244)	0.823	36.6 \pm 13.2	14
POS63 1/2	20	1.381 (5480)	0.118 (34)	0.775 (224)	0.839	36.9 \pm 13.6	7
JD15A	20	1.376 (5461)	0.144 (52)	0.899 (325)	0.976	38.7 \pm 11.6	9
JD17A	20	1.376 (5461)	0.173 (82)	1.181 (560)	0.982	35.4 \pm 8.4	11
JD26A	20	1.376 (5461)	0.125 (80)	0.995 (636)	0.918	30.5 \pm 7.2	10
JD27A	20	1.349 (5354)	0.078 (38)	0.492 (238)	0.933	37.9 \pm 13.2	5
JD38B	11	1.349 (5354) (5354)	0.238 (34) (94)	1.420 (203) (244)	0.996	39.7 \pm 14.8	14
<i>Canning River</i>							
(A)							
POS22B	21	1.376 (5461)	0.421 (132)	1.517 (476)	0.953	66.9 \pm 13.2	15
(B)							
POS24B	23	1.376 (5461)	0.461 (235)	2.371 (1208)	0.871	45.8 \pm 24.0 *	23
POS16A	20	1.376 (5461)	0.168 (71)	1.007 (426)	0.927	40.3 \pm 10.4	10
POS14B	20	1.376 (5461)	0.138 (62)	0.708 (317)	0.894	47.3 \pm 13.2	7
POS35A	25	1.381 (5480)	0.266 (122)	1.379 (632)	0.928	46.8 \pm 9.4	13
(C)							
POS10A	20	1.376 (5461)	0.217 (105)	1.481 (717)	0.863	35.4 \pm 7.4	14
POS08A	20	1.376 (5461)	0.133 (71)	1.066 (569)	0.918	30.2 \pm 7.6	10
JD03B	16	1.450 (5755)	0.412 (112)	2.619 (712)	0.924	32.0 \pm 11.8 #24	
POS07A	15	1.450 (5755)	0.238 (29)	2.011 (245)	0.864	30.2 \pm 11.8	18

Table 1 (continued). Analytical Data For Fission Track Age Determinations

Sample number	Number of grains	Standard track density ($\times 10^6 \text{cm}^{-2}$)	Fossil track density ($\times 10^6 \text{cm}^{-2}$)	Induced track density ($\times 10^6 \text{cm}^{-2}$)	Correlation coefficient	Age (Ma \pm 2 σ)	Uranium content (ppm)
<i>ANWR Coastal Plain</i>							
POS74A	20	1.450 (5755)	0.132 (30)	0.462 (105)	0.925	72.7 \pm 30.2	4
POS74B	20	1.381 (5480)	0.151 (48)	0.514 (163)	0.590	71.3 \pm 23.6	5
POS75A	-	-	-	-	-	-	-
POS67A	20	1.381 (5480)	0.438 (171)	1.347 (526)	0.908	78.7 \pm 14.0	13
POS68A	20	1.381 (5480)	0.263 (75)	0.709 (202)	0.938	89.8 \pm 24.4	7
POS69A	20	1.376 (5461)	0.341 (119)	0.781 (273)	0.831	104.9 \pm 23.2	8
POS64A	10	1.381 (5480)	0.331 (31)	1.378 (129)	0.907	58.3 \pm 23.4	13
JD49A	20	1.349	0.179	0.465	0.267	91.0 \pm 22.2	5

*Number of tracks counted are shown in parenthesis. Standard and induced track densities are measured on mica external detector surfaces. Fossil track densities are measured on internal mineral surfaces. Ages are calculated using Zeta = 352.7 for dosimeter glass SRM612. # Mean age, used where pooled data fail χ^2 test at 5%. Results for each area except Arctic Creek are given in stratigraphic order starting from top to bottom. No stratigraphic control is available for Arctic Creek samples.

Table 2. Fission track length data*

Sample Number	Age ($\pm 2\sigma$) (Ma)	Track Length ($\pm 1\sigma$) (μm)	Standard Deviation (μm)	Number of tracks
<i>Bathtub Ridge</i>				
POS106A	64.0 \pm 13.6	14.52 \pm 0.39	2.58	44
POS104B	63.6 \pm 16.2	15.07 \pm 0.17	1.38	69
POS103B	74.0 \pm 15.2	14.96 \pm 0.09	0.91	102
POS102A	63.8 \pm 14.0	15.21 \pm 0.12	0.97	67
POS97A	69.3 \pm 15.2	15.12 \pm 0.11	1.10	100
POS86A	55.9 \pm 8.4	15.05 \pm 0.09	0.82	81
JD78A	58.2 \pm 19.8	15.51 \pm 0.20	0.64	10
POS96A	64.4 \pm 15.4	14.94 \pm 0.13	1.05	67
POS90A	62.3 \pm 15.0	14.06 \pm 0.16	1.47	84
POS88A	53.6 \pm 14.8	13.39 \pm 0.24	1.00	18
POS111A	60.2 \pm 15.6	14.29 \pm 0.17	1.71	104
POS76A	49.1 \pm 10.4	14.04 \pm 0.24	2.10	80
POS117A	72.4 \pm 27.0	12.87 \pm 0.35	1.89	29
JD87A	61.0 \pm 33.2	13.92 \pm 0.33	0.88	7
POS115A	61.5 \pm 29.2	12.96 \pm 0.34	1.70	25
POS98A	60.4 \pm 27.0	10.95 \pm 1.66	4.40	7
POS99A	60.6 \pm 20.2	14.06 \pm 0.32	1.45	21
POS113A	58.6 \pm 19.0	14.26 \pm 0.39	1.64	18
<i>Arctic Creek</i>				
POS55A	36.6 \pm 13.2	14.06 \pm 0.46	2.10	21
POS63 1/2	36.9 \pm 13.6	14.00 \pm 0.19	1.71	81
JD15A	38.7 \pm 11.6	14.03 \pm 0.16	1.29	61
JD17A	35.4 \pm 8.4	14.02 \pm 0.19	1.55	69
JD26A	30.5 \pm 7.2	14.20 \pm 0.20	1.73	76
JD27A	37.9 \pm 13.2	14.24 \pm 0.18	1.55	75
JD38B	39.7 \pm 14.8	14.48 \pm 0.15	1.31	74

Table 2. Fission track length data (continued)

Sample Number	Age ($\pm 2\sigma$) (Ma)	Track Length ($\pm 1\sigma$) (μm)	Standard Deviation (μm)	Number of tracks
<i>Canning River</i>				
(A)				
POS22B	66.9 ± 13.2	14.47 ± 0.21	1.41	45
(B)				
POS24B	45.8 ± 24.0	14.17 ± 0.32	1.11	12
POS16A	40.3 ± 10.4	14.05 ± 0.23	1.19	28
POS14B	47.3 ± 13.2	13.45 ± 0.21	1.32	41
POS35A	46.8 ± 9.4	12.73 ± 0.20	1.50	57
(C)				
POS10A	35.4 ± 7.4	12.66 ± 0.28	1.75	40
POS08A	30.2 ± 7.6	12.29 ± 0.25	1.81	52
JD03B	32.0 ± 11.8	12.58 ± 0.25	1.37	31
POS07A	30.2 ± 11.8	11.59 ± 0.25	0.72	8
<i>ANWR Coastal Plain</i>				
POS74A	72.7 ± 30.2	14.96 ± 0.18	0.98	31
POS74B	71.3 ± 23.6	14.66 ± 0.27	1.55	32
POS75A	-	14.63 ± 0.21	1.24	35
POS67A	78.7 ± 14.0	14.60 ± 0.12	1.22	107
POS68A	89.8 ± 24.4	13.65 ± 0.29	2.04	50
POS69A	104.9 ± 11.6	13.90 ± 0.17	1.69	100
POS64A	58.3 ± 23.4	14.30 ± 0.36	1.07	9
JD49A	91.0 ± 22.2	14.77 ± 0.21	2.09	101

*Results for each area except Arctic Creek are given in stratigraphic order starting from top to bottom. No stratigraphic control is available for Arctic Creek samples.

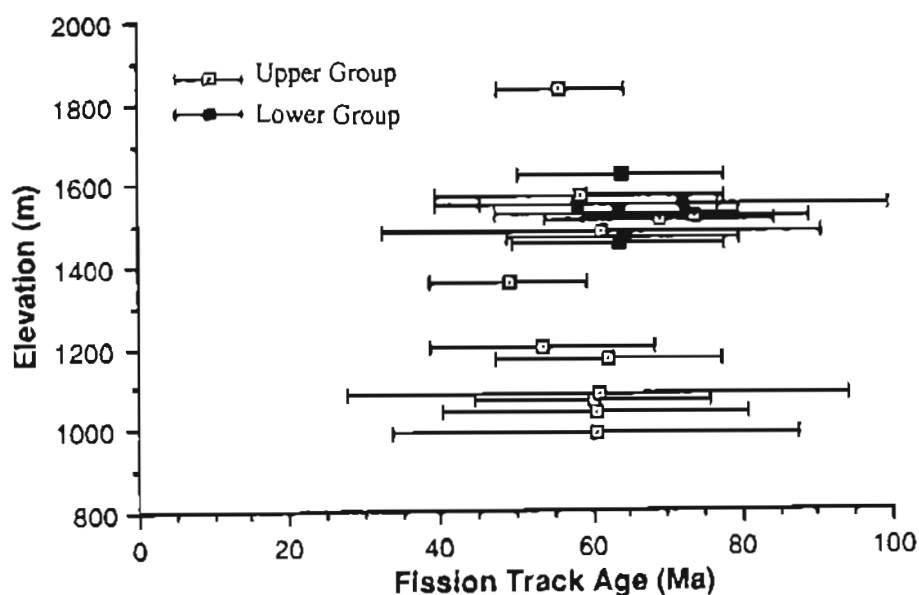


Figure 12. Plot of fission track age vs. elevation for samples collected from Bathtub Ridge. Mean age for 18 samples is ~62 Ma. ± 2 sigma error bars are shown.

BATHTUB RIDGE SECTION

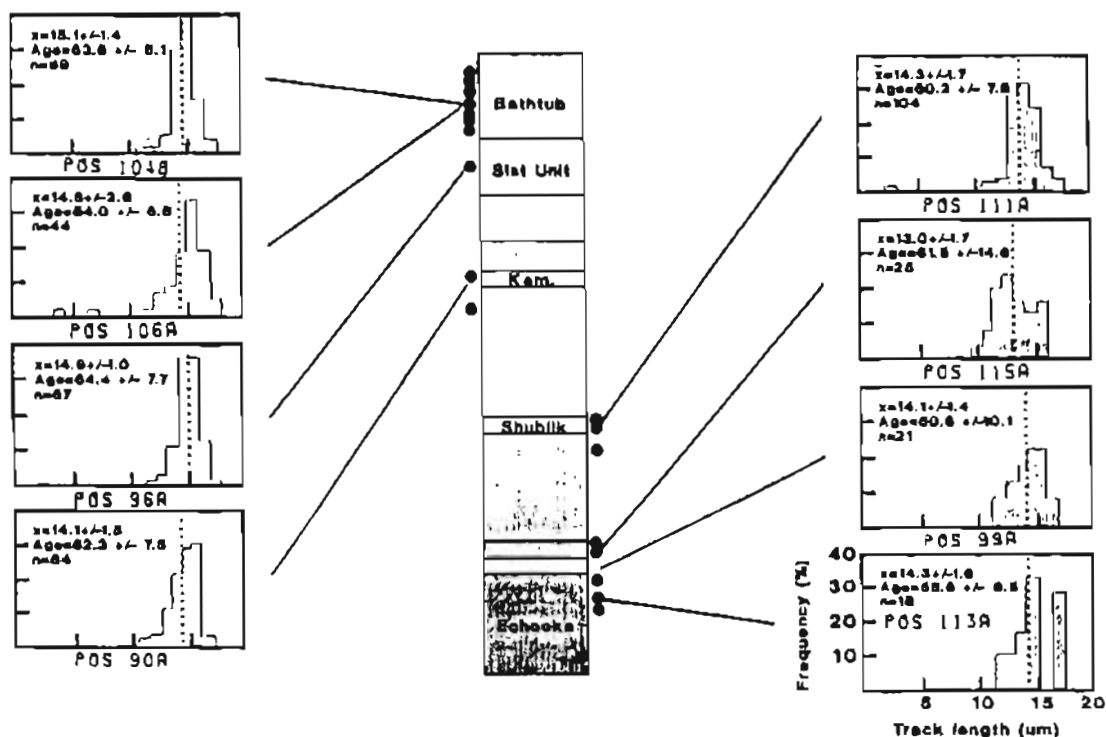


Figure 13. Apatite fission track data from representative samples collected from Bathtub Ridge. Each plot shows track length vs. frequency, mean track length, age (± 1 sigma) and number of tracks measured. Dots represent sample positions.

on page 30. The six samples from the lower group have mean track lengths ranging from 11.0 to 14.3 μm and s.d. between 0.9 and 4.4 μm . The mean track length of these six samples is 13.2 μm with a s.d. of 2.0 μm (Table 2). The shape of these length distributions is typical of a "mixed" distribution, characteristic of a partial thermal overprint (see Appendix A, p. 101).

Arctic Creek Region

The seven samples from the Albian turbidites located at the upper part of the Arctic Creek section possess apatite fission track ages ranging from 31 ± 7 to 40 ± 15 Ma. The mean of the apparent ages for all seven samples is 36.5 Ma (Table 1, Fig. 14). Mean track lengths are all long (between 14 and 15 μm) with s.d. between 1.0 and 2.0 μm (Table 2, Fig. 15). The track length distribution for each of the seven samples is typical of a volcanic-type distribution but with a slight variation. In all but one case there is a distinct tail of short tracks (lengths $< 10 \mu\text{m}$) in each distribution. This tail of short tracks contains less than 4% of the total number of tracks.

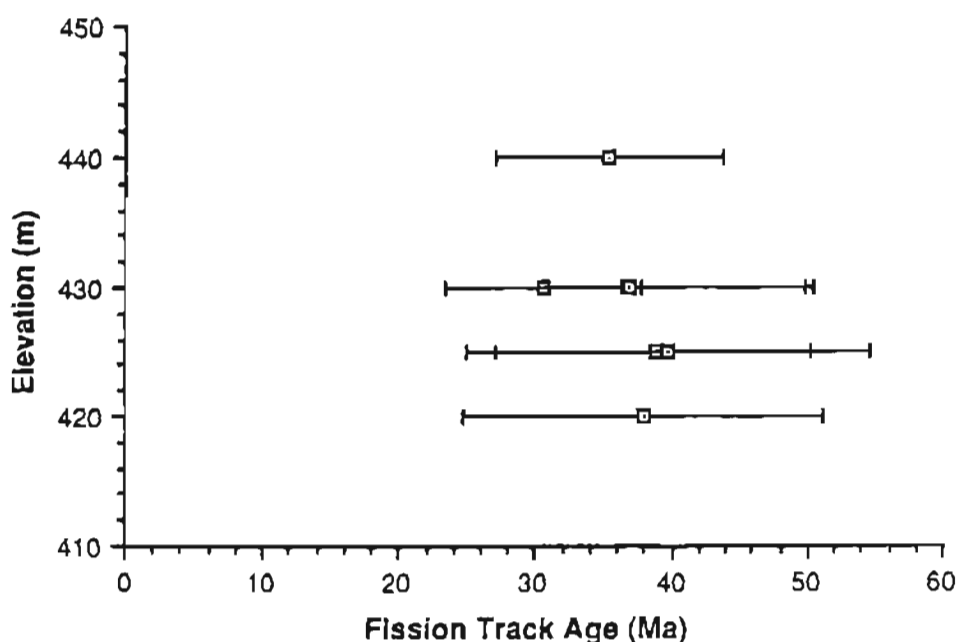


Figure 14. Plot of fission track age vs. elevation for samples collected from the Arctic Creek exposures. Mean age for 7 samples is 36.5 Ma. ± 2 sigma error bars shown.

ARCTIC CREEK REGION

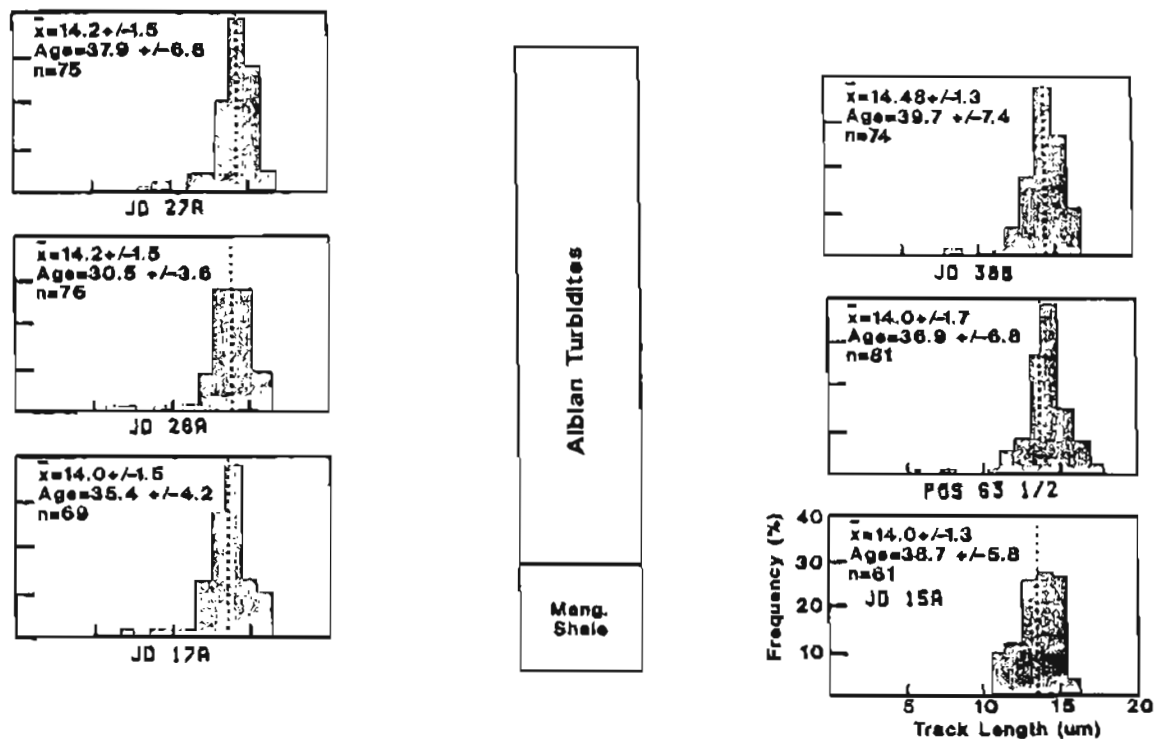


Figure 15. Apatite fission track data from representative samples collected from the Arctic Creek exposures. Each plot shows track length vs. frequency, mean track length, age (± 1 sigma) and number of tracks measured. Sample localities cannot be shown on stratigraphic column due to poor outcrop control.

Canning River Region

The nine samples from the Lower Cretaceous to Paleocene Canning River section possess apatite fission track ages from 67 ± 13 Ma at the top of the section to 30 ± 12 Ma at the base (Table 1, Fig. 16). These data can be divided into three units (Fig. 17): (A) the single sample at the top of the section with an age of ~ 67 Ma, (B) the 4 samples in the upper part of the section with concordant ages between 40 ± 10 and 47 ± 13 Ma (mean age ~ 45 Ma), and (C) the 4 samples near the base of the section with concordant ages between 30 ± 12 and 35 ± 7 Ma (mean age ~ 32 Ma). Mean track lengths decrease from $14.5 \mu\text{m}$ for sample A, to $13.6 \mu\text{m}$ for group B, to $12.3 \mu\text{m}$ for group C. The track length distribution for sample A is a volcanic-type with long mean lengths ($>14 \mu\text{m}$). Track length distributions for group B are volcanic-type at the top but become mixed (Gleadow *et al.*,

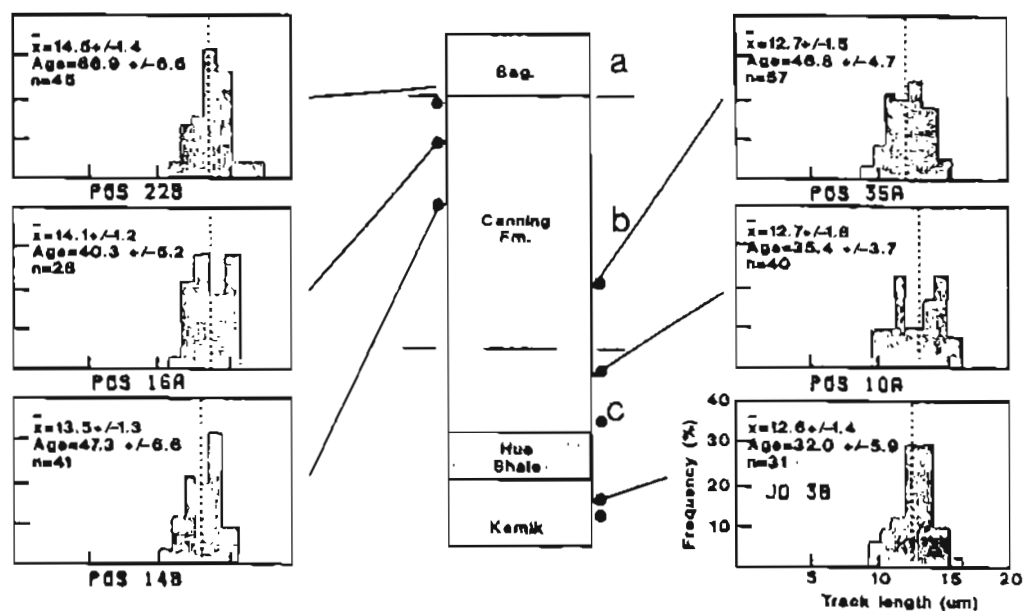


Figure 16. Apatite fission track data from representative samples collected from the Canning River section. Each plot shows track length vs. frequency, mean track length, age (± 1 sigma) and number of tracks measured. Dots represent relative sample positions.

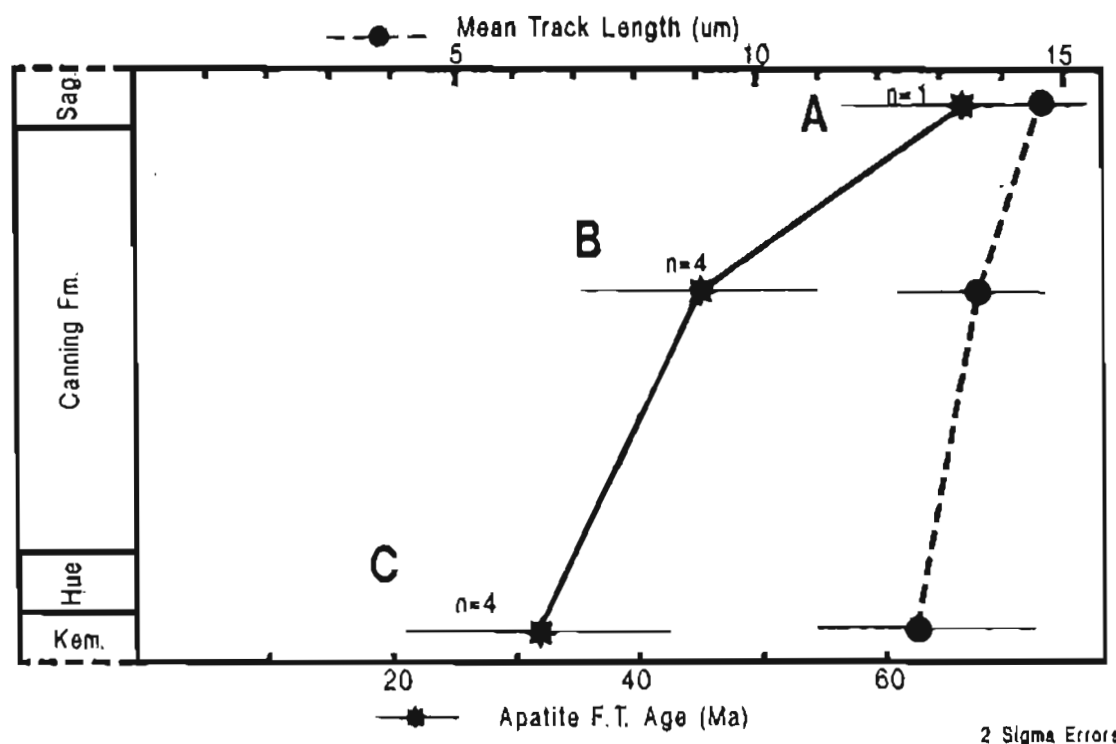


Figure 17. Plot of relative changes in ages and mean track lengths throughout the Canning River section. The section is broken down into three groups based on their ages: (A) ~67 Ma; (B) ~45 Ma; (C) ~32 Ma (± 2 sigma). Sag. = Sagavanirktok Fm., Kem. = Kemick Fm. See text for explanation.

1986b) at the base of the group. The track length distributions for group C are typical of mixed and bimodal distributions (see Appendix A, p. 101).

ANWR Coastal Plain

The eight samples from the ANWR coastal plain with stratigraphic ages ranging from Albian to Eocene give apatite fission track ages from 58 ± 23 to 105 ± 23 Ma (Table 1). Mean track lengths range from 13.7 to 15.0 μm with s.d. from 1.0 to 2.1 μm (Table 2, Fig. 18). All eight samples have a volcanic-type track length distribution defined by a sharp peak centered around ~ 14.5 μm , but four of the samples have a small tail of short tracks ($< 4\%$ of total tracks).

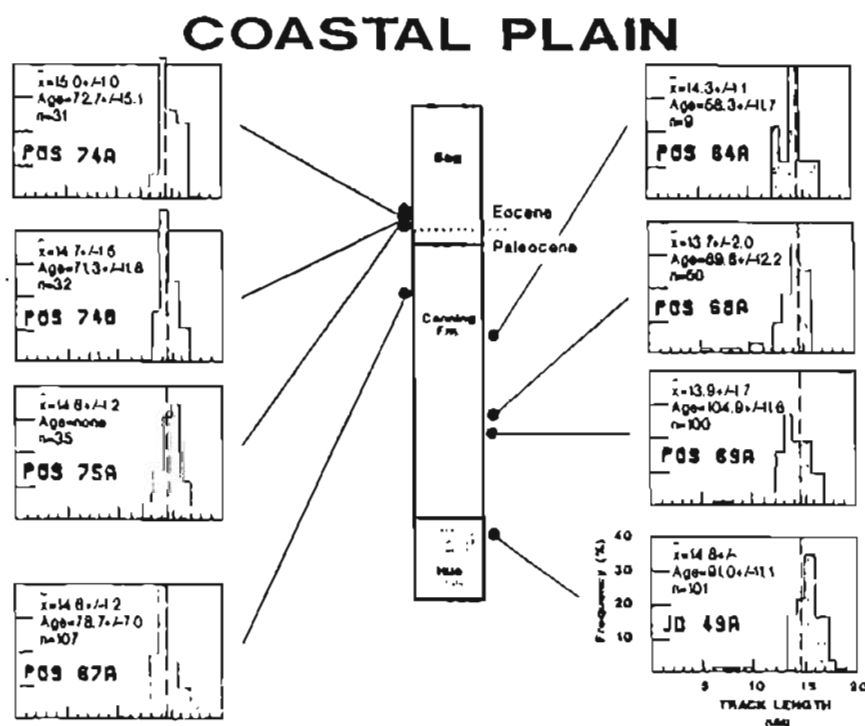


Figure 18. Apatite fission track data from representative samples collected from the Arctic Coastal Plain. Each plot shows track length vs. frequency, mean track length, age (± 1 sigma) and number of tracks measured. Age not calculated for POS 75A due to poor contact between grains and the mica detector during irradiation. Dots represent relative sample positions.

Compositional Variation In Apatites

Although differences in apatite composition were not a major focus of this study, average F and Cl contents of apatites from 12 apatites from the study area have been included. Table 3 shows the ranges in the ratio $\text{Cl}/(\text{F} + \text{Cl})$. Apatites with $\text{Cl}/(\text{F} + \text{Cl}) > 0.01$ are considered Cl-rich, and fission tracks will be stable at higher temperatures than those in F-rich apatites (Duddy, 1988 personal communication). This difference could possibly explain the spread of apatite fission track ages for each area (for example the spread in ages of 49-74 Ma for Bathtub Ridge). However, the sparse data available show no correlation between apparent age and Cl content (Table 3). These differences in apatite composition, which alter the temperature range for the partial stability zone, are not sufficient to explain the rapid cooling ($125^{\circ}\text{--}60^{\circ}\text{C}$) required by the fission track data.

Table 3. Chlorine and Fluorine Contents in Selected Apatite Grains

Sample Number	Fluorine (wt. %)	Chlorine (wt. %)	$\frac{\text{Cl}}{\text{Cl}+\text{F}}$	Age (Ma \pm 2 σ)
<i>Bathtub Ridge</i>				
POS104B	2.35	0.01	0.002	63.6 \pm 16.2
	2.31	0.01	0.002	
JD78A	2.45	0.05	0.020*	58.2 \pm 19.8
	3.10	0.02	0.007	
POS96A	2.90	0.13	0.042*	64.4 \pm 15.4
	2.81	0.07	0.025*	
POS90A	2.66	<0.01	0.000	62.3 \pm 15.0
<i>Arctic Creek</i>				
JD27A	2.60	<0.01	0.000	37.9 \pm 13.2
	1.24	0.01	0.007	
<i>Canning River</i>				
POS08A	2.48	0.19	0.072*	30.2 \pm 7.6
POS07A	2.49	0.01	0.002	30.2 \pm 11.8
<i>ANWR Coastal Plain</i>				
POS75A	2.843	<0.01	0.000	-

Results for each area are shown in stratigraphic order. *Chlorapatites (apatite with $\text{Cl}/(\text{F} + \text{Cl}) > 0.01$). Age not available for POS75A due to poor contact between the grain mount and the mica detector.

INTERPRETATIONS

After results from all 42 samples were obtained, thermal history interpretations were made by comparing the track length distribution of each Alaskan sample to published track length histograms from apatite samples with known thermal histories (e.g. Gleadow *et al.*, 1986b; Green *et al.*, 1985b). Preliminary interpretations were then reviewed by members of the Melbourne University Fission Track Research Group.

As an independent test of the thermal history interpretations obtained by the above method, 3-4 representative sample histograms from each area were compared to model histograms generated by a thermal modeling program developed by A.J.W. Gleadow and P. F. Green (see "Thermal Modeling" in Appendix A). This program utilizes apatite annealing results from the Durango apatite (Green *et al.*, 1986) modeled using formal statistical methods by Laslett *et al.* (1987). These results and all previous mathematical descriptions of fission track annealing in apatite were studied by Laslett *et al.* (1987), prior to presenting a preferred model for the prediction of the annealing processes in apatite (see Appendix A, p. 97). This model was incorporated by A.J.W. Gleadow and P.F. Green into their program which generates model track length distributions from postulated time-temperature histories. Using this program, model histograms were generated for 3-4 representative samples from each study area. The model histograms were compared with the histograms of actual data to provide a test of the postulated thermal histories.

The track length distribution reflects the nature of the thermal history experienced by that apatite (Green, 1986). The continuous production of tracks through time results in distributions of track lengths in which the shorter tracks (<10-12 μm) have experienced higher temperatures than the longest tracks (13-16 μm). In rapidly cooled rocks, such as volcanic rocks or rapidly uplifted basement blocks which have not been heated above $\sim 50^{\circ}\text{C}$ since cooling, the track length distribution is characteristically narrow (s.d. between

~0.8 and 1.3 μm) with nearly all tracks falling between 13 and 16 μm and mean track lengths between 14 and 15 μm . Only for apatite samples with such a track length distribution does the fission track age represent a distinct geologic event in terms of a rapid cooling from above ~125°C (Green *et al.*, 1985b).

Interpretation of Bathtub Ridge Results

Apatite ages of the Bathtub Ridge rocks (49-74 Ma) are much younger than the stratigraphic ages for the same samples (100-280 Ma). This indicates that, subsequent to deposition, the rocks were heated to temperatures greater than 60°C (approximate lower temperature limit of the apatite partial stability zone), causing annealing of existing tracks. This annealing substantially decreased the density of fission tracks and resulted in a decreased age for the sample. The track length distributions for the upper group of the Bathtub Ridge samples are typical volcanic-type distributions. A rapid cooling history for the upper section is therefore indicated. The mixed-type distributions (Gleadow *et al.*, 1986b) for the lower group indicate a more complicated history (Fig. 13).

By combining the fission track age and track length data it is possible to determine a thermal history for the samples in the two parts of the section. The ages from both parts of the section are concordant (Fig. 12). Therefore, at ~62 Ma, the section cooled to below temperatures at which fission tracks become stable.

The track-length data for the upper section indicate that very rapid cooling occurred for these rocks after total annealing of previous tracks and resetting of the fission track age. The narrow track length distributions and high mean track lengths indicate that these rocks must have cooled from temperatures greater than 125°C to approximately 50°C in 3-5 m.y. Figure 19 shows the track length distribution for sample 87POS96A and a best fit model of its thermal history generated by the thermal modelling program. The model results coincide

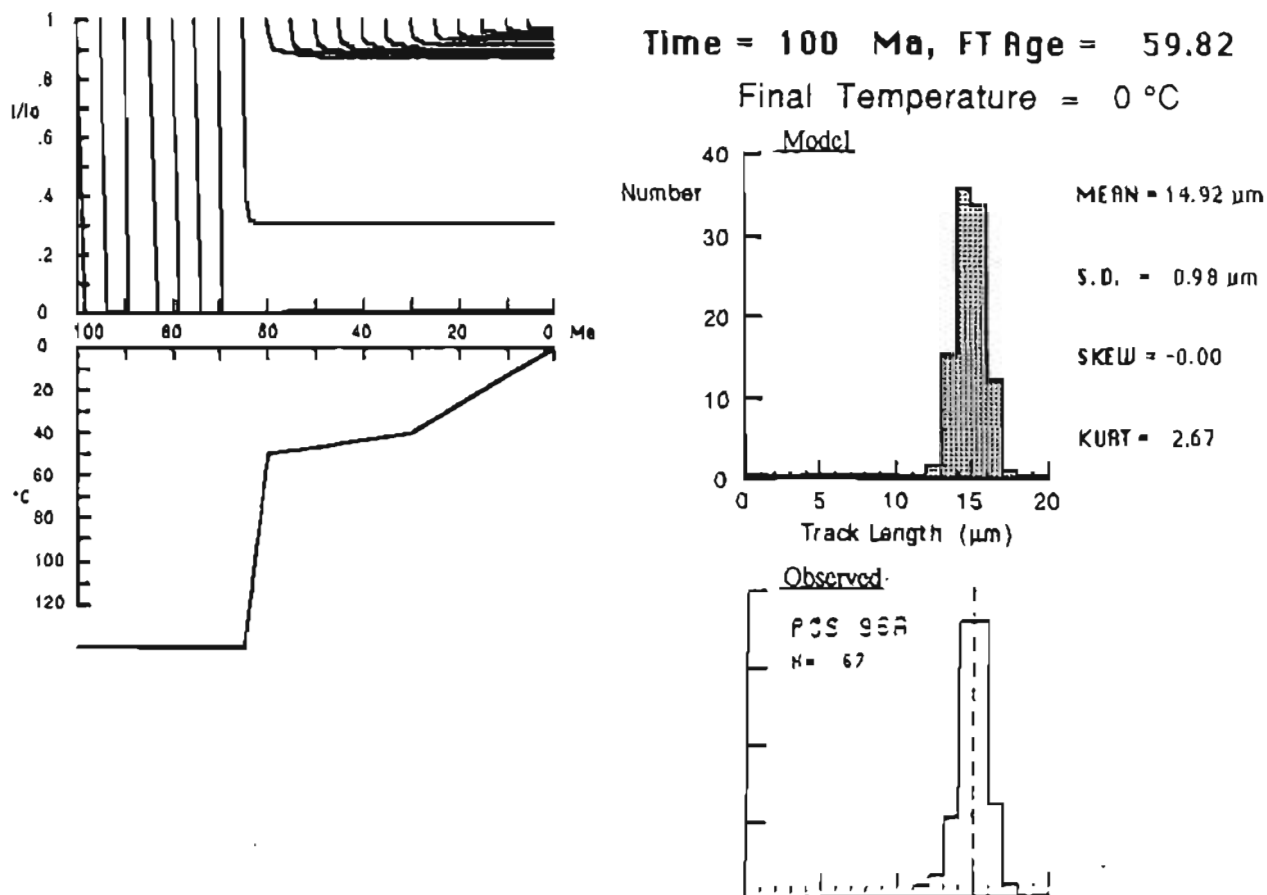


Figure 19. Proposed thermal history for the upper part of the Bathtub Ridge section. This figure shows track length distribution data for the Bathtub Greywacke, sample 87POS96A (unstippled), and its proposed thermal history (suppld) derived using Laslett *et al's* (1987) preferred model. In this "best fit" example, rapid cooling occurs from >125°C to ~50°C between 65 and 60 Ma followed by protracted cooling to present surface temperatures. The positioning of a kink in the curve, after the rapid cooling, has no significance *per se*. In the computer-derived model "Time" represents the actual age of the deposit and "Age" is the apparent fission track age given the time-temperature path since deposition. The dashed line in the sample histogram represents the mean length. The thermal history prior to the cooling event is unknown.

well with the data if cooling occurred over a 5 m.y. period between 65 and 60 Ma. Slower cooling over the same temperature range or rapid cooling to temperatures greater than 50°C would produce some shorter tracks which are not common in the samples. Rapid cooling to temperatures less than 50°C would result in fewer tracks in the 13-14 μm range than seen in these samples. These results indicate cooling rates of approximately 15° to 25°C per m.y. for the temperature interval 125° to 50°C (75°C change over 3 to 5 m.y.).

Track length data for the lower group indicate that rapid cooling, though occurring during the same time period based on the age data, must have terminated at higher temperatures in order to allow the preservation of many short tracks. This can be explained by leaving the lower group of samples at temperatures greater than 60°C after rapid cooling at ~62 Ma. Figure 20 shows the track length distribution for sample 87POS99A and a model of its thermal history. The model shows a time-temperature path with rapid cooling to ~75°C occurring between 60 and 65 Ma. This is followed by slower cooling to present surface temperatures. Leaving the samples at even higher temperatures would result in more short tracks than are actually seen.

In summary, for Bathtub Ridge, all eighteen samples analyzed from both parts of the section have concordant apatite ages averaging ~62 Ma. Since deposition, all apatite fission track ages have been totally reset, requiring heating to temperatures above 125°C. At ~62 Ma, the upper group cooled quickly to ~50°C and has since undergone slow cooling based on the observed high mean track lengths (>14 μm). The lower group appears to have been subjected to a slightly more protracted cooling history, experiencing slightly higher temperatures (~75°C) for a prolonged period upon conclusion of the rapid cooling event at ~62 Ma.

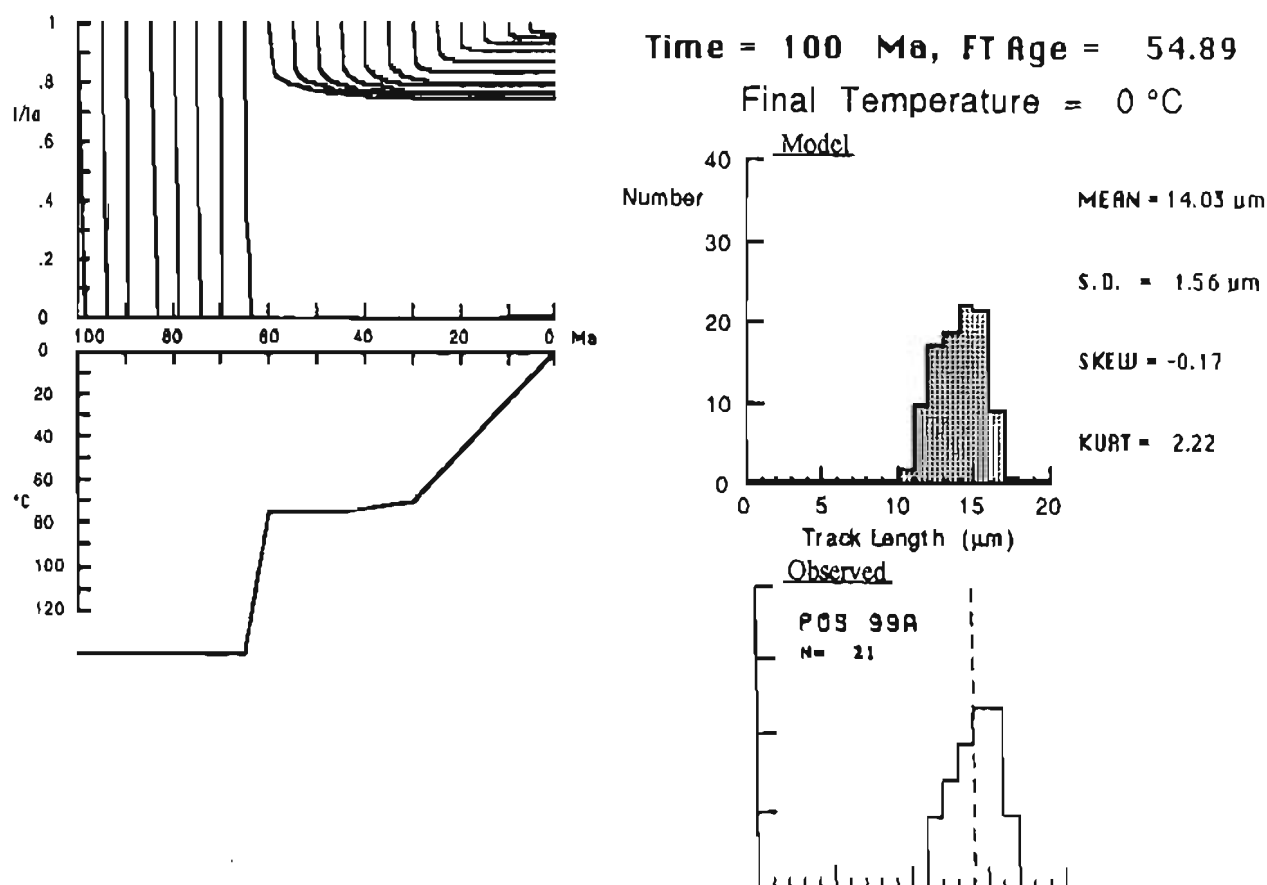


Figure 20. Proposed thermal history for the lower part of Bathtub Ridge. The figure shows track length distribution data for Echooka Fm. sample 87POS99A (unstippled) and its proposed thermal history (stippled) derived for the sample using Laslett *et al*'s (1987) preferred model. In this "best fit" example, rapid cooling from $>125^{\circ}\text{C}$ to $\sim 75^{\circ}\text{C}$ occurs between 65 and 60 Ma followed by protracted cooling to present surface temperatures. The positioning of a kink in the curve, after the rapid cooling, has no significance *per se*. In the computer derived model "Time" represents the actual age of the deposit and "Age" is the apparent fission track age given the time-temperature path since deposition. The dashed line in the sample histogram represents the mean length. The thermal history prior to the cooling event is unknown.

Interpretation of Arctic Creek Results

Apatite ages from the Arctic Creek samples (31-40 Ma) are much younger than their stratigraphic ages (~100 Ma). The younger apatite ages indicate that the samples were heated to temperatures greater than 60°C subsequent to their deposition, resulting in track annealing and a decrease in fission track age. The track length distributions are all indicative of rapid cooling (volcanic-type distributions) but include a small component of short tracks, indicating an extended yet short period of cooling through the track annealing zone.

The combination of age and track length data indicate that at ~37 Ma, these samples underwent rapid cooling from temperatures above 125°C to temperatures below 60°C. Prior to ~37 Ma, the samples experienced temperatures greater than 125°C resulting in total annealing of tracks and a zero fission track age. Rapid cooling at ~37 Ma resulted in the preservation of fission tracks, thus recording the cooling event. The shape of the track-length distribution shows that the samples did not spend more than 10 m.y. in the 60° to 125°C temperature zone or the distribution would have a larger component of shorter tracks (see Appendix A, p. 100). Figure 21 shows the track length distribution for sample 87JD26A and a model of its thermal history showing rapid cooling from 35 to 40 Ma. To allow for the presence of the tail of short tracks, samples are postulated to have cooled to ~125°C prior to rapid cooling to temperatures less than 60°C. At this temperature near the lower temperature portion of the fission track annealing zone, recently-formed tracks would not be fully annealed prior to rapid cooling and would therefore be preserved. Another possible way to explain the short tracks would require the samples to cool from temperatures above 125°C to temperatures about 60°C and then remain at those temperatures for ~10-20 m.y. This would allow some shortening of tracks to occur but

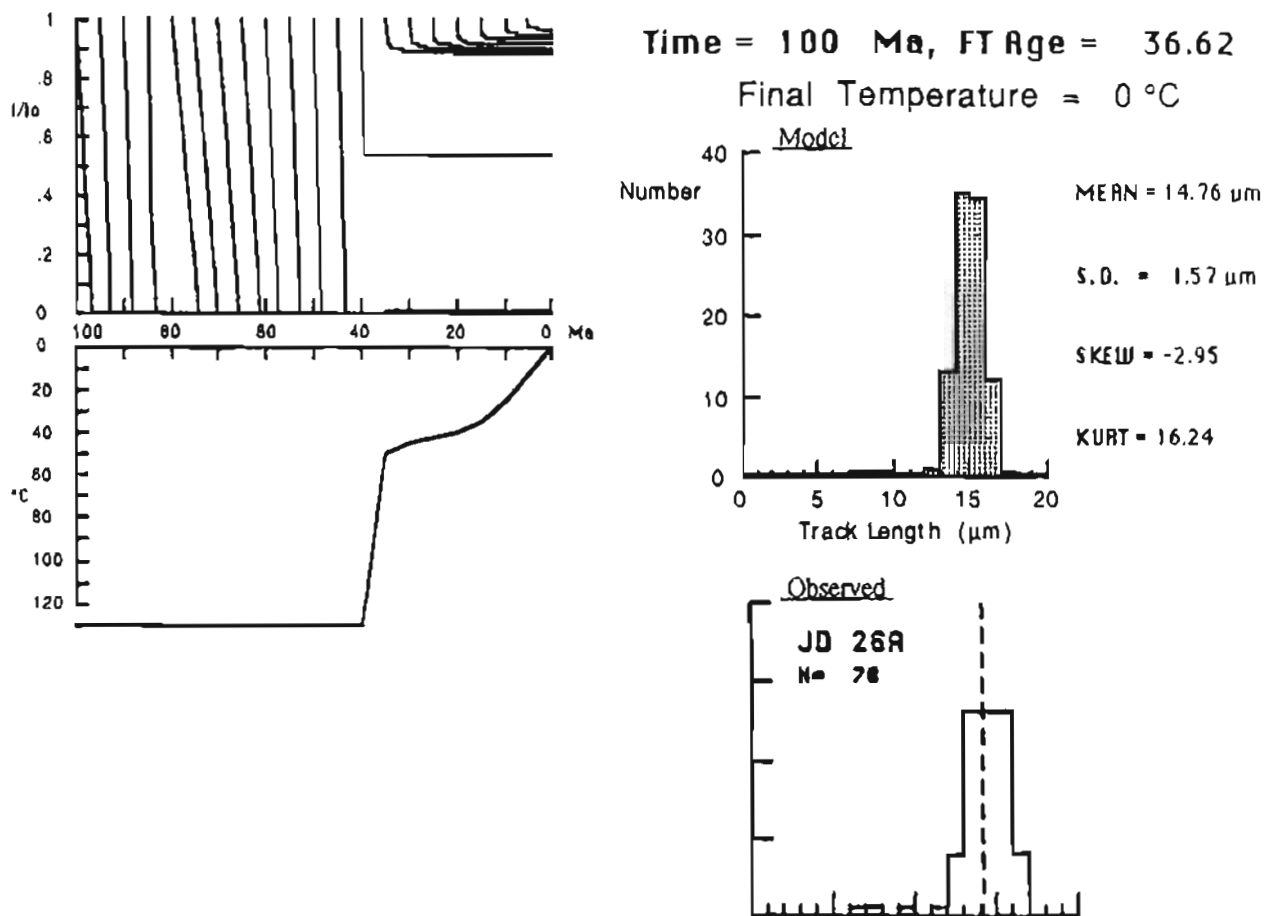


Figure 21. Proposed thermal history for the Albian turbidites of the Arctic Creek section. The figure shows track length distribution data for sample 87JD26A (unstippled) and its proposed thermal history (stippled) derived for the sample using Laslett *et al.*'s (1987) preferred model. In this "best fit" example, rapid cooling from ~125°C to ~50°C occurs between 40 and 35 Ma followed by protracted cooling to present surface temperatures. The positioning of a kink in the curve, after the rapid cooling, has no significance *per se*. In the computer-generated model "Time" represents the actual age of the deposit and "Age" is the apparent fission track age given the time-temperature path since deposition. The dashed line in the sample histogram represents the mean length. The thermal history prior to the cooling event is unknown.

would result in a much broader distribution if the samples remained at those temperatures very much longer.

In summary, all seven samples from the Albian turbidites possess concordant apatite fission track ages averaging ~37 Ma. All apatite fission track ages have been totally reset since deposition, requiring heating to temperatures above 125°C. At ~37 Ma, the entire section cooled quickly through ~60°C and has since undergone slow cooling based on high mean track lengths (>14 µm).

Interpretation of Canning River Results

The samples from the Canning River section can be divided into three units by fission track ages and stratigraphic position. For the sample at the top of the section, the single apatite fission track age (~67 Ma) is older than the stratigraphic age of the host Sagavanirktok Formation. (Paleocene to Pliocene). Its volcanic-type track length distribution indicates that minimal track annealing has occurred since the formation of the tracks. Therefore, the age and lengths apparently reflect the thermal history of the source terrane.

Apatite fission track ages of samples from groups B and C (mean values of ~45 and ~32 Ma) are much younger than their stratigraphic ages. The track length distributions range from volcanic-type at the top of group B in the Canning Formation, to mixed (Gleadow *et al.*, 1986b) and bimodal at the base of the stratigraphically lowest group C (see Table 1, Figure 16, and Appendix C). Moving downsection from the top of group B, mean track lengths decrease from 14 µm to ~11.6 µm at the base of group C. Therefore, following a rapid cooling recorded by the samples in group B at ~45 Ma, group C samples from lower in the section experienced slightly higher temperatures, resulting in more annealing of tracks and shorter mean track lengths. The group C samples record a second event as a maximum age of cooling of ~32 Ma.

The thermal history of these three groups are illustrated in Figure 22. With increasing temperature above $\sim 60^{\circ}\text{C}$, fission tracks in apatite shorten and decrease the apparent age (see Appendix A). This continues until temperatures of $\sim 125^{\circ}\text{C}$ are reached at which point fission tracks are rapidly annealed and samples reach a zero age. To fit the existing data for the Canning River samples, rapid cooling is inferred to have occurred at ~ 45 Ma bringing group B samples from temperatures greater than 125°C to those close to the lower temperature limit of the partial stability zone ($\sim 60^{\circ}\text{C}$). The samples remained at these temperatures long enough for the mean track lengths to shorten to between $14.1\text{--}12.7\text{ }\mu\text{m}$. Group C samples, ~ 1000 m downsection, would have been brought from temperatures

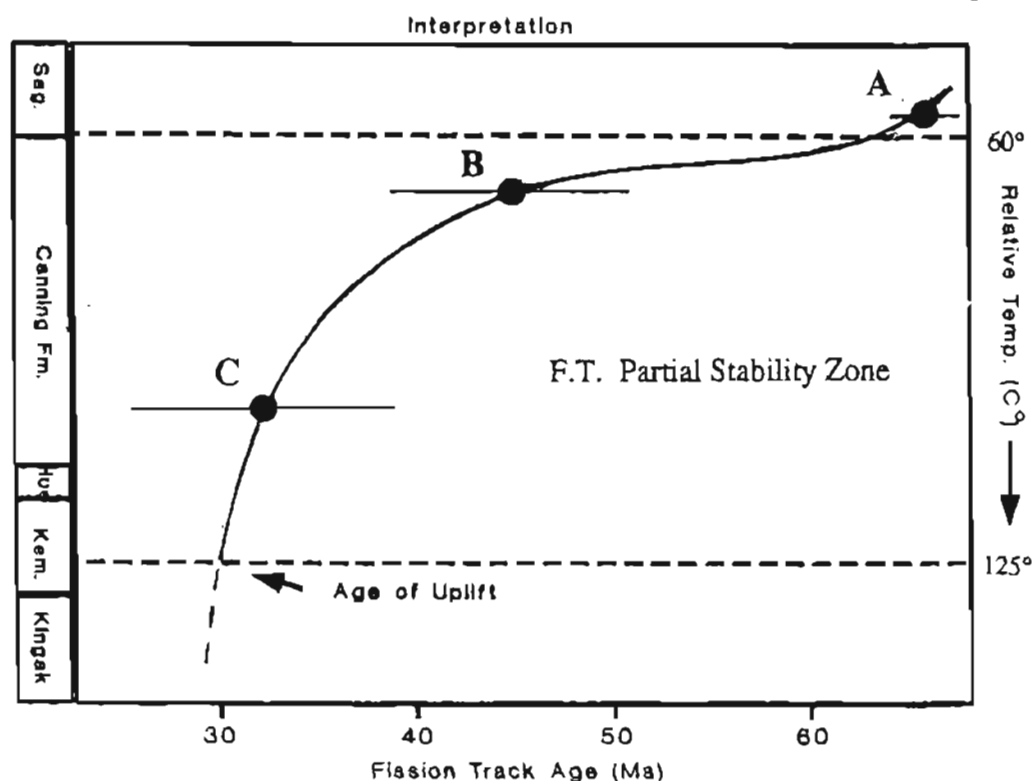


Figure 22. Fission track interpretation of Canning River section. Shows the relative positions within the track annealing zone prior to the second cooling event recorded by the samples in Group C. The section is broken down into three groups based on their ages: (A) ~ 67 Ma; (B) ~ 45 Ma; (C) ~ 32 Ma (± 2 sigma). Sag. = Sagavanirktok Fm., Kem. = Kemick Fm. See text for explanation. Shape of curve is based on variation in fission track ages seen with down-hole temperatures within the track annealing zone from wells in the Otway Basin (Gleadow and Duddy, 1981; also see Fig. A4).

greater than 125°C to ~90°-100°C (assuming a geothermal gradient of 30°C/km). If it were possible to sample farther downsection from the samples giving ages of ~32 Ma (mean of group C), one would expect to encounter rocks which continued to experience temperatures greater than 125°C after the ~45 Ma cooling event. The age of these rocks could record the second cooling event which resulted in the uplift and exposure of the samples from group C. Therefore, the age of the group C samples (~32 Ma) represents a maximum age for the second cooling event. Thermal modeling of a sample from the top of group B and a sample from group C show that this interpretation is possible. In Figures 23 and 24, temperature-time plots and resultant track length distributions are shown for the two samples. Identical cooling paths are followed but these paths are separated by 30°C (1000 m of section).

In summary, data from the sample at the top of the Canning River section reflects the thermal history of its source terrane. Apatite ages from the lower two groups reflect cooling events through ~60°C with the first cooling event occurring at ~45 Ma. The mean age of the lowest group (32 Ma) represents a maximum age for the second cooling event.

Interpretation of ANWR Coastal Plain Results

Ages from the individual samples collected on the ANWR coastal plain (58-105 Ma) are at least as old as their depositional ages (~50-100 Ma). Therefore, subsequent to deposition, the formations have not been subjected to the temperatures necessary to cause resetting of the fission track ages as seen in the three previous examples. The track length distributions are typical volcanic-type distributions but 4 of the samples contain a small percentage of short tracks (2-5%).

The age and track length data indicate that these apatites record events which reset the apatite fission track ages and shortened their lengths prior to inclusion in their present deposits. To produce the observed track length distributions, rapid cooling conditions

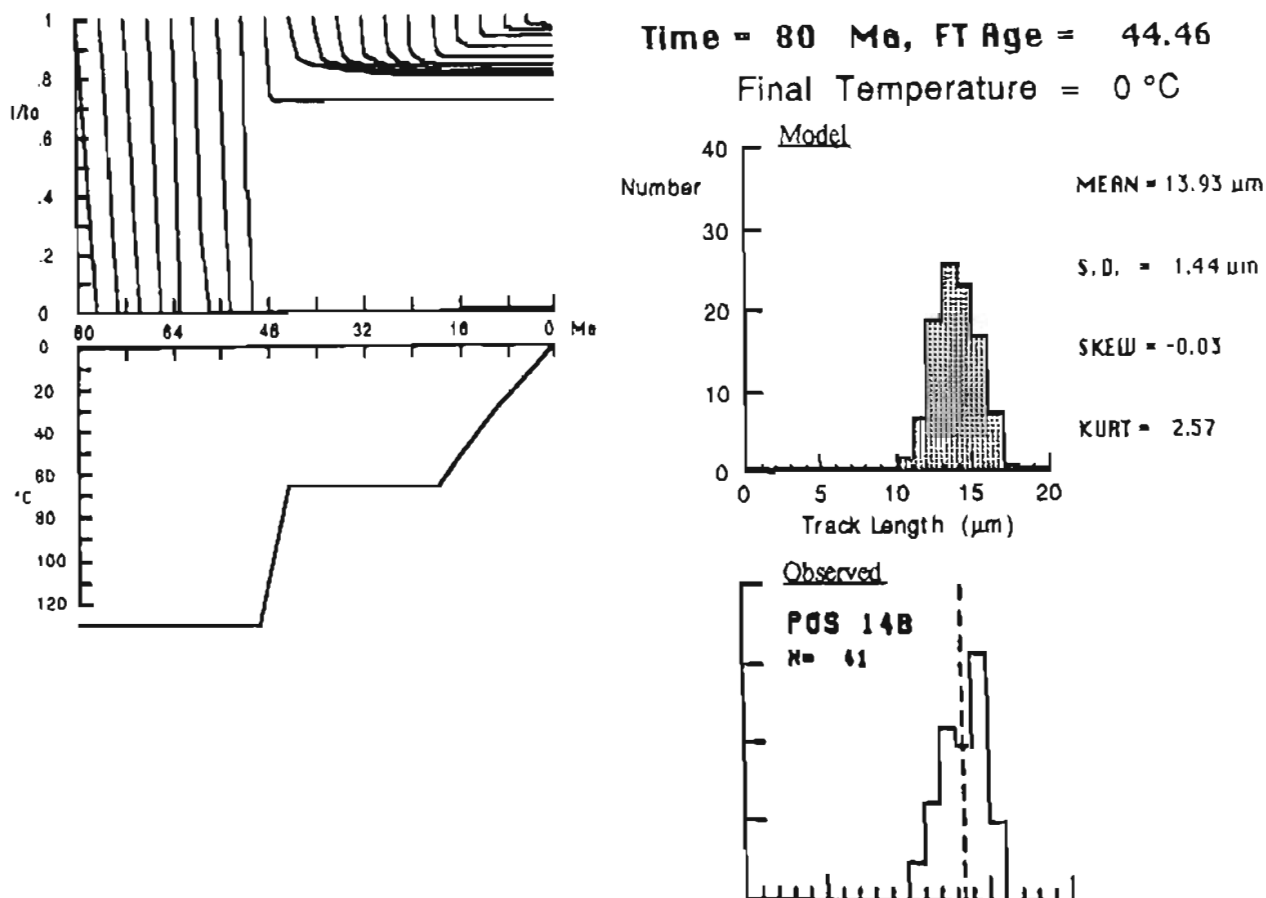


Figure 23. Proposed thermal history for the upper part of the Canning River section. This shows track length distribution data for sample 87POS14B (unstippled) and its proposed thermal history (stippled) derived for the sample using Laslett *et al's* (1987) preferred model. In this example, after deposition ~80 Ma, the sample was cooled to ~65°C between 50 and 45 Ma and remained at that temperature until a second cooling event (<32 Ma) brought it out of the track annealing zone. The dashed line in the sample histogram represents the mean length.

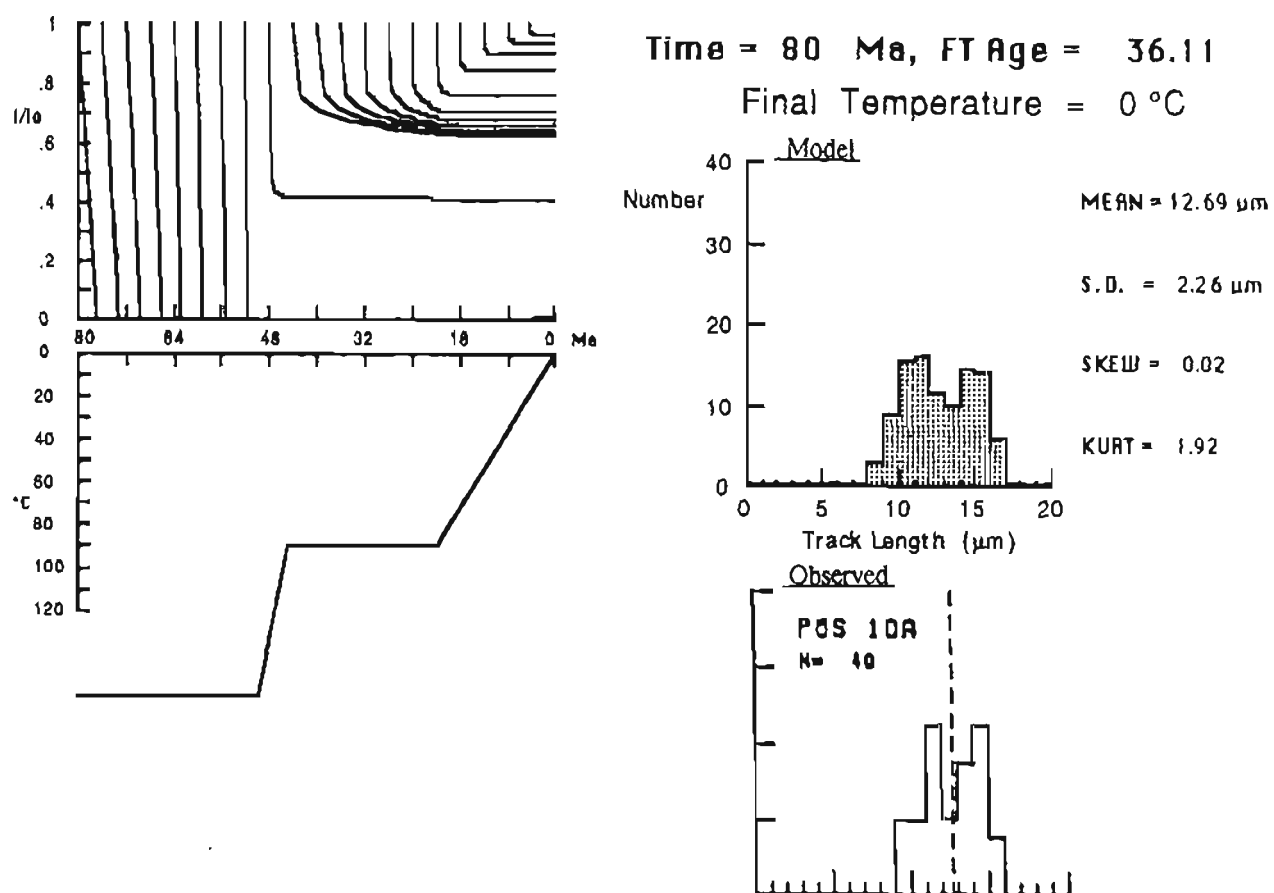


Figure 24. Proposed thermal history for the lower part of the Canning River section. This shows track length distribution data for sample 87POS10A (unstippled) and its proposed thermal history (stippled) derived for the sample using Laslett *et al*'s (1987) preferred model. In this example, after deposition ~80 Ma, the sample was cooled to ~90°C between 50 and 45 Ma and remained at that temperature until a second cooling event (<32 Ma) brought it out of the track annealing zone. In the computer-generated model, "Time" represents the actual age of the deposit and "Age" is the apparent fission track age given the time-temperature path since deposition. The dashed line in the sample histogram represents the mean length.

were necessary, and must have occurred prior to deposition in the sampled units. These rocks have not experienced temperatures greater than 60°C since deposition.

One sample, 87JD49A, was collected from a bentonite bed within the Hue Shale (Albian to Cenomanian). An age of ~91 Ma and a mean track length of 14.8 μm (Fig. 25) were determined for this particular sample. The fission track age appears to date the volcanic event and the length distribution reflects the thermal history of the sample since the event. There are two possibilities to explain the presence of the observed small percentage of short tracks. First, this sample could have experienced temperatures near 60°C for some length of time since deposition but did not experience temperatures which would reset the apatite fission track age. Alternatively, the sample could have been contaminated by grains with short tracks during reworking or inclusion of xenoliths.

In summary, all apatite ages (58-105 Ma) are at least as old as depositional ages (50-100 Ma). These ages and track lengths reflect the thermal histories of the samples' source terranes. Track lengths and ages indicate minimal track annealing since deposition.

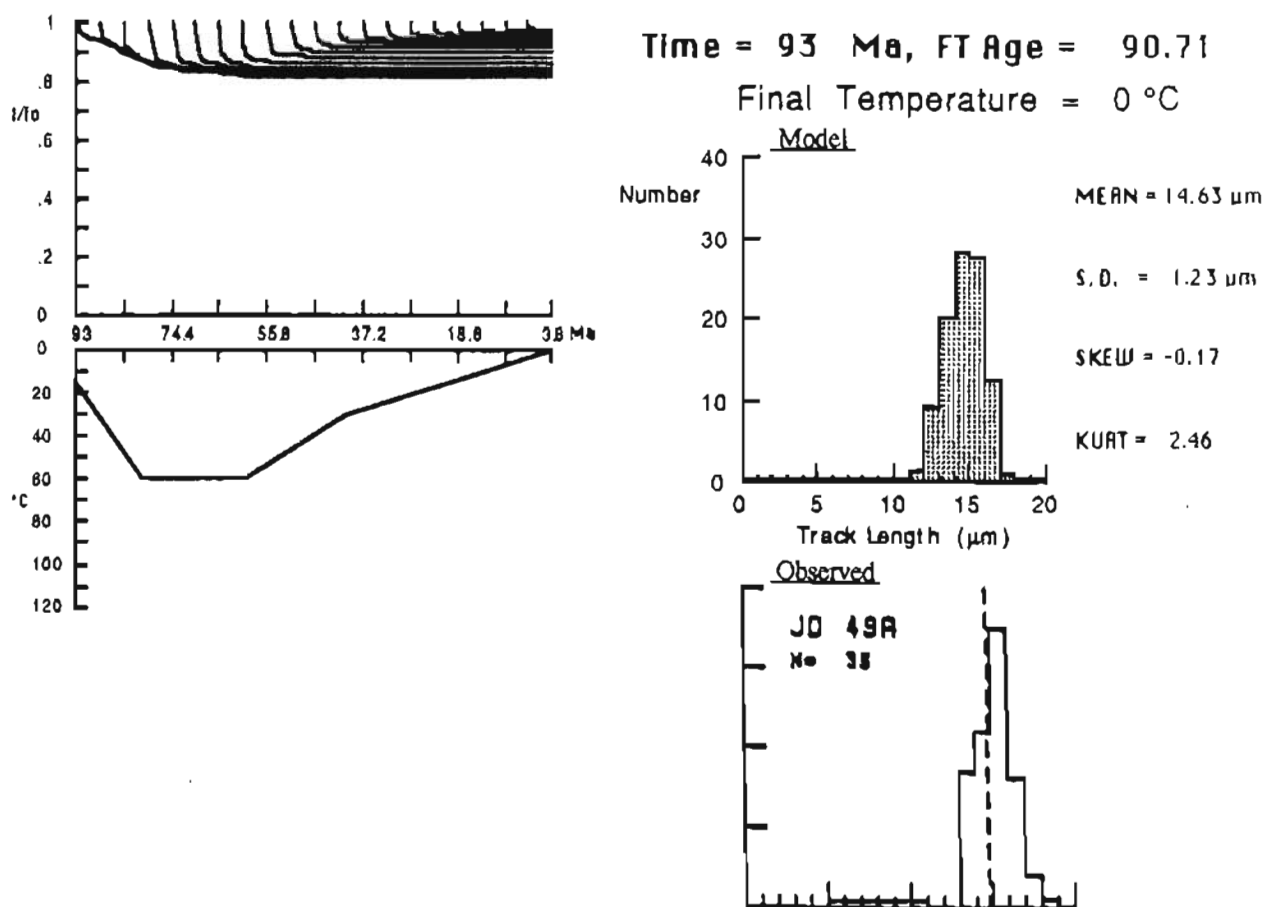


Figure 25. Proposed thermal history for the Hue Shale on the Arctic Coastal Plain. This figure shows track length distribution data for sample 87JD49A (unstippled) and its proposed thermal history (stippled) derived for the sample using Laslett *et al's* (1987) preferred model. In this "best fit" example, after deposition ~93 Ma, the sample has not seen temperatures greater than ~60°C, but has experienced temperatures >50°C in order to accumulate some shorter tracks. In the computer-generated model "Time" represents the actual age of the deposit and "Age" is the apparent fission track age given the time-temperature path since deposition. The dashed line in the sample histogram represents the mean length.

GEOLOGIC INTERPRETATION OF FISSION TRACK DATA

OVERVIEW

Apatite fission track data record cooling events, decreasing in stepwise increments, from ~62 Ma to ~32 Ma northward from Bathtub Ridge to the Canning River. I interpret these events to define times at which the northward-advancing front of the fold and thrust belt was affecting different areas in ANWR. Farther north on the ANWR coastal plain, the rocks studied have not been subjected to temperatures greater than ~60°C for any recordable length of time (by fission track methods) since deposition. Hence the apparent apatite fission track ages for these rocks have not been reset since their deposition.

The Bathtub Ridge, Arctic Creek, and Canning River sections show evidence for rapid cooling from temperatures greater than 125°C to less than 60°C during a period of less than 3-5 m.y. The following brief discussion of heat flow considerations provides a background to a discussion of alternative mechanisms for the rapid cooling.

HEAT FLOW CONSTRAINTS

There are four mechanisms for the transfer of heat: conduction, forced convection, free convection, and radiation. Conductive heat transfer through a medium occurs via a diffusive process wherein molecules transmit their kinetic energy to other molecules by collision. Heat is conducted through a medium in which there is spatial variation in temperature. Convective heat transport occurs by the motion of a medium due to a temperature gradient; it can be *free* where flow patterns are determined by the bouyancy of a heated material or *forced* where flow patterns are determined by external forces (Bird *et al.*, 1960). Electromagnetic radiation also transports heat, for example the radiant energy emitted by the sun, but this is mainly re-radiated back into space and only a small fraction penetrates below a few hundred meters. Therefore radiation need not be considered for the purposes of this discussion.

Cooling of rocks occurs both by conduction and by forced and/or free convection of circulating fluids, mostly groundwater. Thermally conducted heat flow through rock per unit area is the product of the geothermal gradient and the thermal conductivity. In a homogeneous material the thermal conductivity (k) is the sum of conductivities caused by lattice vibrations (Clark, 1966). The equation for one dimensional heat flow through a homogeneous material is given by Fourier's law of heat conduction:

$$Q = -k(dT/dZ)$$

where: Q = the geothermal flux ($\sim 10^{-6}$ calories $\text{cm}^{-2} \text{s}^{-1}$)

k = the thermal conductivity ($\sim 10^{-6}$ calories $\text{cm}^{-1} \text{s}^{-1} \text{ } ^\circ\text{C}$)

(dT/dZ) = the geothermal gradient ($^\circ\text{C cm}^{-1}$) (constants from Wyllie, 1971)

Thermal conductivity varies widely with the composition of rocks (Clark, 1966). Compared with most rocks sandstones have a relatively low thermal conductivity, making them excellent insulators (Lee, 1979). Values of k for rocks include: ~ 5.0 ($\times 10^{-6}$ calories $\text{cm}^{-1} \text{s}^{-1} \text{ } ^\circ\text{C}$) for sandstones, ~ 8.0 for granites, ~ 10.0 for dolomites, and ~ 5.0 for shale (Clark, 1966). These variations cause a variability of geothermal gradient for a given geotectonic regime, whereas values of heat flow are less scattered (Tissot and Welte, 1984). Some average values of heat flow in continental and oceanic regions according to geotectonic conditions are (in 10^{-6} calories $\text{cm}^{-1} \text{s}^{-1} \text{ } ^\circ\text{C}$): Precambrian shields = 0.92; areas stable since Precambrian = 1.32; areas with Mesozoic or Cenozoic orogenies = 1.92; areas of Cenozoic volcanism = 2.16; oceanic basins = 1.28; oceanic ridges = 1.82; and oceanic troughs = 0.99 (Tissot and Welte, 1984).

For basins with a higher heat flow, annealing of fission tracks occurs at relatively shallower depths than in a basin environment with a lower heat flow. Geothermal gradients for foreland basins like the Colville Trough range from $\sim 20^\circ\text{--}30^\circ\text{C/km}$ (North, 1985). Therefore, prior to orogenic activity in the NEBR, it is assumed the foredeep of the advancing Brooks Range experienced a geothermal gradient of between $20^\circ\text{--}30^\circ\text{C/km}$.

With such a gradient, apatite fission tracks would be partially annealed at >2-3 km depths and fully annealed at >4-6 km depths. The area has since been overprinted by the Mesozoic and Cenozoic orogenic activity and would therefore be expected to have a relatively higher heat flow at present.

ALTERNATIVE MECHANISMS FOR RAPID COOLING

Three possible end-member mechanisms to explain how these sections could have cooled from >125°C to <60°C in 3-5 m.y. are: 1) a rapid decrease in geothermal gradient, 2) emplacement of magma nearby followed by rapid cooling, and 3) concurrent rapid uplift and removal of overburden.

Rapid Decrease In Geothermal Gradient

Wells drilled on the North Slope of Alaska in the present foredeep just west of ANWR, have shallow geothermal gradients of ~30°C/km (depths to 4200 to 4700 m and bottom-hole temperatures of 120° to 132°C) (Magoon *et al.*, 1987; Gautier *et al.*, 1987; Lachenbruch *et al.*, 1982; Lachenbruch *et al.*, 1987)). This gradient is at a maximum to the north of the present foredeep, due to uplifted shallow basement material, and decreases slightly to the south as the basin deepens approaching the foredeep (Magoon, 1987 personal communication). Assuming a 20°-30°C/km geothermal gradient for the foredeep as it prograded northward in response to the advancing mountain front, conditions within the actual foredeep have remained relatively constant through time. Local and transient changes in geothermal gradient probably have occurred due to thrusting, uplift, erosion, and/or sedimentation and subsidence.

A rapid decrease in the geothermal gradient would lower isotherm depths, resulting in the cooling of rocks at a given depth as isotherms re-equilibrated. To fit the fission track data, the rocks possessing reset apatite fission track ages must have been below the 125°C isotherm prior to a rapid decrease in thermal gradient, after which most were cooled above

the 60°C isotherm. Let us consider a sample at 60°C under 2 km of overburden (assumed gradient = 30°C/km). A geothermal gradient of ~60°C/km would be required for this sample to be at 125°C under the same 2 km of material. Therefore, if the sample had remained at the same depth and the cooling was related entirely to a decrease in the geothermal gradient, a 50% reduction in gradient would be required. To accommodate the fission track results, the 50% reduction must have occurred over a period of less than 5 m.y. Based on recent limited studies of changes of geothermal gradients in boreholes on the North Slope, there is no evidence to support the idea that such a great change in thermal gradient occurred in the NEBR region since the Albian (Magoon, 1987, personal communication; Lachenbruch and Marshall, 1986), so this hypothesis is considered to be highly unlikely.

Emplacement of Magma And Subsequent Cooling

Plutonic activity is another hypothetical possibility that could explain the resetting of fission track ages and cooling of the apatite samples. If an igneous intrusion occurred near the sampled rocks (within several km depending on the size and composition of the intrusion, and conductivity of the host rocks), the elevated temperatures could possibly reset the apatite fission track ages. Studying temperature gradients away from contacts with granitic plutons of specified diameters and an initial emplacement temperature of 800°C into country rocks at 100 °C, Turner (1981) computed maximum temperature versus distance from the contacts. Results suggest that rocks 4 km from the contact of a 2 km diameter granitic pluton would experience maximum temperatures of ~150°C. For a 10 km diameter granitic pluton, the maximum temperature 4 km from the contact would be ~375°C.

This situation would require distinct plutonic events to occur in the appropriate regions at approximately 62 Ma, 45 Ma, 37 Ma, and 32 Ma. Although Tailleux (1987) proposed

that Cretaceous plutonism has occurred in the Brooks Range, isotopic dating and contact relations led Dillon *et al.* (1987) to conclude that the main granitic plutonic events in the Brooks Range were Devonian and older, and that there is no convincing evidence to indicate post-Devonian plutonism. Dillon *et al.* (1987) also demonstrated that the only plutonic rocks in the NEBR, the Okpilak Batholith and two satellite stocks, are of Devonian age. They suggest that K-Ar biotite ages of ~60-130 Ma from these plutonic rocks were reset in a secondary heating event related to overthrusting. There is no evidence for plutonism younger than 60 Ma in the region.

If emplacement of magma near the sampled areas were to occur, apatite fission track ages could be reset. However, cooling of emplaced magma in convecting magma chambers generally is not rapid (~1-5°C/Ma) (Spera, 1980). Hence apatites in rocks near a cooling magma body probably would not cool rapidly enough to explain the volcanic-type track length distributions characteristic of most of the Alaskan samples.

Rapid Uplift and Denudation

The most feasible hypothesis to explain the observed fission track data is rapid uplift of the sections, with contemporaneous removal of overburden (denudation), producing a cooling from >125° to <60°C in 3-5 m.y. Apatite will begin recording fission tracks upon cooling through its critical track-retention isotherm (Gleadow *et al.*, 1986a). In fission track studies of mountain belts this critical isotherm (~125°C) is commonly assumed to be a static datum at constant depth (Zeitler, 1985). Thus the apatite ages reflect the age of uplift through that isotherm, resulting in a characteristic pattern of ages increasing with elevation.

Here, "uplift" is defined as the total upward movement of the rock body through some fixed datum point. Denudation is defined as the destruction of the landscape by the processes of weathering, mass-wastage, transportation and erosion. Erosion is the wearing away of the land by the natural agents of waves, tidal currents, rivers, glaciers,

ice-sheets, wind and related surficial processes (Buckle, 1978). Uplift and denudation are separate processes which are completely interrelated in terms of cause and effect. Generally in the Earth System uplift is essential in order for denudation to occur. When uplift exceeds base level denudation begins, and will continue until base level is again achieved.

Additional topographic elevation of a land surface resulting from uplift will be equal to the amount of uplift minus the amount of denudation. However, the ascent of a rock body through a static isotherm cannot be distinguished on the basis of fission track ages alone from the downward movement of isotherms. Downward movement of isotherms following an uplift event is likely to occur during the resultant denudation, primarily by erosion since the surface temperature is held constant. Hence, an uplift rate, as determined from the gradient of an apatite age-sample elevation profile is really a denudation rate in this simple case.

Parrish (1982, 1983) called the apatite age-sample elevation gradient the "apparent uplift rate" which he defined as "the rate at which the critical isotherm ($\sim 100^{\circ}\text{C}$) moved downward with respect to the rock column". Kelley and Duncan (1986) re-defined this gradient as the "apparent denudation rate" because it had been pointed out by Morgan and Ashwal (1984) that denudation has more of an effect than uplift on the position of isotherms in the rock column.

According to Parrish (1982, 1983) this "apparent uplift rate" (apparent denudation rate) will equal the true uplift rate when the following conditions are met:

- (1) Critical isotherms must have been horizontal and uninfluenced by surface topography or variable thermal conductivity.
- (2) Critical isotherms must remain at a constant depth with respect to the surface regardless of uplift rate.

(3) Uplift must be equal to "erosion" (denudation).

Unless these conditions are met, it is inappropriate to interpret apatite ages directly as uplift ages and to define an uplift rate.

To explain the fission track results of this study in terms of rapid uplift and denudation, the following conditions must be met: (1) For the apatite fission track ages from the Bathtub Ridge, Arctic Creek, and Canning River sections to have been totally reset since deposition, the rocks must have been subjected to temperatures $>125^{\circ}\text{C}$ in order to allow the fission tracks to anneal. The sampled rocks from the ANWR coastal plain must not have experienced temperatures $>60^{\circ}\text{C}$ since deposition. (2) Assuming a geothermal gradient of $\sim 20^{\circ}\text{--}30^{\circ}\text{C}/\text{km}$, the required $\sim 125^{\circ}\text{C}$ temperatures would be reached at $>4\text{--}6$ km depths.

If these conditions are met, the following conclusions can be made which explain the fission track results in terms of uplift and denudation: (1) The fission track results require that uplift and denudation at Bathtub Ridge and Arctic Creek occurred over periods of time <5 m.y., cooling the samples to temperatures $<60^{\circ}\text{C}$. (2) Two uplift and denudation events are recorded in the Canning River section. The first brought the upper part of the section up to temperatures between $\sim 60\text{--}70^{\circ}\text{C}$ and the lower part of the section to $\sim 90^{\circ}\text{C}$.

In order to account for rapid cooling during uplift and erosion, denudation rate must have approached or equalled uplift rate. A review of several uplift-related thermal history studies using fission track, K-Ar, Rb-Sr, and Ar 40-39 results indicates that all of these studies assume that the denudation rate is equal to the uplift rate (Mailhe *et al.*, 1986; Morgan and Ashwal, 1984; Parrish, 1982; Parrish, 1983; Zeitler, 1985; Zeitler *et al.*, 1982; Royden and Hodges, 1984). This assumption is required, if the apatite data are to be interpreted as a direct indicator of uplift, by the fact that rocks are relatively good insulators, as discussed previously.

Constraint (1) is satisfied by independent thermal history data. Magoon *et al.* (1987), report vitrinite reflectance (R_o) values and thermal alteration index (TAI) values for all four areas. Bathtub Ridge and Arctic Creek values indicate exposure to temperatures $>220^\circ\text{C}$ ($R_o = 1.7-1.8\%$, TAI = 3.3-3.6). Values from rocks along the Canning River show exposure to temperatures $> 130^\circ\text{C}$ ($R_o = 1.3\%$) for the Canning Formation and 80°C ($R_o = 0.6\%$) for the Sagavanirktok Formation (see Fig. 6). Samples from the ANWR coastal plain are thermally immature indicating exposure to temperatures not $>60^\circ\text{C}$ ($R_o = 0.4\%$). Anders *et al.* (1987) report vitrinite values of 1.5-1.8% for the Pebble Shale and 1.0-1.2% for the Canning Formation from samples collected in Ignek Valley near the Canning River. They also give vitrinite values of 0.5% for the Hue Shale and the Canning Formation from the ANWR coastal plain. These vitrinite reflectance and TAI values indicate that the temperatures necessary to reset apatite fission track ages were easily reached.

Since it is assumed that the fission track ages were reset due to burial to high temperatures ($>125^\circ\text{C}$) prior to uplift and denudation, constraint (2) requires that with a geothermal gradient of $\sim 20^\circ\text{C}/\text{km}$ (for a foreland basin) there was once $>4-6$ km of section on top of the presently exposed Albian deposits. A geothermal gradient of between $\sim 20^\circ\text{C}/\text{km}$ is used in this study purely as an average value and the estimate of 4-6 km of section removed is probably a minimum. Geothermal gradients in sedimentary basins from a wide variety of tectonic settings generally range from $15-50^\circ\text{C}/\text{km}$ with an average value of $\sim 30^\circ\text{C}/\text{km}$ (North, 1985). Present and ancient geothermal gradients can be approximately the same in sedimentary basins where no tectonic or magmatic activity has been known since deposition of the rocks (Tissot and Welte, 1984). The similarity of past and present geothermal gradients is not acceptable in basins where the last orogeny and/or magmatic intrusion is contemporaneous with, or younger than, deposition. In these

basins, the geothermal gradient may be high ($>50^{\circ}\text{C}/\text{km}$) and variable (Tissot and Welte, 1984).

Any direct stratigraphic evidence that a section $>4\text{--}6\text{ km}$ once existed on top of the presently exposed deposits has since been removed by denudation, but there is other evidence of its former existence. Bird (1987) reports evidence for over 8,000 m of Upper Cretaceous deposits in the same foredeep farther to the west in NPRA, where the deformation front has not progressed northward since latest Cretaceous earliest Tertiary time. Bird and Bader (1987), working with well data, report that over 7,500 m of Brookian sediments were deposited in the foredeep just northwest of ANWR. To the east, in the MacKenzie Delta region, they report over 9,400 m of Tertiary section alone.

If 4-6 km of section was removed from the top of the Bathtub Ridge and Arctic Creek sections, the eroded material must have been deposited elsewhere. Deposition in the Colville Trough has been prograding east along the strike of the mountain front during the formation of the Brooks Range (Bird, 1987). Material shed northward from the NEBR during Late Cretaceous and Tertiary time would probably be deposited in the foredeep to the northeast of the source. The thickness of Tertiary deposits to the northeast ($>9,400\text{ m}$) and to the northwest ($>7,500\text{ m}$) of the NEBR support the idea that 4 km of material could have been shed from the Bathtub Ridge and Arctic Creek regions.

If conditions 1-2 are accepted, fission track results require minimum uplift and denudation rates of between $\sim 2\text{ km}$ (geothermal gradient = $30^{\circ}\text{C}/\text{km}$) and $\sim 3\text{ km}$ (geothermal gradient = $20^{\circ}\text{C}/\text{km}$) in 3-5 m.y., over the temperature range $\sim 125\text{--}60^{\circ}\text{C}$. These correspond to minimum uplift and denudation rates of between $\sim 0.4\text{--}0.7\text{ mm yr}^{-1}$ ($30^{\circ}\text{C}/\text{km}$) and $\sim 0.6\text{--}1.0\text{ mm yr}^{-1}$ ($20^{\circ}\text{C}/\text{km}$). Uplift and denudation of the upper part of the Bathtub Ridge and Arctic Creek sections occurred over a 3-5 m.y. period, over a temperature range of 125°C to $\sim 50^{\circ}\text{C}$. These values give a rate for uplift and denudation of

between $\sim 0.5\text{--}0.8 \text{ mm yr}^{-1}$ (30°C/km) and $\sim 0.8\text{--}1.3 \text{ mm yr}^{-1}$ (20°C/km). Uplift and denudation of the Canning River section occurred over a 3-5 m.y. period, over a temperature range of 125°C to $\sim 60\text{--}70^\circ\text{C}$ giving rates of $\sim 0.4\text{--}0.6 \text{ mm yr}^{-1}$ (geothermal gradient = 30°C/km) and $\sim 0.6\text{--}0.9 \text{ mm yr}^{-1}$ (geothermal gradient = 20°C/km).

These rates are consistent with other reported rates of uplift from other orogenic areas. In the Himalayas, Zeitler (1985), reported rates for uplift and erosion as high as 0.2 to 0.5 mm yr^{-1} . In the European Alps, Clark and Jager (1969) calculated mean uplift and erosion rates of 0.4 to 1.0 mm yr^{-1} and Wagner *et al.*, (1977) reported values from different tectonic blocks ranging between 0.2 to 1.3 mm yr^{-1} . In the Lepontine Alps, Hurford (1986) reported mean rates of uplift and erosion of 0.5 mm yr^{-1} with local rates up to 2.2 mm yr^{-1} . In New Zealand, rates as high as 2.0 mm yr^{-1} have been reported (Harrison and McDougall, 1980).

The rates of uplift and denudation determined from the ANWR samples are also consistent with reported rates of denudation for mountain belts. In southeast Alaska, Corbel (1959) reported denudation rates of between $0.6\text{--}0.8 \text{ mm yr}^{-1}$. Bloom (1978) reported denudation rates between 0.5 and 1.0 mm yr^{-1} for Cretaceous alpine erosion in the Sierra Nevada. Using sedimentological evidence, Menard (1961) reported erosion rates for the Himalayas ranging from 0.2 mm yr^{-1} at 40 Ma to 1.0 mm yr^{-1} under present conditions. Dodson and McClelland-Brown (1985), infer erosion rates of 2.0 to 15.0 mm yr^{-1} for the western Himalayas on the basis of paleomagnetic and isotopic data.

The inferred rates for the NEBR are minima because the temperature range over which fission tracks in apatite can describe a thermal history is limited to approximately $<125^\circ\text{C}$. Vitrinite values show that some of the samples were buried to depths at which temperatures were much greater than 125°C , but neither vitrinite nor fission track data constrain the maximum depth to which the samples were buried.

SUMMARY AND CONCLUSIONS

The northeastern Brooks Range in the Arctic National Wildlife Refuge is part of a complex, northward-advancing fold and thrust belt. Apatite fission track results from this study indicate that the uplift and denudation events responsible for building the northeastern Brooks Range are younger to the north.

Bathtub Ridge

The fission track results from the Bathtub Ridge section indicate that rapid cooling during a 3-5 m.y. period occurred at ~62 Ma. This cooling event, believed to be related to uplift and denudation, brought the section up from temperatures greater than 125°C to ~50°C for the upper part of the section and to ~75°C for the lower part of the section. This indicates a cooling rate of ~20°C/m.y. and minimum rates of uplift between ~0.5 and 0.8 mm yr⁻¹ (geothermal gradient = 30°C/km) and 0.8-1.3 mm yr⁻¹ (geothermal gradient = 20°C/km). After this event, the section has undergone slower uplift at a rate on the order of ~0.03 mm yr⁻¹ (~2 km in 60 Ma) to reach present surface conditions.

Arctic Creek Region

The fission track results from the Arctic Creek exposures indicate that rapid cooling during a 3-5 m.y. period occurred at ~37 Ma. This cooling event, related to uplift and denudation, brought the section up from temperatures greater than 125°C to ~60°C. This gives a cooling rate of ~20°C/m.y. during uplift and denudation and a minimum rate of between 0.5 and 0.8 mm yr⁻¹ (geothermal gradient = 30°C/km) and 0.8-1.3 mm yr⁻¹ (geothermal gradient = 20°C/km). Since this event, the section has undergone slower uplift on the order of ~0.06 mm yr⁻¹.

Canning River Region

The fission track results from the Canning River exposures indicate two periods of rapid uplift, the first at ~45 Ma and the second at ≤ 32 Ma. The first uplift event may

explain the presence of an Eocene unconformity reported by Bruns *et al.* (1987) and Kelley and Foland (1987) (Fig. 6). Uplift and denudation in the region at ~45 Ma was followed by deposition of the Sagavanirktok Formation. Fission tracks in rocks below the unconformity record the uplift events whereas those from rocks above the unconformity reflect the history of the sediment source terrane. The ~67 Ma age from the Sagavanirktok Formation sample may represent a provenance age of material shed northward from the region uplifted during the event recorded in the Bathtub Ridge section.

ANWR Coastal Plain

The fission track and vitrinite reflectance results from the ANWR coastal plain exposures indicate that the rocks have not been subjected to temperatures necessary to reset apatite ages since deposition. The rocks from these exposures are thermally immature and thus it is not possible to determine an uplift/denudation history for the area since deposition. Instead, the apatite ages reflect the thermal histories of the sediment source terranes. One of the ages (~58 Ma) could possibly represent a provenance age of material shed northward from the region uplifted during the event recorded in the Bathtub Ridge section.

Overview of Proposed Uplift/Denudation History

It has been proposed (Namson and Wallace, 1986; Wallace and Hanks, 1988a, b, and in review) that Cenozoic shortening in the NEBR (Fig. 26) has been accommodated by a duplex thrust system (Fig. 27) consisting of a roof thrust and a floor thrust bounding a series of hinterland-dipping horses (e.g. Boyer and Elliot, 1983). The floor thrust of this proposed duplex is at depth in pre-Mississippian rocks, and the roof thrust is near the base of the Ellesmerian Sequence. The duplex thrust geometry requires that the faults formed from south to north in a forward-propagating thrust sequence (Boyer and Elliot, 1983).

TECTONIC MAP OF THE NORTHEASTERN BROOKS RANGE

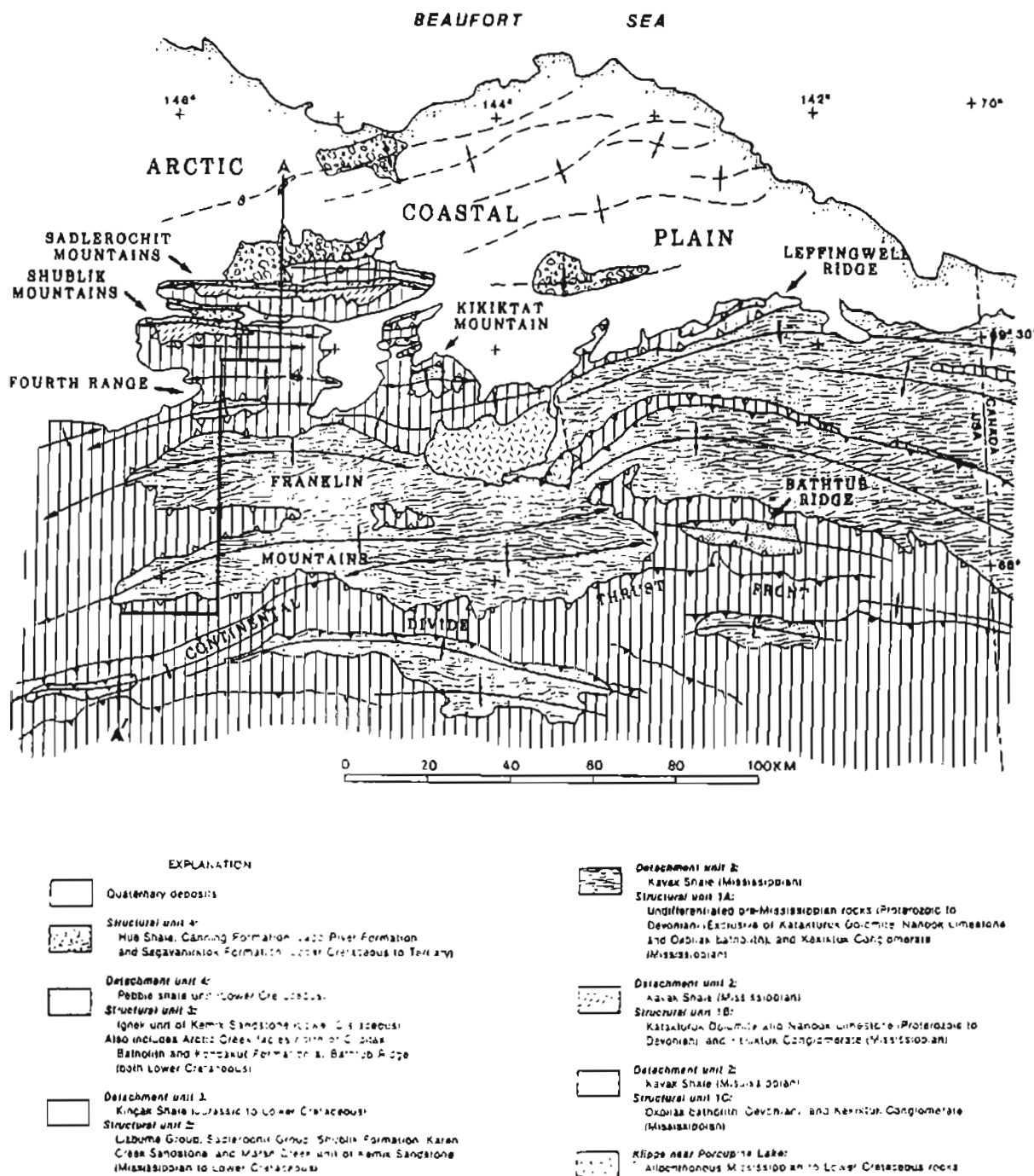


Figure 26. Tectonic map of the NEBR. (from Wallace and Hanks, 1988)

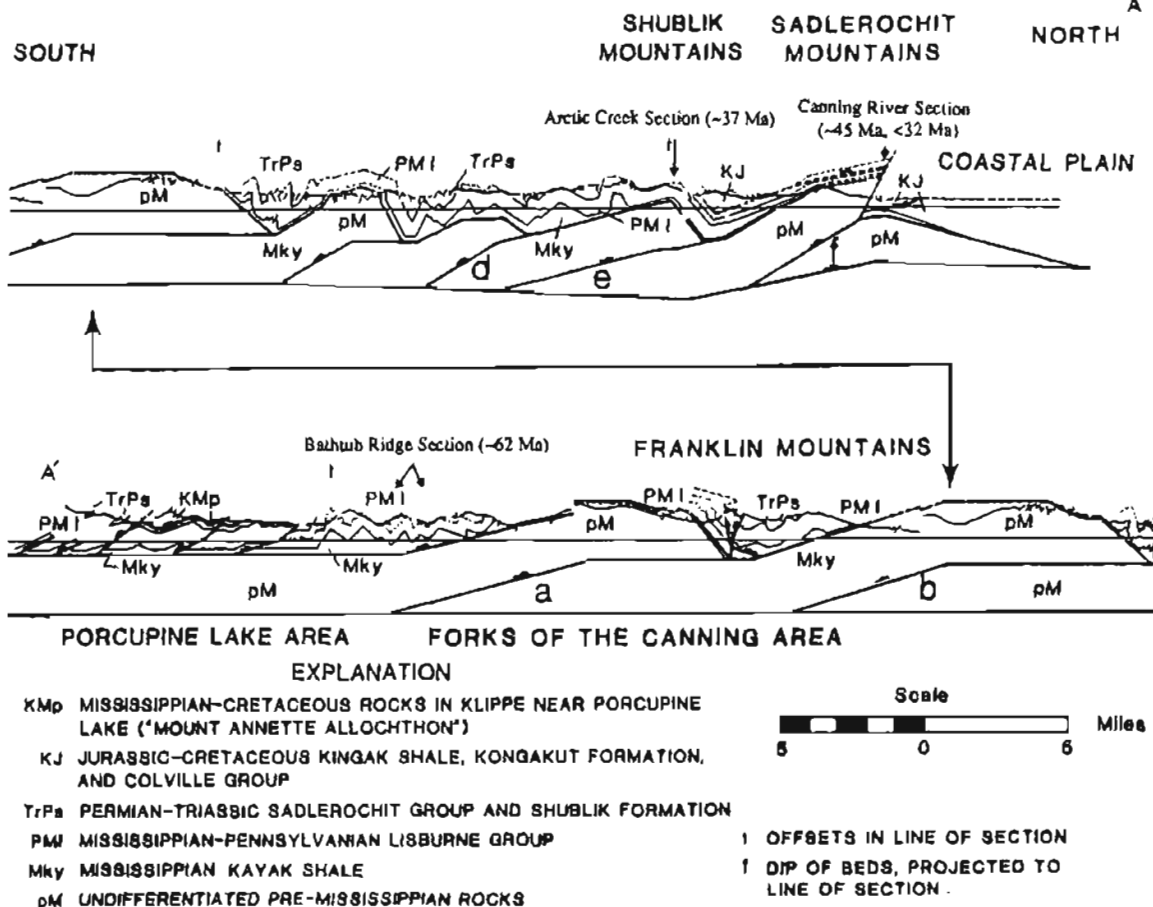


Figure 27. Preliminary cross-section across the NEBR. The apatite fission track ages for the Bathub Ridge section, the Arctic Creek area, and the Canning River section have been projected into equivalent structural positions along the line of section. Ages of displacement over footwall ramps decrease in age northward from a (~62Ma) to f (<32 Ma). See text for explanation. (Data projected onto cross-section described in Namson and Wallace, 1986)

Shortening in rocks above the duplex was accommodated by a combination of detachment folding and imbricate thrust faulting (Wallace and Hanks, 1988a, b, and in review).

Fission track results, discussed below in context with Figure 27, have been projected into the line of the section to the approximately equivalent structural position along strike. Because data are being projected from a considerable distance off the section, the specific structures and history on the line of section may differ from the areas sampled.

Before deformation began in the NEBR (Wallace and Hanks, in review), the Lower Cretaceous deposits at Bathtub Ridge and the Arctic Creek area were deposited in a foredeep to the north of the front of the ancestral Brooks Range (Bird *et al.*, 1987). Deformation during Paleocene time (~62 Ma) resulted in the emplacement of a major horse above ramp (a) in the Franklin Mountains, resulting in the rapid uplift and denudation of the Bathtub Ridge section. Continued shortening resulted in the migration of the deformation front northward and formation of subsequent horses. At ~37 Ma (~Eocene-Oligocene boundary) displacement occurred over ramp (e) resulting in the rapid uplift and denudation of the Arctic Creek exposures. The Canning River exposures to the west of the Sadlerochit Mountains underwent two phases of uplift and denudation. The first occurred during the Eocene (~45 Ma) and the second occurred during the last 32 m.y, both over ramp (f). The first uplift event may have resulted in a regional unconformity on which subsequent deposition of the Sagvanirktok Formation occurred. The ANWR coastal plain surface exposures are thermally immature where studied and do not show any fission track annealing effects due to uplift associated with the advancing fold and thrust belt. Uplift due to deformation in the coastal plain has been insufficient to expose rocks which have been buried deeply enough for fission track annealing to occur.

APPENDIX A

FISSION TRACK ANALYSIS: A SUMMARY OF THE TECHNIQUE AND INTERPRETATION OF RESULTS

INTRODUCTION

Fission tracks are damage zones formed as charged particles, produced by fission of a heavy atom (^{232}Th , ^{235}U , and ^{238}U), pass through a crystal lattice. It is assumed for all practical purposes that all fission tracks have come from ^{238}U because ^{232}Th and ^{235}U possess very low fission decay rates compared to ^{238}U (Naeser, 1979a). ^{238}U decays by both spontaneous fission and alpha particle emission but alpha particles themselves do not create tracks in natural minerals (Fleischer *et al.*, 1975).

The density of spontaneous fossil tracks is proportional to the length of time during which tracks have accumulated and to the ^{238}U concentration of the sample. The concentration of ^{238}U can be determined by irradiating the sample alongside a standard in a nuclear reactor, using a monitored thermal neutron flux. Thermal neutrons in the reactor induce fission in a fraction of ^{235}U present in the sample. A count of the induced tracks produced from the decay of ^{235}U can be related to the ^{238}U concentration using the constant $^{235}\text{U}/^{238}\text{U}$ ratio in natural materials (7.252×10^{-3}). By determining the ratio of fossil tracks to induced tracks, a geological age can be determined. The ratio of ^{238}U to fission track density is analogous to the ratio of parent to daughter isotopes in other radiometric dating systems.

FISSION TRACKS AND FISSION TRACK TECHNIQUES

The Formation of a Fission Track

A fission track is formed when a nucleus of an element such as uranium undergoes fission. Fission decay results in two fast-moving highly-charged fission fragments

recoiling from each other in opposite directions due to electrostatic repulsion. The best explanation for the formation of fission tracks is the "ion explosion spike" (Fleischer *et al.*, 1975) (Fig. A1). A "burst" of ionization along the path of the charged particles creates an electrostatically unstable array of adjacent ions which eject one another from their normal sites into interstitial positions. As the fission fragment passes, it strips electrons and leaves a zone of net positive charge in its wake. This causes the remaining positively-charged ions along the particles path to repel each other, forming the track or damage zone. Some have speculated that a phase change occurs in the vicinity of the fission track.

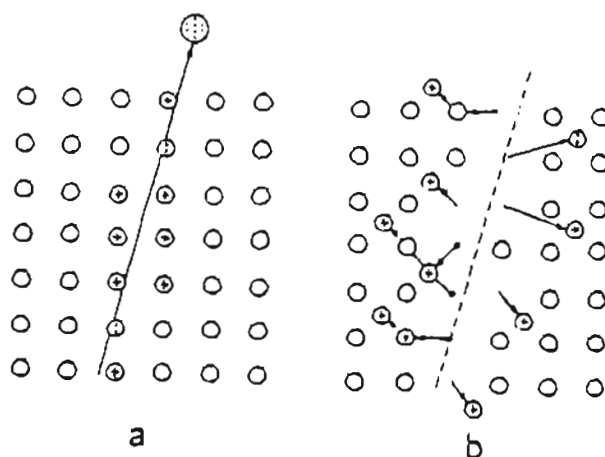


Figure A1. The ion explosion spike mechanism for track formation in a simple crystalline solid; (a) atoms are ionized by passage of a massive charged particle (fission fragment), (b) causing instability and ejecting ions into the lattice by mutual repulsion (after Fleischer *et al.*, 1975).

The resultant track is only a few angstroms wide and $\sim 10\text{-}20\text{ }\mu\text{m}$ long (Naeser, 1979a). It remains stable in all insulating solids, but conducting and semi-conducting solids do not retain tracks as movement of electrons rapidly neutralizes the ions produced. These tracks can be observed by transmission electron microscopy but the electron beam anneals them

quickly. It is also possible to observe them under a petrographic microscope once the tracks have been revealed by chemical etching.

Track Etching

Fission tracks are made visible by chemical etching because the etchant preferentially attacks the highly disordered (glassy?) material along the track. The geometry of track etching is determined by the simultaneous action of two etching processes (Gleadow, 1984). These are the rate of etching along the particle track surface at a linear rate (V_T) and the rate of etching along an undamaged surface, or bulk etching rate (V_G). Selective etching of a track depends on V_T being greater than V_G , with the shape of the resulting track being dependent on the difference between these two etching rates. For example, if $V_T \gg V_G$, a narrow conical track is produced (Fig. A2). If V_T is only slightly greater

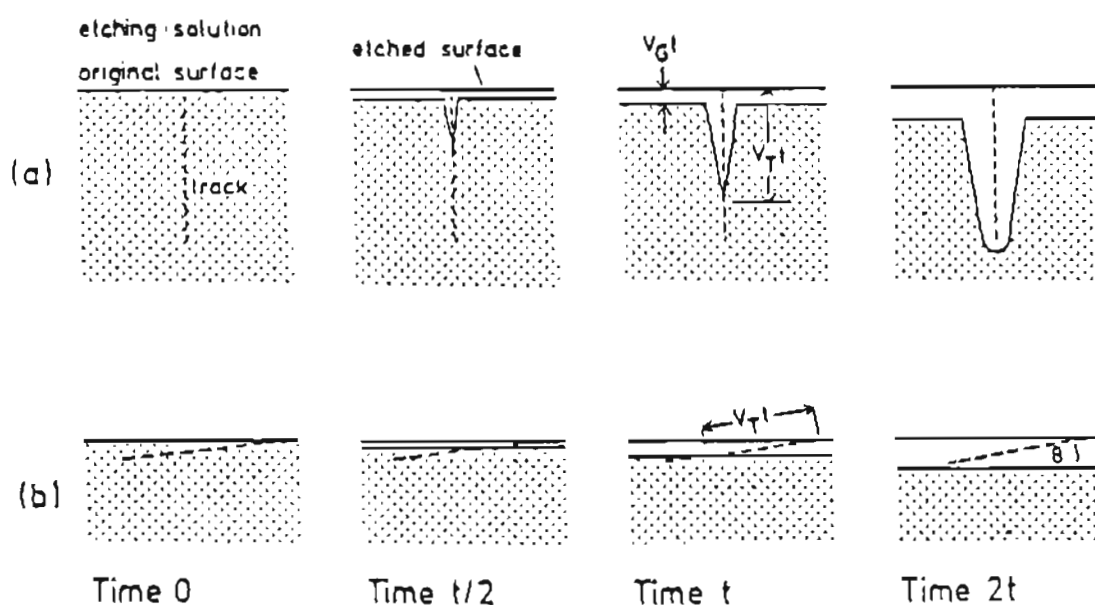


Figure A2. Track geometry showing $V_G t$ (bulk surface etching with time) and $V_T t$ (track etching with time). Tracks intersecting the surface at angles less than the critical angle ϕ will not be revealed. See text for explanation (from Gleadow, 1984).

than V_G , a shallow, wide, poorly defined track results. Another factor that controls the observation of tracks is the angle at which a track intersects the surface. Tracks intersecting the surface at less than the minimum intersection angle ϕ are not revealed by etching because the vertical component of V_T is not as great as V_G (Fleischer and Price, 1963) (Fig. A2). Therefore, where ϕ is greater than zero, an etching efficiency (π) exists, defined as the fraction of tracks intersecting a given surface that are actually etched on the surface. Only those tracks intersecting at angles greater than ϕ (defined by $\sin\phi = V_T/V_G$) will be revealed by etching.

The concepts of V_T and V_G explain track etching well for isotropic minerals, however V_G is anisotropic in most minerals (Fleischer *et al.*, 1975). This anisotropy is reduced by accumulating radiation damage from the alpha decay of uranium and thorium in the host mineral (Gleadow, 1978). Working with sphene, Gleadow, (1978) found that the mineral became more isotropic with accumulating radiation damage causing progressive change in the etching characteristics of fission tracks. The consequences of anisotropic etching (shape of etched fission tracks with different crystallographic orientations and different V_G values on different crystallographic planes) and accumulated radiation damage are discussed in more detail by Gleadow (1981) and Gleadow (1984).

Etching Conditions

In order to reveal tracks clearly it is important to establish proper etching conditions. Under-etching results in tracks being faint and easy to miss so that track density is underestimated. Over-etching makes it difficult to distinguish tracks from other etch features or intersecting tracks. Apatites of widely different composition and age seem to be very consistent in their etching behavior, unlike sphene and zircon; therefore an etching time of approximately 20 seconds in 5 mol HNO_3 at 20°C is sufficient to reveal fission tracks (Gleadow, 1984). Sphene and zircon have highly variable etching times dependent

on general radiation damage plus a number of other compositional and crystallographic features (Gleadow, 1978; Hurford and Green, 1982; Gleadow, 1984).

Fleischer *et al.* (1975) has summarized the characteristics of fission tracks which make them easily distinguishable from dislocations and other spurious etch pits. Fission tracks are randomly orientated linear defects of finite length with a limited thermal stability, and should have a statistical distribution related to spatial variation of uranium concentration.

Fission Track Dating Methods

Different fission track dating methods are described by Hurford and Green (1982) and Gleadow (1981). These include the population method and the external detector method (EDM). In the population method, the spontaneous and induced track densities are measured on two aliquots of the separated mineral grains. In the EDM, spontaneous and induced tracks are measured in exactly matching areas from the same internal surface of an individual crystal.

The EDM is now the most commonly used technique for fission track mineral dating. There are many advantages of the EDM, including the ability to date and analyze individual grains and its adaptability to automation. It also requires less counting times, gives more reproducible results, and requires less complicated handling after irradiation.

The External Detector Method

In this method spontaneous tracks are measured on an internal surface of a mineral grain. During irradiation induced tracks from ^{235}U are registered on an external surface of a detector mineral held in contact with the same surface on which the spontaneous tracks are counted. This detector, usually a sheet of low-uranium muscovite (<5 ppb), is subsequently etched to reveal the registered tracks. Spontaneous and induced tracks are counted in exactly matching areas from the same surface plane of an individual crystal so

that inhomogeneity in uranium concentration between grains and within grains is not a problem as it is with the population method.

Since dating involves determining ages for individual grains it is important to avoid selecting grains that are badly etched or contain dislocations. When selecting grains one should count only grains which have a low V_G , identified by the presence of sharp polishing scratches. Scratches indicate a very slow bulk etching rate for that exposed surface and hence a high etching efficiency for tracks (Gleadow, 1978). Other features one looks for when selecting grains include alignment of etch pits elongated along the c-axis, and optical characteristics which indicate that the surface is parallel to the c-axis.

Gleadow (1978) and Hurford and Green (1982) discuss the EDM in more detail. Hurford and Green (1982) also conclude that sphene and zircon, which are known to accumulate alpha-recoil damage, can only be dated reliably by the EDM. This is because laboratory annealing used in the population method removes the alpha-recoil damage as well the spontaneous fission tracks thereby restoring the initial highly anisotropic pattern of bulk etch rates. An overestimation of age with sphene can result because etching of the induced tracks in the annealed sphene will be anisotropic and weakly etched tracks may be overlooked during counting.

THE FISSION TRACK EQUATION, ZETA CALIBRATION, AND ERROR ANALYSIS

The Fission Track Equation

The fission track age equation is a specialized form of the general age equation used in all other forms of radiometric dating (Gleadow, 1984). In fission track dating however, the ratio of daughter atoms to parent atoms remaining is a function of the ratio of spontaneous to induced track densities of the form (Price and Walker, 1963):

$$T = \frac{1}{\lambda_D} \ln \left(1 + \frac{\lambda_D \phi \sigma I \rho_s}{\lambda_f \rho_i} \right) \quad (1)$$

- I = isotopic ratio $^{235}\text{U}/^{238}\text{U} = 7.252 \times 10^{-3}$ (Conran and Adler, 1976).
 λ_D = total decay constant for $^{238}\text{U} = 1.55125 \times 10^{10} \text{ yr}^{-1}$ (Jaffey *et al.*, 1971).
 λ_f = spontaneous fission decay constant of ^{238}U ; two values, 6.85 or $8.42 \times 10^{-17} \text{ yr}^{-1}$ (Fleischer and Price, 1964; Galliker *et al.*, 1970); see following page for explanation.
 σ = thermal neutron cross section for $^{235}\text{U} = 580 \times 10^{-24} \text{ cm}^2$ (Hannah *et al.*, 1969).
 ϕ = thermal neutron fluence.
 ρ_s = spontaneous track density.
 ρ_i = induced track density.

Two or more standard glass/mica pairs are included in each irradiation package to monitor neutron fluence and the possible presence of a gradient along the package. The standard glass (NBS glass SRM612) contains uniform U concentration (~50 ppm) that produces manageable track densities in the mica detectors. The flux is directly related to the track density in the mica ρ_d by:

$$\phi = B \rho_d \quad (2)$$

where B is a calibration constant for the standard glass ($\sim 5.736 \times 10^9$; Hurford and Green, 1983).

To determine an age using equation (1) requires the measurement of ρ_s and ρ_i , the determination of neutron fluence (ϕ), and the use of the constants B and λ_f . The use of this equation, its systematics, and calibrations have been reviewed by Hurford and Green (1982).

The value of the spontaneous fission decay constant for ^{238}U (λ_f) has been in doubt for some time. Fleischer and Price (1964) reported a value $6.85 (\pm 0.20) \times 10^{-17} \text{ yr}^{-1}$ based on a comparison of fission track dates of tektites with K-Ar dates. However, when the effect

of track fading, causing decreased ages, is taken into consideration, a value of $8.4 \times 10^{-17} \text{yr}^{-1}$ is obtained (Storzer and Wagner, 1971). A more precise determination is by Galliker *et al.*, (1970), who reported a value of $8.46 (\pm 0.06) \times 10^{-17} \text{yr}^{-1}$. This value for λ_f was confirmed by Storzer (1970) and Wagner *et al.*, (1975). Both values ($6.85 \times 10^{-17} \text{yr}^{-1}$ and $8.46 \times 10^{-17} \text{yr}^{-1}$) have been used for dating by the fission track method (e.g. Gleadow and Lovering, 1974; Bar *et al.*, 1974).

The value of B is often determined against independent measurements of the fluence or by reference to fission track dating of an age standard using an assumed value of λ_f . Green and Hurford (1984), report that neutron dosimetry using activation foils can be extremely unreliable. They also report that reproducibility of fluence calibrations between different laboratories is poor and that this is expected because in many cases determinations of λ_f have depended of fluence measurements (Hurford and Green, 1982). They concluded that any value of λ_f calculated using a system of thermal neutron dosimetry is only valid for that system.

Zeta Calibration

Fission track dates are subject to systematic errors arising from the uncertainty of λ_f and from difficulties with measurements of the neutron dose (ϕ). Hurford and Green (1982) proposed that until independent values of λ_f and ϕ are known, fission track dating should be empirically calibrated against independently known ages. Substituting equation (2) into equation (1) gives:

$$T = \frac{1}{\lambda_D} \ln \left(1 + \frac{\rho_c}{\rho_i} \sigma I \lambda_D \left(\frac{B \rho_1}{\lambda_f} \right) \right) \quad (3)$$

The constants in equation (3), except for λ_D (which effectively cancels out for young ages under 100 Ma) can be grouped into a single factor, "zeta" (ζ) which is calibrated directly from age standards.

$$\zeta = \frac{e^{\lambda_D T_{STD}} - 1}{\lambda_D (P_s/P_i)_{STD} P_d} \quad (4)$$

Equation (3) becomes:

$$T = \frac{1}{\lambda_D} \ln \left(1 + \lambda_D \zeta \frac{P_s}{P_i} P_d \right) \quad (5)$$

Ratios of counts obtained over different standard glasses in common use in laboratories have been given by Hurford and Green (1983) and Green (1985).

Personal Zeta Calibration

I used three apatite standards for zeta calibration before any unknowns were counted. The three standards were the Fish Canyon Tuff (27.9 ± 0.7 Ma), Durango apatite (31.4 ± 0.5 Ma), and Mt. Dromedary apatite (98.7 ± 1.1 Ma). These three standards are discussed by Hurford and Green (1983) and Green (1985). My results are listed Table A1; the weighed mean zeta of 352.7 was used when determining unknown apatite ages in this study.

Determination of Error

The fundamental assumption of fission track statistics is that track counts, like radioactive decay, will follow a poisson distribution. The "conventional analysis" of errors (e.g. Lindsay *et al.*, 1975) assumes that no further sources of variation are present in the measurement of track densities. Green (1981), in his discussion on the use of statistics in fission track dating, discusses this assumption in detail. For a poisson distribution the

Table A1. Fission Track Counting of Standards for Personal Zeta Determination

Sample number	Number of grains	Standard track density ($\times 10^6 \text{cm}^{-2}$)	Fossil track density ($\times 10^5 \text{cm}^{-2}$)	Induced track density ($\times 10^6 \text{cm}^{-2}$)	Correlation coefficient	Zeta
Durango apatite						
8122-3B	20	1.422 (321)	1.987 (2353)	1.456	0.824	324.5
8122-3A	15	1.422 (218)	1.700 (1927)	1.503	0.354	391.3
8122-3B	15	1.422 (234)	2.200 (1734)	1.630	0.981	328.1
Sample Mean Zeta = 348.0						
Fish Canyon tuff						
72N8-24	20	1.422 (336)	2.192 (2856)	1.863	0.754	333.1
72N8-01	20	1.422 (298)	1.860 (2845)	1.775	0.903	374.1
Sample Mean Zeta = 353.6						
Mt. Dromedary apatite						
8322-39	20	1.422 (884)	10.57 (2216)	2.651	0.781	350.7
8322-42	20	1.422 (767)	8.708 (2004)	2.275	0.771	365.5
8322-39	20	1.422 (775)	12.64 (1962)	3.201	0.857	354.1
Sample Mean Zeta = 357.8						
Overall Mean Zeta = 352.7						

Number of tracks counted are given in parenthesis. Standard and induced track densities are measured on mica detectors, and fossil track densities on internal mineral surfaces.

standard deviation S of a track count is given by the square root of the total number of tracks counted N :

$$S = \sqrt{N} \quad (6)$$

A standard deviation can be assigned to each track density measurement used in calculating a fission track age. These errors are combined to give the standard deviation of the age S_T :

$$S_T = T \sqrt{(1 / N_s) + (1 / N_i) + (1 / N_d)} \quad (7)$$

where N_s , N_i , and N_d are the total number of tracks counted for spontaneous, induced, and standard glass track densities. Other non-poissonian sources of variation are possible

(Green, 1981; see below) so the conventional analysis (equation 7) is actually a limiting best case.

The EDM is designed so that sampling problems should be eliminated because both ρ_s and ρ_i ideally originate from the same amount of uranium. Therefore, ρ_s and ρ_i should give approximately the same ratio within the variation allowed by the poisson distribution. However, when using the EDM, some experimental factors can make this "ideal case" unattainable:

- [1] Careless counting of track-like features as tracks leads to an overestimate of ρ_s . This results in determination of an incorrect older age. Experience in the careful identification of tracks is necessary to overcome this factor.
- [2] Poor contact between the grain mount and mica detector results in a lower ρ_i as fewer induced tracks are recorded in the detector. This leads to a higher ρ_s/ρ_i ratio and hence an older age. Bad contact over a large region of the mount can be recognized by the absence of shallow-dipping tracks and blurred replicas of grain boundaries in the mica. Apatite grains adjacent to zircon grains should not be counted as the higher relief of the zircon may result in poor contact locally and a decrease in ρ_i .
- [3] High track densities make determination of true ρ_s/ρ_i difficult. A high spontaneous track density makes determination of the correct ρ_s difficult whereas a high induced track density does the same for ρ_i .
- [4] A low ρ_i makes location of the grain replica and the correct counting area difficult and in some cases, next to impossible. This can be overcome by subjecting the sample to sufficiently large neutron fluences in the reactor.
- [5] Incomplete etching of tracks leads to an underestimate of either ρ_i or ρ_s . Overetching may also result in an underestimate of either ρ_i or ρ_s as it is difficult in this case to

distinguish between tracks when they overlap. Overetching also results in the loss of short tracks.

[6] Spontaneous tracks may not be completely revealed. Zircon or sphene grains containing different spontaneous track densities or compositions will etch at different rates due to differing degrees of alpha damage. Therefore, at any given etch time, tracks will be completely revealed only for a limited range of ρ_s . Below this range, tracks are incompletely revealed, whereas at high ρ_s tracks are lost. Therefore at either low or high track densities, the measured values may be depressed, leading to low ρ_s/ρ_i ratios.

[7] Incorrect identification of the crystal or mica "mirror image" may yield totally incorrect ρ_s/ρ_i ratios. This problem can be eliminated by using a meticulous and careful technique.

[8] Spatial variation of the thermal neutron fluence may occur in the nuclear reactor and cause problems (Burchart, 1981). Standard glasses, included within a package of irradiated samples, are used to determine ρ_d and check on uniformity of fluence on a scale of centimeters. If the neutron fluence is not consistent on this scale, this might introduce an additional variation in ρ_s/ρ_i .

[9] Uranium may be vertically heterogeneous in the apatite grain (Burchart, 1981): ρ_i is measured in a mica detector exposed to fissions occurring below the sample surface, while ρ_s originates from fissions occurring both above and below the exposed sample surface. Therefore, in relating ρ_s to ρ_i , it is assumed that the amount of uranium above and below the sample surface is identical over the range of a fission event ($\sim 15\text{-}20\text{ }\mu\text{m}$).

All of the above experimental factors are capable of introducing non-poissonian variations to or errors in the measured values of ρ_i and ρ_s , and, therefore, to the final age determination. However, with experience and careful sample preparation, factors [1] through [7] should be neutralized. Factors [8] and [9] plus contamination may be impossible to identify. The conventional method (equation 7) allows no check to be made

on the way in which the data are affected by the above factors (Green, 1981). Thus, the final estimate of ρ_s/ρ_i may be strongly affected by data with a non-poissonian variation.

A χ^2 test can be used to test whether variation is present in excess of that predicted from poisson statistics and determines whether or not the data represents a single population (Galbraith, 1981). In geological situations, failure of the χ^2 test usually indicates that some external factor is acting on the variation of ρ_s/ρ_i . This is not always the case. Green (1985) has shown that an age determination can fail the χ^2 test by chance alone when non-poissonian errors were not present. For those instances when the value of χ^2 was not acceptable, Green (1981) determined that the mean of individual grain ratios of $\rho_s/\rho_i (\pm 1\sigma)$ takes into account non-poissonian variation where present and gives a more realistic estimate of the precision of the determination of ρ_s/ρ_i . The value of ρ_s/ρ_i is then:

$$\rho_s/\rho_i = \left(\frac{(\rho_s/\rho_i)}{n} \right) \quad (8)$$

and its standard deviation is:

$$\sigma(\rho_s/\rho_i) = \frac{\sqrt{\sum (\rho_s/\rho_i)^2 - (\sum (\rho_s/\rho_i))^2}}{n(n-1)} \quad (9)$$

The same analysis is often applied to results obtained by both the EDM and the population method. While this is valid for the EDM in most cases, it will be valid for the population method only in the case where the uranium concentration is the same for all the grains. Where there is a variation in uranium between grains, which is likely in most cases, the uncertainty calculated from equation (7) will be an underestimate.

APATITE FISSION TRACK LENGTHS

The length of fission tracks is an important parameter because tracks decrease in length (anneal) in response to time and temperature (Wagner and Storzer, 1972) and hence can be used as geothermometers. During the annealing of fission tracks, the effects of both time and temperature are important. A higher temperature for a shorter period of time can anneal tracks the same amount as a lower temperature over a longer time span.

Fission Track Annealing

Annealing has been discussed in detail by several authors: laboratory annealing by Naeser and Faul (1969), Storzer and Wagner (1971), and Wagner (1986); natural annealing by Naeser (1979a), and Gleadow and Duddy (1981); and fission track length annealing by Green *et al.* (1985a, 1986).

Laboratory Annealing Studies: In laboratory annealing studies, a mineral is heated for varying periods of time at different temperatures. The degree of observed track density reduction with time and temperature is presented on an Arrhenius plot which relates the logarithm of time to the inverse of temperature. Early studies investigating the annealing properties of apatite found that heating apatite for a period of one hour produced total track annealing between 250° and 350°C (Naeser and Faul, 1969; Wagner, 1968). An Arrhenius plot representing the data (Figure A3: from Naeser and Faul, 1969), could then be used to extrapolate to a time period of 1 m.y. where 100% annealing would occur at ~175°C. The slope of the lines on the plot increase from that for 100% track retention to that for total track loss, with the difference in the slope of these two extremes ranging by a factor of 2 or 3 (Green *et al.*, 1985a). This *fanning array* has been interpreted in terms of activation energies increasing with degree of annealing (Storzer and Wagner, 1971). However, in another study, Wagner (1986), found a parallel-type Arrhenius plot describing a single activation energy when he carried out an annealing experiment on a single apatite crystal.

Natural Annealing Studies: A more direct way to study fission track annealing in apatite under geologic conditions is to look at the change in apatite age with depth in a drill hole (Naeser, 1981; Gleadow and Duddy, 1981). In three studies (Naeser and Forbes,

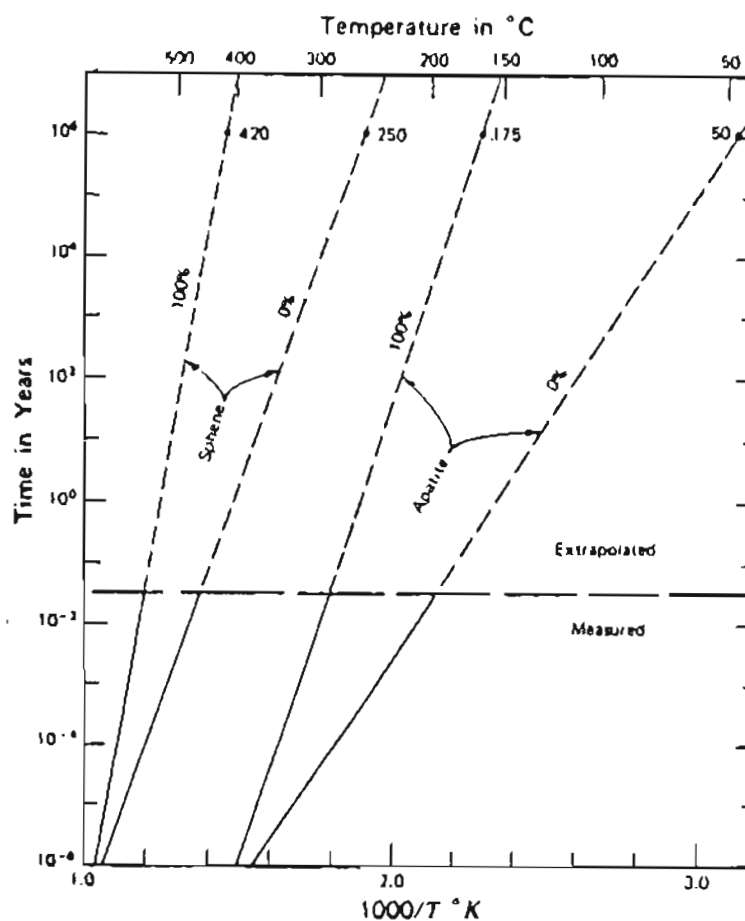


Figure A3. Results of a laboratory study of fading of fission tracks in apatite and sphene. The lines marked 0% indicate temperature and time periods in which no tracks are lost. The lines marked 100% indicate temperature and time periods at which all tracks are lost (from Naeser and Faul, 1969).

1976; Naeser, 1979a; Gleadow and Duddy, 1981), apatite fission track ages relative to depth in drill holes were reported. Naeser and Forbes (1976) found that apatite fission track ages decreased from 100 Ma at the surface to 12 Ma at 3000 m ($\sim 95^{\circ}C$ present

downhole temperature) in the Eielson Air Force Base, Alaska, deep drill hole. Naeser (1979a) reported a zero apparent age at 2000 m depth ($\sim 135^{\circ}\text{C}$ present downhole temperature) from the Los Alamos, New Mexico, geothermal test wells 1 and 2. Gleadow and Duddy (1981), studying apatites from drill-holes located in the Otway Basin of southeastern Australia, identified both the top and the base of the track annealing zone. In this basin, stratigraphic evidence indicates that the sediments reached their maximum depth of burial at ~ 30 Ma and have essentially remained at this depth in a uniform temperature regime since then. Apatite ages start to decrease downhole at $\sim 60^{\circ}\text{C}$ (Fig. A4), are reduced by about half at $\sim 95^{\circ}\text{C}$, and reach zero at $\sim 125^{\circ}\text{C}$. The entire partial stability zone was therefore revealed. Combining their results with laboratory data from Wagner (1968) and Naeser and Faul (1969), Gleadow and Duddy (1981) constructed an Arrhenius plot (Fig.

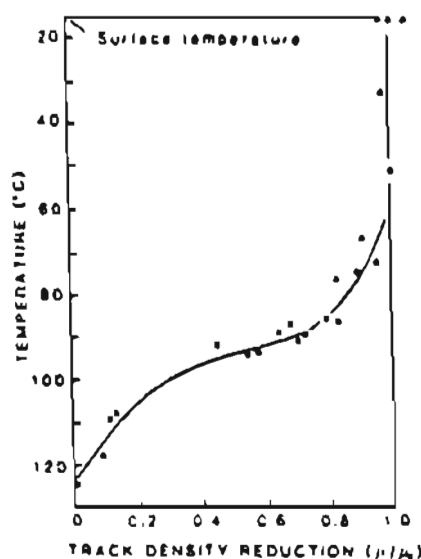


Figure A4. Variation in apparent apatite fission track age with down-hole temperature in wells of the Otway Basin, South Australia. Ages here are expressed as a fraction of their original age (120 Ma) giving a measure of p/p_0 , the ratio of fission track density after and before natural annealing (from Gleadow and Duddy, 1981).

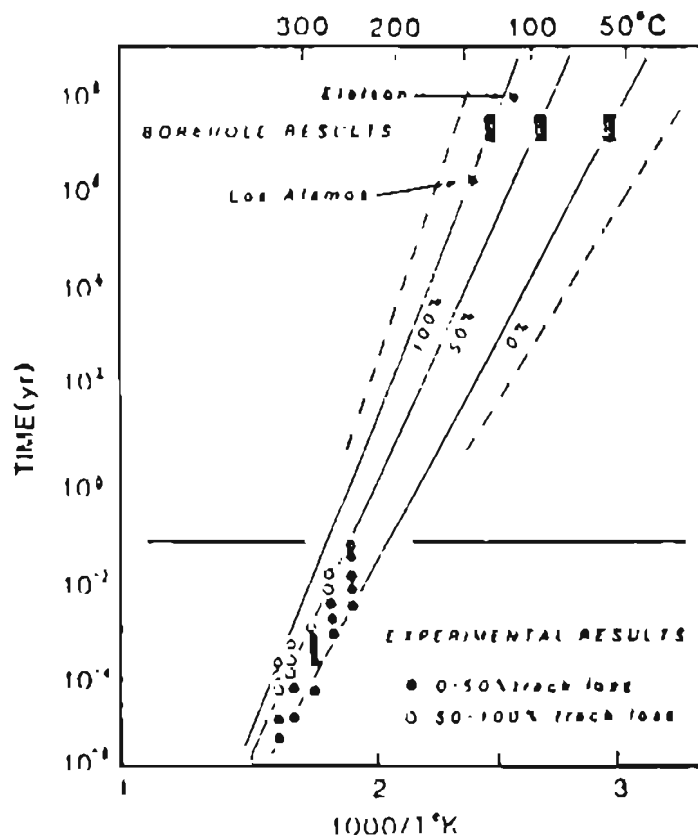


Figure A5. Arrhenius plot for fission track fading in apatite. Shows results from the Otway Group drill-hole data, laboratory annealing results of Naeser (1969) and results from the Eielson, Alaska, and Los Alamos, New Mexico deep drill-holes (Naeser, 1979). Dashed lines represent the 0 and 100% track loss lines extrapolated from laboratory annealing data alone (from Gleadow and Duddy, 1981).

A5). This plot shows that the temperature interval over which annealing occurs at geological time intervals is less than that predicted from laboratory studies. The variation of mean track length of confined tracks with change in depth and temperature down a drill hole has also been studied (Gleadow and Duddy, 1981; Gleadow *et al.*, 1983). Proportional lengths were expressed as a ratio of L (present measured length) over L_0 (the average length of fresh induced tracks in apatite). The results showed the mean lengths to be reduced relative to the original length of $16.4 \pm 0.8 \mu\text{m}$ even in surface samples and that some long tracks still existed in samples that were 90% reduced in age. Plotting track length reduction versus temperature, they were able to locate the apatite partial stability zone

in the Otway Basin as being between the temperatures of $\sim 60^{\circ}$ - 70° and 125°C for times in the order of 10 m.y. They concluded that the unique contribution of apatite fission track analysis is the ability to define maximum paleotemperatures and variations in temperature through time. Gleadow and Duddy (1981) also observed that single grain ages varied considerably for samples in the partial stability zone. They suggested that this indicated that different apatites can have different annealing properties, presumably controlled by apatite composition.

The Effect of Composition on Apatite Annealing

Gleadow and Duddy (1981) proposed that chemical composition of individual apatite grains must play some part in the considerable spread of *single grain ages* from apatites subjected to temperatures within the partial stability zone. Green et al. (1985a) analyzed apatite grains from a single sample residing within the partial stability zone in an Otway Basin borehole. This sample displayed wide variation in single grain ages. The age for the bulk sample was 53 ± 2 Ma, but single grain ages ranged from 0 to 120 Ma. The single grain ages were plotted against the number of Cl atoms per $\text{Ca}_{10}(\text{PO}_4)_6(\text{F},\text{OH},\text{Cl})_2$ molecule (Fig. A6). Cl-rich grains are observed to be more resistant to annealing than F-rich grains.

Fission Track Length Annealing Studies

In a laboratory study of confined induced fission track lengths in a single, previously annealed, Durango apatite crystal, Green *et al.*, (1985a), determined a single activation energy (~ 1.64 eV). This implied a near parallelism of lines on the Arrhenius plot for various degrees of length reduction. Because the annealing characteristics of individual apatite grains are strongly controlled by Cl content, they suggested that the widely fanning Arrhenius plots could be the result of the superposition of a series of near-parallel

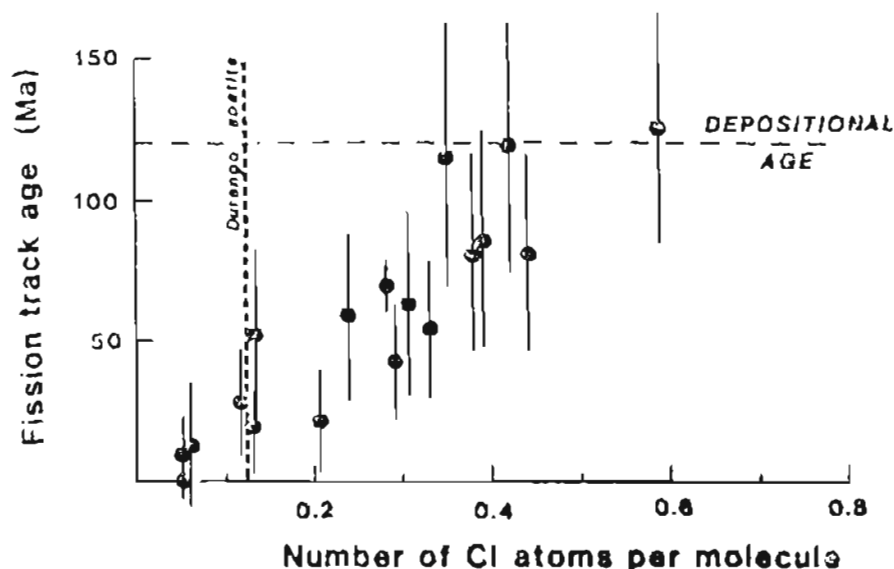


Figure A6. Variation of apatite single grain ages with composition. This sample is from the Otway Basin S. Australia. Composition is expressed as a number of Cl-atoms in the (F, OH, Cl) group of the apatite molecule. This shows Cl-rich grains are more resistant to annealing than F-rich grains (from Green *et al.*, 1985a).

Arrhenius curves. Each curve would correspond to the range of compositions present and represent slightly different activation energies.

Green *et al.*, (1986) observed that in all annealed samples, the mean confined track length is always less than that in unannealed control samples. As annealing progresses, the mean length is reduced and the length distribution broadens, slowly at first, and then more rapidly below a length reduction (L/L_0) of ~ 0.65 . In addition, the anisotropy of annealing becomes more pronounced in apatite as annealing progresses. Tracks aligned parallel to the crystallographic c-axis are more resistant than tracks perpendicular to it. As the mean length decreases, the only tracks preserved are those more closely aligned parallel to the c-axis. In heavily annealed samples ($L/L_0 < 0.65$) sequential etching indicated the presence of non-etchable (in terms of normal etch times) gaps along the length of a small proportion

of tracks. These gaps, which delay the progress of the etchant during that process, are not common and may be breached with continued etching Green *et al.*, (1986).

A two-stage model for the annealing of fission tracks in apatite emerges. For mean lengths above $\sim 10.5 \mu\text{m}$ ($L/L_0 \geq 0.65$) the form of the track length distribution changes only slightly with the degree of annealing because the anisotropy is not very pronounced. Below $\sim 10.5 \mu\text{m}$, the form of the confined track length distribution changes rapidly as annealing progresses. The dominant process causes a shortening of the etchable portion of the track from each end, with the rate of shortening increasing with increasing angle to the c-axis. For a given combination of temperature and time there is a characteristic maximum etchable length, which depends on the orientation of the track. As annealing becomes severe, gaps may appear in the etchable portions which may delay the progress of the etchant. With continued etching the gaps may be breached, allowing the characteristic etchable length to be revealed. The observed length distributions thus result from a combination of the anisotropy of annealing, and to a much lesser degree, the presence of gaps (Green *et al.*, 1986).

Laslett *et al.*, (1987) used the results of Green *et al.*, (1986) to determine whether the results were best explained by a parallel or slightly fanning Arrhenius plot. The best fitting parallel model accounted for only 96.7% of the variation of transformed length reductions. A slightly fanning model gave the best match, accounting for 98.0% of the variation.

For a slightly fanning Arrhenius model:

$$\ln(t) = A(r) + B(r) T^{-1} \quad (\text{equation 20, Laslett } et al, 1987)$$

where: t = annealing time

T = absolute temperature

$r = L/L_0$

$A(r)$ = an unknown function of r subject to constraints that when $t = 0$ or $T = 0$,
 $r = 1$ so that: $A(1) = -\infty$

$B(r)$ = a function where B is normally interpreted in terms of E/K where K is Boltzmanns constant and E is an activation energy

This model is difficult to fit since $A(r)$ and $B(r)$ are unknowns. Therefore, by statistical means they derived the following preferred model (see also Fig. 7):

$$\left[\left\{ (1-r^{2.7}) / 2.7 \right\}^{0.35} - 1 \right] / 0.35 = -4.87 + 0.000168T [\ln(t) + 28.12]$$

(equation 27, Laslett *et al.*, 1987)

Measuring Fission Track Lengths

There are three ways of measuring fission track lengths:

[1] By measuring the projected lengths of tracks intersecting an exposed internal surface (Wagner and Storzer, 1972); [2] measuring the true length of tracks in an internal surface by measuring the vertical as well as the horizontal component of the track length and correcting for the dip of the track; or [3] measuring the true length of internal *confined tracks* (Fig. A7) which do not intersect the surface. Confined tracks, as defined by Lal *et al.* (1969), are tracks etched either via contact with a track which reaches the exposed surface or via a fracture or crack.

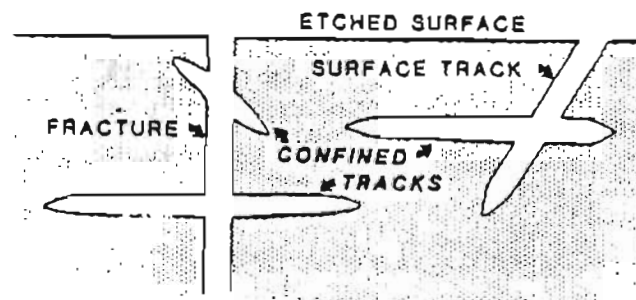


Figure A7. Confined fission track lengths as etched through fractures or other tracks (modified from Gleadow *et al.*, 1983).

To measure the true length of a confined track, one measures tracks present in the grain in a horizontal plane perpendicular to the line of sight. However, from a practical standpoint, it is possible to measure tracks that are not quite horizontal. Laslett *et al.* (1982) considered confined tracks with true dips $<15^\circ$ as horizontal because their measurement resulted in an underestimate of the actual length by only a few percent. With reflected light illumination, horizontal confined tracks exhibit a very bright image and can be easily located. This only occurs for tracks very close to horizontal. In transmitted light, a track is considered horizontal only if it remains in sharp focus along its entire length.

Confined tracks should be measured in prismatic grains (parallel to the c-crystallographic axis). This is because annealing in apatite is anisotropic causing tracks perpendicular to the c-axis to shorten faster than tracks parallel to the c-axis (Laslett *et al.*, 1984). Thus in a grain orientated parallel to the c-axis the whole range of track lengths will be present. In a basal section the mean track length will be shorter because the longest tracks will not be present.

In this study, confined fission track lengths in apatite were measured using the criteria outlined in Laslett *et al.* (1982, 1984) and Gleadow *et al.* (1986a, 1986b). To properly calibrate track length measurements I measured many track length standards with known distributions. Only after I displayed an acceptable level of competence determined by P.F. Green and A.J.W. Gleadow were the Alaskan samples measured for this study.

APATITE FISSION TRACK THERMAL HISTORIES

As previously discussed on page 29, annealing of fission tracks in apatite can be used to determine the thermal history of a sample. Gleadow and Duddy (1981), in a study of the annealing properties of apatite from subsurface samples in the Otway basin of southeastern Australia, defined a temperature range over which fission tracks anneal. In the Otway

Basin, apatite ages and mean track lengths began to decrease at $\sim 60^{\circ}\text{C}$ and reached 0 at $\sim 125^{\circ}\text{C}$ (Fig. A4). The entire apatite partial stability zone was therefore revealed and defined as $\sim 60\text{--}125^{\circ}\text{C}$ (based on the data in Fig. A4). Green (1986), presented data in which some annealing occurs even at ambient surface temperatures.

Track Length Distributions

Heating through the apatite partial stability zone, as track densities and mean track lengths decrease with increasing temperature, track length distributions have characteristic distributions relative to their length of residence time within the partial stability zone (Fig. A8). The transition from unaffected ages through partial overprints to total resetting is reflected in the shape of the track length distribution. For samples that were subjected to lower temperatures in the partial stability zone, track length distributions show a high mean

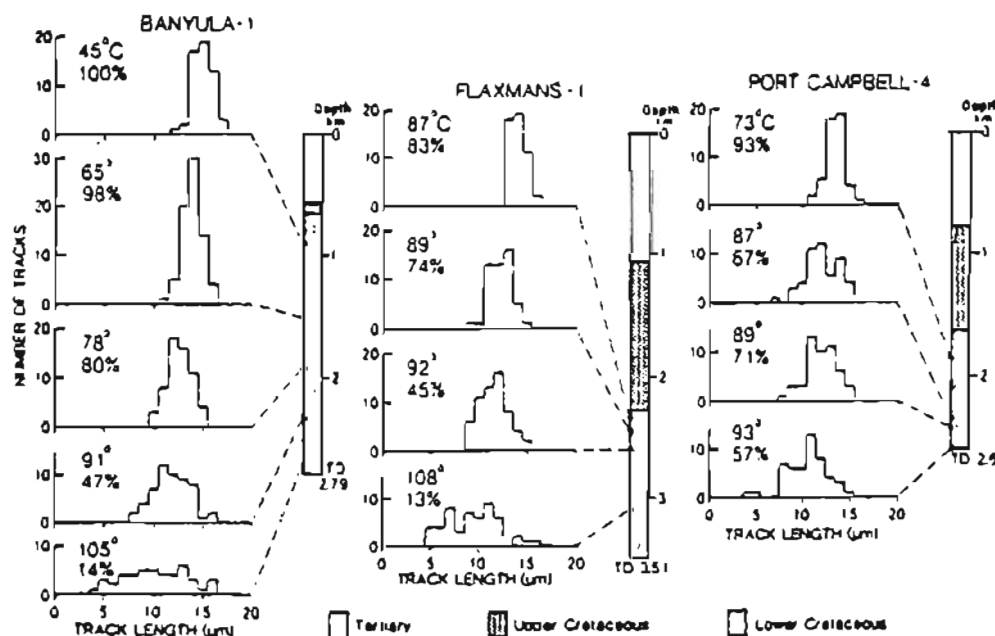


Figure A8. Fission track length distributions observed in apatites from the Otway Basin, South Australia, at various depths (temperatures) in three drill-holes. Estimated formation temperature and the percentage to which the apparent fission track age has been reduced is also shown (from Gleadow *et al.*, 1986a).

length with a low standard deviation. As temperature increases the length distribution broadens. This results in a decrease in the mean length and an increase in standard deviation. Samples from the base of the partial stability zone show very broad and relatively flat length distributions with mean lengths $\sim 50\%$ of the unannealed mean length. The maximum track length seen in the samples ($\sim 16 \mu\text{m}$) doesn't change because new tracks are continually being formed.

Several possible patterns of track lengths in apatites arising from distinct thermal histories as described by Gleadow *et al.*, (1983) are shown in Figure A9. This Figure shows a number of hypothetical temperature vs. time plots and the resulting track-length distributions. The examples A-C show simple burial histories giving unimodal apatite length patterns essentially in equilibrium with different levels in the partial stability zone.

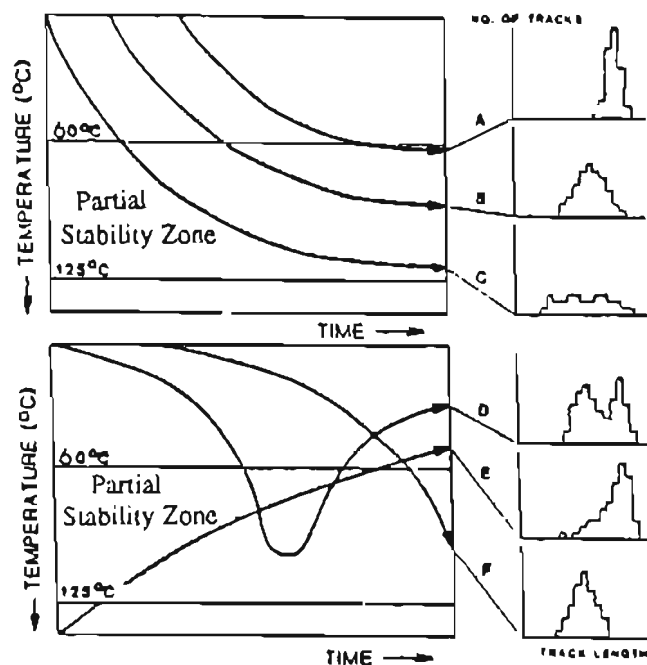


Figure A9. Idealized time-temperature paths with the resultant apatite track length distributions. See text for explanation (modified Gleadow *et al.*, 1983). The 60°C value for the upper boundary of the partial annealing zone is based on the work of Wagner *et al.*, 1977.

Examples D-F show a bimodal length distribution resulting from a past heating event, a skewed distribution typical of slow cooling through the partial stability zone, and an entirely shortened unimodal distribution produced by a recent temperature increase.

Bimodal distributions consist of two major length components: those that were annealed during a heating event and those that have formed since cooling to lower temperatures. By statistically separating the two components and estimating the contribution of the later group to the age of the mineral, the timing of the heating event can be estimated. Skewed distributions are essentially the summation of the three length distributions shown in simple burial. The shortened distribution resulting from a recent temperature increase is produced when all previous tracks are shortened together.

Gleadow *et al.* (1986b) determined apatite fission track length distribution patterns for a number of geologic environments. They divided confined track length distributions into five characteristic shapes (Fig. A10):

(1) Induced Track Length Distributions. Induced track length distributions from many apatite samples have mean track lengths which fall within a narrow range between 15.8 μm and 16.6 μm and have s.d. of $\sim 0.9 \mu\text{m}$ (Fig. A10a). It is reasonable to conclude that induced tracks in all apatite samples will have a distribution typified by a mean of $\sim 16.3 \mu\text{m}$ and a s.d. $< 1 \mu\text{m}$ (Gleadow *et al.* 1986b). Track length distributions of spontaneous tracks from a wide variety of different apatites can therefore be compared without the need to refer back to lengths of induced tracks in the same apatite sample (Gleadow *et al.* 1986b), as had been previously suggested by Green (1980).

(2) "Undisturbed Volcanic" Distributions. These distributions are characterized by mean lengths between 14.0 and 15.7 μm and s.d. from 0.8 to 1.3 μm (Fig. A10b) although most range from 0.8 to 1.0 μm . This type of distribution reflects rapid cooling after formation, and subsequent exposure to temperatures $< 50^\circ\text{C}$ (Gleadow *et al.* 1986b). An undisturbed

volcanic-type" length distribution can also be found in rocks of non-volcanic origin, where this distribution is diagnostic of a rapid cooling, followed by residence at low temperatures (<50°C).

(3) "Undisturbed Basement" Distributions. This form of distribution (Fig. A10c) is typical of plutonic rocks and high-grade metamorphic rocks that formed at high temperatures (>500°C) deep within the earth's crust, were uplifted with overburden removed by denudation and have now cooled to ambient surface temperatures. They are characterized by a distinct negative skewness, mean track lengths of ~12.5 to 13.5 μm , and standard deviations of ~1.3 to 1.7 μm .

(4) Bimodal and (5) Mixed Distributions. These are characteristic of thermally affected, but not totally overprinted, samples. A "mixed" distribution reflects a partial thermal overprint which may become more prominent to form a "bimodal" distribution (Fig. A10d and A10e).

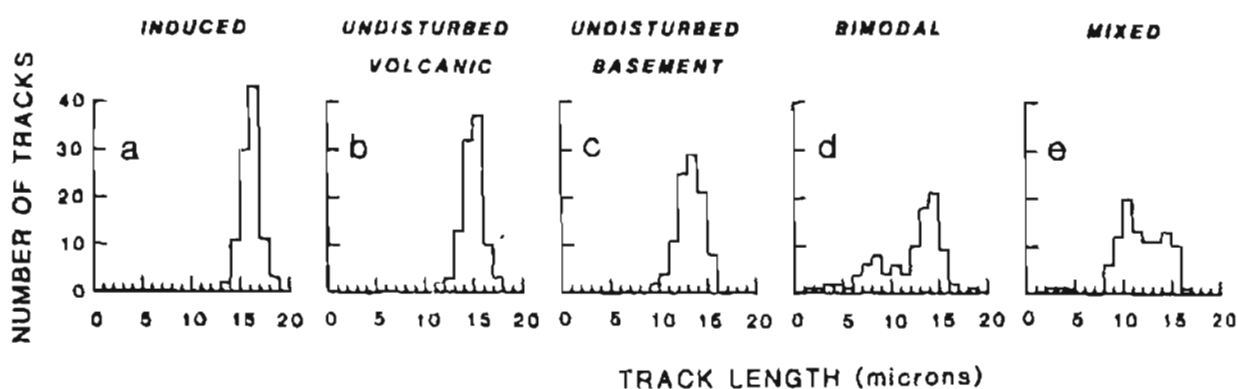


Figure A10. Characteristic apatite confined track length distributions for different thermal histories. See text for explanation (from Gleadow *et al.*, 1986b)

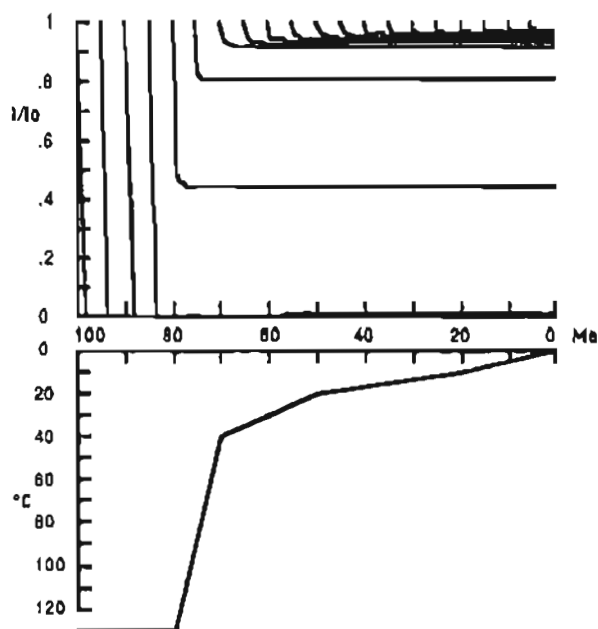
Upon completion of my results, the Alaskan sample track length distributions were compared to the above length distribution models and to interpretations of various thermal histories (Green *et al.*, 1985b; Gleadow *et al.*, 1986b; Gleadow *et al.*, 1986a) in order to work out the thermal histories for the Alaskan sedimentary sequences.

Thermal Modeling

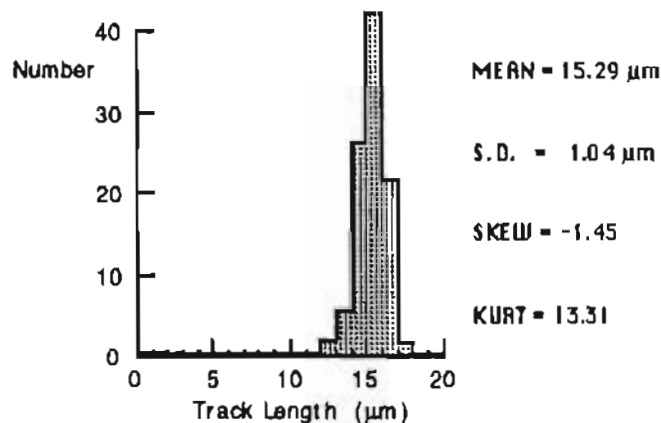
Thermal modeling is an important tool in predicting a thermal history for a sample based on its apparent fission track age and the shape of its track length distribution. Figure A11 illustrates three examples with different rates of cooling and their resultant apatite ages and track length distributions as predicted by a thermal modeling program written by P.F. Green and A.J.W. Gleadow based on Laslett *et al.*'s. (1987) preferred model. In (A), rapid uplift resulting in cooling at a uniform rate from 130°C to 40°C over 10 m.y. is followed by much slower cooling to 0°C. The computer model produces a volcanic-type distribution for this cooling history. In (B) and (C), decreasing the rates of cooling (130°C to 40°C over times of 20 m.y. and 40 m.y. respectively) results in decreasing the mean track length and increasing the standard deviation. These effects result from the sample spending longer periods of time within the annealing zone (~60°-125°C) where more short tracks accumulate.

Figure A12 shows how sensitive this thermal modeling can be. In (A), the sample was at 130°C prior to a rapid cooling to 40°C between 50 and 60 Ma. The resultant track length distribution is a *volcanic-type* and contains no short tracks. In (B) and (C), the sample was at 120°C and 110°C, respectively, prior to rapid cooling and results in the preservation of higher percentages of shortened tracks. A small difference in the temperature prior to cooling (110-130°C) is easy to distinguish by the shape of the track length distribution. The sample at 130°C prior to cooling shows no short tracks. The sample at 120°C has a

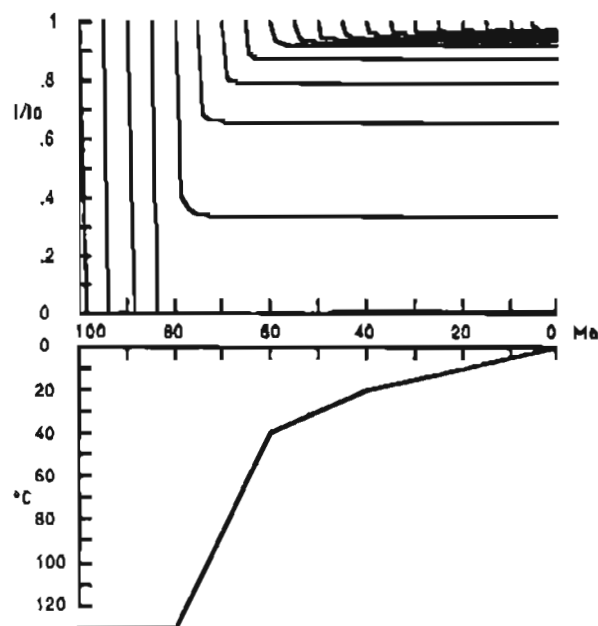
very small *tail* of tracks $<12\mu\text{m}$ ($\sim 4\%$) and the sample at 110°C shows a larger tail of tracks $<12\mu\text{m}$ ($\sim 8\%$).



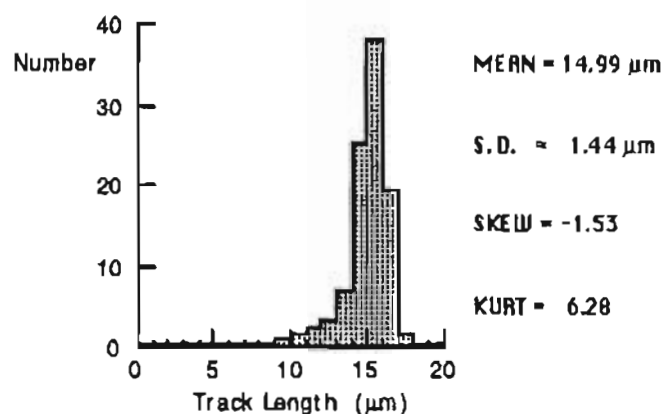
Time = 100 Ma, FT Age = 76.81
Final Temperature = 0°C



(A)



Time = 100 Ma, FT Age = 74.58 Ma
Final Temperature = 0°C



(B)

Figure A11. Figure caption on next page.

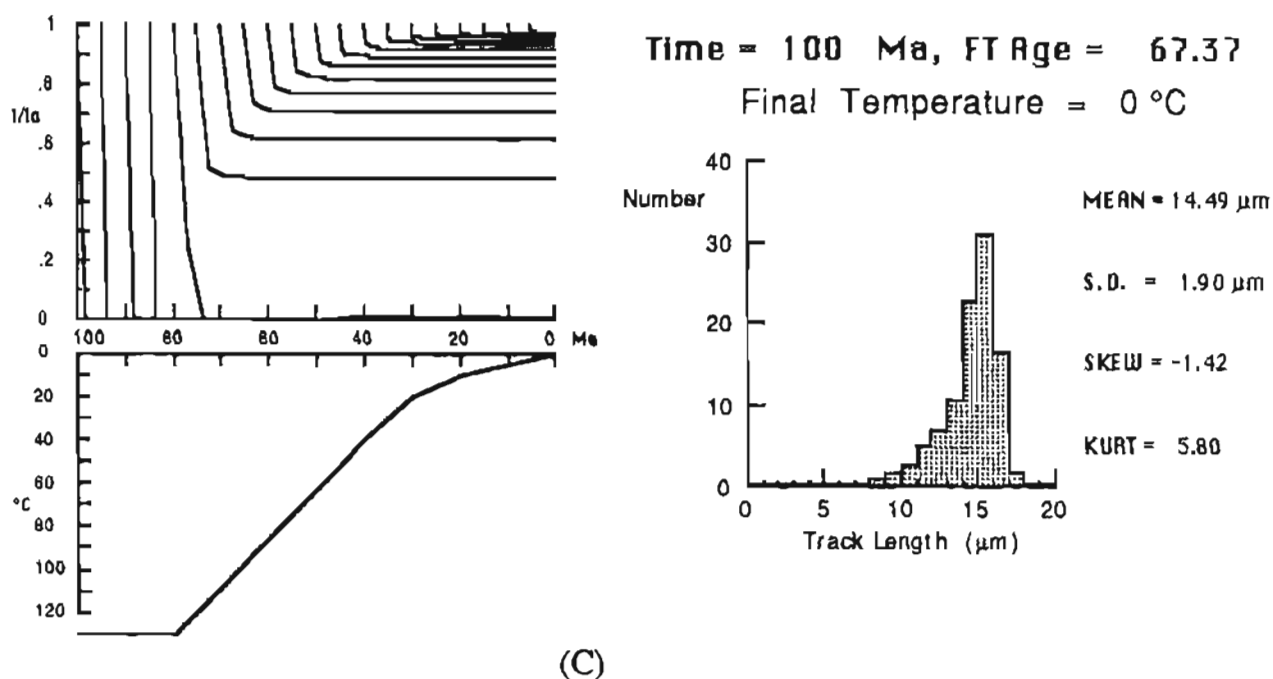
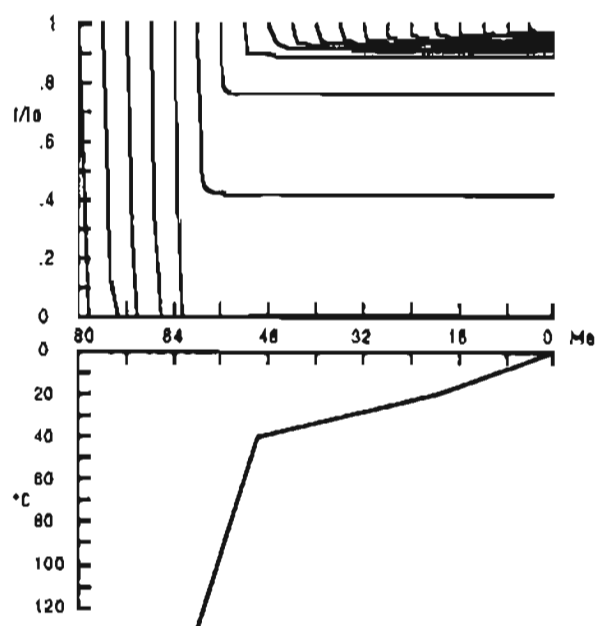
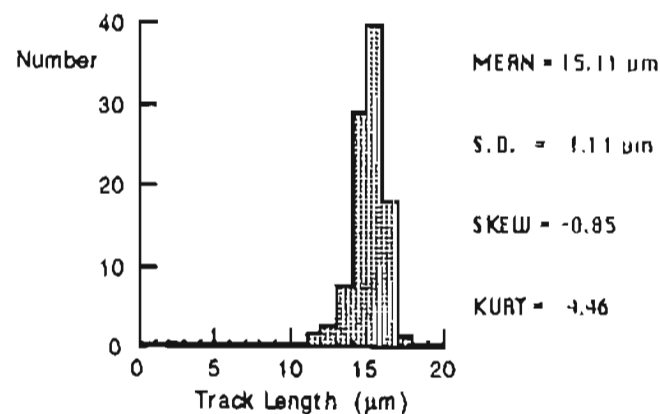


Figure A11. Apatite track length distributions resulting from different assumed thermal histories. Examples show expected distributions resulting from decreasing cooling rates (interpreted in terms of increasing rates of uplift). See text for explanation. These diagrams are produced from a program written by P.F. Green and A.J.W. Gleadow based on Laslett *et al.*'s (1987) preferred model of apatite fission track annealing. The thermal history being modelled is shown on the bottom left diagram in terms of a time-temperature path. "Time" represents the total time elapsed since fission tracks start forming. The history of track shortening is shown for 20 hypothetical tracks at different times (in each top left diagram), expressed as l/l_0 (measured length/ length of original track). The length distributions from each are summed to give the histogram on the right.

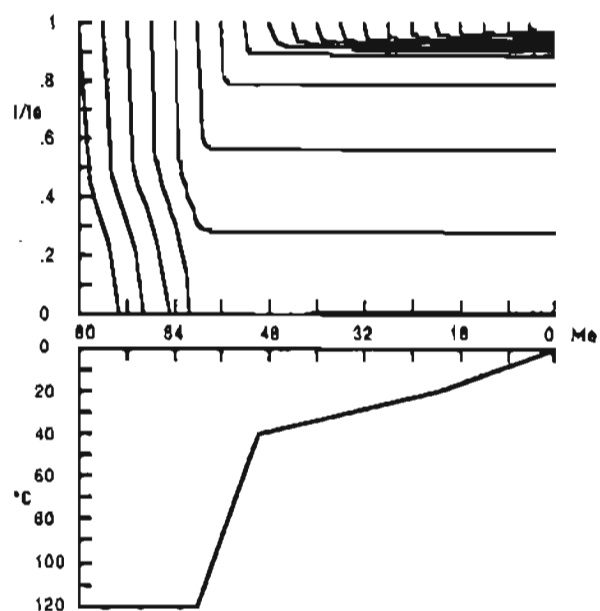


Time = 80 Ma, FT Age = 56.45

Final Temperature = 0 °C

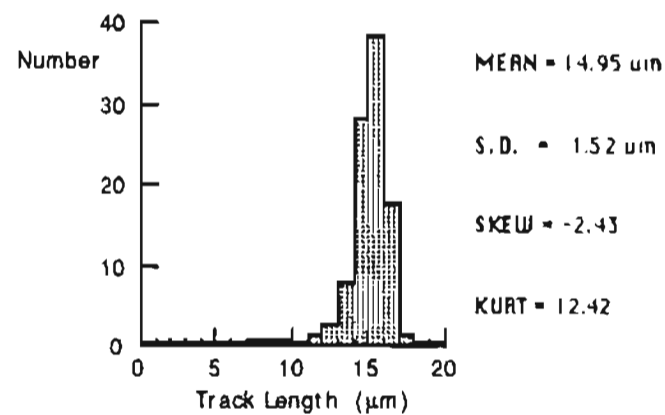


(A)



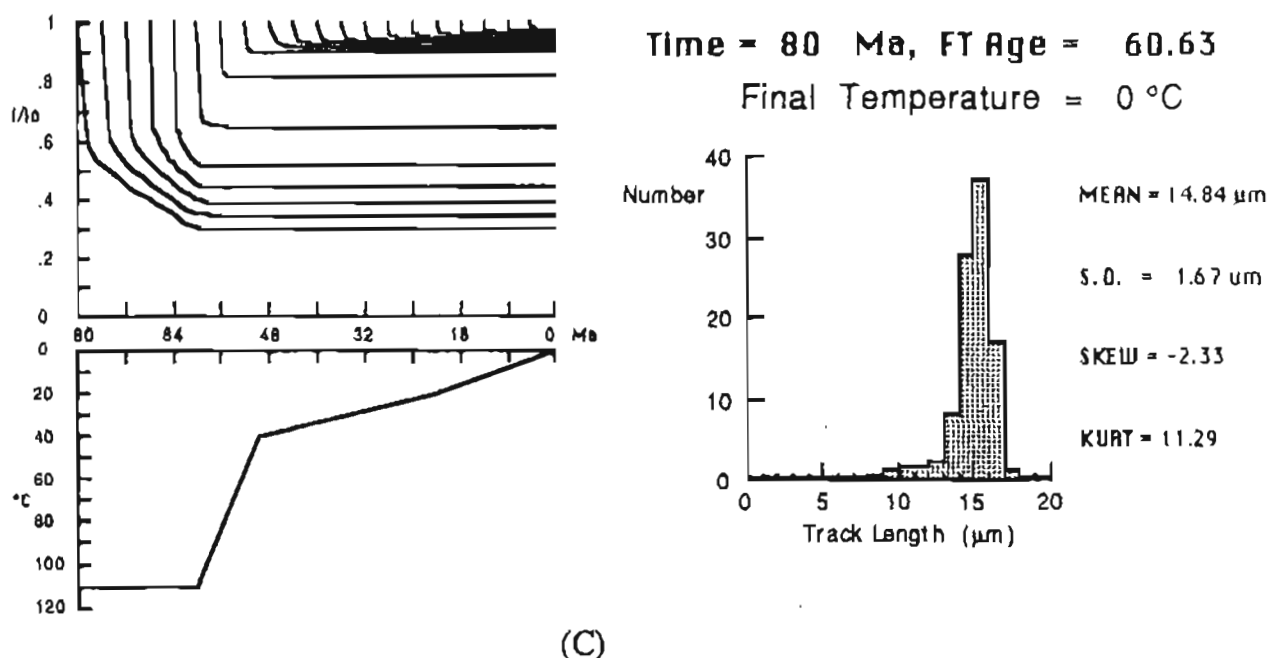
Time = 80 Ma, FT Age = 58.24

Final Temperature = 0 °C



(B)

Figure A12. Figure caption next page.



(C)

Figure A12. Thermal modeling of different thermal histories prior to identical cooling histories. Examples show expected distributions resulting from rapid cooling from different initial temperatures. See text for explanation. These diagrams are produced from a program written by P.F. Green and A.J.W. Gleadow based on Laslett *et al.*'s (1987) preferred model of apatite fission track annealing. The thermal history being modelled is shown on the bottom left diagram in terms of a time-temperature path. The history of track shortening is shown for 20 hypothetical tracks at different times, (in each top left diagram), expressed as l/l_0 (measured length/ length of original track). The length distributions from each are summed to give the final distribution histogram on the right of each diagram.

Applications

An age and a track length distribution from a single sample can yield a relatively minor amount of information compared to a sequence of samples selected to reveal variations within a sedimentary section. The sequence may be taken from drill holes (e.g. Gleadow and Duddy, 1981), or taken from long vertical profiles in mountain ranges (e.g. Gleadow and Fitzgerald, 1987).

Apatite fission track analysis has been used to constrain the thermal histories of many different geologic settings. These include dating the emplacement of igneous bodies (e.g. Gleadow and Ollier, 1987), evolution of sedimentary basins (e.g. Gleadow and Duddy, 1984), evolution of continental margins (e.g. Moore *et al.*, 1986), uplift and erosion of mountain ranges (e.g. Fitzgerald *et al.*, 1986), and "regional thermo-tectonic evolution" (Green, 1986). By using the observed fission track parameters and apatite thermal history models discussed above, it is possible to constrain the thermal history of a terrane. This approach has been applied to the Alaskan sedimentary rock units in this study.

APPENDIX B
APATITE FISSION TRACK ANALYSIS
SAMPLE PREPARATION

INTRODUCTION

Sample preparation techniques described below are those in routine use by the Fission Track Research Group of the University of Melbourne Geology Department, recently described by Fitzgerald (1987). They have evolved over a 17 year period and have been improved by many people during that period. The techniques described below are those developed by A.J.W. Gleadow.

SAMPLE TREATMENT

Rock samples used in this study varied from about 3 to 6 kg. Sample numbers contain the year collected (87), my initials (POS) or those of John Decker (JD), and then number of the field location. Multiple samples from the same location were designated by A, B, or C. Sample numbers ranged from 87POS1A through 87POS117A and 87JD3B through 87JD87A. Weathering rinds were trimmed and the initial rock crushing was performed in the Geochronology Laboratory of the Geophysical Institute, University of Alaska, Fairbanks. The samples were then shipped to Melbourne for the remainder of the sample preparation. At every stage of the preparation, from crushing through mineral separation, pre-irradiation and then post-irradiation handling, measures were taken to insure cleanliness of equipment to prevent any possible contamination. A reference hand specimen was retained and a thin section was prepared for each sample.

ROCK CRUSHING AND MINERAL SEPARATION

Rock crushing and mineral separation procedures are summarized in Table B1 followed by a discussion of the subsequent steps.

Table B1. Rock Crushing and Mineral Separation Summary

-
- (1) Crush to size range 200-75 μm .
 - (a) Large jaw crusher
 - (b) Bico Braun disk mill
 - (2) Wash thoroughly in water to remove fines (dust), or if the sample is too large, use a Wilfley Table to wash sample and concentrate heavy minerals.
 - (3) Oven dry at low temperatures ($< 60^\circ \text{C}$).
 - (4) First magnetic separation.
 - (a) Frantz-full scale (1.9A), vertical paper funnel, removes ferromagnesian minerals
 - (b) Frantz-0.4A, vertical feed, removes biotite
 - (5) First TBE. Nonmagnetic fraction from (4b) into TBE, remove quartz, feldspar etc. as float.
 - (6) Second magnetic separation-sink from (5). Frantz at forward slope of 25° and side slope of 10° .
 - (a) Frantz-0.5A, removes biotite and epidote as magnetic fraction
 - (b) Frantz-0.8A, removes sphene and monazite as magnetic fraction
 - (c) Frantz-1.1A, removes sphene composites as magnetic fraction
 - (d) Frantz-full scale, magnetic cleanup
 - (7) Second TBE. Nonmagnetic fraction from (6d) into TBE, removes remaining quartz, feldspar, etc. as float.
 - (8) DIM. Sink from (7) into DIM, sink is zircon fraction, float is apatite fraction.
 - (9) Clean up apatite and zircon fraction.
 - (a) Apatite, Frantz-full scale, 2° to 5° side slope
 - (b) Zircon, Frantz-full scale, 0° side slope
-

TBE = Tetrabromoethane (sym) (specific gravity = 2.96-2.97)

DIM = Di-iodo methane (specific gravity = 3.32)

MINERAL MOUNTING, GRINDING, POLISHING, AND ETCHING TECHNIQUES

The following methods outline the procedure for mounting and preparing apatite for fission track analysis. The purpose of the mounting medium is to support the grains while they are ground, polished, etched, and eventually counted. Grinding exposes an internal surface, polishing removes the grinding scratches plus any surface imperfections, and etching reveals the tracks so they can be seen with a petrographic microscope. At all stages of preparation the sample numbers were labeled on the mounts.

Summary of Materials and Methods

<i>Mounting medium:</i>	epoxy on a glass slide. Araldite MY753 resin and HY956 hardener, 5:1 by volume or weight.
<i>Grinding:</i>	400 and 600 grit SiC waterproof abrasive paper on a wet rotating lap (400 rpm).
<i>Polishing:</i>	0.3 μm corundum polishing powder in a H_2O slurry on a nylon cloth lap rotating at 400 rpm (1:5 ratio, $\text{Al}_2\text{O}_3:\text{H}_2\text{O}$).
<i>Etchant:</i>	5M HNO_3 for ~20 (15-30) seconds at 20-22°C.

Mounting

Apatite grains were mounted in Araldite on a hot-plate at 120°C. Approximately 10 mg of 100-200 μm size grains are enough to adequately cover a 1 cm x 1.5 cm area so that the grains are not touching, yet not excessively isolated. Mounting with excessive grain density makes locating the grain image on the mica replica difficult. Once in the warm epoxy, the slurry was stirred with a needle to ensure that apatite grains sank to the bottom of the araldite. The slide was then left on the hot-plate for 5 minutes to cure the Araldite. Heating to 120°C for this very short period of time has been shown not to affect track lengths (Gleadow, 1984).

Grinding and Polishing

During this stage the slide was held in a specially made recessed brass holder. Excess epoxy was removed using the 400 grit paper. Internal surfaces of the grains were exposed using the 600 grit paper. In the grinding stage the slide is held stationary in one orientation. Mounts were polished for at least two periods of 45 seconds each.

Etching

Mounts were etched by placing two slides back to back, holding them together using tweezers and submerging them for 20 seconds in a beaker of 5M nitric acid. To stop the etching, they were submerged in a beaker of tap water and then rinsed with tap water. At this stage the mounts were trimmed down to a 1 x 1.5 cm size by snapping off the excess slide glass after scoring with a diamond pencil and ruler. Final trimming was accomplished using a rotating diamond-impregnated metal grinding wheel.

PRE-IRRADIATION SAMPLE HANDLING FOR THE EXTERNAL DETECTOR METHOD

Mount - Mica Pairs and Wrapping

The mounts were all trimmed to 1 x 1.5 cm at this stage. Pre-packaged rectangles (~50 μm thick x 1.3 cm x 0.85 cm) of low-uranium muscovite (<5 ppb) were used for the external detector. The sample number was scribed on the back of the mica prior to wrapping. The mount-mica pair was then placed in an envelope of heat shrink polythene/polyester laminate plastic using tweezers and then sealed using a heat sealer. The envelope corners were trimmed off to allow air to escape when the heat-shrinking takes place. Heat shrinking was done between two pre-heated glass slides on the hot plate at ~100°C. Considerable care was necessary at this stage to ensure the mica was aligned correctly over the mount, not overlapping the edges of the glass, and that good contact was achieved between the mount and the mica. Pinpricks were used to mark the corners of the

mount-mica pair for use during the coarse alignment procedure on the Autoscan™ stage. Standard glass-mica pairs (for determining P_d , the standard track density) were wrapped in the same way.

The Irradiation Package

Up to 15 mount-mica pairs, all labeled and in known order, were placed in a stack with a standard glass-mica pair at either end for monitoring the neutron fluence. The stacks were wrapped tightly in Al-foil, the top labeled and placed in a high-purity aluminum irradiation tube. It is important to know the order of the samples within the tube so that if a fluence gradient is measured by the standard glasses at either end of the package then individual standard track densities can be assigned to individual mount-mica pairs.

Neutron Irradiation and Fluence Monitoring

Neutron irradiations were carried out in the X-7 position of the Australian Atomic Energy Commission HIFAR Research Reactor, Canberra, which has a well thermalized flux of $\sim 3 \times 10^{12} \text{ ncm}^{-1}\text{sec}^{-1}$. No flux gradients were detected from any of the 4 packages when using between 12-15 mount-mica pairs and 2 standard glasses (package thickness ~ 5 cm). Thermal neutron fluences were monitored by recording the standard track density in the mica external detectors placed over standard glass discs of the National Bureau of Standards (NBS) reference glass SRM612 (~ 50 ppm U). The standard neutron dose requested for the apatite packages was $1 \times 10^{16} \text{ neutrons cm}^{-2}$. The apatites from the ANWR region were of such low uranium concentration (5-30 ppm U) that future irradiations should be given higher neutron fluences.

POST-IRRADIATION SAMPLE HANDLING

After irradiation, the mount-mica pairs were removed from the irradiation tube and unwrapped when a safe level of radiation was achieved. Micras were etched in 40% HF for 20 minutes, thoroughly washed overnight in tap water, and then allowed to stand for at

least 12 hours. This allowed evaporation of any residual HF and therefore prevented any possible damage to microscope objectives. The mount-mica pairs were mounted on 1 x 3 inch glass slides using epoxy (Figure B1). Care was necessary at this stage to ensure the pairs were aligned in a mirror-image configuration and that the mica was not glued face down. The micas that were put over the standard glasses were mounted together on a separate slide.

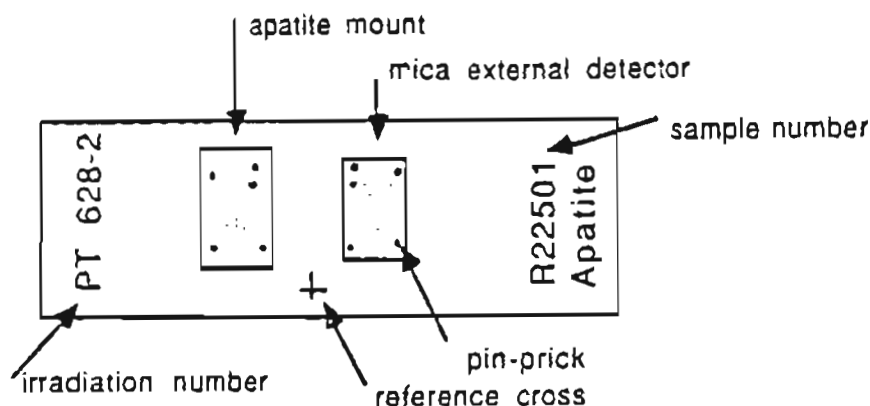


Figure B1. Mount/mica pair as mounted on a glass slide ready for counting and measuring track lengths. Pin pricks are used during coarse alignment and the scribed cross is used as the reference point for automated alignment (from Fitzgerald, 1987).

MICROSCOPE EQUIPMENT AND COUNTING PROCEDURES

Fission Track Ages

A Zeiss Universal microscope system, equipped with dry, epiplan objectives mounted on a revolving nose turret, was used for all fission track counting. Objectives used were corrected for use without cover slips. The 80x objective used for counting had a numerical aperture of 0.95 and the condenser had a numerical aperture of 1.4. The tube factor was variable using an Optivar magnification chamber, either 1.25x, 1.6x, or 2.0x being available. A Zeiss KPL wideangle binocular eyepiece with a magnification of 12.5x was

used. A 10 x 10 grid located in one of the eyepieces was used for counting tracks over a known area.

Fission tracks were counted at a total magnification of 1250x ($80 \times 1.25 \times 12.5 =$ objective magnification \times tube factor \times eyepiece magnification). The size and area of the grid in the eyepiece was calibrated using a diffraction grating (stage micrometer), one line on the diffraction grating being equal to 1.5678 μm .

Standard track densities (P_d) were obtained by scanning across the mica external detector and counting the number of tracks in a given area at a given number of locations. Tracks lying on the lines defining the top and right side of each square in the grid were counted as being within that square. The exact position of a track was defined by the position of the track *head* (the intersection of each track and the exposed surface of the grain). The requested dose of 1×10^{16} neutrons cm^{-2} for NBS glass SRM612 usually gave a standard track density (p_d) of $\sim 1.35\text{--}1.45 \times 10^6$ tracks per cm^{-2} .

A microcomputer-controlled Autoscan™ 3 axis motorized stage system (Gleadow *et al.*, 1982; Smith and Leigh-Jones, 1985) mounted on the Zeiss Universal microscope was used for counting fission tracks. This stage system permits the automatic location of matching points on the mineral mount and its mirror image on the mica detector. The coordinates of all counting sites are recorded relative to the position of a small cross scribed on the slide (Fig.B1). The mount and the mica were first roughly aligned using the pin pricks and then fine-tuned using distinctive grains and their images. Alignment usually took about 10 minutes and had a precision of 5-10 μm .

The mount was usually scanned using the 16x objective under reflected light to look for grains with good polishing scratches (indicating proper etching conditions on the crystal face). Once a good grain was found it was examined under transmitted light to determine whether it was suitable for counting (dislocation free, and not zoned). The area counted on

each grain varied according to the suitable area available (area on individual grains ranged from 4 to 70 grids with each grid $\sim 8.548 \times 10^{-7} \text{ cm}^2$). This area had to lie within a one-track-length distance of the grain margin. Usually 20 suitable grains were located (or as many grains as possible up to 20) before counting tracks in the apatite (N_s) and in their muscovite replica (N_i). A mechanical hand counter was used to record the number of tracks.

Confined Fission Track Lengths

A drawing tube was attached to the Zeiss Universal microscope and the images of confined fission tracks were measured on a Hipad™ digitizing tablet. This tablet had been previously calibrated using a stage micrometer marked at 10 and 2 μm intervals. A light emitting diode was attached to the cross hairs of the the digitizing tablet's cursor so it could be more clearly seen. Only horizontal, confined fission tracks with clearly defined ends were measured. Confined tracks were located by scanning the mount using a 40x objective under reflected light. Horizontal confined tracks usually appear as highly birefringent, cigar-shaped tubes. Track lengths were measured using an 80x dry objective. 100 track lengths (or as many as possible up to 100) were measured in each sample. Locating this many on most of the samples took 2-3 hours but some particularly young or low-U samples took up to 4 hours.

APPENDIX C

INDIVIDUAL SAMPLE DATA

SAMPLE LOCATIONS

Table C1. Sample Locations.

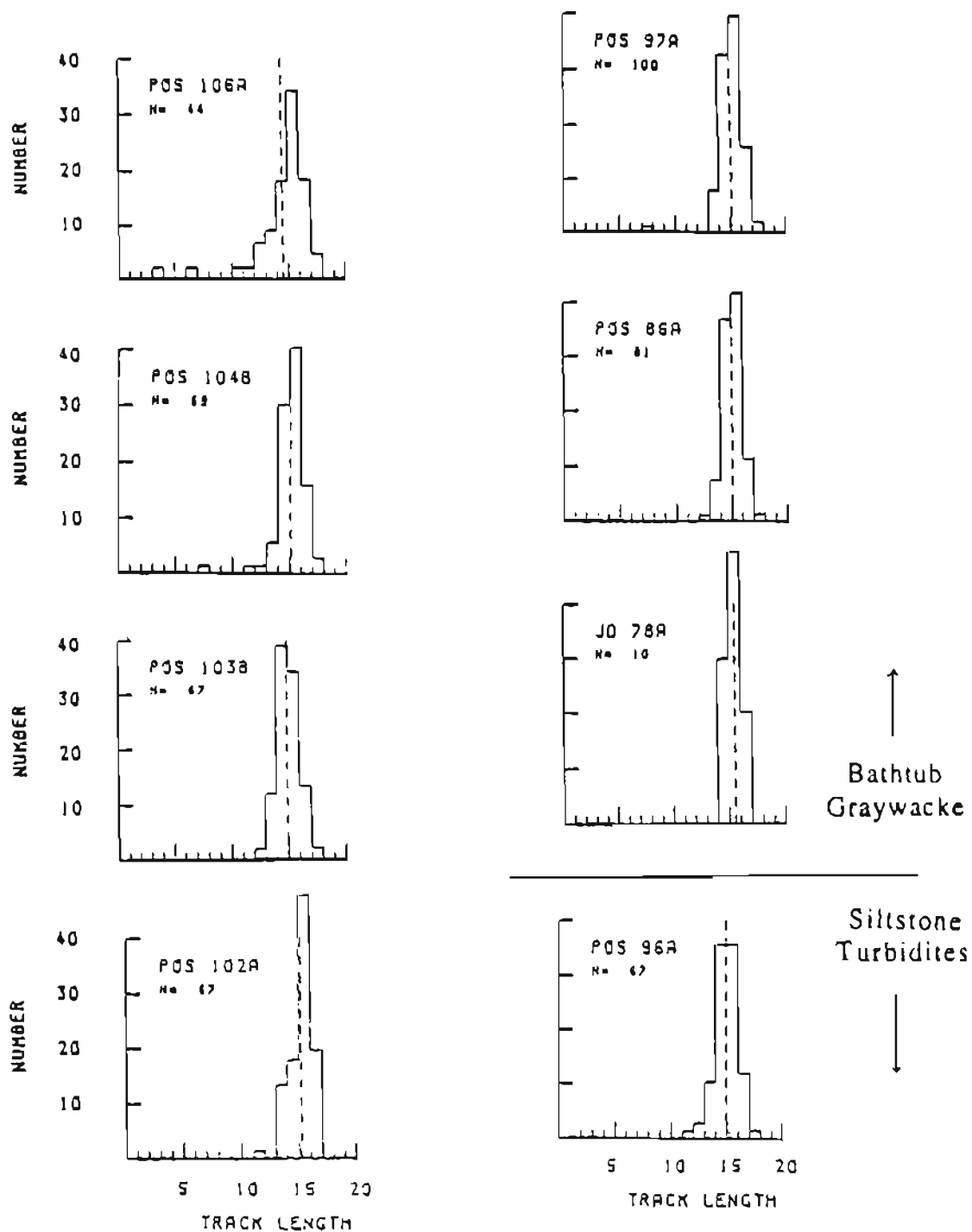
Sample Number	Latitude (North)	Longitude (West)	Quadrangle (1:250,000)
<i>Bathub Ridge</i>			
POS76A	69.14	142.77	Demarcation Pt.
POS86A	69.14	142.77	Demarcation Pt.
POS88A	69.12	142.75	Demarcation Pt.
POS90A	69.12	142.75	Demarcation Pt.
POS96A	69.12	142.75	Demarcation Pt.
POS97A	69.12	142.75	Demarcation Pt.
POS98A	69.13	142.53	Demarcation Pt.
POS99A	69.13	142.53	Demarcation Pt.
POS102A	69.13	142.53	Demarcation Pt.
POS103B	69.13	142.53	Demarcation Pt.
POS104B	69.13	142.53	Demarcation Pt.
POS106A	69.13	142.53	Demarcation Pt.
POS111A	69.13	142.53	Demarcation Pt.
POS113A	69.14	142.80	Demarcation Pt.
POS115A	69.14	142.80	Demarcation Pt.
POS117A	69.14	142.80	Demarcation Pt.
JD78A	69.13	142.53	Demarcation Pt.
JD87A	69.13	142.53	Demarcation Pt.
<i>Arctic Creek Area</i>			
POS55A	69.49	144.61	Mt. Michelson
POS63 1/2	69.50	144.46	Mt. Michelson
JD15A	69.49	144.55	Mt. Michelson
JD17A	69.49	144.54	Mt. Michelson
JD26A	69.50	144.54	Mt. Michelson
JD27A	69.50	144.55	Mt. Michelson
JD38B	69.49	144.49	Mt. Michelson
<i>Canning River Area</i>			
POS07A	69.53	146.31	Mt. Michelson
POS08A	69.55	146.29	Mt. Michelson
POS10A	69.58	146.30	Mt. Michelson
POS14A	69.60	146.32	Mt. Michelson
POS16A	69.63	146.28	Mt. Michelson
POS22B	69.73	146.24	Mt. Michelson
POS24B	69.66	146.24	Mt. Michelson
POS35A	69.56	146.26	Mt. Michelson
JD03B	69.53	146.31	Mt. Michelson

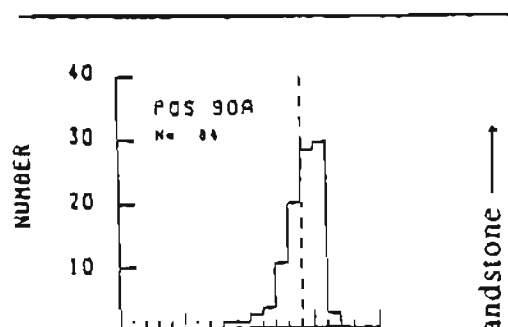
Table C1 (continued). Sample Locations.

Sample Number	Latitude (North)	Longitude (West)	Quadrangle (1:250,000)
<i>ANWR Coastal Plain</i>			
POS64A	69.92	143.38	Demarcation Pt.
POS67A	69.94	142.94	Demarcation Pt.
POS68A	69.90	142.95	Demarcation Pt.
POS69A	69.90	142.95	Demarcation Pt.
JD49A	69.90	143.04	Demarcation Pt.
POS74A	69.95	144.67	Mt. Michelson
POS74B	69.95	144.67	Mt. Michelson
POS75A	69.95	144.67	Mt. Michelson

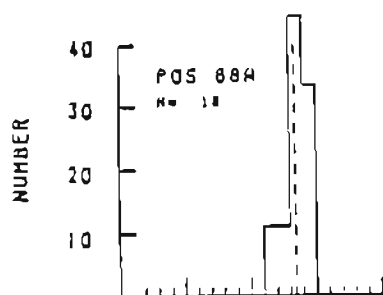
TRACK LENGTH DATA
(Arranged in Stratigraphic Order Where Known)

Bathtub Ridge

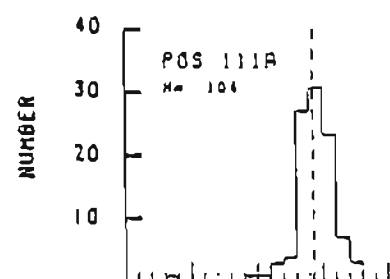




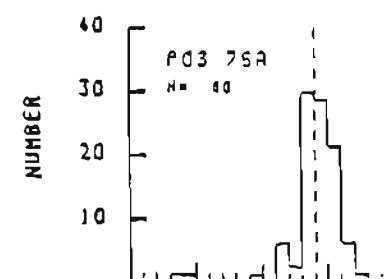
↑ Sandstone



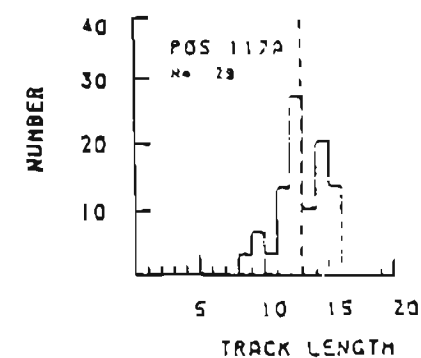
↓ Kemik



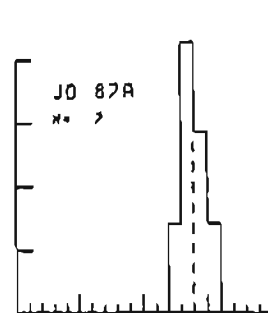
↑ Shublik



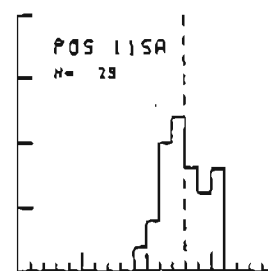
↓ Shublik



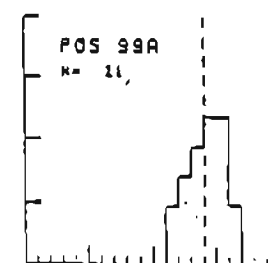
↓ Shublik



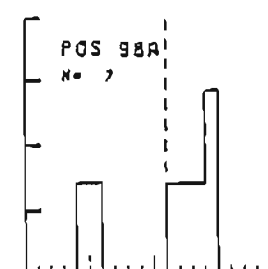
↑ Ivishak



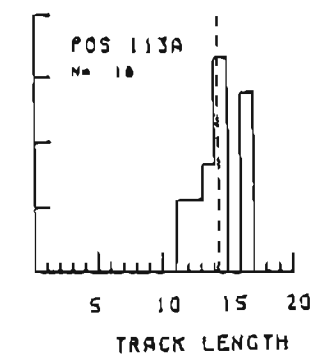
↓ Ivishak



↑ Echooka



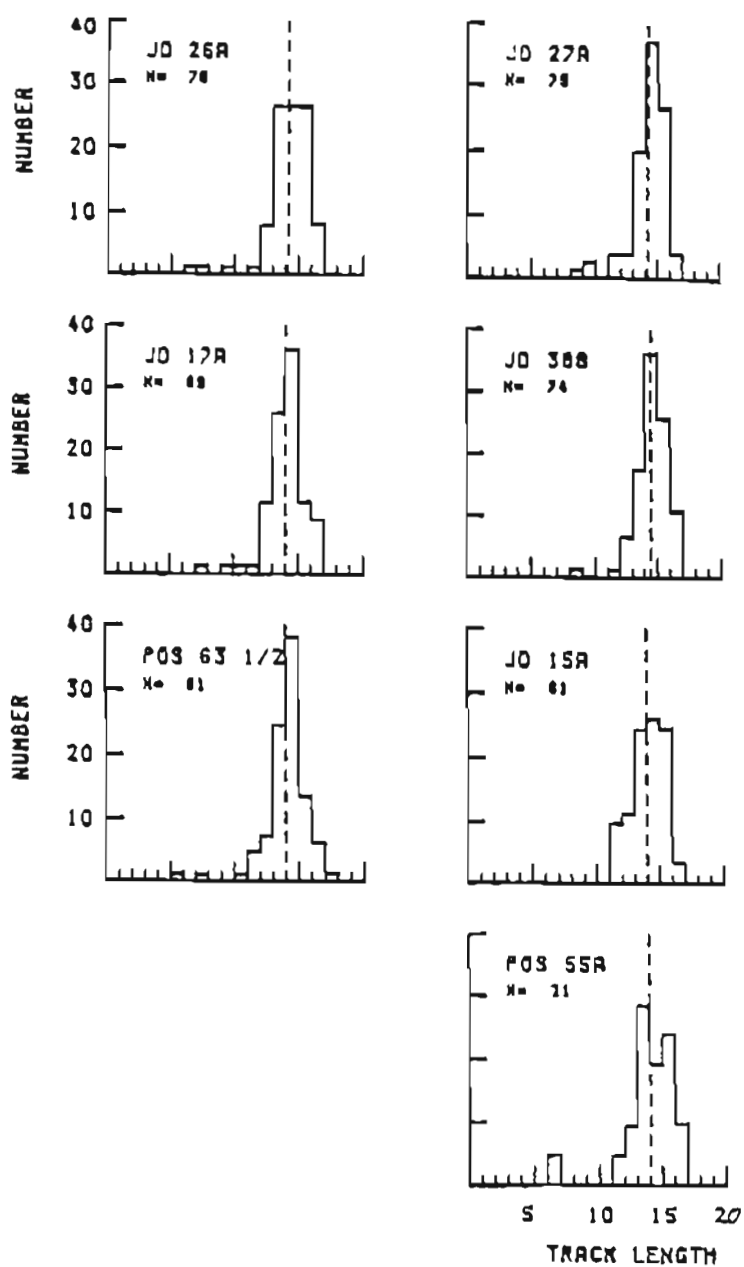
↓ Echooka



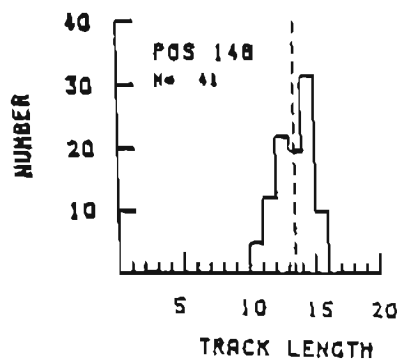
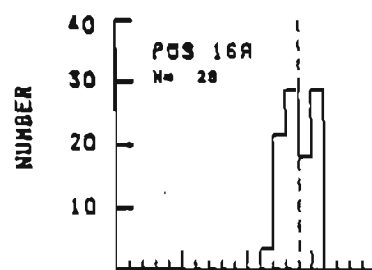
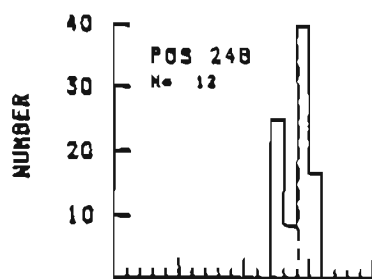
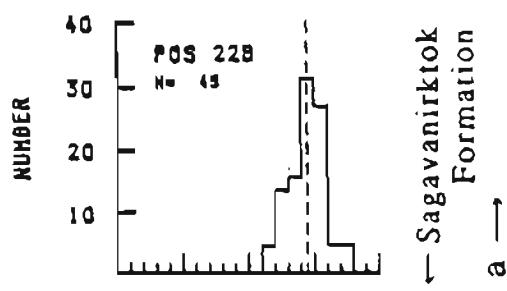
↓ Echooka

Arctic Creek Region

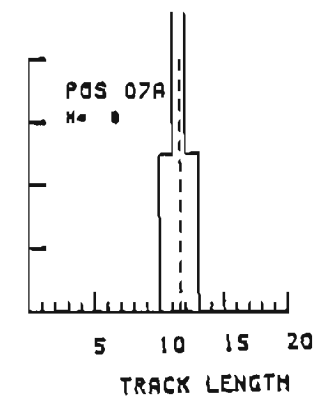
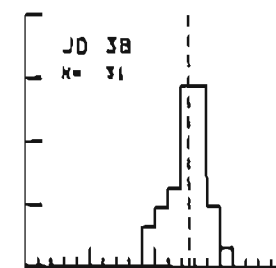
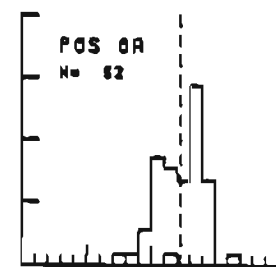
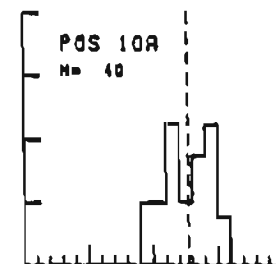
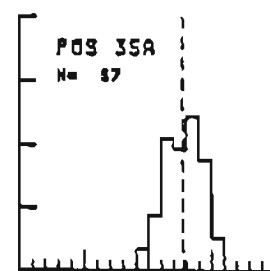
Albian turbidites



Canning River Region



Canning Formation



Kemik Formation

ANWR Coastal Plain

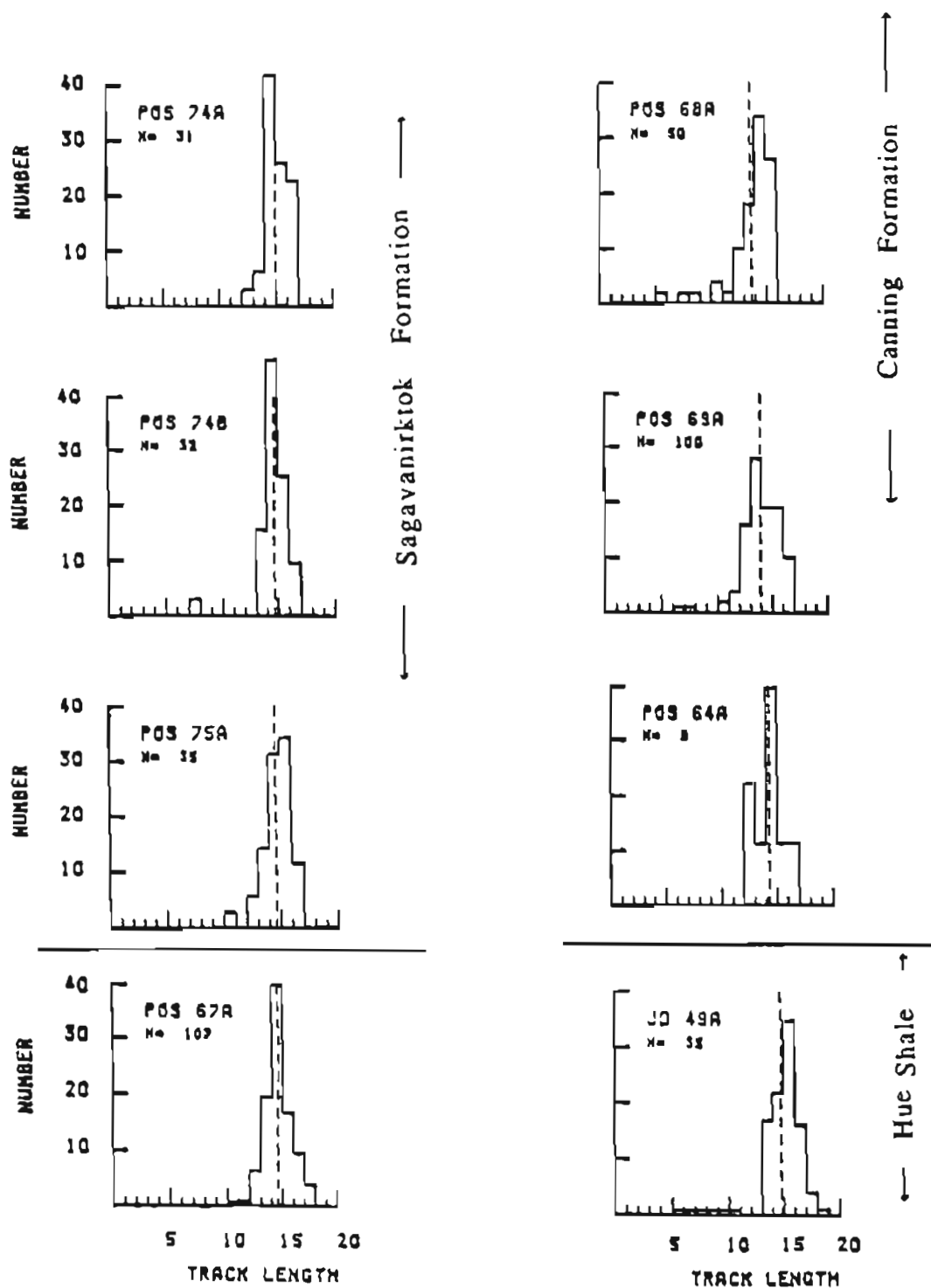


Table C2. Distribution of Individual Track Lengths

Sample	Track Length Range (μm)													
Number	≤ 5	5-6	6-7	7-8	8-9	9-10	10-11	11-12	12-13	13-14	14-15	15-16	16-17	> 17
<i>Bathtub Ridge</i>														
POS106A	1	0	1	0	0	0	1	1	3	4	8	15	8	2
POS104B	0	0	0	1	0	0	0	1	1	4	21	28	11	2
POS103B	0	0	0	0	0	0	0	0	2	12	39	34	13	2
POS102A	0	0	0	0	0	0	0	1	0	9	12	32	13	0
POS97A	0	0	0	1	0	0	0	0	0	8	33	40	16	2
POS86A	0	0	0	0	0	0	0	0	1	6	30	34	9	1
JD78A	0	0	0	0	0	0	0	0	0	0	3	5	2	0
POS96A	0	0	0	0	0	0	0	1	2	7	24	24	8	1
POS90A	0	0	0	0	1	1	2	3	9	17	24	25	2	0
POS88A	0	0	0	0	0	0	0	2	2	8	6	0	0	0
POS111A	1	0	0	0	0	1	1	3	4	28	32	24	7	3
POS76A	2	0	0	0	0	1	0	5	2	24	23	17	5	1
POS117A	0	0	0	0	1	2	1	4	8	3	6	4	0	0
JD87A	0	0	0	0	0	0	0	0	1	3	2	1	0	0
POS115A	0	0	0	0	0	1	2	5	6	4	3	4	0	0
POS99A	0	0	0	0	0	0	0	2	3	4	5	5	2	0
POS98A	1	1	0	0	0	0	0	1	1	1	2	0	0	0
POS113A	0	0	0	0	0	0	0	2	2	3	6	0	5	0
<i>Arctic Creek</i>														
POS55A	0	0	1	0	0	0	0	1	2	6	4	5	2	0
POS63 1/2	0	1	0	1	0	0	1	4	6	20	31	11	5	1
JD15A	0	0	0	0	0	0	0	6	7	15	16	15	2	0
JD17A	0	0	0	1	0	1	1	1	8	18	25	8	6	0
JD26A	0	0	1	1	0	1	0	1	6	20	20	20	6	0
JD27A	0	0	0	0	1	2	0	3	3	15	28	20	3	0
JD38B	0	0	0	0	1	0	0	1	5	13	27	19	8	0
<i>Canning River</i>														
(A)														
POS22B	0	0	0	0	0	0	0	2	6	7	14	12	2	2
(B)														
POS24B	0	0	0	0	0	0	0	0	3	1	6	2	0	0
POS16A	0	0	0	0	0	0	0	1	6	8	5	8	0	0
POS14B	0	0	0	0	0	0	2	5	9	8	13	4	0	0
POS35A	0	0	0	0	0	2	5	12	11	14	10	3	0	0
(C)														
POS10A	0	0	0	0	0	4	4	9	4	7	9	3	0	0
POS08A	0	0	0	1	1	3	9	8	7	15	7	0	1	0
JD03B	0	0	0	0	0	2	3	4	9	9	3	1	0	0
POS07A	0	0	0	0	0	0	2	4	2	0	0	0	0	0

Table C2 (continued). Distribution of Individual Track Lengths

Sample	Track Length Range (μm)													
Number	<5	5-6	6-7	7-8	8-9	9-10	10-11	11-12	12-13	13-14	14-15	15-16	16-17	>17
<i>ANWR Coastal Plain</i>														
POS74A	0	0	0	0	0	0	0	0	1	2	13	8	7	0
POS74B	0	0	0	1	0	0	0	0	0	5	15	8	3	0
POS75A	0	0	0	0	0	0	1	0	2	5	11	12	4	0
POS67A	0	0	0	0	0	0	1	1	7	21	45	18	10	4
POS68A	0	1	0	1	1	0	2	1	5	9	17	13	0	0
POS69A	0	0	1	1	0	0	2	4	16	28	19	19	10	0
POS64A	0	0	0	0	0	0	0	0	2	1	4	1	1	0
JD49A	0	0	0	0	0	2	3	4	9	9	3	1	0	0

Results for each area except Arctic Creek are given in stratigraphic order from top to bottom. No stratigraphic control is available on Arctic Creek samples.

AGE DATA

(Arranged in Stratigraphic Order Where Known)

Explanation of Terms

Each analysis shows a listing of the individual grain ages, the resulting age and pertinent information used in determining the age.

POS 07A	-Sample number
Irradiation:	-Laboratory number for samples irradiated in the same package
NS	-Number of spontaneous tracks counted
NI	-Number of induced tracks counted
Area Units	-Number of area units counted in grain
Ratio	-Ratio of (NS/NI) for each grain
RHO S	-Density of spontaneous tracks (per cm ²)
RHO I	-Density of induced tracks (per cm ²)
Age(MYR)	-Individual grain ages (Ma)
Variance of SQR	-Statistical comparison of values of NS or NI for all grains
CHI Squared	-Statistical test for determining multiple grain populations: Pass = grains represent a single population Fail = grains represent multiple populations
NS/NI	-Pooled ratio of (NS/NI). Uses total number of spontaneous and induced tracks counted for whole sample. Value used in age calculation if sample is part of a single population
Mean Ratio	-Average ratio of (NS/NI) for grains
Pooled Age	-Age (Ma) calculated using NS/NI(single population)
Mean Age	-Age (Ma) calculated Using "Mean Ratio" (multiple populations)

Bathtub Ridge
POS 106A

IRRADIATION: PT938-06
 ANALYSIS BY POS 5/16/88

CRYSTAL	NS	NI	AREA UNITS	RATIO	RHO S	RHO I	AGE(MYR)
1	6	31	18	0.194	3.31E+05	1.71E+06	49.3 +- 22.8
2	3	9	15	0.333	1.99E+05	5.96E+05	84.7 +- 56.5
3	12	42	12	0.266	9.93E+05	3.48E+06	72.7 +- 23.8
4	3	16	12	0.188	2.48E+05	1.32E+06	47.8 +- 38.1
5	12	61	12	0.197	9.93E+05	5.85E+06	58.1 +- 15.8
6	5	21	9	0.238	5.52E+05	2.32E+06	68.6 +- 30.2
7	14	49	9	0.286	1.55E+06	5.41E+06	72.7 +- 22.8
8	28	75	8	0.267	2.48E+06	9.31E+06	67.8 +- 17.1
9	8	2	9	0.888	0.88E+00	2.21E+05	8.8 +- 8.8
10	15	41	9	0.366	1.66E+06	4.52E+06	92.9 +- 28.8
11	6	38	15	0.288	3.97E+05	1.99E+06	58.9 +- 22.8
12	1	5	6	0.288	1.66E+05	8.28E+05	58.9 +- 55.8
13	8	4	8	0.888	0.88E+00	4.97E+05	8.8 +- 8.8
14	4	14	12	0.286	3.31E+05	1.16E+06	72.7 +- 41.2
15	2	9	18	0.222	1.18E+05	4.97E+05	56.6 +- 44.2
16	8	4	28	0.888	0.88E+00	1.99E+05	8.8 +- 8.8
17	2	6	12	0.333	1.66E+05	4.97E+05	84.7 +- 69.1
18	5	28	28	0.258	2.48E+05	9.93E+05	63.6 +- 31.8
19	8	2	9	0.888	0.88E+00	2.21E+05	8.8 +- 8.8
28	3	8	9	0.375	3.31E+05	8.83E+05	95.2 +- 64.4

113

449

4.638E+05

1.843E+06

AREA OF BASIC UNIT = 1.8868E-06 CM²

VARIANCE OF SQR(NIS) = 1.86

VARIANCE OF SQR(NI) = 4.82447

CORRELATION COEFFICIENT = 0.961

CHI SQUARED = 7.18183 WITH 19 DEGREES OF FREEDOM PASS

NS/NI = 0.252 +- 0.026

MEAN RATIO = 0.211 +- 0.027

AGE CALCULATED USING A ZETA OF 352.7 FOR SRM612 GLASS

RHO D = 1.45E+06 NO = 5755

POOLED AGE = 64.0 +- 6.8 MYR

MEAN AGE = 53.7 +- 7.0 MYR

POS 104B

IRRADIATION: PT930-00
ANALYSIS BY POS 5/15/88

CRYSTAL	NS	NI	AREA UNITS	RATIO	RHO S	RHO I	AGE(MYR)
1	1	12	12	0.083	9.45E+04	1.13E+05	21.3 +- 22.1
2	3	13	30	0.231	1.13E+05	4.91E+05	50.7 +- 37.6
3	6	15	18	0.400	3.78E+05	9.45E+05	101.5 +- 49.0
4	6	12	15	0.500	4.54E+05	9.87E+05	126.6 +- 63.3
5	6	12	25	0.500	2.72E+05	5.44E+05	126.6 +- 63.3
6	2	10	12	0.200	1.09E+05	9.45E+05	50.9 +- 39.5
7	1	8	12	0.125	9.45E+04	7.56E+05	31.9 +- 33.8
8	0	3	8	0.000	0.00E+00	4.25E+05	0.0 +- 0.0
9	0	9	20	0.000	0.00E+00	5.10E+05	0.0 +- 0.0
10	4	7	20	0.571	2.27E+05	3.97E+05	144.5 +- 90.6
11	3	9	20	0.333	1.78E+05	5.10E+05	84.7 +- 56.5
12	2	9	15	0.222	1.51E+05	6.00E+05	56.6 +- 44.2
13	1	8	10	0.125	6.30E+04	5.04E+05	31.9 +- 33.8
14	2	6	10	0.333	2.27E+05	6.00E+05	84.7 +- 69.1
15	1	10	16	0.100	7.09E+04	7.09E+05	25.5 +- 26.0
16	0	0	15	0.000	0.00E+00	6.05E+05	0.0 +- 0.0
17	11	36	20	0.306	6.24E+05	2.04E+06	77.7 +- 26.0
18	14	55	15	0.255	1.06E+06	4.16E+06	64.0 +- 19.4
19	15	62	10	0.242	9.45E+05	3.91E+06	61.6 +- 17.7
20	0	0	15	0.000	0.00E+00	6.05E+05	0.0 +- 0.0

<u>70</u>	<u>312</u>	<u>2.640E+05</u>	<u>1.059E+06</u>
-----------	------------	------------------	------------------

AREA OF BASIC UNIT = 8.819E-07 CM²

VARIANCE OF SQR(NS) = 1.4128

VARIANCE OF SQR(NI) = 2.54046

CORRELATION COEFFICIENT = 0.923

CHI SQUARED = 17.5343 WITH 19 DEGREES OF FREEDOM PASS

NS/NI = 0.250 +- 0.032

MEAN RATIO = 0.226 +- 0.039

AGE CALCULATED USING A ZETA OF 352.7 FOR SRM612 GLASS

RHO D = 1.45E+06 ID = 5755

POOLED AGE = 63.6 +- 3.1 MYR

MEAN AGE = 57.6 +- 10.1 MYR

POS 103B

IRRADIATION: PT930-03
ANALYSIS BY POS 5/9/88

CRYSTAL	NS	NI	AREA UNITS	RATIO	RHO S	RHO I	AGE(MYR)
1	6	28	15	0.214	4.68E+05	2.18E+06	54.6 +- 24.5
2	9	43	12	0.209	8.77E+05	4.19E+06	53.3 +- 19.5
3	5	16	15	0.313	3.98E+05	1.25E+06	79.4 +- 40.7
4	2	8	12	0.258	1.95E+05	7.88E+05	63.6 +- 58.3
5	5	14	28	0.357	2.92E+05	8.19E+05	96.7 +- 47.2
6	14	35	38	0.408	5.46E+05	1.36E+06	181.5 +- 32.1
7	6	28	16	0.214	4.39E+05	2.85E+06	54.6 +- 24.5
8	5	18	9	0.588	6.58E+05	1.38E+06	126.6 +- 69.3
9	1	6	9	0.167	1.38E+05	7.88E+05	42.5 +- 45.4
10	3	13	15	0.231	2.34E+05	1.81E+06	58.7 +- 37.6
11	7	26	36	0.269	2.27E+05	8.45E+05	68.5 +- 29.2
12	13	41	18	0.317	1.52E+06	4.88E+06	88.6 +- 25.6
13	5	16	18	0.313	3.25E+05	1.84E+06	79.4 +- 40.7
14	5	18	9	0.278	6.58E+05	2.34E+06	78.6 +- 35.7
15	28	69	15	0.298	1.56E+06	5.38E+06	73.7 +- 18.7
16	2	8	15	0.258	1.56E+05	6.24E+05	63.6 +- 58.3
17	3	12	42	0.258	8.36E+04	3.34E+05	63.6 +- 41.1
18	8	18	9	0.444	1.84E+06	2.34E+06	112.7 +- 47.9
19	5	13	38	0.385	1.95E+05	5.87E+05	97.6 +- 51.4
20	8	4	24	0.888	8.88E+08	1.95E+05	8.8 +- 8.8
			<u>124</u>	<u>426</u>	<u>4.818E+05</u>	<u>1.381E+06</u>	

AREA OF BASIC UNIT = 8.548E-07 CM²

VARIANCE OF SQR(NS) = .981729

VARIANCE OF SQR(NI) = 2.48611

CORRELATION COEFFICIENT = 0.935

CHI SQUARED = 7.8665 WITH 19 DEGREES OF FREEDOM PASS

NS/NI = 0.291 +- 0.038

MEAN RATIO = 0.283 +- 0.024

AGE CALCULATED USING A ZETA OF 352.7 FOR SRM612 GLASS

RHO D = 1.45E+06 NO = 5755

POOLED AGE = 74.8 +- 7.6 MYR

MEAN AGE = 71.8 +- 6.2 MYR

POS 102A

IRRADIATION: PT930-05
ANALYSIS BY POS 5/15/80

CRYSTAL	NS	NI	AREA UNITS	RATIO	RHO S	RHO I	AGE(MYR)
1	0	5	7	0.000	0.00E+00	0.10E+05	0.0 +- 0.0
2	12	47	6	0.255	2.27E+04	0.00E+04	65.8 +- 21.8
3	4	3	18	1.333	4.54E+05	3.40E+05	332.2 +- 253.7
4	0	56	25	0.143	3.63E+05	2.54E+04	36.4 +- 13.8
5	7	31	20	0.226	3.97E+05	1.74E+04	57.5 +- 24.1
6	1	4	0	0.250	1.89E+05	7.56E+05	63.6 +- 71.1
7	17	06	9	0.190	2.14E+04	1.00E+07	50.3 +- 13.4
8	5	26	21	0.192	2.70E+05	1.40E+04	49.0 +- 23.9
9	2	4	0	0.500	2.03E+05	5.67E+05	126.6 +- 109.6
10	3	4	10	0.750	1.89E+05	2.52E+05	109.0 +- 144.3
11	2	2	10	1.000	2.27E+05	2.27E+05	250.0 +- 250.0
12	2	3	24	0.667	9.45E+04	1.42E+05	160.3 +- 153.6
13	1	3	6	0.333	1.89E+05	5.67E+05	84.7 +- 97.0
14	21	06	36	0.244	6.61E+05	2.71E+06	62.1 +- 15.1
15	1	3	24	0.333	4.72E+04	1.42E+05	84.7 +- 97.0
16	0	3	6	0.000	0.00E+00	5.67E+05	0.0 +- 0.0
17	2	2	6	1.000	3.70E+05	3.70E+05	250.0 +- 250.0
18	5	8	12	0.625	4.72E+05	7.56E+05	157.9 +- 90.0
19	4	12	9	0.333	5.04E+05	1.51E+06	04.7 +- 48.9
20	0	31	10	0.250	5.04E+05	1.95E+06	65.7 +- 26.0

1054194.237E+051.601E+06

AREA OF BASIC UNIT = 0.019E-07 CM²

VARIANCE OF SQR(NS) = 1.45495

VARIANCE OF SQR(NI) = 7.19546

CORRELATION COEFFICIENT = 0.955

CHI SQUARED = 23.2545 WITH 19 DEGREES OF FREEDOM PASS

NS/NI = 0.251 +- 0.027

MEAN RATIO = 0.432 +- 0.080

AGE CALCULATED USING A ZETA OF 352.7 FOR SRM312 GLASS

RHO O = 1.45E+00 NO = 5755

POOLED AGE = 63.3 +- 7.0 MYR

MEAN AGE = 109.5 +- 20.3 MYR

POS 97A

IRRADIATION: PT931-03
ANALYSIS BY POS 5/9/88

CRYSTAL	NS	NI	AREA UNITS	RATIO	RHO S	RHO I	AGE(MYR)
1	10	30	16	0.333	7.31E+05	2.19E+06	80.7 +- 29.5
2	3	18	24	0.167	1.46E+05	8.77E+05	48.5 +- 25.2
3	2	6	12	0.333	1.95E+05	5.85E+05	80.7 +- 65.9
4	7	27	12	0.259	6.82E+05	2.63E+06	62.8 +- 26.7
5	3	6	20	0.500	1.75E+05	3.51E+05	120.6 +- 85.3
6	14	56	12	0.250	1.36E+06	5.46E+06	60.6 +- 18.1
7	5	26	12	0.192	4.87E+05	2.53E+06	46.7 +- 22.8
8	2	5	12	0.400	1.95E+05	4.87E+05	96.7 +- 80.9
9	2	6	16	0.333	1.46E+05	4.39E+05	80.7 +- 65.9
10	6	17	30	0.353	2.34E+05	6.63E+05	85.4 +- 40.5
11	3	6	30	0.500	1.17E+05	2.34E+05	120.6 +- 85.3
12	9	42	30	0.214	3.51E+05	1.64E+06	52.8 +- 19.1
13	2	5	20	0.400	1.17E+05	2.92E+05	96.7 +- 80.9
14	4	11	30	0.364	1.56E+05	4.29E+05	80.0 +- 51.4
15	3	8	12	0.375	2.92E+05	7.80E+05	90.7 +- 61.4
16	14	47	20	0.298	8.19E+05	2.75E+06	72.1 +- 22.0
17	1	6	16	0.167	7.31E+04	4.39E+05	48.5 +- 43.7
18	7	16	20	0.438	4.89E+05	9.36E+05	105.7 +- 47.9
19	12	39	18	0.300	7.80E+05	2.53E+06	74.5 +- 24.6
20	0	4	15	0.800	0.800E+00	3.12E+05	0.0 +- 0.0

1893813.382E+051.182E+06

AREA OF BASIC UNIT = 8.548E-07 CM²

VARIANCE OF SQR(NS) = .945042

VARIANCE OF SQR(NI) = 3.1821

CORRELATION COEFFICIENT = 0.948

CHI SQUARED = 7.05549 WITH 19 DEGREES OF FREEDOM PASS

NS/NI = 0.286 +- 0.031

MEAN RATIO = 0.309 +- 0.027

AGE CALCULATED USING A ZETA OF 352.7 FOR SRM612 GLASS

RHO D = 1.381E+06 ND = 5480

POOLED AGE = 69.3 +- 7.6 MYR

MEAN AGE = 74.9 +- 6.7 MYR

POS 86A

IRRADIATION: PT916-09
ANALYSIS BY POS 5/7/88

CRYSTAL	NS	NI	AREA UNITS	RATIO	RHO S	RHO I	AGE(MYR)
1	11	67	32	0.164	3.41E+05	2.00E+06	39.7 +- 12.9
2	7	42	38	0.167	2.32E+05	1.39E+06	40.3 +- 16.5
3	16	72	32	0.222	4.97E+05	2.23E+06	53.7 +- 14.0
4	5	16	20	0.313	2.48E+05	7.95E+05	75.4 +- 38.6
5	14	58	24	0.280	5.79E+05	2.07E+06	67.6 +- 28.4
6	26	97	32	0.268	0.07E+05	3.01E+06	64.7 +- 14.3
7	11	33	25	0.333	4.37E+05	1.31E+06	80.4 +- 26.0
8	2	8	22	0.250	9.03E+04	3.61E+05	60.4 +- 47.7
9	9	31	24	0.290	3.72E+05	1.20E+06	70.1 +- 26.5
10	10	100	36	0.167	4.97E+05	2.98E+06	40.3 +- 10.3
11	8	37	25	0.216	3.10E+05	1.47E+06	52.3 +- 20.4
12	2	10	30	0.200	6.62E+04	3.31E+05	48.3 +- 37.5
13	3	6	32	0.500	9.31E+04	1.06E+05	120.2 +- 85.0
14	4	26	25	0.154	1.59E+05	1.03E+06	37.2 +- 20.0
15	11	43	36	0.256	3.03E+05	1.19E+06	61.0 +- 20.9
16	24	88	27	0.273	0.83E+05	3.24E+06	65.0 +- 15.2
17	27	126	25	0.214	1.07E+06	5.01E+06	51.8 +- 11.0
18	25	111	28	0.225	1.24E+06	5.51E+06	54.4 +- 12.0
19	2	5	24	0.400	0.20E+04	2.07E+05	96.3 +- 80.6
20	3	9	18	0.333	1.66E+05	4.97E+05	30.4 +- 53.6
					<u>4.201E+05</u>	<u>1.015E+06</u>	

AREA OF BASIC UNIT = $1.0068E-06$ CM²

VARIANCE OF SQR(NS) = 1.70548

VARIANCE OF SQR(NI) = 0.50176

CORRELATION COEFFICIENT = 0.954

CHI SQUARED = 9.52736 WITH 19 DEGREES OF FREEDOM PASS

NS/NI = 0.231 +- 0.017

MEAN RATIO = 0.261 +- 0.019

AGE CALCULATED USING A ZETA OF 352.7 FOR GRM612 GLASS

RHO D = $1.376E+06$ ND = 5461

POOLED AGE = 55.9 +- 4.2 MYR

MEAN AGE = 53.1 +- 4.7 MYR

JD 78A

IRRADIATION: PT917-05
ANALYSIS BY POS 5/17/88

CRYSTAL	NS	NI	AREA UNITS	RATIO	RHO S	RHO I	AGE(MYR)
1	5	18	9	0.278	5.52E+05	1.99E+06	65.7 +- 33.2
2	18	46	9	0.217	1.10E+06	5.08E+06	51.5 +- 18.0
3	8	36	25	0.222	3.18E+05	1.43E+06	52.7 +- 28.6
4	3	9	20	0.333	1.49E+05	4.47E+05	70.8 +- 52.5
5	7	30	7	0.104	9.93E+05	5.39E+06	43.7 +- 18.0
6	2	7	6	0.286	3.31E+05	1.16E+06	67.6 +- 54.2
7	6	18	18	0.333	5.96E+05	1.79E+06	70.8 +- 37.2
8	2	3	12	0.667	1.66E+05	2.40E+05	156.7 +- 143.0

<u>43</u>	<u>175</u>	<u>4.358E+05</u>	<u>1.774E+06</u>
-----------	------------	------------------	------------------

AREA OF BASIC UNIT = 1.0868E-06 CM²

VARIANCE OF SQR(NS) = .432437

VARIANCE OF SQR(NI) = 3.36207

CORRELATION COEFFICIENT = 0.966

CHI SQUARED = 2.7097 WITH 7 DEGREES OF FREEDOM PASS

NS/NI = 0.246 +- 0.042

MEAN RATIO = 0.315 +- 0.054

AGE CALCULATED USING A ZETA OF 352.7 FOR SRM612 GLASS

RHO D = 1.349E+06 ND = 5354

POOLED AGE = 58.2 +- 9.9 MYR

MEAN AGE = 74.5 +- 12.8 MYR

POS 96A

IRRADIATION: PT931-08
ANALYSIS BY POS 5/9/88

CRYSTAL	NS	NI	AREA UNITS	RATIO	RHO S	RHO I	AGE(MYR)
1	1	7	20	0.143	4.97E+04	3.48E+05	34.7 +- 37.1
2	2	3	5	0.667	3.97E+05	5.96E+05	160.3 +- 146.4
3	4	11	15	0.364	2.65E+05	7.20E+05	80.8 +- 51.4
4	1	4	10	0.250	9.93E+04	3.97E+05	60.6 +- 67.7
5	0	4	10	0.000	0.00E+00	3.97E+05	0.0 +- 0.0
6	5	21	15	0.238	3.31E+05	1.39E+06	57.7 +- 29.7
7	2	8	40	0.250	4.97E+04	1.99E+05	60.6 +- 47.9
8	7	21	16	0.333	4.35E+05	1.38E+06	80.7 +- 35.2
9	11	32	21	0.344	5.20E+05	1.51E+06	83.2 +- 29.1
10	3	16	10	0.100	1.66E+05	0.83E+05	45.5 +- 20.6
11	1	5	15	0.200	6.62E+04	3.31E+05	48.5 +- 53.2
12	10	16	10	0.625	9.93E+05	1.59E+06	150.4 +- 60.6
13	3	11	30	0.273	9.93E+04	3.64E+05	66.1 +- 43.0
14	17	86	21	0.190	0.04E+05	4.07E+06	40.8 +- 12.7
15	1	4	15	0.250	6.62E+04	2.65E+05	60.6 +- 67.7
16	0	2	10	0.000	0.00E+00	1.99E+05	0.0 +- 0.0
17	2	9	15	0.222	1.32E+05	5.96E+05	53.9 +- 42.1
18	16	62	20	0.250	7.95E+05	3.00E+06	62.5 +- 17.5
19	1	7	8	0.143	1.24E+05	0.69E+05	34.7 +- 37.1
20	2	6	40	0.333	4.97E+04	1.49E+05	80.7 +- 65.9

393352.497E+059.397E+05AREA OF BASIC UNIT = 1.0860E-06 CM²

VARIANCE OF SQR(NS) = 1.34816

VARIANCE OF SQR(NI) = 4.15772

CORRELATION COEFFICIENT = 0.929

CHI SQUARED = 11.1033 WITH 19 DEGREES OF FREEDOM PASS

NS/NI = 0.266 +- 0.032

MEAN RATIO = 0.264 +- 0.036

AGE CALCULATED USING A ZETA OF 352.7 FOR SRM612 GLASS

RHO D = 1.381E+06 MD = 5400

POOLED AGE = 54.4 +- 7.7 MYR

MEAN AGE = 63.9 +- 6.9 MYR

POS 90A

IRRADIATION: PT931-12
ANALYSIS BY POS 5/9/88

CRYSTAL	NS	NI	AREA UNITS	RATIO	RHO S	RHO I	AGE(MYR)
1	14	32	8	0.438	1.74E+06	3.97E+06	105.7 +- 33.9
2	4	12	4	0.333	9.93E+05	2.98E+06	88.7 +- 46.6
3	2	11	9	0.182	2.21E+05	1.21E+06	44.1 +- 33.9
4	2	7	18	0.286	1.99E+05	6.95E+05	69.2 +- 55.5
5	5	22	8	0.227	6.21E+05	2.73E+06	55.1 +- 27.3
6	2	6	8	0.333	2.48E+05	7.45E+05	88.7 +- 65.9
7	18	46	8	0.217	1.24E+06	5.71E+06	52.7 +- 18.4
8	4	25	12	0.168	3.31E+05	2.87E+06	38.9 +- 28.9
9	6	29	12	0.207	4.97E+05	2.48E+06	58.2 +- 22.5
10	3	13	8	0.231	3.72E+05	1.61E+06	56.8 +- 35.8
11	3	14	18	0.214	2.98E+05	1.39E+06	52.8 +- 33.1
12	2	5	18	0.488	1.99E+05	4.97E+05	96.7 +- 88.9
13	3	18	12	0.388	2.48E+05	8.28E+05	72.7 +- 47.8
14	3	11	16	0.273	1.86E+05	6.83E+05	66.1 +- 43.8
15	8	29	9	0.276	8.83E+05	3.28E+06	66.8 +- 26.7
16	1	8	18	0.125	5.52E+04	4.41E+05	38.4 +- 32.2
17	5	19	9	0.263	5.52E+05	2.18E+06	63.8 +- 32.1
18	6	21	15	0.286	3.97E+05	1.39E+06	69.2 +- 32.8
19	4	17	9	0.235	4.41E+05	1.88E+06	57.1 +- 31.7
20	2	9	6	0.222	3.31E+05	1.49E+06	53.9 +- 42.1

<u>89</u>	<u>346</u>	<u>4.398E+05</u>	<u>1.718E+06</u>
-----------	------------	------------------	------------------

AREA OF BASIC UNIT = 1.0868E-06 CM²

VARIANCE OF SQR(NS) = .452024

VARIANCE OF SQR(NI) = 1.48146

CORRELATION COEFFICIENT = 0.859

CHI SQUARED = 5.74935 WITH 19 DEGREES OF FREEDOM PASS

NS/NI = 0.257 +- 0.031

MEAN RATIO = 0.260 +- 0.017

AGE CALCULATED USING A ZETA OF 352.7 FOR SPN612 GLASS

RHO D = 1.331E+06 ND = 5480

POOLED AGE = 62.3 +- 7.5 MYR

MEAN AGE = 63.1 +- 4.2 MYR

POS 88A

IRRADIATION: PT916-10
ANALYSIS BY POS 5/9/88

CRYSTAL	NS	NI	AREA UNITS	RATIO	RHO S	RHO I	AGE(MYR)
1	44	197	30	0.223	1.46E+06	6.52E+06	54.0 +- 9.8
2	0	4	6	0.000	0.00E+00	6.62E+05	0.0 +- 0.0
3	2	5	8	0.400	2.40E+05	6.21E+05	96.3 +- 88.6
4	1	0	0	0.125	1.24E+05	9.93E+05	30.3 +- 32.1
5	1	5	0	0.200	1.24E+05	6.21E+05	40.3 +- 53.0
6	4	17	10	0.235	3.97E+05	1.69E+06	56.0 +- 31.6
7	13	57	20	0.220	4.61E+05	2.02E+06	55.1 +- 16.9

<u>65</u>	<u>293</u>				<u>6.500E+05</u>	<u>2.970E+06</u>	
-----------	------------	--	--	--	------------------	------------------	--

AREA OF BASIC UNIT = 1.0060E-06 CM²

VARIANCE OF SQR(NS) = 4.9996

VARIANCE OF SQR(NI) = 19.6514

CORRELATION COEFFICIENT = 0.999

CHI SQUARED = 1.72092 WITH 6 DEGREES OF FREEDOM PASS

NS/NI = 0.222 +- 0.030

MEAN RATIO = 0.202 +- 0.046

AGE CALCULATED USING A ZETA OF 352.7 FOR SRM612 GLASS

RHO D = 1.376E+06 ND = 5461

POOLED AGE = 53.6 +- 7.4 MYR

MEAN AGE = 48.8 +- 11.1 MYR

POS 111A

IRRADIATION: PT931-07
ANALYSIS BY POS 5/16/88

CRYSTAL	NS	NI	AREA UNITS	RATIO	RHO S	RHO I	AGE(MYR)
1	6	18	18	0.333	5.96E+05	1.79E+06	80.7 +- 38.0
2	2	8	8	0.250	2.48E+05	9.93E+05	60.6 +- 47.7
3	6	15	18	0.400	3.31E+05	8.28E+05	96.7 +- 46.7
4	4	12	8	0.333	4.97E+05	1.49E+06	80.7 +- 46.6
5	3	7	4	0.429	7.45E+05	1.74E+06	103.5 +- 71.4
6	8	34	9	0.235	8.03E+05	3.75E+06	57.1 +- 22.4
7	3	16	9	0.180	3.31E+05	1.77E+06	45.5 +- 28.6
8	3	27	9	0.111	3.31E+05	2.98E+06	27.0 +- 16.4
9	7	31	6	0.226	1.16E+06	5.13E+06	54.8 +- 22.9
10	6	12	12	0.500	4.97E+05	9.93E+05	120.6 +- 60.3
11	4	14	6	0.286	6.62E+05	2.32E+06	69.2 +- 39.2
12	5	24	15	0.200	3.31E+05	1.59E+06	50.5 +- 24.8
13	2	18	4	0.200	4.97E+05	2.48E+06	40.5 +- 37.6
14	3	12	4	0.250	7.45E+05	2.98E+06	60.6 +- 39.1
15	1	6	6	0.167	1.66E+05	9.93E+05	40.5 +- 43.7
16	3	8	6	0.375	4.97E+05	1.32E+06	90.7 +- 61.4
17	3	13	9	0.231	3.31E+05	1.43E+06	56.0 +- 35.8
18	3	15	9	0.200	3.31E+05	1.66E+06	40.5 +- 38.7
19	1	5	6	0.200	1.66E+05	8.28E+05	40.5 +- 53.2
20	2	15	9	0.133	2.21E+05	1.66E+06	32.4 +- 24.4

<u>75</u>	<u>302</u>	<u>4.461E+05</u>	<u>1.796E+06</u>
-----------	------------	------------------	------------------

AREA OF BASIC UNIT = 1.0068E-06 CM²

VARIANCE OF SQR(NS) = .261357

VARIANCE OF SQR(NI) = .995079

CORRELATION COEFFICIENT = 0.729

CHI SQUARED = 8.09865 WITH 19 DEGREES OF FREEDOM PASS

NS/NI = 0.248 +- 0.032

MEAN RATIO = 0.263 +- 0.023

AGE CALCULATED USING A ZETA OF 352.7 FOR GRM612 GLASS

RHO D = 1.381E+06 MD = 5480

POOLED AGE = 60.2 +- 7.8 MYR

MEAN AGE = 63.7 +- 5.6 MYR

POS 760

IRRADIATION: PT931-11
ANALYSIS BY POS 5/9/88

CRYSTAL	NS	NI	AREA UNITS	RATIO	RHO S	RHO I	AGE(MYR)
1	1	4	12	0.250	0.28E+04	3.31E+05	60.6 +- 67.7
2	6	56	24	0.107	2.48E+05	2.32E+06	26.0 +- 11.2
3	4	16	8	0.250	4.97E+05	1.99E+06	60.6 +- 33.9
4	20	121	8	0.165	2.48E+06	1.50E+07	40.1 +- 9.7
5	6	16	6	0.375	9.93E+05	2.65E+06	90.7 +- 43.4
6	1	4	10	0.250	9.93E+04	3.97E+05	60.6 +- 67.7
7	3	6	4	0.500	7.45E+05	1.49E+06	120.6 +- 85.3
8	4	17	6	0.235	6.62E+05	2.81E+06	57.1 +- 31.7
9	6	27	8	0.222	7.45E+05	3.35E+06	93.9 +- 24.3
10	4	23	12	0.174	3.31E+05	1.90E+06	42.2 +- 22.9
11	6	24	7	0.250	8.51E+05	3.41E+06	60.6 +- 27.7
12	1	6	8	0.167	1.24E+05	7.45E+05	40.5 +- 43.7
13	3	9	4	0.333	7.45E+05	2.23E+06	80.7 +- 53.8
14	4	13	18	0.308	2.21E+05	7.17E+05	74.5 +- 42.6
15	2	8	8	0.250	2.48E+05	9.93E+05	60.6 +- 47.9
16	5	18	3	0.278	1.66E+06	5.96E+06	67.3 +- 34.0
17	17	59	9	0.288	1.88E+06	6.51E+06	69.8 +- 19.2
18	13	95	15	0.137	8.61E+05	6.29E+06	33.2 +- 9.8
19	2	15	8	0.133	2.48E+05	1.86E+06	32.4 +- 24.4
20	2	6	8	0.333	2.48E+05	7.45E+05	80.7 +- 65.9

<u>110</u>	<u>543</u>	<u>5.874E+05</u>	<u>2.900E+06</u>
------------	------------	------------------	------------------

AREA OF BASIC UNIT = 1.0068E-06 CM²

VARIANCE OF SQR(NS) = .9369

VARIANCE OF SQR(NI) = 6.39069

CORRELATION COEFFICIENT = 0.917

CHI SQUARED = 12.8013 WITH 19 DEGREES OF FREEDOM PASS

NS/NI = 0.203 +- 0.021

MEAN RATIO = 0.250 +- 0.021

AGE CALCULATED USING A ZETA OF 352.7 FOR SRM612 GLASS

RHO D = 1.381E+06 ND = 5480

POOLED AGE = 49.1 +- 5.2 MYR

MEAN AGE = 60.7 +- 5.1 MYR

POS 117A

IRRADIATION: PT930-02
ANALYSIS BY POS 5/17/88

CRYSTAL	NS	NI	AREA UNITS	RATIO	RHO S	RHO I	AGE(MYR)
1	3	10	9	0.300	3.31E+05	1.10E+06	76.3 +- 50.2
2	2	7	4	0.286	4.97E+05	1.74E+06	72.7 +- 50.2
3	1	5	6	0.200	1.66E+05	8.20E+05	50.9 +- 55.8
4	3	6	4	0.500	7.45E+05	1.49E+06	126.6 +- 89.5
5	2	7	9	0.286	2.21E+05	7.73E+05	72.7 +- 50.2
6	6	26	6	0.231	9.93E+05	4.30E+06	50.7 +- 26.6
7	1	4	4	0.250	2.40E+05	9.93E+05	63.6 +- 71.1
8	1	3	5	0.333	1.99E+05	5.96E+05	84.7 +- 97.8
9	1	5	4	0.200	2.40E+05	1.24E+06	50.9 +- 55.8
10	1	5	4	0.200	2.40E+05	1.24E+06	50.9 +- 55.8
11	5	10	6	0.500	8.20E+05	1.66E+06	126.6 +- 69.3
12	1	2	9	0.500	1.10E+05	2.21E+05	126.6 +- 155.1
13	4	11	3	0.364	1.32E+06	3.64E+06	92.3 +- 53.9
14	8	11	9	0.800	0.80E+00	1.21E+06	0.0 +- 0.0
15	4	10	8	0.400	4.97E+05	1.24E+06	101.5 +- 60.0
16	2	8	8	0.250	2.40E+05	9.93E+05	63.6 +- 50.3

<u>37</u>	<u>138</u>	<u>3.750E+05</u>	<u>1.318E+06</u>
-----------	------------	------------------	------------------

AREA OF BASIC UNIT = 1.0060E-06 CM²

VARIANCE OF SQR(NS) = .377437

VARIANCE OF SQR(NI) = .730373

CORRELATION COEFFICIENT = 0.742

CHI SQUARED = 6.19307 WITH 15 DEGREES OF FREEDOM PASS

NS/NI = 0.285 +- 0.053

MEAN RATIO = 0.300 +- 0.033

AGE CALCULATED USING A ZETA OF 352.7 FOR SRM612 GLASS

RHO D = 1.45E+06 NO = 5755

POOLED AGE = 72.4 +- 13.5 MYR

MEAN AGE = 76.2 +- 8.5 MYR

JD 87A

IRRADIATION: PT917-06
ANALYSIS BY POS 5/17/88

CRYSTAL	NS	NI	AREA UNITS	RATIO	RHO S	RHO I	AGE(MYR)
1	1	4	12	0.250	0.20E+04	3.31E+05	59.2 +- 66.2
2	2	7	20	0.286	9.93E+04	3.48E+05	67.6 +- 54.2
3	3	6	25	0.500	1.19E+05	2.38E+05	117.9 +- 83.3
4	1	5	16	0.200	6.21E+04	3.10E+05	47.4 +- 51.9
5	2	7	12	0.286	1.66E+05	5.79E+05	67.6 +- 54.2
6	5	17	16	0.294	3.10E+05	1.06E+06	69.6 +- 35.4
7	3	20	16	0.150	1.06E+05	1.24E+06	35.6 +- 22.0

<u>17</u>	<u>66</u>				<u>1.443E+05</u>	<u>5.603E+05</u>	
-----------	-----------	--	--	--	------------------	------------------	--

AREA OF BASIC UNIT = 1.0068E-06 CM²

VARIANCE OF SQR(NS) = .194016

VARIANCE OF SQR(NI) = .923343

CORRELATION COEFFICIENT = 0.746

CHI SQUARED = 1.84994 WITH 6 DEGREES OF FREEDOM PASS

NS/NI = 0.258 +- 0.070

MEAN RATIO = 0.291 +- 0.042

AGE CALCULATED USING A ZETA OF 352.7 FOR SRM612 GLASS

RHO O = 1.349E+06 ND = 5354

POOLED AGE = 61.0 +- 16.6 MYR

MEAN AGE = 66.5 +- 9.9 MYR

POS 115A

IRRADIATION: PT930-11
ANALYSIS BY POS 5/16/88

CRYSTAL	NS	NI	AREA UNITS	RATIO	RHO S	RHO I	AGE(MYR)
1	1	5	8	0.288	1.24E+05	6.21E+05	58.9 +- 55.8
2	3	9	4	0.333	7.45E+05	2.23E+06	84.7 +- 56.5
3	3	8	6	0.375	4.97E+05	1.32E+06	95.2 +- 64.4
4	1	2	3	0.588	3.31E+05	6.62E+05	126.6 +- 155.1
5	8	3	4	0.888	0.88E+08	7.45E+05	8.8 +- 8.8
6	8	4	4	0.888	0.88E+08	9.93E+05	8.8 +- 8.8
7	8	2	6	0.888	0.88E+08	3.31E+05	8.8 +- 8.8
8	5	17	6	0.294	8.28E+05	2.81E+06	74.8 +- 38.8
9	4	19	9	0.211	4.41E+05	2.18E+06	53.6 +- 29.5
10	2	9	6	0.222	3.31E+05	1.49E+06	56.6 +- 44.2
11	8	3	8	0.888	0.88E+08	3.72E+05	8.8 +- 8.8
12	3	18	9	0.388	3.31E+05	1.18E+06	76.3 +- 58.2

22912.993E+051.238E+06

AREA OF BASIC UNIT = $1.8868E-06$ D¹²

VARIANCE OF SQR(NS) = .749766

VARIANCE OF SQR(NI) = .991811

CORRELATION COEFFICIENT = 0.919

CHI SQUARED = 4.2922 WITH 11 DEGREES OF FREEDOM PASS

NS/NI = 0.242 +- 0.057

MEAN RATIO = 0.283 +- 0.049

AGE CALCULATED USING A ZETA OF 352.7 FOR SRM612 GLASS

RHO D = $1.45E+06$ ND = 5755

POOLED AGE = 61.5 +- 14.6 MYR

MEAN AGE = 51.7 +- 12.5 MYR

POS 99A

IRRADIATION: PT931-13
ANALYSIS BY POS 5/15/88

CRYSTAL	NS	NI	AREA UNITS	RATIO	RHO S	RHO I	AGE(MYR)
1	9	21	5	0.238	1.17E+06	4.91E+06	57.7 +- 28.7
2	2	28	28	0.108	1.17E+05	1.17E+06	24.3 +- 18.8
3	1	4	2	0.258	5.85E+05	2.34E+06	68.6 +- 67.7
4	8	3	2	0.888	8.88E+08	1.75E+06	8.8 +- 8.8
5	8	3	4	0.888	8.88E+08	8.77E+05	8.8 +- 8.8
6	9	18	15	0.588	7.82E+05	1.48E+06	128.6 +- 49.2
7	1	9	9	0.111	1.38E+05	1.17E+06	27.8 +- 28.5
8	8	5	6	0.888	8.88E+08	9.75E+05	8.8 +- 8.8
9	2	3	18	0.667	1.38E+05	1.95E+05	168.3 +- 146.4
10	3	8	16	0.375	2.19E+05	5.85E+05	98.7 +- 61.4
11	1	2	5	0.588	2.34E+05	4.68E+05	128.6 +- 147.7
12	1	4	6	0.258	1.95E+05	7.88E+05	68.6 +- 67.7
13	1	6	6	0.167	1.95E+05	1.17E+06	48.5 +- 43.7
14	3	4	18	0.758	3.51E+05	4.68E+05	188.1 +- 137.6
15	6	28	25	0.388	2.81E+05	9.36E+05	72.7 +- 33.8
16	2	18	9	0.288	2.68E+05	1.38E+06	48.5 +- 37.6
17	2	5	16	0.488	1.46E+05	3.66E+05	96.7 +- 88.9
18	8	4	6	0.888	8.88E+08	7.88E+05	8.8 +- 8.8
19	4	12	9	0.333	5.28E+05	1.56E+06	88.7 +- 46.6
20	2	19	18	0.185	2.34E+05	2.22E+06	25.6 +- 19.8

451882.645E+051.858E+06

AREA OF BASIC UNIT = 8.548E-07 CM²

VARIANCE OF SQR(NS) = .694513

VARIANCE OF SQR(NI) = 1.18707

CORRELATION COEFFICIENT = 0.693

CHI SQUARED = 15.3456 WITH 19 DEGREES OF FREEDOM PASS

NS/NI = 0.250 +- 0.042

MEAN RATIO = 0.262 +- 0.049

AGE CALCULATED USING A ZETA OF 352.7 FOR SRM612 GLASS

RHO O = 1.381E+06 NO = 5488

POOLED AGE = 68.6 +- 10.1 MYR

MEAN AGE = 63.6 +- 11.9 MYR

POS 98A

IRRADIATION: PT916-11
ANALYSIS BY POS 5/15/88

CRYSTAL	NS	NI	AREA UNITS	RATIO	RHO S	RHO I	AGE(MYR)
1	8	3	24	0.000	0.00E+00	1.46E+05	0.0 +- 0.0
2	8	8	16	0.000	0.00E+00	5.85E+05	0.0 +- 0.0
3	2	5	15	0.400	1.56E+05	3.90E+05	96.3 +- 80.6
4	8	3	9	0.000	0.00E+00	3.90E+05	0.0 +- 0.0
5	1	3	9	0.333	1.38E+05	3.90E+05	80.4 +- 92.0
6	3	16	18	0.188	3.51E+05	1.07E+06	45.3 +- 20.5
7	1	2	20	0.500	5.85E+04	1.17E+05	120.2 +- 147.2
8	0	3	12	0.000	0.00E+00	2.92E+05	0.0 +- 0.0
9	6	15	21	0.400	3.34E+05	8.36E+05	96.3 +- 46.5
10	0	1	9	0.000	0.00E+00	1.38E+05	0.0 +- 0.0
11	2	5	12	0.400	1.95E+05	4.07E+05	96.3 +- 80.6
12	5	18	24	0.500	2.44E+05	4.07E+05	120.2 +- 63.0
13	2	4	9	0.500	2.68E+05	5.20E+05	120.2 +- 104.1
14	8	8	9	0.000	0.00E+00	1.04E+06	0.0 +- 0.0
15	2	6	16	0.333	1.46E+05	4.39E+05	80.4 +- 65.6
16	1	3	8	0.333	1.46E+05	4.39E+05	80.4 +- 92.0
17	0	5	20	0.000	0.00E+00	2.92E+05	0.0 +- 0.0

<u>25</u>	<u>180</u>	<u>1.204E+05</u>	<u>4.014E+05</u>
-----------	------------	------------------	------------------

AREA OF BASIC UNIT = 0.540E-07 CM²

VARIANCE OF SQR(NS) = .727061

VARIANCE OF SQR(NI) = .679781

CORRELATION COEFFICIENT = 0.713

CHI SQUARED = 12.4843 WITH 16 DEGREES OF FREEDOM PASS

NS/NI = 0.250 +- 0.056

MEAN RATIO = 0.229 +- 0.051

AGE CALCULATED USING A ZETA OF 352.7 FOR SRM612 GLASS

RHO D = 1.376E+06 NO = 5461

POOLED AGE = 60.4 +- 13.5 MYR

MEAN AGE = 55.3 +- 12.4 MYR

POS 113A

IRRADIATION: PT936-13
ANALYSIS BY POS 5/16/88

CRYSTAL	NS	NI	AREA UNITS	RATIO	RHO S	RHO I	AGE(MYR)
1	4	8	24	0.500	1.66E+05	3.31E+05	126.6 +- 77.5
2	6	46	12	0.130	4.97E+05	3.81E+06	33.3 +- 14.4
3	7	37	6	0.189	1.16E+06	6.13E+06	48.2 +- 19.9
4	4	18	12	0.222	3.31E+05	1.49E+06	56.6 +- 31.3
5	4	16	6	0.250	6.62E+05	2.65E+06	63.6 +- 35.6
6	4	9	6	0.444	6.62E+05	1.49E+06	112.7 +- 67.7
7	13	53	21	0.243	6.15E+05	2.51E+06	62.4 +- 19.3
8	3	7	9	0.429	3.31E+05	7.73E+05	188.7 +- 75.8
9	2	18	12	0.200	1.66E+05	8.28E+05	58.9 +- 39.5
<hr/>							
<u>47</u>		<u>284</u>			<u>4.322E+05</u>	<u>1.876E+06</u>	

AREA OF BASIC UNIT = 1.0868E-06 CM²

VARIANCE OF SQR(NS) = .404088

VARIANCE OF SQR(NI) = 3.25077

CORRELATION COEFFICIENT = 0.865

CHI SQUARED = 5.85106 WITH 8 DEGREES OF FREEDOM PASS

NS/NI = 0.230 +- 0.037

MEAN RATIO = 0.290 +- 0.044

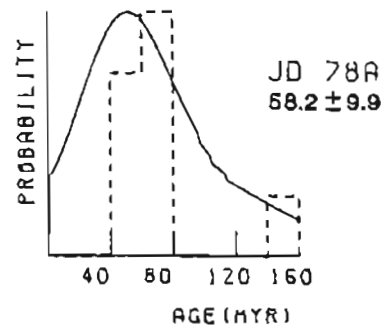
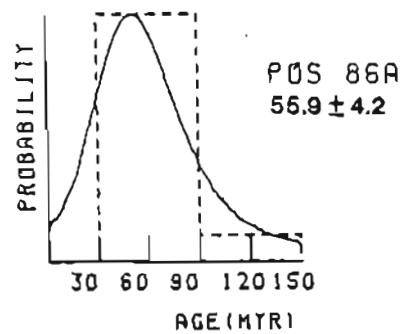
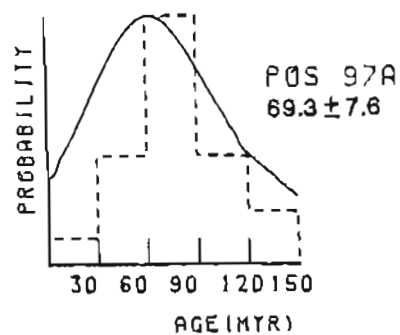
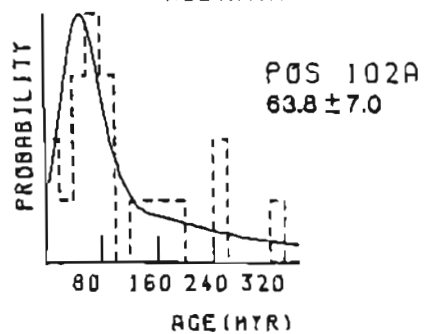
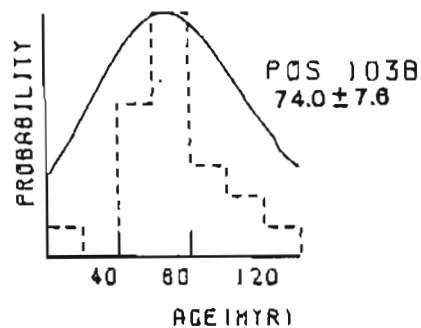
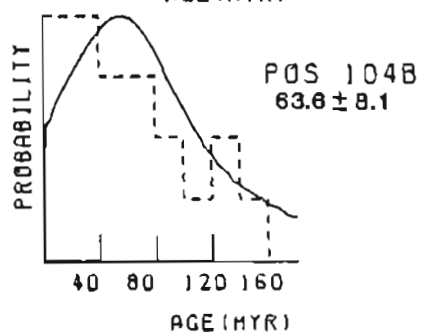
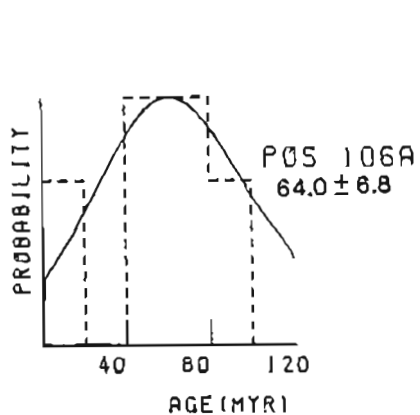
AGE CALCULATED USING A ZETA OF 352.7 FOR SRM612 GLASS

RHO O = 1.45E+06 NO = 5755

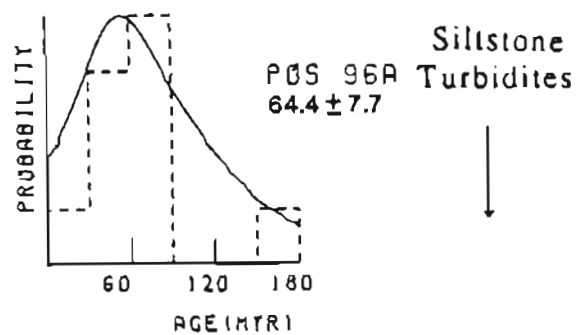
POOLED AGE = 58.6 +- 9.5 MYR

MEAN AGE = 73.7 +- 11.2 MYR

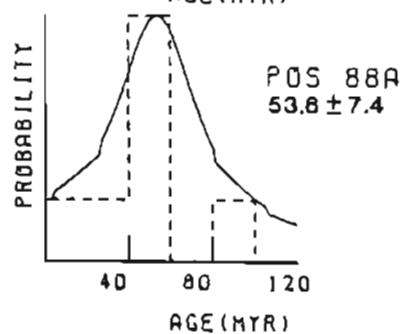
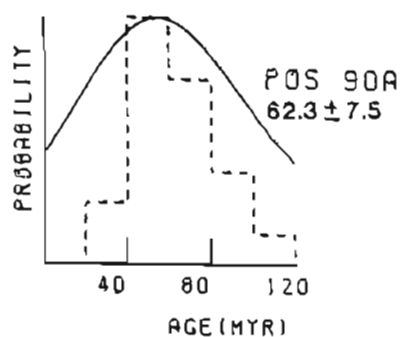
Single-Grain Age Distributions: Bathtub Ridge



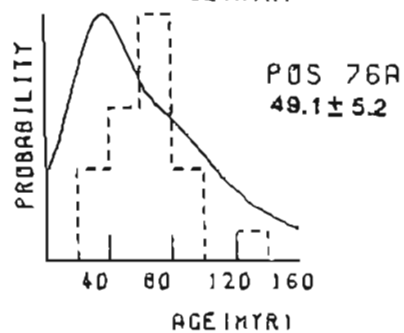
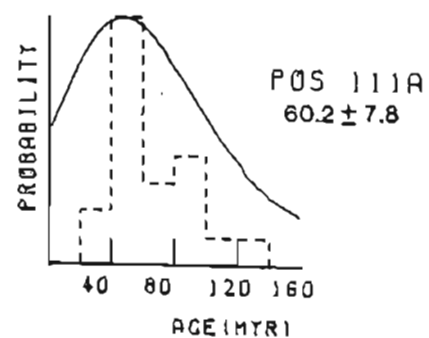
↑
Bathtub
Graywacke



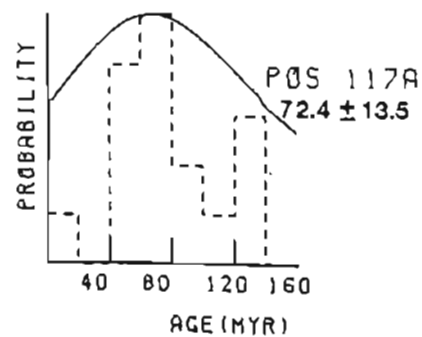
Siltstone
Turbidites
↓



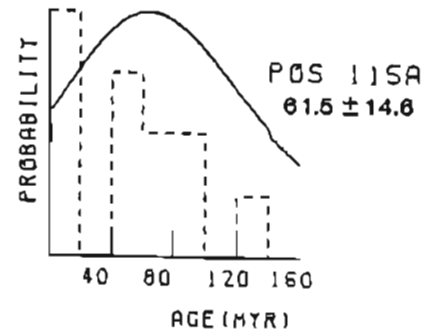
↑
Kemik Sandstone
↓

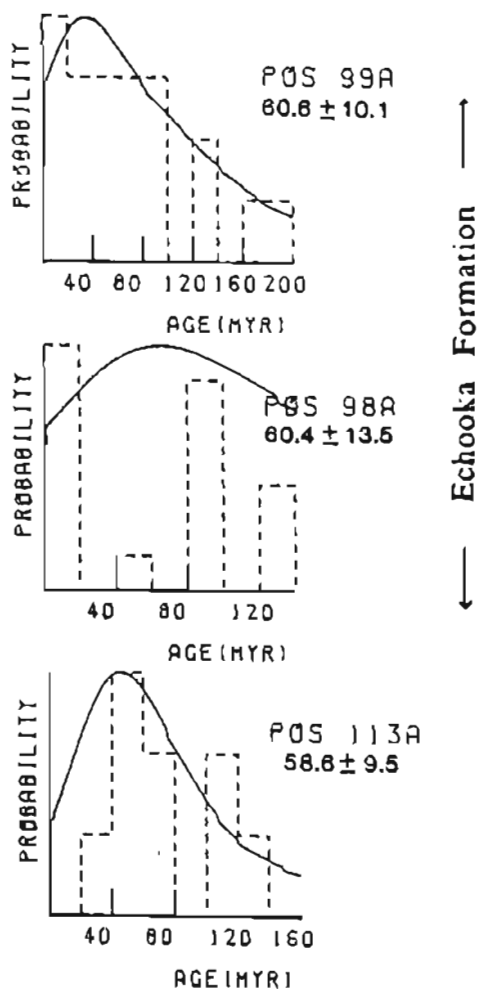


—
Shublik Formation
↓



↑
Ivishak Formation
↓





Arctic Creek Region

JD 26A

IRRADIATION: PT916-15
ANALYSIS BY POS 4/28/88

CRYSTAL	NS	NI	AREA UNITS	RATIO	RHO S	RHO I	AGE(MYR)
1	1	10	36	0.100	2.76E+04	2.76E+05	24.2 +- 25.4
2	6	96	70	0.063	8.51E+04	1.36E+06	15.1 +- 6.4
3	0	1	27	0.000	0.00E+00	3.60E+04	0.0 +- 0.0
4	4	10	20	0.400	1.99E+05	4.97E+05	96.3 +- 57.0
5	1	3	49	0.333	2.03E+04	6.00E+04	80.4 +- 92.0
6	1	5	40	0.200	2.40E+04	1.24E+05	48.3 +- 53.0
7	9	46	45	0.196	1.99E+05	1.02E+06	47.3 +- 17.2
8	0	5	50	0.000	0.00E+00	9.93E+04	0.0 +- 0.0
9	10	101	36	0.099	2.76E+05	2.79E+06	24.0 +- 0.0
10	1	2	15	0.500	6.62E+04	1.32E+05	120.2 +- 147.2
11	16	171	20	0.094	7.95E+05	8.49E+06	22.7 +- 5.9
12	10	121	20	0.149	8.94E+05	6.01E+06	36.0 +- 9.1
13	0	33	25	0.242	3.18E+05	1.31E+06	50.6 +- 23.1
14	2	9	30	0.222	6.62E+04	2.90E+05	53.7 +- 42.0
15	1	0	20	0.125	3.55E+04	2.04E+05	30.3 +- 32.1
16	0	1	21	0.000	0.00E+00	4.73E+04	0.0 +- 0.0
17	1	7	28	0.143	3.55E+04	2.40E+05	34.6 +- 37.0
18	0	1	27	0.000	0.00E+00	3.60E+04	0.0 +- 0.0
19	0	3	32	0.000	0.00E+00	9.31E+04	0.0 +- 0.0
20	1	3	16	0.333	6.21E+04	1.06E+05	80.4 +- 92.0

806361.251E+059.940E+05AREA OF BASIC UNIT = 1.0060E-06 CM²

VARIANCE OF SQR(NS) = 1.02676

VARIANCE OF SQR(NI) = 14.3114

CORRELATION COEFFICIENT = 0.913

CHI SQUARED = 13.967 WITH 19 DEGREES OF FREEDOM PASS

NS/NI = 0.126 +- 0.015

MEAN RATIO = 0.160 +- 0.032

AGE CALCULATED USING A ZETA OF 352.7 FOR SRM612 GLASS

RHO 0 = 1.376E+06 ND = 5461

POOLED AGE = 30.5 +- 3.6 MYR

MEAN AGE = 38.7 +- 7.8 MYR

JD 17A

IRRADIATION: PT916-14
ANALYSIS BY POS 4/27/88

CRYSTAL	NS	NI	AREA UNITS	RATIO	RHO S	RHO I	AGE(MYR)
1	8	11	38	0.000	0.00E+00	3.44E+05	0.0 +- 0.0
2	9	98	20	0.100	4.47E+05	4.47E+06	24.2 +- 0.5
3	2	18	21	0.200	9.46E+04	4.73E+05	48.3 +- 37.5
4	0	4	16	0.000	0.00E+00	2.48E+05	0.0 +- 0.0
5	2	14	20	0.143	9.93E+04	6.95E+05	34.6 +- 26.1
6	2	17	15	0.110	1.32E+05	1.13E+06	28.5 +- 21.3
7	4	31	20	0.129	1.42E+05	1.10E+06	31.2 +- 16.6
8	0	3	32	0.000	0.00E+00	9.31E+04	0.0 +- 0.0
9	1	9	24	0.111	4.14E+04	3.72E+05	26.9 +- 28.4
10	3	12	48	0.250	6.21E+04	2.48E+05	68.4 +- 39.8
11	39	263	30	0.148	1.29E+06	8.71E+06	35.9 +- 6.2
12	1	7	10	0.143	5.32E+04	3.86E+05	34.6 +- 37.0
13	0	3	20	0.000	0.00E+00	1.49E+05	0.0 +- 0.0
14	0	1	30	0.000	0.00E+00	2.61E+04	0.0 +- 0.0
15	0	2	6	0.000	0.00E+00	3.31E+05	0.0 +- 0.0
16	0	1	4	0.000	0.00E+00	2.48E+05	0.0 +- 0.0
17	1	4	16	0.250	6.21E+04	2.48E+05	68.4 +- 67.5
18	3	16	25	0.100	1.19E+05	6.36E+05	45.3 +- 28.5
19	12	46	24	0.261	4.97E+05	1.98E+06	63.8 +- 20.4
20	3	16	36	0.100	8.28E+04	4.41E+05	45.3 +- 20.5
<u>92</u>			<u>560</u>		<u>1.729E+05</u>	<u>1.181E+06</u>	

AREA OF BASIC UNIT = 1.8068E-06 CM²

VARIANCE OF SQR(NS) = 2.37629

VARIANCE OF SQR(NI) = 12.4686

CORRELATION COEFFICIENT = 0.982

CHI SQUARED = 9.75851 WITH 19 DEGREES OF FREEDOM PASS

NS/NI = 0.146 +- 0.017 MEAN RATIO = 0.111 +- 0.021

AGE CALCULATED USING A ZETA OF 352.7 FOR SPM612 GLASS

RHO D = 1.376E+06 ND = 5461

POOLED AGE = 35.4 +- 4.2 MYR

MEAN AGE = 27.0 +- 5.1 MYR

PDS 63 1/2

IRRADIATION: PT931-06
ANALYSIS BY PDS 4/27/88

CRYSTAL	NS	NI	AREA UNITS	RATIO	RHO S	RHO I	AGE(MYR)
1	2	10	7	0.200	2.84E+05	1.42E+06	48.5 +- 37.6
2	0	4	16	0.000	0.00E+00	2.48E+05	0.0 +- 0.0
3	3	23	10	0.130	1.66E+05	1.27E+06	31.7 +- 19.5
4	5	30	10	0.132	4.97E+05	3.77E+06	32.0 +- 15.2
5	0	5	4	0.000	0.00E+00	1.24E+06	0.0 +- 0.0
6	3	14	20	0.214	1.49E+05	6.95E+05	52.0 +- 33.1
7	0	2	4	0.000	0.00E+00	4.97E+05	0.0 +- 0.0
8	3	9	20	0.333	1.06E+05	3.19E+05	00.7 +- 53.8
9	3	12	30	0.250	9.93E+04	3.97E+05	60.6 +- 39.1
10	0	11	0	0.000	0.00E+00	1.37E+06	0.0 +- 0.0
11	1	9	12	0.111	0.20E+04	7.45E+05	27.0 +- 20.5
12	1	7	16	0.143	6.21E+04	4.35E+05	34.7 +- 37.1
13	2	12	20	0.167	7.09E+04	4.26E+05	40.5 +- 30.9
14	0	5	6	0.000	0.00E+00	0.20E+05	0.0 +- 0.0
15	0	3	6	0.000	0.00E+00	4.97E+05	0.0 +- 0.0
16	3	10	16	0.167	1.06E+05	1.12E+06	40.5 +- 25.2
17	2	12	20	0.167	9.93E+04	5.96E+05	40.5 +- 30.9
18	2	12	0	0.167	2.40E+05	1.49E+06	40.5 +- 30.9
19	1	5	15	0.200	6.62E+04	3.31E+05	40.5 +- 53.2
20	3	13	15	0.231	1.99E+05	0.61E+05	56.0 +- 35.0
					<u>1.177E+05</u>	<u>7.752E+05</u>	

AREA OF BASIC UNIT = 1.0068E-06 CM²

VARIANCE OF SQR(NS) = .597203

VARIANCE OF SQR(NI) = 1.21648

CORRELATION COEFFICIENT = 0.839

CHI SQUARED = 7.86213 WITH 19 DEGREES OF FREEDOM PASS

NS/NI = 0.152 +- 0.028

MEAN RATIO = 0.131 +- 0.022

AGE CALCULATED USING A ZETA OF 352.7 FOR SRM612 GLASS

RHO O = 1.381E+06 ND = 5400

POOLED AGE = 36.9 +- 6.8 MYR

MEAN AGE = 31.7 +- 5.5 MYR

JD 27A

IRRADIATION: PT917-01
ANALYSIS BY POS 4/28/88

CRYSTAL	NS	NI	AREA UNITS	RATIO	RHO S	RHO I	AGE(MYR)
1	0	1	14	0.000	8.00E+00	7.89E+04	0.0 +- 0.0
2	2	5	36	0.400	5.52E+04	1.30E+05	94.5 +- 79.0
3	1	6	32	0.167	3.10E+04	1.86E+05	39.5 +- 42.7
4	7	69	36	0.101	1.93E+05	1.90E+06	24.1 +- 9.5
5	0	3	25	0.000	0.00E+00	1.19E+05	0.0 +- 0.0
6	0	1	12	0.000	0.00E+00	8.20E+04	0.0 +- 0.0
7	4	27	10	0.140	2.21E+05	1.49E+06	35.1 +- 18.0
8	0	2	30	0.000	0.00E+00	6.62E+04	0.0 +- 0.0
9	0	2	25	0.000	0.00E+00	7.95E+04	0.0 +- 0.0
10	0	1	35	0.000	0.00E+00	2.04E+04	0.0 +- 0.0
11	0	2	21	0.000	0.00E+00	9.46E+04	0.0 +- 0.0
12	0	5	27	0.000	0.00E+00	1.04E+05	0.0 +- 0.0
13	1	3	16	0.333	6.21E+04	1.86E+05	70.0 +- 91.0
14	2	6	36	0.333	5.52E+04	1.66E+05	70.0 +- 64.4
15	2	12	24	0.167	0.20E+04	4.97E+05	39.5 +- 30.2
16	15	76	30	0.197	4.97E+05	2.52E+06	46.0 +- 13.2
17	2	4	12	0.500	1.66E+05	3.31E+05	117.9 +- 102.1
18	0	3	20	0.000	0.00E+00	1.49E+05	0.0 +- 0.0
19	1	0	20	0.125	4.97E+04	3.97E+05	29.7 +- 31.5
20	1	2	12	0.500	0.20E+04	1.66E+05	117.9 +- 144.4

<u>30</u>	<u>230</u>	<u>7.047E+04</u>	<u>4.915E+05</u>
-----------	------------	------------------	------------------

AREA OF BASIC UNIT = 1.0060E-06 CM²

VARIANCE OF SQR(NS) = 1.13065

VARIANCE OF SQR(NI) = 4.92713

CORRELATION COEFFICIENT = 0.933

CHI SQUARED = 10.6348 WITH 19 DEGREES OF FREEDOM PASS

NS/NI = 0.160 +- 0.020

MEAN RATIO = 0.149 +- 0.039

AGE CALCULATED USING A ZETA OF 352.7 FOR SRM612 GLASS

RHO D = 1.349E+06 ND = 5354

POOLED AGE = 37.9 +- 6.0 MYR

MEAN AGE = 35.3 +- 9.3 MYR

JD 388

IRRADIATION: PT917-03
ANALYSIS BY POS 4/28/88

CRYSTAL	NS	NI	AREA UNITS	RATIO	RHO S	RHO I	AGE(MYR)
1	1	6	18	0.167	5.52E+04	3.31E+05	39.5 +- 42.7
2	1	3	12	0.333	8.28E+04	2.48E+05	78.8 +- 91.8
3	10	61	16	0.164	6.21E+05	3.79E+06	38.9 +- 13.3
4	0	3	18	0.000	0.00E+00	1.66E+05	0.0 +- 0.0
5	1	7	12	0.143	8.28E+04	5.79E+05	33.9 +- 36.2
6	1	2	9	0.500	1.18E+05	2.21E+05	117.9 +- 144.4
7	2	12	6	0.167	3.31E+05	1.99E+06	39.5 +- 38.2
8	0	2	9	0.000	0.00E+00	2.21E+05	0.0 +- 0.0
9	4	20	10	0.200	3.97E+05	1.99E+06	47.4 +- 26.0
10	13	82	24	0.159	5.38E+05	3.39E+06	37.6 +- 11.2
11	1	5	8	0.200	1.24E+05	6.21E+05	47.4 +- 51.9

342032.378E+051.420E+06

AREA OF BASIC UNIT = 1.0868E-06 CM²

VARIANCE OF SQR(NS) = 1.3046

VARIANCE OF SQR(NI) = 6.87695

CORRELATION COEFFICIENT = 0.996

CHI SQUARED = 2.27835 WITH 10 DEGREES OF FREEDOM PASS

NS/NI = 0.167 +- 0.031

MEAN RATIO = 0.185 +- 0.042

AGE CALCULATED USING A ZETA OF 352.7 FOR SRM612 GLASS

RHO D = 1.349E+06 ND = 5354

POOLED AGE = 39.7 +- 7.4 MYR

MEAN AGE = 43.8 +- 10.0 MYR

JD 15A

IRRADIATION: PT916-13
ANALYSIS BY POS 4/27/88

CRYSTAL	NS	NI	AREA UNITS	RATIO	RHO S	RHO I	AGE(MYR)
1	1	10	12	0.100	0.20E+04	0.20E+05	24.2 +- 25.4
2	0	14	10	0.000	0.00E+00	7.73E+05	0.0 +- 0.0
3	1	3	10	0.333	9.93E+04	2.90E+05	80.4 +- 92.0
4	2	10	12	0.200	1.66E+05	0.20E+05	40.3 +- 37.5
5	3	22	30	0.136	9.93E+04	7.20E+05	33.0 +- 28.3
6	0	6	20	0.000	0.00E+00	2.90E+05	0.0 +- 0.0
7	1	9	6	0.111	1.66E+05	1.49E+06	26.9 +- 20.4
8	0	3	10	0.000	0.00E+00	2.90E+05	0.0 +- 0.0
9	5	23	20	0.217	2.40E+05	1.14E+06	52.5 +- 25.9
10	0	3	24	0.000	0.00E+00	1.24E+05	0.0 +- 0.0
11	3	0	21	0.375	1.42E+05	3.70E+05	90.4 +- 61.2
12	3	19	10	0.150	1.66E+05	1.05E+06	30.2 +- 23.7
13	0	2	0	0.000	0.00E+00	2.40E+05	0.0 +- 0.0
14	19	110	20	0.173	6.74E+05	3.90E+06	41.0 +- 10.4
15	3	16	50	0.100	5.96E+04	3.10E+05	45.3 +- 20.5
16	2	7	10	0.200	1.99E+05	6.95E+05	69.0 +- 55.3
17	3	13	14	0.231	2.13E+05	9.22E+05	55.0 +- 35.7
18	3	20	21	0.150	1.42E+05	9.46E+05	36.3 +- 22.5
19	3	25	15	0.120	1.99E+05	1.66E+06	29.1 +- 17.0
20	0	2	12	0.000	0.00E+00	1.66E+05	0.0 +- 0.0
					<u>52</u>	<u>325</u>	
							<u>1.439E+05</u> <u>8.992E+05</u>

AREA OF BASIC UNIT = 1.0060E-06 CM²

VARIANCE OF SQR(NS) = 1.15107

VARIANCE OF SQR(NI) = 4.05333

CORRELATION COEFFICIENT = 0.975

CHI SQUARED = 9.0304 WITH 19 DEGREES OF FREEDOM PASS

NS/NI = 0.160 +- 0.024

MEAN RATIO = 0.139 +- 0.026

AGE CALCULATED USING A ZETA OF 352.7 FOR SRM612 GLASS

RHO D = 1.376E+06 ND = 5461

POOLED AGE = 30.7 +- 5.0 MYR

MEAN AGE = 33.6 +- 6.3 MYR

POS 55A

IRRADIATION: PT930-09
ANALYSIS BY POS 4/27/88

CRYSTAL	NS	NI	AREA UNITS	RATIO	RHO S	RHO I	AGE(MYR)
1	1	12	15	0.083	6.62E+04	7.95E+05	21.3 +- 22.1
2	2	10	10	0.200	1.10E+05	5.52E+05	50.9 +- 39.5
3	0	20	6	0.286	9.93E+05	3.48E+06	72.7 +- 29.1
4	9	91	15	0.899	5.94E+05	6.03E+06	25.2 +- 0.0
5	0	3	6	0.000	0.00E+00	4.97E+05	0.0 +- 0.0
6	0	4	6	0.000	0.00E+00	6.62E+05	0.0 +- 0.0
7	0	4	6	0.000	0.00E+00	6.62E+05	0.0 +- 0.0
8	1	3	4	0.333	2.48E+05	7.45E+05	84.7 +- 97.0
9	1	8	4	0.125	2.48E+05	1.99E+06	31.9 +- 33.8
10	0	1	2	0.000	0.00E+00	4.97E+05	0.0 +- 0.0
11	1	13	12	0.877	8.20E+04	1.00E+06	19.6 +- 20.4
12	3	5	6	0.600	4.97E+05	0.20E+05	151.6 +- 110.7
13	0	6	4	0.000	0.00E+00	1.49E+06	0.0 +- 0.0
14	0	4	3	0.000	0.00E+00	1.32E+06	0.0 +- 0.0
15	1	6	5	0.167	1.99E+05	1.19E+06	42.5 +- 45.9
16	0	1	2	0.000	0.00E+00	4.97E+05	0.0 +- 0.0
17	4	12	4	0.333	9.93E+05	2.98E+06	84.7 +- 48.9
18	0	8	6	0.000	0.00E+00	1.32E+06	0.0 +- 0.0
19	3	13	0	0.231	3.72E+05	1.61E+06	50.7 +- 37.6
20	1	12	20	0.883	4.97E+04	5.96E+05	21.3 +- 22.1
					<u>2.257E+05</u>	<u>1.574E+06</u>	

AREA OF BASIC UNIT = $1.0060E-06$ CM²

VARIANCE OF SQR(NS) = .921205

VARIANCE OF SQR(NI) = 3.41491

CORRELATION COEFFICIENT = 0.023

CHI SQUARED = 17.7482 WITH 19 DEGREES OF FREEDOM PASS

NS/NI = 0.143 +- 0.026

MEAN RATIO = 0.131 +- 0.036

AGE CALCULATED USING λ ZETA OF 352.7 FOR GRM612 GLASS

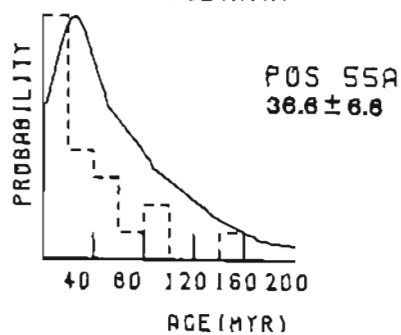
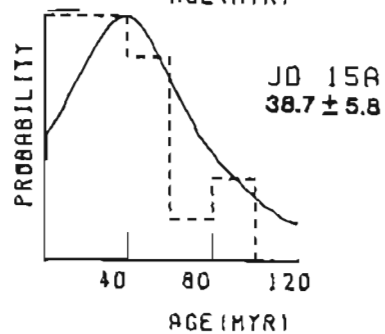
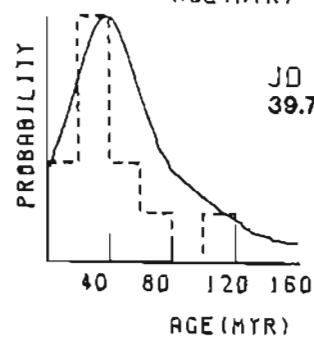
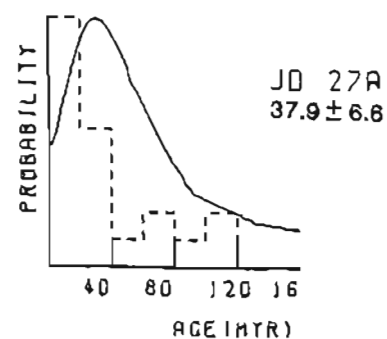
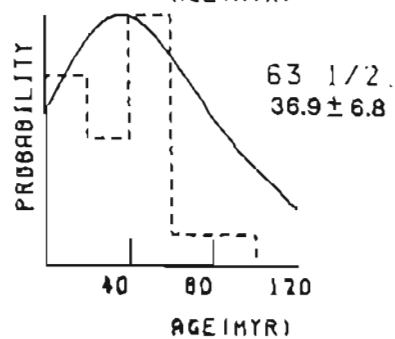
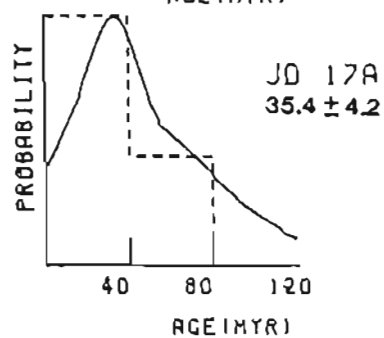
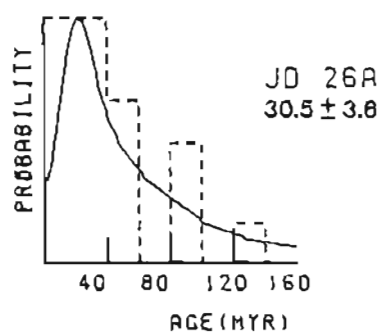
RHO O = $1.45E+06$ ND = 5755

POOLED AGE = 36.6 +- 6.6 MYR

MEAN AGE = 33.4 +- 9.1 MYR

Single-Grain Age Distributions: Arctic Creek Region

Albian turbidites



Canning River Region

POS 228IRRADIATION: PT916-06
ANALYSIS BY POS 4/21/88

CRYSTAL	NS	NI	AREA UNITS	RATIO	RHO S	RHO I	AGE(MYR)
1	3	14	23	0.214	1.53E+05	7.12E+05	51.8 +- 32.9
2	8	6	27	0.888	8.88E+00	2.68E+05	8.8 +- 8.8
3	2	2	12	1.088	1.95E+05	1.95E+05	238.2 +- 238.2
4	15	68	21	0.258	8.36E+05	3.34E+06	68.4 +- 17.4
5	27	187	19	0.252	1.66E+06	6.59E+06	68.9 +- 13.1
6	2	3	22	0.667	1.06E+05	1.68E+05	159.8 +- 145.9
7	6	27	21	0.222	3.34E+05	1.58E+06	53.7 +- 24.2
8	9	35	24	0.257	4.39E+05	1.71E+06	62.1 +- 23.2
9	1	1	18	1.888	1.17E+05	1.17E+05	238.2 +- 336.9
10	1	2	15	0.588	7.88E+04	1.56E+05	128.2 +- 147.2
11	3	28	7	0.158	5.81E+05	3.34E+06	36.3 +- 22.5
12	8	18	25	0.888	8.88E+00	4.68E+05	8.8 +- 8.8
13	8	1	16	0.888	8.88E+00	7.31E+04	8.8 +- 8.8
14	6	12	19	0.588	3.69E+05	7.39E+05	128.2 +- 68.1
15	4	6	6	0.588	7.88E+05	1.56E+06	128.2 +- 73.6
16	7	27	24	0.259	3.41E+05	1.32E+06	62.6 +- 26.6
17	4	4	12	1.888	3.98E+05	3.98E+05	238.2 +- 168.4
18	22	77	14	0.286	1.84E+06	6.43E+06	69.8 +- 16.7
19	15	29	12	8.517	1.46E+06	2.83E+06	124.3 +- 39.5
20	5	28	28	8.179	2.92E+05	1.64E+06	43.2 +- 21.8
21	8	3	18	0.888	8.88E+00	1.95E+05	8.8 +- 8.8

<u>132</u>	<u>476</u>	<u>4.288E+05</u>	<u>1.517E+06</u>
------------	------------	------------------	------------------

AREA OF BASIC UNIT = 3.548E-07 CM²

VARIANCE OF SQR(NS) = 3.25784

VARIANCE OF SQR(NI) = 6.89556

CORRELATION COEFFICIENT = 0.953

CHI SQUARED = 22.1738 WITH 20 DEGREES OF FREEDOM PASS

NS/NI = 0.277 +- 0.027 MEAN RATIO = 0.369 +- 0.071

AGE CALCULATED USING A ZETA OF 352.7 FOR SRM612 GLASS

RHO D = 1.376E+06 ND = 5461

POOLED AGE = 66.9 +- 6.6 MYR

MEAN AGE = 89.8 +- 17.0 MYR

POS 248

IRRADIATION: PT916-67
ANALYSIS BY POS 4/22/88

CRYSTAL	NS	NI	AREA UNITS	RATIO	RHO S	RHO I	AGE(MYR)
1	15	188	25	0.158	7.82E+05	4.68E+06	36.3 +- 18.1
2	4	29	28	0.138	2.34E+05	1.78E+06	33.4 +- 17.8
3	19	184	54	0.183	4.12E+05	2.25E+06	44.2 +- 11.8
4	8	29	12	0.888	8.88E+08	2.83E+06	8.8 +- 8.8
5	47	116	48	0.485	1.37E+06	3.39E+06	97.6 +- 16.9
6	12	76	21	0.158	6.68E+05	4.23E+06	38.2 +- 11.9
7	1	1	16	1.888	7.31E+04	7.31E+04	238.2 +- 336.9
8	2	3	16	0.667	1.46E+05	2.19E+05	159.8 +- 145.9
9	2	31	38	0.865	7.88E+04	1.21E+06	15.6 +- 11.4
10	8	14	48	0.888	8.88E+08	4.89E+05	8.8 +- 8.8
11	8	1	24	0.888	8.88E+08	4.87E+04	8.8 +- 8.8
12	1	7	48	8.143	2.92E+04	2.85E+05	34.6 +- 37.8
13	2	26	12	0.877	1.95E+05	2.53E+06	18.6 +- 13.7
14	2	12	8	8.167	2.92E+05	1.75E+06	48.3 +- 38.8
15	2	62	18	0.832	2.34E+05	7.25E+06	7.8 +- 5.6
16	14	125	48	0.112	4.89E+05	3.66E+06	27.1 +- 7.6
17	76	284	24	8.373	3.42E+06	9.18E+06	89.8 +- 12.1
18	8	6	17	8.888	8.88E+08	4.13E+05	8.8 +- 8.8
19	11	53	42	0.288	3.86E+05	1.48E+06	58.2 +- 16.6
20	8	58	28	8.888	8.88E+08	2.42E+06	8.8 +- 8.8
21	5	28	15	8.258	3.98E+05	1.56E+06	68.4 +- 38.2
22	19	95	28	8.288	1.11E+06	5.56E+06	48.3 +- 12.2
23	1	36	48	8.828	2.92E+04	1.85E+06	6.7 +- 6.8

23512884.613E+052.371E+06AREA OF BASIC UNIT = 8.548E-07 CM²

VARIANCE OF SQR(NS) = 5.13174

VARIANCE OF SQR(NI) = 13.8883

CORRELATION COEFFICIENT = 0.871

CHI SQUARED = 91.3505 WITH 22 DEGREES OF FREEDOM FAIL

NS/NI = 0.195 +- 0.014

MEAN RATIO = 0.189 +- 0.058

AGE CALCULATED USING A ZETA OF 352.7 FOR SRM612 GLASS

PHO 0 = 1.376E+06 ND = 5461

POOLED AGE = 47.8 +- 3.4 MYR

MEAN AGE = 45.8 +- 12.8 MYR

POS 15A

IRRADIATION: PT916-05
ANALYSIS BY POS 4/22/88

CRYSTAL	NS	NI	AREA UNITS	RATIO	RHO S	RHO I	AGE(MYR)
1	24	148	64	0.162	4.39E+05	2.71E+06	39.2 +- 8.6
2	0	2	36	0.000	0.00E+00	6.50E+04	0.0 +- 0.0
3	2	21	20	0.095	1.17E+05	1.23E+06	23.1 +- 17.1
4	4	11	27	0.364	1.73E+05	4.77E+05	07.6 +- 51.2
5	1	3	12	0.333	9.75E+04	2.92E+05	08.4 +- 92.8
6	0	1	12	0.000	0.00E+00	9.75E+04	0.0 +- 0.0
7	1	1	4	1.000	2.92E+05	2.92E+05	238.2 +- 336.9
8	2	2	24	1.000	9.75E+04	9.75E+04	238.2 +- 238.2
9	18	120	24	0.003	4.87E+05	5.85E+06	20.2 +- 6.6
10	1	6	15	0.167	7.00E+04	4.60E+05	40.3 +- 43.5
11	1	10	30	0.100	3.90E+05	3.90E+05	96.3 +- 00.6
12	2	5	15	0.400	1.56E+05	2.92E+05	96.3 +- 00.6
13	2	5	20	0.400	1.17E+05	2.92E+05	96.3 +- 00.6
14	2	12	0	0.167	2.92E+05	1.75E+06	40.3 +- 30.8
15	1	1	16	1.000	7.31E+04	7.31E+04	230.2 +- 336.9
16	0	1	30	0.000	0.00E+00	3.90E+04	0.0 +- 0.0
17	3	13	20	0.231	1.75E+05	7.60E+05	55.0 +- 35.7
18	7	25	42	0.200	1.95E+05	6.96E+05	67.6 +- 20.9
19	1	5	16	0.200	7.31E+04	3.66E+05	48.3 +- 53.8
20	7	34	60	0.200	1.36E+05	6.63E+05	49.8 +- 20.7

71 426 1.670E+05 1.007E+06

AREA OF BASIC UNIT = 0.540E-07 CM²

VARIANCE OF SQR(NS) = 1.34374

VARIANCE OF SQR(NI) = 9.59981 CORRELATION COEFFICIENT = 0.927

CHI SQUARED = 21.0999 WITH 19 DEGREES OF FREEDOM PASS

NS/NI = 0.167 +- 0.021 MEAN RATIO = 0.309 +- 0.072

AGE CALCULATED USING A ZETA OF 352.7 FOR SRM612 GLASS
RHO D = 1.376E+06 ND = 5461

POOLED AGE = 40.3 +- 5.2 MYR

MEAN AGE = 74.6 +- 17.4 MYR

POS 148

IRRADIATION: PT916-84
ANALYSIS BY POS 4/26/88

CRYSTAL	NS	NI	AREA UNITS	RATIO	RHO S	RHO I	AGE(MYR)
1	8	3	25	0.888	0.88E+00	1.40E+05	0.0 +- 0.0
2	2	4	28	0.500	0.36E+04	1.67E+05	120.2 +- 104.1
3	2	18	8	0.280	2.92E+05	1.46E+06	40.3 +- 37.5
4	3	13	48	0.231	0.77E+04	3.88E+05	55.8 +- 35.7
5	8	2	24	0.888	0.88E+00	9.75E+04	0.0 +- 0.0
6	10	28	28	0.357	5.85E+05	1.64E+06	86.1 +- 31.7
7	3	11	28	0.273	1.75E+05	6.43E+05	65.8 +- 42.9
8	9	39	24	0.231	4.39E+05	1.98E+06	55.8 +- 28.6
9	1	4	12	0.250	9.75E+04	3.98E+05	68.4 +- 67.5
10	3	9	35	0.333	1.88E+05	3.81E+05	80.4 +- 53.6
11	5	34	38	0.147	1.95E+05	1.33E+06	35.6 +- 17.0
12	8	5	28	0.888	0.88E+00	2.92E+05	0.0 +- 0.0
13	6	29	26	0.287	2.78E+05	1.38E+06	50.8 +- 22.4
14	8	9	38	0.888	0.88E+00	3.51E+05	0.0 +- 0.0
15	2	14	38	0.143	7.88E+04	5.46E+05	34.6 +- 26.1
16	11	61	40	0.188	3.22E+05	1.78E+06	43.6 +- 14.3
17	2	25	48	0.888	5.85E+04	7.31E+05	19.4 +- 14.2
18	2	8	28	0.258	8.36E+04	3.34E+05	68.4 +- 47.7
19	0	4	38	0.888	0.88E+00	1.56E+05	0.0 +- 0.0
20	1	5	14	0.280	0.36E+04	4.18E+05	48.3 +- 53.8

<u>62</u>	<u>317</u>	<u>1.384E+05</u>	<u>7.877E+05</u>
-----------	------------	------------------	------------------

AREA OF BASIC UNIT = 0.548E-07 CM²

VARIANCE OF SQR(NS) = 1.13589

VARIANCE OF SQR(NI) = 3.10425

CORRELATION COEFFICIENT = 0.894

CHI SQUARED = 12.0365 WITH 19 DEGREES OF FREEDOM PASS

NS/NI = 0.196 +- 0.027

MEAN RATIO = 0.179 +- 0.031

AGE CALCULATED USING A ZETA OF 352.7 FOR SRM612 GLASS

RHO D = 1.376E+06 IND = 5461

POOLED AGE = 47.3 +- 6.6 MYR

MEAN AGE = 43.3 +- 7.4 MYR

POS 35A

IRRADIATION: PT931-09
ANALYSIS BY POS 4/22/88

CRYSTAL	NS	NI	AREA UNITS	RATIO	RHO S	RHO I	AGE(MYR)
1	7	34	12	0.286	6.82E+05	3.31E+06	49.9 +- 28.7
2	4	19	12	0.211	3.90E+05	1.85E+06	51.1 +- 28.1
3	8	3	35	0.800	8.88E+08	1.00E+05	0.0 +- 0.0
4	1	3	12	0.333	9.75E+04	2.92E+05	88.7 +- 93.2
5	1	5	28	0.288	5.85E+04	2.92E+05	48.5 +- 53.2
6	7	29	27	0.241	3.03E+05	1.26E+06	58.5 +- 24.6
7	8	15	36	0.800	8.88E+08	4.87E+05	8.0 +- 8.0
8	8	18	28	0.800	8.88E+08	4.18E+05	0.0 +- 0.0
9	8	9	48	0.800	8.88E+08	2.63E+05	0.0 +- 0.0
10	14	189	38	0.128	5.46E+05	4.25E+06	31.2 +- 8.9
11	1	12	15	0.883	7.88E+04	9.36E+05	28.3 +- 21.1
12	17	52	18	0.327	1.18E+06	3.38E+06	79.1 +- 22.1
13	3	8	16	0.375	2.19E+05	5.85E+05	98.7 +- 61.4
14	16	67	58	0.239	3.74E+05	1.57E+06	57.9 +- 16.1
15	6	28	8	0.388	8.77E+05	2.92E+06	72.7 +- 33.8
16	1	18	24	0.188	4.87E+04	4.87E+04	8.0 +- 0.0
17	8	1	24	0.888	0.88E+08	3.90E+05	0.0 +- 0.0
18	8	5	15	0.888	0.88E+08	3.90E+05	48.5 +- 53.2
19	1	5	15	0.288	7.88E+04	1.51E+06	47.8 +- 28.9
20	6	31	24	0.194	2.92E+05	3.12E+06	66.6 +- 22.7
21	11	48	15	0.275	8.58E+05	6.82E+05	8.0 +- 0.0
22	8	7	12	0.888	0.88E+08	6.82E+05	48.9 +- 18.7
23	25	124	24	0.282	1.22E+06	6.84E+06	0.0 +- 0.0
24	8	6	12	0.888	0.88E+08	5.85E+05	0.0 +- 0.0
25	1	8	12	0.125	9.75E+04	7.88E+05	38.4 +- 32.2

122 8322.663E+05 1.379E+06AREA OF BASIC UNIT = 8.548E-07 CM²

VARIANCE OF SQR(NS) = 2.40279

VARIANCE OF SQR(NI) = 7.0737

CORRELATION COEFFICIENT = 0.928

CHI SQUARED = 21.997 WITH 24 DEGREES OF FREEDOM PASS

NS/NI = 0.193 +- 0.019 MEAN RATIO = 0.150 +- 0.025

AGE CALCULATED USING μ ZETA OF 352.7 FOR SRM612 GLASS

RHO D = 1.381E+06 RD = 5480

POOLED AGE = 46.8 +- 4.7 MYR

MEAN AGE = 36.3 +- 5.1 MYR

PQS 10A

IRRADIATION: PT916-03
ANALYSIS BY PQS 4/26/88

CRYSTAL	NS	NI	AREA UNITS	RATIO	RHO S	RHO I	AGE(MYR)
1	1	9	30	0.111	3.31E+04	2.98E+05	26.9 +- 28.4
2	7	99	72	0.071	9.66E+04	1.37E+06	17.1 +- 6.7
3	3	6	16	0.500	1.86E+05	3.72E+05	120.2 +- 85.8
4	16	57	42	0.281	3.78E+05	1.35E+06	67.8 +- 19.2
5	0	17	27	0.000	0.00E+00	6.25E+05	0.0 +- 0.0
6	3	16	16	0.168	1.86E+05	9.93E+05	45.3 +- 28.5
7	3	18	18	0.167	1.66E+05	9.93E+05	40.3 +- 25.1
8	10	45	14	0.222	7.09E+05	3.19E+06	53.7 +- 10.8
9	7	47	21	0.149	3.31E+05	2.22E+06	36.8 +- 14.6
10	3	26	36	0.115	8.20E+04	7.17E+05	27.9 +- 17.0
11	20	140	24	0.143	0.20E+05	5.79E+06	34.6 +- 8.3
12	3	36	12	0.083	2.48E+05	2.98E+06	20.2 +- 12.1
13	0	3	9	0.000	0.00E+00	3.31E+05	0.0 +- 0.0
14	0	22	15	0.000	0.00E+00	1.46E+06	0.0 +- 0.0
15	0	3	20	0.000	0.00E+00	1.49E+05	0.0 +- 0.0
16	13	62	30	0.210	4.30E+05	2.05E+06	50.7 +- 15.5
17	2	13	16	0.154	1.24E+05	8.07E+05	37.2 +- 28.3
18	0	1	10	0.000	0.00E+00	9.93E+04	0.0 +- 0.0
19	12	93	10	0.129	6.62E+05	5.13E+06	31.2 +- 9.6
20	2	4	35	0.500	5.60E+04	1.14E+05	120.2 +- 104.1

1057172.168E+051.431E+06

AREA OF BASIC UNIT = 1.0860E-06 CM²

VARIANCE OF SQR(NS) = 2.02342

VARIANCE OF SQR(NI) = 9.22566

CORRELATION COEFFICIENT = 0.863

CHI SQUARED = 25.3818 WITH 19 DEGREES OF FREEDOM PASS

NS/NI = 0.146 +- 0.015

MEAN RATIO = 0.151 +- 0.032

AGE CALCULATED USING A ZETA OF 352.7 FOR SRM612 GLASS

RHO D = 1.376E+06 IND = 5461

POOLED AGE = 35.4 +- 3.7 MYR

MEAN AGE = 36.6 +- 7.9 MYR

POS 08A

IRRADIATION: PT916-02
ANALYSIS BY POS 4/26/88

CRYSTAL	NS	NI	AREA UNITS	RATIO	RHO S	RHO I	AGE(MYR)
1	2	15	12	0.133	1.66E+05	1.24E+06	32.3 +- 24.3
2	1	24	20	0.042	3.55E+04	0.51E+05	18.1 +- 10.3
3	7	72	40	0.097	1.74E+05	1.79E+06	23.5 +- 9.3
4	4	36	10	0.111	2.21E+05	1.99E+06	26.9 +- 14.2
5	2	21	32	0.095	6.21E+04	6.52E+05	23.1 +- 17.1
6	1	0	20	0.125	4.97E+04	3.97E+05	30.3 +- 32.1
7	1	7	40	0.143	2.40E+04	1.74E+05	34.6 +- 37.0
8	0	55	16	0.145	4.97E+05	3.41E+06	35.2 +- 13.3
9	3	39	20	0.077	1.49E+05	1.94E+06	10.6 +- 11.2
10	3	12	35	0.250	0.51E+04	3.41E+05	60.4 +- 39.0
11	3	27	36	0.111	0.28E+04	7.45E+05	26.9 +- 16.4
12	17	95	35	0.179	4.02E+05	2.70E+06	43.3 +- 11.4
13	2	24	24	0.083	0.28E+04	9.93E+05	20.2 +- 14.9
14	0	1	24	0.000	0.00E+00	4.14E+04	0.0 +- 0.0
15	9	40	25	0.100	3.50E+05	1.91E+06	45.3 +- 16.5
16	0	5	10	0.000	0.00E+00	4.97E+05	0.0 +- 0.0
17	1	26	40	0.030	2.40E+04	6.46E+05	9.3 +- 9.5
18	0	7	20	0.000	0.00E+00	3.48E+05	0.0 +- 0.0
19	4	21	30	0.190	1.32E+05	6.95E+05	46.1 +- 25.1
20	3	26	25	0.115	1.19E+05	1.03E+06	27.9 +- 17.0

71 569 1.331E+05 1.066E+06

AREA OF BASIC UNIT = 1.0060E-06 CM²

VARIANCE OF SQR(NS) = 1.00102

VARIANCE OF SQR(NI) = 4.73973

CORRELATION COEFFICIENT = 0.918

CHI SQUARED = 11.1711 WITH 19 DEGREES OF FREEDOM PASS

NS/NI = 0.125 +- 0.016

MEAN RATIO = 0.106 +- 0.015

AGE CALCULATED USING A ZETA OF 352.7 FOR GRM512 GLASS

RHO O = 1.376E+06 NO = 5461

POOLED AGE = 30.2 +- 3.8 MYR

MEAN AGE = 25.7 +- 3.7 MYR

JD 038

IRRADIATION: PT930-04
ANALYSIS BY POS 4/21/88

CRYSTAL	NS	NI	AREA UNITS	RATIO	RHO S	RHO I	AGE(MYR)
1	43	174	40	0.247	1.26E+06	5.09E+06	62.9 +- 10.7
2	5	83	28	0.060	2.09E+05	3.47E+06	15.4 +- 7.1
3	13	40	50	0.271	3.04E+05	1.12E+06	60.9 +- 21.5
4	2	20	9	0.100	2.60E+05	2.60E+06	25.5 +- 10.9
5	0	30	0	0.000	0.00E+00	4.39E+06	0.0 +- 0.0
6	3	21	20	0.143	1.25E+05	8.77E+05	36.4 +- 22.5
7	1	19	9	0.053	1.30E+05	2.47E+06	13.4 +- 13.0
8	2	41	10	0.049	1.30E+05	2.66E+06	12.5 +- 9.0
9	1	16	24	0.063	4.07E+04	7.00E+05	16.0 +- 16.5
10	2	9	12	0.222	1.95E+05	0.77E+05	56.6 +- 44.2
11	0	16	0	0.000	0.00E+00	2.34E+06	0.0 +- 0.0
12	1	19	15	0.053	7.00E+04	1.40E+06	13.4 +- 13.0
13	3	16	10	0.100	3.51E+05	1.07E+06	47.0 +- 30.1
14	10	39	10	0.256	1.17E+06	4.56E+06	65.2 +- 23.1
15	7	55	24	0.127	3.41E+05	2.60E+06	32.5 +- 13.0
16	19	106	25	0.179	0.89E+05	4.96E+06	45.7 +- 11.4
<u>112</u> <u>712</u>			<u>4.120E+05</u>		<u>2.619E+06</u>		

AREA OF BASIC UNIT = 8.548E-07 CM²

VARIANCE OF SQR(NS) = 2.85386

VARIANCE OF SQR(NI) = 7.58119

CORRELATION COEFFICIENT = 0.924

CHI SQUARED = 31.6494 WITH 15 DEGREES OF FREEDOM FAIL

NS/NI = 0.157 +- 0.016

MEAN RATIO = 0.126 +- 0.023

AGE CALCULATED USING A ZETA OF 352.7 FOR SRM612 GLASS
RHO D = 1.45E+06 NO = 5755

POOLED AGE = 40.1 +- 4.1 MYR

MEAN AGE = 32.0 +- 5.9 MYR

POS 07A

IRRADIATION: PT930-12
ANALYSIS BY POS 4/26/88

CRYSTAL	NS	NI	AREA UNITS	RATIO	RHO S	RHO I	AGE(MYR)
1	1	7	6	0.143	1.66E+05	1.16E+06	36.4 +- 38.9
2	1	9	10	0.111	9.93E+04	8.94E+05	20.3 +- 29.9
3	1	8	12	0.125	8.28E+04	6.62E+05	31.9 +- 33.8
4	2	3	12	0.667	1.66E+05	2.40E+05	160.3 +- 153.6
5	2	14	5	0.143	3.97E+05	2.78E+06	36.4 +- 27.5
6	6	45	8	0.133	7.45E+05	5.59E+06	34.0 +- 14.8
7	8	18	3	0.888	8.88E+00	3.31E+06	0.0 +- 0.0
8	4	25	6	0.160	6.62E+05	4.14E+06	40.0 +- 22.0
9	3	27	9	0.111	3.31E+05	2.98E+06	20.3 +- 17.3
10	4	24	12	0.167	3.31E+05	1.99E+06	42.5 +- 22.9
11	1	11	8	0.891	1.24E+05	1.37E+06	23.2 +- 24.2
12	2	20	16	0.108	1.24E+05	1.24E+06	25.5 +- 18.9
13	8	18	4	0.888	8.88E+00	2.48E+06	0.0 +- 0.0
14	2	27	4	0.874	4.97E+05	6.78E+06	10.9 +- 13.9
15	8	5	6	0.888	8.88E+00	8.28E+05	0.0 +- 0.0
					<u>2.381E+05</u>	<u>2.811E+06</u>	

AREA OF BASIC UNIT = 1.8868E-06 CM²

VARIANCE OF SQR(NS) = .556151

VARIANCE OF SQR(NI) = 1.86705

CORRELATION COEFFICIENT = 0.864

CHI SQUARED = 8.96987 WITH 14 DEGREES OF FREEDOM PASS

NS/NI = 0.118 +- 0.023

MEAN RATIO = 0.135 +- 0.041

AGE CALCULATED USING A ZETA OF 352.7 FOR SRM612 GLASS

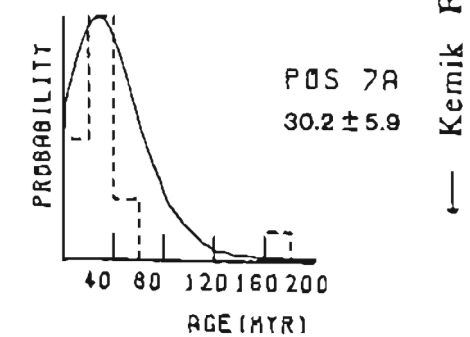
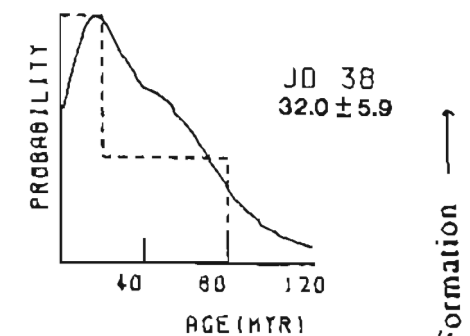
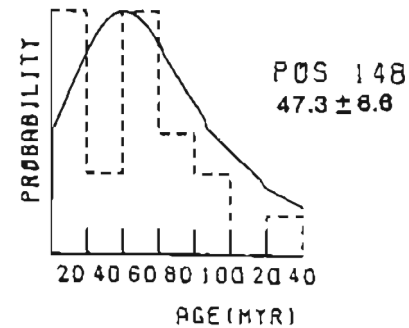
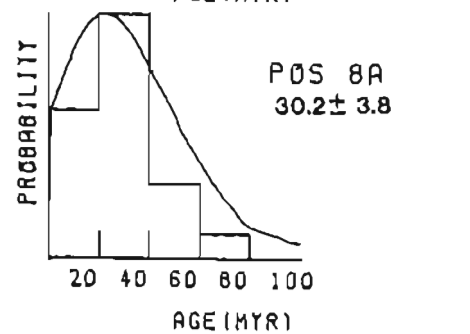
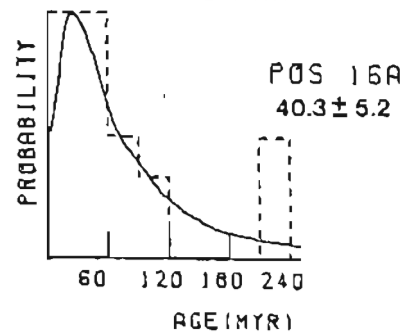
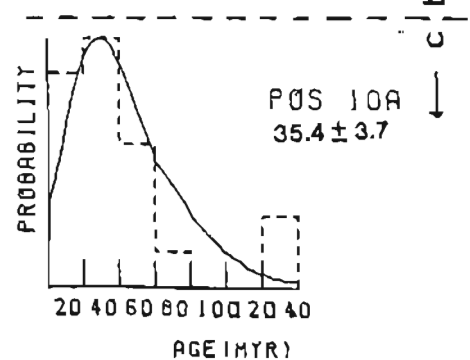
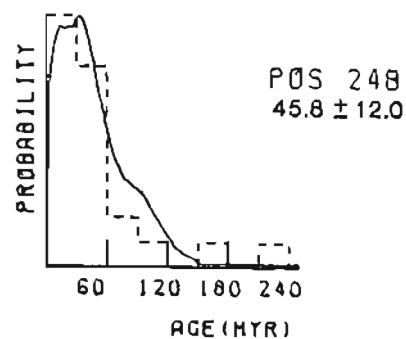
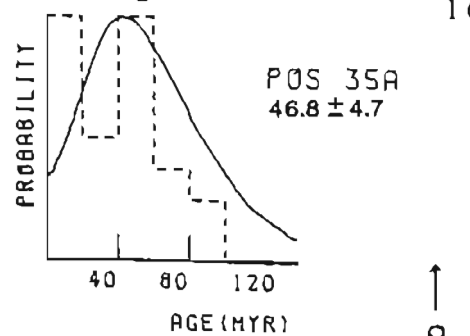
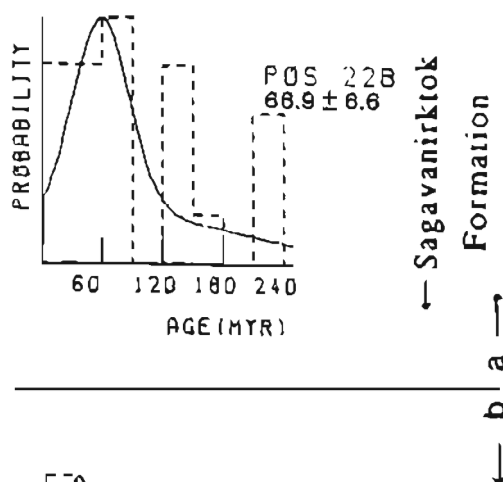
RHO D = 1.45E+06 ND = 5755

POOLED AGE = 30.2 +- 5.9 MYR

MEAN AGE = 34.4 +- 10.4 MYR

Single-Grain Age Distributions: Canning River Region

167



ANWR Coastal Plain
POS 74A

IRRADIATION: PT930-01
 ANALYSIS BY POS 4/29/88

CRYSTAL	NS	NI	AREA UNITS	RATIO	RHO S	RHO I	AGE(MYR)
1	1	2	6	0.500	1.66E+05	3.31E+05	126.6 +- 155.1
2	0	1	6	0.000	0.00E+00	1.66E+05	0.0 +- 0.0
3	2	2	12	1.000	1.66E+05	1.66E+05	250.0 +- 250.0
4	0	3	12	0.000	0.00E+00	2.40E+05	0.0 +- 0.0
5	1	1	4	1.000	2.40E+05	2.40E+05	250.0 +- 354.6
6	0	3	18	0.000	0.00E+00	2.98E+05	0.0 +- 0.0
7	2	7	12	0.286	1.66E+05	5.79E+05	72.7 +- 58.2
8	1	2	10	0.500	5.52E+04	1.18E+05	126.6 +- 155.1
9	2	6	6	0.333	3.31E+05	9.93E+05	84.7 +- 69.1
10	1	2	8	0.500	1.24E+05	2.40E+05	126.6 +- 155.1
11	0	2	12	0.000	0.00E+00	1.66E+05	0.0 +- 0.0
12	2	4	6	0.500	3.31E+05	6.62E+05	126.6 +- 189.6
13	0	3	20	0.000	0.00E+00	1.49E+05	0.0 +- 0.0
14	1	7	10	0.143	9.93E+04	6.95E+05	36.4 +- 38.9
15	3	16	18	0.100	2.98E+05	1.59E+06	47.8 +- 30.1
16	0	3	10	0.000	0.00E+00	2.98E+05	0.0 +- 0.0
17	2	6	36	0.333	5.52E+04	1.66E+05	84.7 +- 69.1
18	0	1	6	0.000	0.00E+00	1.66E+05	0.0 +- 0.0
19	2	4	18	0.500	1.99E+05	3.97E+05	126.6 +- 189.6
20	10	30	12	0.333	8.28E+05	2.40E+06	84.7 +- 30.9

<u>30</u>	<u>105</u>	<u>1.318E+05</u>	<u>4.615E+05</u>
-----------	------------	------------------	------------------

AREA OF BASIC UNIT = 1.0060E-06 CM²

VARIANCE OF SQR(NS) = .689974

VARIANCE OF SQR(NI) = 1.1742

CORRELATION COEFFICIENT = 0.925

CHI SQUARED = 9.89239 WITH 19 DEGREES OF FREEDOM PASS

NS/NI = 0.286 +- 0.059

MEAN RATIO = 0.306 +- 0.070

AGE CALCULATED USING A ZETA OF 352.7 FOR GRM612 GLASS

RHO D = 1.45E+06 MD = 5755

POOLED AGE = 72.7 +- 15.1 MYR

MEAN AGE = 77.7 +- 17.8 MYR

POS 74B

IRRADIATION: PT931-05
ANALYSIS BY POS 4/29/88

CRYSTAL	NS	NI	AREA UNITS	RATIO	RHO S	RHO I	AGE(MYR)
1	1	3	15	0.333	6.62E+04	1.99E+05	88.7 +- 93.2
2	1	4	30	0.250	3.31E+04	1.32E+05	68.6 +- 67.7
3	0	2	21	0.000	0.00E+00	9.46E+04	0.0 +- 0.0
4	1	2	16	0.500	6.21E+04	1.24E+05	128.6 +- 147.7
5	0	1	18	0.000	0.00E+00	5.52E+04	0.0 +- 0.0
6	3	11	9	0.273	3.31E+05	1.21E+06	66.1 +- 43.0
7	2	6	15	0.333	1.32E+05	3.97E+05	88.7 +- 65.9
8	3	27	15	0.111	1.99E+05	1.79E+06	27.0 +- 16.4
9	6	33	6	0.182	9.93E+05	5.46E+06	44.1 +- 19.6
10	3	6	9	0.500	3.31E+05	6.62E+05	128.6 +- 85.3
11	1	3	8	0.333	1.24E+05	3.72E+05	88.7 +- 93.2
12	7	10	8	0.700	0.69E+05	1.24E+06	168.3 +- 82.9
13	0	5	30	0.000	0.00E+00	1.66E+05	0.0 +- 0.0
14	4	4	16	1.000	2.48E+05	2.48E+05	239.1 +- 169.0
15	5	16	6	0.313	0.28E+05	2.65E+06	75.7 +- 38.8
16	2	5	30	0.400	6.62E+04	1.66E+05	96.7 +- 88.9
17	6	7	12	0.857	4.97E+05	5.79E+05	285.4 +- 114.3
18	0	2	15	0.000	0.00E+00	1.32E+05	0.0 +- 0.0
19	1	8	24	0.125	4.14E+04	3.31E+05	38.4 +- 32.2
20	2	8	12	0.250	1.66E+05	6.62E+05	68.6 +- 47.9

<u>48</u>	<u>163</u>	<u>1.514E+05</u>	<u>5.140E+05</u>
-----------	------------	------------------	------------------

AREA OF BASIC UNIT = 1.0060E-06 CM²

VARIANCE OF SQR(NS) = .717192

VARIANCE OF SQR(NI) = 1.51777

CORRELATION COEFFICIENT = 0.520

CHI SQUARED = 19.3723 WITH 19 DEGREES OF FREEDOM PASS

NS/NI = 0.294 +- 0.048

MEAN RATIO = 0.323 +- 0.063

AGE CALCULATED USING A ZETA OF 352.7 FOR SRM612 GLASS

RHO D = 1.381E+06 ND = 5480

POOLED AGE = 71.3 +- 11.8 MYR

MEAN AGE = 78.2 +- 15.2 MYR

POS 67A

IRRADIATION: PT931-04
ANALYSIS BY POS 4/30/88

CRYSTAL	NS	NI	AREA UNITS	RATIO	RHO S	RHO I	AGE(MYR)
1	0	2	12	0.000	0.00E+00	1.66E+05	0.0 +- 0.0
2	1	3	12	0.333	0.20E+04	2.40E+05	80.7 +- 93.2
3	14	37	14	0.370	9.93E+05	2.63E+06	91.5 +- 20.7
4	4	4	20	1.000	1.99E+05	1.99E+05	239.1 +- 169.0
5	4	20	30	0.200	1.32E+05	6.62E+05	40.5 +- 26.6
6	14	51	12	0.275	1.16E+06	4.22E+06	66.5 +- 20.1
7	1	7	10	0.143	5.52E+04	3.06E+05	34.7 +- 37.1
8	9	15	6	0.600	1.49E+06	2.40E+06	144.5 +- 60.9
9	15	61	24	0.246	6.21E+05	2.52E+06	59.6 +- 17.2
10	0	3	20	0.000	0.00E+00	1.49E+05	0.0 +- 0.0
11	5	13	10	0.385	2.76E+05	7.17E+05	93.0 +- 40.9
12	16	61	16	0.262	9.93E+05	3.79E+06	63.6 +- 17.9
13	0	1	30	0.000	0.00E+00	3.31E+04	0.0 +- 0.0
14	17	49	15	0.347	1.13E+06	3.24E+06	83.9 +- 23.6
15	11	31	35	0.355	3.12E+05	0.00E+05	05.0 +- 30.1
16	1	6	14	0.167	7.09E+04	4.26E+05	40.5 +- 43.7
17	1	4	12	0.250	0.20E+04	3.31E+05	60.6 +- 67.7
18	6	10	16	0.600	3.72E+05	6.21E+05	144.5 +- 74.6
19	27	106	24	0.255	1.12E+06	4.39E+06	61.7 +- 13.3
20	25	42	40	0.595	6.21E+05	1.04E+06	143.4 +- 36.2

<u>171</u>	<u>526</u>	<u>4.377E+05</u>	<u>1.347E+06</u>
------------	------------	------------------	------------------

AREA OF BASIC UNIT = 1.0068E-06 CM²

VARIANCE OF SQR(NS) = 2.76442

VARIANCE OF SQR(NI) = 7.17754

CORRELATION COEFFICIENT = 0.900

CHI SQUARED = 19.7615 WITH 19 DEGREES OF FREEDOM PASS

NS/NI = 0.325 +- 0.029

MEAN RATIO = 0.320 +- 0.054

AGE CALCULATED USING A ZETA OF 352.7 FOR SRM612 GLASS

RHO D = 1.381E+06 NO = 5400

POOLED AGE = 73.7 +- 7.0 MYR

MEAN AGE = 77.3 +- 13.1 MYR

POS 68A

IRRADIATION: PT931-02
ANALYSIS BY POS 4/30/88

CRYSTAL	NS	NI	AREA UNITS	RATIO	RHO S	RHO I	AGE(MYR)
1	5	14	16	0.357	3.18E+05	0.69E+05	86.4 +- 45.6
2	1	4	12	0.250	0.28E+04	3.31E+05	68.6 +- 67.7
3	0	1	8	0.000	0.00E+00	1.24E+05	0.0 +- 0.0
4	0	3	18	0.000	0.00E+00	1.66E+05	0.0 +- 0.0
5	9	11	0	0.810	1.12E+06	1.37E+06	196.2 +- 88.2
6	2	5	18	0.400	1.10E+05	2.76E+05	96.7 +- 80.9
7	2	3	12	0.667	1.66E+05	2.48E+05	160.3 +- 146.4
8	1	3	12	0.333	0.28E+04	2.48E+05	88.7 +- 93.2
9	1	3	20	0.333	4.97E+04	1.49E+05	88.7 +- 93.2
10	2	5	18	0.400	1.10E+05	2.76E+05	96.7 +- 80.9
11	10	31	14	0.323	7.09E+05	2.28E+06	78.1 +- 28.4
12	0	2	12	0.000	0.00E+00	1.66E+05	0.0 +- 0.0
13	1	3	16	0.333	6.21E+04	1.06E+05	88.7 +- 93.2
14	2	14	12	0.143	1.66E+05	1.16E+06	34.7 +- 26.2
15	2	6	21	0.333	9.46E+04	2.04E+05	88.7 +- 65.9
16	12	30	6	0.400	1.99E+06	4.97E+06	96.7 +- 33.0
17	7	16	6	0.438	1.16E+06	2.65E+06	105.7 +- 47.9
18	4	10	10	0.400	3.97E+05	9.93E+05	96.7 +- 57.2
19	0	2	16	0.000	0.00E+00	1.24E+05	0.0 +- 0.0
20	14	36	28	0.389	4.97E+05	1.28E+06	94.8 +- 29.6

752022.632E+057.090E+05

AREA OF BASIC UNIT = 1.0068E-06 CM²

VARIANCE OF SQR(NS) = 1.36579

VARIANCE OF SQR(NI) = 2.25543

CORRELATION COEFFICIENT = 0.938

CHI SQUARED = 8.92728 WITH 19 DEGREES OF FREEDOM PASS

NS/NI = 0.371 +- 0.050

MEAN RATIO = 0.316 +- 0.048

AGE CALCULATED USING A ZETA OF 352.7 FOR SRM612 GLASS

RHO D = 1.391E+06 ND = 5480

FOOLED AGE = 89.8 +- 12.2 MYR

MEAN AGE = 76.5 +- 11.6 MYR

POS 69A

IRRADIATION: PT916-08
ANALYSIS BY POS 4/30/88

CRYSTAL	NS	NI	AREA UNITS	RATIO	RHO S	RHO I	AGE(MYR)
1	2	8	11	0.250	1.81E+05	7.22E+05	68.4 +- 47.7
2	5	16	12	0.313	4.14E+05	1.32E+06	75.4 +- 38.6
3	13	27	9	0.481	1.43E+06	2.98E+06	115.8 +- 39.1
4	4	8	16	0.500	2.48E+05	4.97E+05	120.2 +- 73.6
5	4	3	27	1.333	1.47E+05	1.18E+05	315.7 +- 241.1
6	7	28	24	0.250	2.98E+05	1.16E+06	68.4 +- 25.5
7	1	2	21	0.500	4.73E+04	9.46E+04	120.2 +- 147.2
8	15	23	15	0.652	9.93E+05	1.52E+06	156.3 +- 51.9
9	3	9	36	0.333	8.28E+04	2.48E+05	88.4 +- 53.6
10	4	4	12	1.000	3.31E+05	3.31E+05	238.2 +- 168.4
11	4	12	16	0.333	2.48E+05	7.45E+05	88.4 +- 46.4
12	16	18	24	0.889	6.62E+05	7.45E+05	212.2 +- 72.9
13	14	33	18	0.424	1.39E+06	3.28E+06	182.1 +- 32.6
14	16	38	9	0.533	1.77E+06	3.31E+06	128.1 +- 39.7
15	8	6	16	0.800	8.00E+04	3.72E+05	8.8 +- 8.8
16	4	12	28	0.333	1.99E+05	5.96E+05	88.4 +- 46.4
17	6	25	16	0.240	3.72E+05	1.55E+06	58.8 +- 26.4
18	8	1	8	0.800	8.00E+04	1.24E+05	8.8 +- 8.8
19	8	4	28	0.800	8.00E+04	1.99E+05	8.8 +- 8.8
20	1	4	25	0.250	3.97E+04	1.59E+05	68.4 +- 67.5

1192733.486E+057.814E+05

AREA OF BASIC UNIT = 1.0068E-06 CM²

VARIANCE OF SQR(NS) = 1.68762

VARIANCE OF SQR(NI) = 2.22549

CORRELATION COEFFICIENT = 0.831

CHI SQUARED = 20.5285 WITH 19 DEGREES OF FREEDOM PASS

NS/NI = 0.436 +- 0.048

MEAN RATIO = 0.431 +- 0.075

AGE CALCULATED USING A ZETA OF 352.7 FOR SRM612 GLASS

RHO O = 1.376E+06 NO = 5461

POOLED AGE = 104.9 +- 11.6 MYR

MEAN AGE = 103.7 +- 18.2 MYR

POS 64A

IRRADIATION: PT931-01
ANALYSIS BY POS 4/30/88

CRYSTAL	NS	NI	AREA UNITS	RATIO	RHO S	RHO I	AGE(MYR)
1	5	43	8	0.116	6.21E+05	5.34E+06	28.3 +- 13.4
2	4	9	15	0.444	2.65E+05	5.96E+05	107.3 +- 64.5
3	1	2	15	0.500	6.62E+04	1.32E+05	120.6 +- 147.7
4	17	58	10	0.293	1.69E+06	5.76E+06	71.0 +- 19.6
5	1	2	8	0.500	1.24E+05	2.40E+05	120.6 +- 147.7
6	2	5	2	0.400	9.93E+05	2.40E+06	96.7 +- 88.9
7	0	3	15	0.000	0.00E+00	1.99E+05	0.0 +- 0.0
8	1	4	5	0.250	1.99E+05	7.95E+05	60.6 +- 67.7
9	0	1	6	0.000	0.00E+00	1.66E+05	0.0 +- 0.0
10	0	2	9	0.000	0.00E+00	2.21E+05	0.0 +- 0.0

<u>31</u>	<u>129</u>			<u>3.311E+05</u>	<u>1.370E+06</u>		
-----------	------------	--	--	------------------	------------------	--	--

AREA OF BASIC UNIT = 1.0068E-06 CM²

VARIANCE OF SQR(NS) = 1.63156

VARIANCE OF SQR(NI) = 5.38167

CORRELATION COEFFICIENT = 0.907

CHI SQUARED = 3.63706 WITH 9 DEGREES OF FREEDOM PASS

NS/NI = 0.240 +- 0.048

MEAN RATIO = 0.250 +- 0.066

AGE CALCULATED USING A ZETA OF 352.7 FOR SRM612 GLASS

RHO D = 1.381E+06 ND = 5480

POOLED AGE = 58.3 +- 11.7 MYR

MEAN AGE = 60.7 +- 16.0 MYR

JD 49A

IRRADIATION: PT917-04
ANALYSIS BY POS 4/28/88

CRYSTAL	NS	NI	AREA UNITS	RATIO	RHO S	RHO I	AGE(MYR)
1	5	7	15	0.714	3.31E+05	4.64E+05	167.7 +- 98.2
2	4	17	48	0.235	9.93E+04	4.22E+05	55.7 +- 31.0
3	6	17	36	0.353	1.66E+05	4.69E+05	83.4 +- 39.6
4	10	9	20	1.111	4.97E+05	4.47E+05	259.1 +- 119.0
5	6	12	24	0.500	2.48E+05	4.97E+05	117.9 +- 58.9
6	3	6	20	0.500	1.86E+05	2.13E+05	117.9 +- 83.3
7	12	18	24	0.667	4.97E+05	7.45E+05	156.7 +- 58.4
8	2	6	18	0.333	1.18E+05	3.31E+05	78.8 +- 64.4
9	4	10	27	0.400	1.47E+05	3.68E+05	94.5 +- 55.9
10	2	11	24	0.182	0.28E+04	4.55E+05	43.1 +- 33.1
11	4	20	40	0.200	9.93E+04	4.97E+05	47.4 +- 26.0
12	3	4	12	0.750	2.48E+05	3.31E+05	176.0 +- 134.4
13	5	11	20	0.455	1.77E+05	3.98E+05	107.2 +- 57.8
14	3	12	40	0.250	7.45E+04	2.98E+05	59.2 +- 38.2
15	3	18	20	0.167	1.86E+05	6.39E+05	39.5 +- 24.7
16	3	14	18	0.214	1.66E+05	7.73E+05	50.8 +- 32.3
17	7	14	24	0.500	2.98E+05	5.79E+05	117.9 +- 54.6
18	4	11	15	0.364	2.65E+05	7.28E+05	85.9 +- 50.2
19	4	13	36	0.300	1.18E+05	3.59E+05	72.0 +- 41.6
20	4	14	24	0.286	1.66E+05	5.79E+05	67.6 +- 38.3

942441.792E+054.652E+05

AREA OF BASIC UNIT = 1.8868E-06 CM²

VARIANCE OF SQR(NS) = .276054

VARIANCE OF SQR(NI) = .45105

CORRELATION COEFFICIENT = 0.267

CHI SQUARED = 17.9573 WITH 19 DEGREES OF FREEDOM PASS

NS/NI = 0.385 +- 0.047

MEAN RATIO = 0.424 +- 0.053

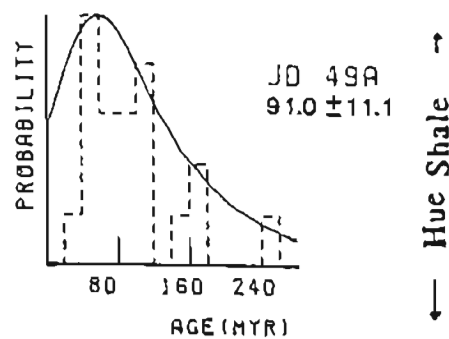
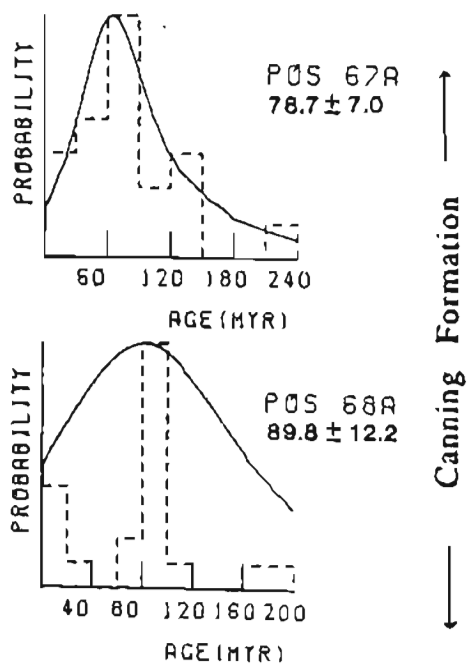
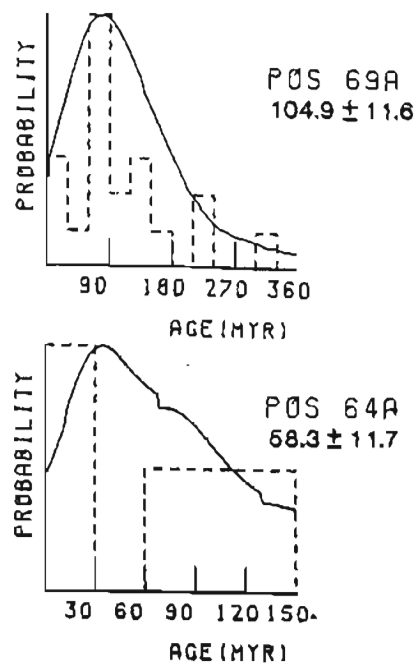
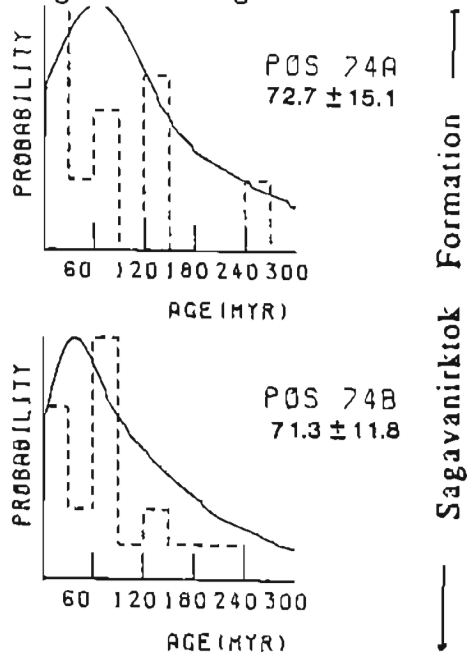
AGE CALCULATED USING A ZETA OF 352.7 FOR SRM612 GLASS

RHO D = 1.349E+03 ND = 5354

POOLED AGE = 91.0 +- 11.1 MYR

MEAN AGE = 100.2 +- 12.6 MYR

Single-Grain Age Distributions: ANWR Coastal Plain



REFERENCES

- Anders, D.E., Magoon, L.B. and Lubeck, Sister C. (1987). Geochemistry of surface oil shows and potential source rocks. In: Bird, K.J. and Magoon, L.B., (eds), Petroleum Geology of the Northern Part of the Arctic National Wildlife Refuge, Northeastern Alaska. U.S. Geological Survey Bulletin 1778: 181-198.
- Bar, K.D., Kolodny, Y. and Bentor, Y.K. (1974). Dating faults by fission track dating of epidotes--an attempt. Earth and Planetary Science Letters, v. 22: 157-162.
- Bird, K.J. (1987). The framework geology of the north slope of Alaska as related to oil-source rock correlations. In: Tailleux, I.L. and Weimer, P., (eds.), Alaskan North Slope Geology. Society of Economic Paleontologists and Mineralogists Pacific Section Publication 50: 121-143.
- Bird, K.J. and Bader, J.W. (1987). Regional geologic setting and history of petroleum exploration. In: Bird, K.J. and Magoon, L.B., (eds), Petroleum Geology of the Northern Part of the Arctic National Wildlife Refuge, Northeastern Alaska. U.S. Geological Survey Bulletin 1778: 17-25.
- Bird, K.J. and Molenaar, C.M., (1987). Stratigraphy. In: Bird, K.J. and Magoon, L.B., (eds.), Petroleum Geology of the Northern Part of the Arctic National Wildlife Refuge, Northeastern Alaska. U.S. Geological Survey Bulletin 1778: 37-59.
- Bird, K.J., Griscom, S.B., Bartsch-Winkler, S. and Giovannetti, D.M. (1987). Petroleum reservoir rocks. In: Bird, K.J. and Magoon, L.B., (eds), Petroleum Geology of the Northern Part of the Arctic National Wildlife Refuge, Northeastern Alaska. U.S. Geological Survey Bulletin 1778: 79-100.
- Bird, R.B., Stewart, W.E. and Lightfoot, E.N. (1960). Transport phenomena. J. Wiley and sons, New York, New York. 780 p.
- Bloom, A.L. (1978). Geomorphology. Prentice-Hall Inc., Englewood Cliffs, New Jersey: 510 p.
- Boyer, S.E. and Elliot, D. (1982). Thrust systems. American Association of Petroleum Geologists Bulletin, v. 66: 1196-1230.
- Brosge, W.P. and Tailleux, I.L., (1970). Depositional history of northern Alaska. In: Adkison, W.L., and Brosge, M.M., (eds.), Proceedings of the geological seminar on the North Slope of Alaska. American Association of Petroleum Geologists Pacific Section Meeting, Los Angeles: D1-D18.
- Bruns, T.R., Fisher, M.A., Leinbach, W.J. and Miller, J.J. (1987). Regional structure of rocks beneath the coastal plain. In: Bird, K.J. and Magoon, L.B., (eds), Petroleum Geology of the Northern Part of the Arctic National Wildlife Refuge, Northeastern Alaska. U.S. Geological Survey Bulletin 1778: 249-254.
- Buckle, C. (1978). Landforms in Africa. Longman, London, United Kingdom: 249 p.

- Burchart, J. (1981). Evaluation of uncertainties in fission track dating: some statistical and geochemical problems. *Nuclear Tracks* 5: 87-92.
- Clark, S.P. (1966). *Handbook of Physical Constants*. Geological Society of America Memoir 97: 587 p.
- Clark, S.P. and Jager, E. (1969). Denudation rate in the Alps from geochronologic and heat flow data. *American Journal of Science*, v. 267: 1143-1160.
- Conran, G.A. and Adler, H.H. (1976). The variability of the natural abundance of ^{235}U . *Geochim. Cosmochim. Acta*. 40: 1487-1490.
- Corbel, J. (1959). Vitesse de l'erosion. *Zeitschr. fur Geomorph.*, v. 3: 1-28.
- Decker, J., Camber, W., Vandergon, M.A. and Crowder, R.K., (1988). Arctic Creek facies, Arctic National Wildlife Refuge, Northeastern Alaska (abs.). *American Association of Petroleum Geologists Bulletin* 72: p. 176.
- Detterman, R.L., Reiser, H.N., Brosge, W.P. and Dutro Jr., J.T., (1975). Post-Carboniferous Stratigraphy, Northeastern Alaska. U.S. Geological Survey Professional Paper 886: 46 p.
- Dodge, F.C.W. and Naeser, C.W., (1968). Ages of apatites from granitic rocks of the Sierra Nevada Batholith (abs). *Transactions of the American Geophysical Union*, v. 49: p. 348.
- Dillon, J.T., Tilton, G.R., Decker, J. and Kelly, M.J. (1987). Resource Implications of magmatic and metamorphic ages for Devonian igneous rocks in the Brooks Range. In: Tailleux, I.L. and Weimer, P., (eds.), *Alaskan North Slope Geology*. Society of Economic Paleontologists and Mineralogists Pacific Section Publication 50: 713-723.
- Dodson M.H. and McClelland-Brown, E. (1985). Isotope and paleomagnetic evidence for rates of cooling, uplift and erosion. *The Chronology of the Geological Record*. Geological Society of America Memoir 10: 315-325.
- Fitzgerald, P.G. (1987). Uplift History of the Transantarctic Mountains in the Ross Sea Sector and a Model for Their Formation. Ph.D. Thesis, University of Melbourne, Australia: 327 p.
- Fitzgerald, P.G., Sandiford, M., Barrett, P.J. and Gleadow, A.J.W. (1986). Asymmetric extension associated with uplift and subsidence of the Transantarctic Mountains and Ross Embayment. *Earth and Planetary Science Letters*, v. 81: 67-78.
- Fleischer, R.L. and Price, P.B. (1963). Charged particle tracks in glass. *Journal Applied Physics*, v. 34: 2903-2904.
- Fleischer, R.L. and Price, P.B. (1964). Fission track evidence for the simultaneous origin of tektites and other natural glasses. *Geochim. Cosmochim. Acta*. 28: 755-760.

- Fleischer, R.L., Price, P.B. and Walker, R.M. (1975). Nuclear tracks in solids: Principles and applications. University of California Press, Berkeley: 605 p.
- Galbraith, R.F. (1981). On statistical models for fission track counts. *Mathematical Geology*, v. 13: 471-488.
- Galliker, D., Hugentobler, E. and Hahn, B. (1970). Spontane Kernspaltung von U-238 und Am-241. *Helv. Phys. Acta.*, v. 43: p. 593.
- Gautier, D.L., Bird, K.J. and Colten-Bradley, V.A. (1987). Relationship of clay mineralogy, thermal maturity, and geopressure in wells of the Point Thompson area. In: Bird, K.J. and Magoon, L.B., (eds), *Petroleum Geology of the Northern Part of the Arctic National Wildlife Refuge, Northeastern Alaska*. U.S. Geological Survey Bulletin 1778: 199-207.
- Gleadow, A.J.W. (1978). Anisotropic and variable track etching characteristics in natural sphenes. *Nuclear Tracks* 2: 105-117.
- Gleadow, A.J.W. (1981). Fission-track dating: what are the real alternatives? *Nuclear Tracks* 5: 3-14.
- Gleadow, A.J.W. (1984). Fission track dating methods - II: a manual of principles and techniques. Workshop on fission track analysis: principles and applications. James Cook University, Townsville, Australia, Sept. 4-6, 1984: 35 p.
- Gleadow, A.J.W. and Lovering, J.L. (1974). The effect of weathering on fission track dating. *Earth and Planetary Science Letters*, v. 22: 163-168.
- Gleadow, A.J.W. and Brooks, C.K., (1979). Fission track dating, thermal histories and tectonics of igneous intrusions in east Greenland. *Contributions to Mineral Petrology*, v. 71: 45-60.
- Gleadow, A.J.W. and Duddy, I.R. (1981). A natural long term annealing experiment for apatite. *Nuclear Tracks* 5: 169-174.
- Gleadow, A.J.W., Leigh-Jones, P., Duddy, I.R. and Lovering, J.F. (1982). An automated microscope stage system for fission track dating and particle track mapping (abs). Workshop on fission track dating, Nikko, Japan, Fifth International Conference on Geochronology, Cosmochronology and Isotope Geology.
- Gleadow, A.J.W., Duddy, I.R. and Lovering, J.F. (1983). Fission track analysis: a new tool for the evaluation of thermal histories and hydrocarbon potential. *Petroleum Exploration Association of Australia Journal* 23: 93-102.
- Gleadow, A.J.W. and Duddy, I.R. (1984). Fission track dating and thermal history analysis of apatites from wells in the north-west Canning Basin. In: Purcell, P.G. (ed.), *The Canning Basin, W. A., Proceedings of the Geological Society of Australia and Petroleum Exploration Society of Australia Symposium*, Perth, 1984: 377-387.

- Gleadow, A.J.W. and Fitzgerald, P.G. (1984). Uplift history of the Transantarctic Mountains in the Dry Valleys area, southern Victoria Land, Antarctica, from apatite fission track ages. *New Zealand Journal of Geology and Geophysics*, v. 27: 457-464.
- Gleadow, A.J.W., Duddy, I.R., Green, P.F. and Hegarty, K.A. (1986a). Fission track lengths in the apatite annealing zone and the interpretation of mixed ages. *Earth and Planetary Science Letters*, v. 78: 245-254.
- Gleadow, A.J.W., Duddy, I.R., Green, P.F. and Lovering J.F. (1986b). Confined fission track lengths in apatite: a diagnostic tool for thermal history analysis. *Contributions to Mineral Petrology*, v. 94: 405-415.
- Gleadow, A.J.W. and Fitzgerald, P.G. (1987). Uplift history and structure of the Transantarctic Mountains: new evidence from fission track dating of basement apatites in the Dry Valleys area, southern Victoria Land. *Earth and Planetary Science Letters*, v. 82: 1-14.
- Gleadow, A.J.W. and Ollier, C.D. (1987). The age of gabbro at The Crescent, New South Wales. *Australian Journal of Earth Sciences*, v. 34: 209-212.
- Grantz, A. and May, S.D. (1983). Rifting history and structural development of the continental margin north of Alaska. In: Watkins, J.S. and Drake, C.L. (eds.), *Studies in continental margin geology*. American Association of Petroleum Geologists Memoir 34: 77-100.
- Green, P.F. (1980). On the cause of shortening of spontaneous fission tracks in certain minerals. *Nuclear Tracks* 4: 91-100.
- Green, P.F. (1981). A new look at statistics in fission track dating. *Nuclear Tracks* 5: 77-86.
- Green, P.F. (1985). Comparison of zeta calibration baselines for fission-track dating of apatite, zircon and sphene. *Chemical Geology*, v. 58: 1-22.
- Green, P.F. (1986). On the thermo-tectonic evolution of Northern England: evidence from fission track analysis. *Geology*, v. 5: 493-506.
- Green, P.F. and Hurford, A.J. (1984). Neutron dosimetry for fission track dating. *Nuclear Tracks* 9: 231-241.
- Green, P.F., Duddy, I.R., Gleadow, A.J.W., Tingate, P.T. and Laslett, G.M. (1985a). Fission-track annealing in apatite: track length measurements and the form of the Arrhenius plot. *Nuclear Tracks* 10: 323-328.
- Green, P.F., Duddy, I.R., Gleadow, A.J.W. and Lovering, J.F. (1985b). Apatite fission track analysis as a paleotemperature indicator for hydrocarbon exploration. In: Naeser, N.D. (ed.), *Society of Economic Paleontologists and Mineralogists Special Publication*, (in press).

- Green, P.F., Duddy, I.R., Gleadow, A.J.W., Tingate, P.T. and Laslett, G.M. (1986). Thermal annealing of fission tracks in apatite: 1 - a qualitative description. *Isotope Geoscience*, v. 59: 237-253.
- Hannah, G.C., Wescott, C.H., Lemmel, H.D., Leonard, B.R., Story, J.S. and Attree, P.M. (1969). Revision of values for the 2200 m/s neutron constants for four fissile nuclides. *Gen. Elec. Co. Atomic Energy Rev.* 7: 3-92.
- Harrison, T.M. and McDougall, I. (1980). Investigations of an intrusive contact, northwest Nelson, New Zealand. 1, Thermal, chronological and isotopic constraints. *Geochim. Cosmochim. Acta*. v. 44: 1985-2003.
- Harrison, T.M., Armstrong, R.L., Naeser, C.W. and Harakal, J.E. (1979). Geochronology and thermal history of the Coast Plutonic Complex, near Prince Rupert, British Columbia. *Canadian Journal of Earth Sciences*, v. 16: 400-410.
- Hubbard, R.J., Edrich, S.P. and Rattey, R.P. (1987). Geologic evolution and hydrocarbon habitat of the 'Arctic Alaska Microplate. In: TAILLEUR, I.L. and WEIMER, P., (eds.), *Alaskan North Slope Geology*. Society of Economic Paleontologists and Mineralogists Pacific Section Publication 50: 797-830.
- Hurford, A.J. (1986). Cooling and uplift patterns in the Lepontine Alps South Central Switzerland and an age of vertical movement on the Insubric fault line. *Contributions to Mineral Petrology*, v. 92: 413-427.
- Hurford, A.J. and Green, P.F. (1982). A users' guide to fission-track dating calibration. *Earth and Planetary Science Letters*, v. 59: 343-354.
- Hurford, A.J. and Green, P.F. (1983). The zeta calibration of fission track dating. *Isotope Geoscience*, v. 1: 285-317.
- Jaffey, A.H., Flynn, K.F., Glendenin, L.E., Bentley, W.C. and Essling, A.M. (1971). Precision measurements of the half-lives and specific activities of ^{235}U and ^{238}U . *Physics Review*, v. 4: 1889-1906.
- Kelley, J.S. and Foland, R.L. (1987). Structural style and framework geology of the coastal plain and adjacent Brooks Range. In: Bird, K.J. and Magoon, L.B., (eds), *Petroleum Geology of the Northern Part of the Arctic National Wildlife Refuge, Northeastern Alaska*. U.S. Geological Survey Bulletin 1778: 255-270.
- Kelley, S.A. and Duncan, I.J. (1986). Late Cretaceous to Middle Tertiary tectonic history of the northern Rio Grande Rift, New Mexico. *Journal of Geophysical Research*, v. 91: 6246-6262.
- Lachenbruch, A.H. and Marshall, B.V. (1986). Changing climate--Geothermal evidence from permafrost in the Alaskan Arctic. *Science*, v. 234, 689-696.
- Lachenbruch, A.H., Sass, J.H., Marshall, B.V. and Moses, T.R. Jr. (1982). Permafrost, heat flow, and the geothermal regime at Prudhoe Bay, Alaska. *Journal of Geophysical Research*, v. 87: 9301-9316.

- Lachenbruch, A.H., Sass, J.H., Lawver, L.A., Brewer, M.C., Marshall, B.V., Munroe, R.J., Kennelly, Jr., J.P., Galanis, Jr., S.P. and Moses, Jr., T.H. (1987). Temperature and Depth of Permafrost on the Alaskan North Slope. In: Tailleux, I.L. and Weimer, P., (eds.), *Alaskan North Slope Geology*. Society of Economic Paleontologists and Mineralogists Pacific Section Publication 50: 545-558.
- Lal, D., Rajan, R.S. and Tarnhane, A.S. (1969). Chemical composition of nuclei of $Z > 22$ in cosmic rays using meteoric minerals as detectors. *Nature*, v. 221: 33-37.
- Laslett, G.M., Kendall, W.S., Gleadow, A.J.W. and Duddy, I.R. (1982). Bias in measurement of fission-track length distributions. *Nuclear Tracks* 6: 79-85.
- Laslett, G.M., Gleadow, A.J.W. and Duddy, I.R. (1984). The relationship between fission track length and density in apatite. *Nuclear Tracks* 9: 29-38.
- Laslett, G.M., Green, P.F., Duddy, I.R. and Gleadow, A.J.W. (1987). Thermal modelling of fission tracks in apatite: 2. A quantitative analysis. *Chemical Geology*, v. 65: 1-13.
- Lee, T. (1979). Erosion, uplift, exponential heat source Distribution, and transient heat flux. *Journal of Geophysical Research*, v. 84: 585-590.
- Lerand, Monti (1973). Beaufort Sea. In: McCrossan, R.G. (ed.), *The Future Petroleum Provinces of Canada--Their Geology and Potential*. Canadian Society Petroleum Geologists Memoir 1: 315-386.
- Leiggi, P.A. (1987). Style and age of tectonism of Sadlerochit Mountains to Franklin Mountains, Arctic National Wildlife Refuge (ANWR), Alaska. In: Tailleux, I.L. and Weimer, P., (eds.), *Alaskan North Slope Geology*. Society of Economic Paleontologists and Mineralogists Pacific Section Publication 50, 749-756.
- Lindsay, D.A., Naeser, C.W. and Shawe, D.R. (1975). Age of volcanism, intrusion and mineralization in the Thomas Range, Keg Mountains and Desert Mountain, western Utah. *Journal of Research U.S. Geological Survey* 3: 597 p.
- Magoon, L.B., Woodward, P.V., Banet Jr., A.C., Griscom, S.B. and Daws, T.A. (1987). Thermal maturity, richness, and type of organic matter of source-rocks units. In: Bird, K.J. and Magoon, L.B., (eds), *Petroleum Geology of the Northern Part of the Arctic National Wildlife Refuge, Northeastern Alaska*. U.S. Geological Survey Bulletin 1778: 127-180.
- Mailhe, D., Lucazeau, F and Vasseur, G. (1986). Uplift history of thrust belts: an approach based on fission track data and thermal modelization. *Tectonophysics*, v. 124: 177-191.
- Mast, R.F., McMullen, R.H., Bird, K.J. and Brosge, W.P. (1980). Resource appraisal of undiscovered oil and gas resources in the William O. Douglas Arctic Wildlife Range. U.S. Geological Survey Open-file Report 80-916: 80 p.

- Menard, H.W. (1961). Some rates of regional erosion. *Journal of Geology*, v. 69: 154-161.
- Miller, D.S. and Lakatos, S. (1983). Uplift rate of Adirondack anorthosite measured by fission tracks in apatite. *Geology*, 11: 284-286.
- Moore, M.E., Gleadow, A.J.W. and Lovering, J.F. (1986). Thermal evolution of rifted continental margins: new evidence from fission tracks in basement apatites from southeastern Australia. *Earth and Planetary Science Letters*, v. 78: 255-270.
- Morgan, P. and Ashwal, L.D. (1984). Comment and reply on "Uplift rate of Adirondack anorthosite measured by fission-track analysis of apatite". *Geology*, v. 12, 124-125.
- Mull, C.G. (1982). Tectonic evolution and structural style of the Brooks Range and Arctic Slope, Alaska. In: Powers, R.B., (ed.), *Geologic Studies of the Cordilleran Thrust belt*. Rocky Mountain Association of Geologists, Denver, Colorado, 1: 1-45.
- Mull, C.G. (1985). Cretaceous tectonics, depositional cycles, and the Nanushak Group, Brooks Range and Arctic Slope, Alaska. In: Huffman, A.C. Jr., (ed.), *Geology of the Nanushak Group and related rocks, North Slope, Alaska*. U.S. Geological Survey Bulletin 1614: 7-36.
- Naeser, C.W. (1979a). Fission track dating and geologic annealing of fission tracks. In: Jager, E. and Hunziker, J.C. (eds.), *Lectures in Isotope Geology*. Springer Verlag, New York: 154-169.
- Naeser, C.W. (1979b). Thermal history of sedimentary basins: fission track dating of subsurface rocks. *Society of Economic Paleontologists and Mineralogists Special Publication* 26: 109-112.
- Naeser, C.W. (1981). The fading of fission-tracks in the geologic environment - data from deep drill holes (abs.). *Nuclear Tracks* 5: 248-250.
- Naeser, C.W. and Faul, H. (1969). Fission track annealing in apatite and sphene. *Journal of Geophysical Research*, v. 74: 705-710.
- Naeser, C.W. and Forbes, R.B., (1976). Variation of fission track ages with depth in two deep drill-holes (abs.). *Transactions of the American Geophysical Union*, v. 57: p. 353.
- Naeser, C.W., Bryant, B., Crittenden, M.D. and Sorensen, M.L. (1983). Fission-track ages of apatite in the Wasatch Mountains, Utah: An uplift study. *Geological Society of America Memoir* 157: 29-36.
- Namson, J.S. and Wallace, W.K. (1986). A structural transect across the northeastern Brooks Range, Alaska (abs.). *Geological Society of America Abstracts with Programs*, v. 18: 163.
- North, F.K. (1985). *Petroleum Geology*. Allen and Unwin Inc., London, United Kingdom: 607 p.

- Oldow, J.S., Seidensticker, C.M., Phelps, J.C., Julian, F.E., Gottschalk, R.R., Boler, K.W., Handschy, J.W. and Ave Lallement, H.G. (1987). Balanced cross sections through the central Brooks Range and North Slope, Arctic Alaska. American Association of Petroleum Geologists Publication: 19 p., 8 plates.
- Palmer, I.F., Bolmm, J.R., Maxey, L.R. and Lyle, W.M. (1979). Petroleum source rock and reservoir quality data from outcrop samples, onshore North Slope of Alaska east of Prudhoe Bay. U.S. Geological Survey Open-File Report 79-1634: 14 plates, 52 p.
- Parrish, R.R. (1982). Cenozoic thermal and tectonic history of the Coast Mountains of British Columbia as revealed by fission-track and geological data. PhD Thesis, University of British Columbia, Vancouver, 166 p.
- Parrish, R.R. (1983). Cenozoic thermal evolution and tectonics of the coast mountains of British Columbia. 1. Fission track dating, apparent uplift rates and patterns of uplift. *Tectonics*, v. 2: 601-631.
- Price, P.B. and Walker, R.L. (1963). Fossil tracks of charged particles in mica and the age of minerals. *Journal of Geophysical Research*, v. 68: 4847-4862.
- Rathey, R.P. (1987). Northeastern Brooks Range, Alaska--new evidence for complex thin-skinned thrusting (abs). In: TAILLEUR, I.L. and WEIMER, P., (eds.), *Alaskan North Slope Geology*. Society of Economic Paleontologists and Mineralogists Pacific Section Publication 50: p.757.
- Royden, L. and Hodges, K.V. (1984). A technique for analyzing the thermal and uplift histories of eroding orogenic belts: a Scandinavian example. *Journal of Geophysical Research*, v. 89: 7091-7106.
- Sable, E.G. (1977). Geology of the western Romanazof Mountains, Brooks Range, northeastern Alaska. U.S. Geological Survey Professional Paper 897: 84 p.
- Sedivy, R.A., Penfield, I.E., Halpern, H.I., Drozd, R.J., Cole, G.A. and Burwood, R. (1987). Investigation of source rock-crude oil relationships in the northern Alaska hydrocarbon habitat. In: TAILLEUR, I.L. and WEIMER, P., (eds.), *Alaskan North Slope Geology*. Society of Economic Paleontologists and Mineralogists Pacific Section Publication 50: 169-179.
- Smith, M.J. and Leigh-Jones, P. (1985). An automated microstage for fission track dating. *Nuclear Tracks* 10, 395-400.
- Spera, F.J. (1980). Aspects of magma transport. In: HARGRAVES, R.B. (ed), *Physics of Magmatic Processes*. Princeton University Press, New Jersey: 264-323.
- Storzer, D. (1970). Fission track dating of volcanic glass and the thermal history of rocks. *Earth and Planetary Science Letters*, v. 8: 55-60.
- Storzer, D. and Wagner, G.A. (1971). Fission track ages of North American tektites. *Earth and Planetary Science Letters*, v. 10: 435-440.

- Tailleur, I.L. (1987). Argument for Cretaceous instead of Devonian plutonism in the Brooks Range, Northern Alaska (abs.). In: Tailleir, I.L. and Weimer, P., (eds.), Alaskan North Slope Geology. Society of Economic Paleontologists and Mineralogists Pacific Section Publication 50: 724.
- Tissot, B.P. and Welte, D.H. (1984). Petroleum Formation and Occurrence. Springer-Verlag, New York, New York: 699 p.
- Turner, F.J. (1981). Metamorphic Petrology. Hemisphere Publishing Corp., New York, New York: 524 p.
- Wagner, G.A. (1968). Fission track dating of apatites. Earth and Planetary Science Letters, v. 4: 411-415.
- Wagner, G.A. (1986). Comments on the paper "Fission track annealing in apatite: Track length measurements and the form of the Arrhenius plot". Nuclear Tracks 11: p. 269.
- Wagner, G.A. and Storzer, D. (1972). Fission track length reductions in minerals and the thermal history of rocks. Trans. Am. Nucl. Soc. 15: 127-128.
- Wagner, G.A., Reimer, G.M., Carpenter, G.S., Faul, H., Van der Linden, R. and Gijbels, R. (1975). The spontaneous fission rate of U-238 and fission track dating. Geochim. Cosmochim. Acta. 39: 1279-1286.
- Wagner, G.A., Reimer, G.M. and Jager, E. (1977). The cooling ages derived by apatite fission track, mica Rb-Sr, and K-Ar dating: the uplift and cooling history of the central Alps. Inst. Geol. Mineral., Univ. Padova, Italy, Mem. 30: 27 p.
- Wallace, W.K. and Hanks, C.L. (1988a). Stratigraphic controls on lateral variations in the structural style of the northeastern Brooks Range, Arctic National Wildlife Refuge (ANWR), Alaska. American Association of Petroleum Geologists Bulletin, v. 72/2: p. 256.
- Wallace, W.K. and Hanks, C.L. (1988b). Lateral variations in the range-front structure of the northeastern Brooks Range, Arctic National Wildlife Refuge (ANWR), Alaska. Geological society of America, Cordillera Section Abstracts with Programs. v. 20/3: p. 241.
- Wallace, W.K. and Hanks, C.L. (1988). Systematic vertical and lateral variations in structural geometry in the northeastern Brooks Range, Alaska. American Association of Petroleum Geologists Bulletin (submitted).
- Wyllie, P.J. (1971). The Dynamic Earth. Wyley and Sons Inc., New York: 416 p.
- Zeitler, P.K. (1985). Cooling history of the NW Himalaya, Pakistan. Tectonics, 4, 127-151.
- Zeitler, P.K., Tahirkhell, R.A.K., Naeser, C.W. and Johnson, N.M. (1982). Unroofing history of a suture zone in the Himalaya of Pakistan by means of fission track annealing ages. Earth and Planetary Science Letters, v. 57: 227-240.